Effect of Pyrethroid Insecticides on Gene Expression in the Mammalian Central Nervous System

Joshua A. Harrill

"A dissertation submitted to the faculty of the University of North Carolina at Chapel Hill in partial fulfillment of the requirements for the degree of doctor of philosophy in the Curriculum in Toxicology."

Chapel Hill
2008

Approved by:
Kevin M. Crofton, Ph.D.
Lee M. Graves, Ph.D.
David J. Holbrook, Ph.D.
A. Leslie Morrow, Ph.D.
Nigel Walker, Ph.D.
Fred A. Wright, Ph.D.

Abstract

Joshua A. Harrill

Effect of Pyrethroid Insecticides on Gene Expression in the Mammalian Central Nervous System

(Under the direction of Kevin M. Crofton, Ph.D.)

Pyrethroids interfere with nervous system function by increasing neuronal excitability. Increased excitability underlies the toxicity observed at the whole organism level following an acute pyrethroid exposure. However, changes in neuronal excitability also trigger *de novo* gene expression which may impact neuronal function. This aspect of pyrethroid toxicity has not been extensively examined. The present studies test the hypothesis that *in vivo* pyrethroid exposures, at doses surrounding the threshold for neurobehavioral effects, result in changes in gene expression in the rat cortex. In the first aim, adult rats were orally dosed with deltamethrin (DLT: 0.3, 1, 3 mg/kg), permethrin (PERM: 1, 10, 100 mg/kg) or vehicle. Frontal cortex was collected at 6 hr and global transcriptional profiles were generated. Dose-dependent changes in gene expression were identified using penalized linear and isotonic regressions. A set of altered transcripts were then confirmed by qRT-PCR. In addition, rats were dosed with either DLT (3 mg/kg), PERM (100 mg/kg) or vehicle and cortical tissue collected at 1,3,6 and 9 hr. Expression of transcripts examined by qRT-PCR in the dose-response studies were investigated in this time course cohort. Functional category analysis identified 'branching morphogenesis' as a biological process potentially sensitive to pyrethroids. This prediction was confirmed in an

in vitro model of neuronal morphogenesis. The time course of expression for *Camk1g* was further examined by qRT-PCR and Western blot. Expression of the *Camk1g1* mRNA splice variant changed in response to pyrethroids with no detectable change in *Camk1g1* protein. The second aim determined if Type I and Type II pyrethroids produce similar effects on gene transcription in the cortex. Rats were dosed with vehicle or either a Type I or Type II pyrethroid at doses that produce the same effect on an apical behavior. Cortex was sampled at 3 and 6 hr and global transcriptional profiles were generated. Qualitatively similar but quantitatively different patterns of expression between Type I and Type II pyrethroids were observed that is consistent with increases in neuronal excitability. These data contribute to a comprehensive mode-of-action model for pyrethroids.

This work is dedicated to the whole of the Harrill family for their love, support and advice for which my everlasting love and gratitude is due:

Thomas L. and Olivia Harrill
Robert A. and Mary Anne Harrill
Thomas L. Harrill, Jr. and Paula H. Yount & their loving families
Eunice L. Conway

And to Ms. Alison I. Hege, the constant source of joy and light in my life.

Acknowledgements

The author would like to thank Kevin M. Crofton, Ph.D. for his valuable mentorship during the preparation and execution of this work.

Thanks are also due to: A. Leslie Morrow, Ph.D., Lee M Graves, Ph.D., David J. Holbrook, Ph.D., Nigel Walker, Ph.D. and Fred A. Wright, Ph.D. for their input throughout the project, Chris Miller and Terry Cagle at Applied Biosystems, Inc. for help in the design and supply of the custom *Camk1g1* and *Camk1g2* qRT-PCR assays, Hongzu Ren, Ph.D., Chris Corton, Ph.D., Susan Hester, Ph.D. and Geremy Knapp for their technical expertise relating to RNA preparation, genomics applications and RNA quantification, Fred A. Wright, Ph.D., Zhen Li and Dan Gatti for their assistance with gene array data analysis, Rogelio-Tornero-Velez for pharmacokinetic modeling of the pyrethroid data, William R. Mundy, Ph.D. and Nick M. Radio, Ph.D. for work with the neuronal morphogenesis assays, Timothy J. Shafer, Ph.D., David W. Herr, Ph.D., and Mary E. Gilbert, Ph.D., for a variety of collaborations not featured in the present work, the University of North Carolina Curriculum in Toxicology, the EPA/UNC Toxicology Research Program Training Agreement (CR833237) and the National Institute of Environmental Health Science Training Grant (T32-ES07126).

Also, special thanks to Joan M. Hedge for her support during my tenure at US EPA, Marcelo J. Wolansky, Ph.D. for stimulating scientific discourse and tireless efforts towards the publication of a previous pyrethroid review article and Stephanie Padilla, Ph.D. for initiating my recruitment to Dr. Crofton's laboratory.

Table of Contents

List of Tables

List of Figures

List of Abbreviations

BIF:	bifenthrin
CYF:	cyfluthrin
CYP:	cypermethrin
DLT:	deltamethrin
EDL:	Equipotent Dose Level
FDR:	false discovery rate
GCOS:	GeneChip® Operating Software
GO:	Gene ontology
HPA:	hypothalamic-pituitary-adrenal axis
IEG:	immediate early gene
KEGG:	Kyoto encyclopedia of genes and genomes
MAP:	mitogen activated protein
mRNA:	messenger ribonucleic acid
PERM:	permethrin
PIR:	Penalized Isotonic Regression
qRT-PCR:	Quantitative Real-Time Polymerase Chain Reaction
RMA:	Robust Multi-Array Analysis
SAFE:	Significant Analysis of Function and Expression
SAM:	Significant Analysis of Microarrays
TEF:	tefluthrin
TRT:	treatment

List of Symbols

Acpl2:	acid phosphatase-like 2
Adipor:	adiponectin receptor 2
Angpt14:	angiopoietin-like 4
Arc:	activity regulated cytoskeletal-associated protein
Arhgap7:	deleted in liver cancer 1
Arrdc2:	arrestin domain containing 2
Asah3l:	N-acylsphingosine amidohydrolase 3-like
Asph:	aspartate beta-hydroxylase
Axud1:	AXIN1 up-regulated 1
B3galt3:	UDP-Gal:betaGlcNAc beta 1,3-galactosyltransferase, polypeptide 3
B3galt5:	UDP-Gal:betaGlcNAc beta 1,3-galactosyltransferase, polypeptide 5
Bag3:	BCL2-associated athanogene 3
Bcat:	branched chain aminotransferase 1, cytosolic
Bcl2l1:	Bcl2-like 1
Bcl6:	B-cell leukemia/lymphoma 6 (predicted)
Bdnf:	brain derived neurotrophic factor
Bves:	blood vessel epicardial substance
c-fos:	FBJ murine osteosarcoma viral oncogene homolog
Cables1:	Cdk5 and Abl enzyme substrate 1 (predicted)
Cacng2:	calcium channel, voltage-dependent, gamma subunit 2
Camk1g:	calcium/calmodulin-dependent protein kinase I gamma
Camk1g1:	calcium/calmodulin-dependent protein kinase I gamma 1

Camk1g2: calcium/calmodulin-dependent protein kinase I gamma 2

Cbr3: carbonyl reductase 3 (predicted)

Cebpb: CCAAT/enhancer binding protein (C/EBP), beta

Cd163: CD163 antigen (predicted)

Cdc42ep4: CDC42 effector protein (Rho GTPase binding) 4 (predicted)

Cdkn1a: cyclin-dependent kinase inhibitor 1A

Chrm4: cholinergic receptor, muscarinic 4

Clec14a: C-type lectin domain family 14, member a

Cnksr3: Cnksr family member 3

Ctrl: chymotrypsin-like

Cttnbp2nl: CTTNBP2 N-terminal like (predicted)

Cxcr4: chemokine (C-X-C motif) receptor 4

CREB: cAMP responsive element binding protein

Crh: corticotropin releasing hormone

Cryab: crystallin, alpha B

Cxcl12: chemokine (C-X-C motif) ligand 12 (stromal cell-derived factor 1)

Ddc: dopa decarboxylase (aromatic L-amino acid decarboxylase)

Degs: degenerative spermatocyte homolog 1

Dnajb5: DnaJ (Hsp40) homolog, subfamily B, member 5 (predicted)

Dusp1: dual specificity phosphatase 1

Dusp5: dual specificity phosphatase 5

Dusp6: dual specificity phosphatase 6

Dync1i1: dynein cytoplasmic 1 intermediate chain 1

Egr1: early growth response 1

Egr2: early growth response 2

Ephb3: Eph receptor B3 (predicted)

ERK: extracellular regulated MAP kinase

Errfi1: ERBB receptor feedback inhibitor 1

Ets2: v-ets erythroblastosis virus E26 oncogene homolog 2

Fbxo22: F-box only protein 22

Finb: ras responsive element binding protein 1 (predicted)

Fkbp51: FK506 binding protein 5

Fmo2: flavin containing monooxygenase 2

Fmo3: flavin containing monooxygenase 3

Fst: follistatin

Gad45b: growth arrest and DNA-damage-inducible, beta

Gfpt2: glutamine-fructose-6-phosphate transaminase 2

Gjb6: gap junction protein, beta 6, 30kDa

Gna14: guanine nucleotide binding protein, alpha 14

Gpd1: glycerol-3-phosphate dehydrogenase 1

Heatr1: HEAT repeat containing 1 (predicted)

Hes1: hairy and enhancer of split 1

Homer1: homer homolog 1

Hs3st1: heparan sulfate (glucosamine) 3-O-sulfotransferase 1

Hsp27: heat shock 27kDa protein 1

Hyal2: hyaluronoglucosaminidase 2

Hyou1:	hypoxia up-regulated 1
Id1:	inhibitor of DNA binding 1
Ier2:	immediate early response 2
Ier5:	immediate early response 5
Ier5l:	immediate early response 5-like
Igfpb3:	insulin-like growth factor binding protein 3
Il6r:	interleukin 6 receptor
Irs2:	insulin receptor substrate 2
Junb:	jun B proto-oncogene
Kcn1a:	potassium voltage-gated channel, shaker-related subfamily, member 1
Kcnf1:	potassium voltage-gated channel, subfamily F, member 1
Kcnk12:	potassium channel, subfamily K, member 12
Klf2:	Kruppel-like factor 2 (lung) (predicted)
Klf4:	Kruppel-like factor 4
Klf10:	Kruppel-like factor 10
Lcn7:	lipocalin 7
Lfng:	LFNG O-fucosylpeptide 3-beta-N-acetylglucosaminyltransferase
Lims2:	LIM and senescent cell antigen like domains 2
Lpin2:	lipin 2 (predicted)
Lrg1:	leucine-rich alpha-2-glycoprotein 1
Madh3:	MAD homolog 3
Map2k3:	mitogen activated protein kinase kinase 3
Map3k6:	mitogen-activated protein kinase kinase kinase 6 (predicted)

Max:	Max protein
Medl19:	mediator of RNA polymerase II transcription, subunit 19 homolog
MEK:	MAP kinase-ERK kinase
Mertk:	c-mer proto-oncogene tyrosine kinase
Mgl1:	macrophage galactose N-acetyl-galactosamine specific lectin 1
Midn:	midnolin (predicted)
Mkl1:	megakaryoblastic leukemia (translocation) 1
Mrc1:	mannose receptor, C type 1
Mybbp1a:	MYB binding protein (P160) 1a
Mycn:	v-myc myelocytomatosis viral related oncogene, neuroblastoma derived
Nab2:	Ngfi-A binding protein 2
Ndrg1:	N-myc downstream regulated gene 1
Nedd4l:	neural precursor cell expressed, developmentally down-regulated 4-like
Nfkbia:	nuclear factor of kappa light polypeptide gene enhancer in B-cells inhibitor, alpha
Nid67:	putative small membrane protein NID67
Nr4a1:	nuclear receptor subfamily 4, group A, member 1
Nr4a3:	nuclear receptor subfamily 4, group A, member 3
Nppc:	natriuretic peptide precursor type C
PACAP:	pituitary adenylate cyclase-activating polypeptide
Pal2g3:	phospholipase A2, group III (predicted)
Pde10a:	phosphodiesterase 10A
Pdk4:	pyruvate dehydrogenase kinase, isozyme 4
Pdlm7:	PDZ and LIM domain protein 7

Per1:	period homolog 1
Per2:	period homolog 2
Pim3:	serine/threonine-protein kinase pim-3
Pkp2:	plakophilin 2
Pld1:	phospholipase D1
Plekhf1:	pleckstrin homology domain containing, family F (with FYVE domain) member 1
Pnp1a2:	patatin-like phospholipase domain containing 2 (predicted)
Polr2c:	polymerase (RNA) II (DNA directed) polypeptide C, 33kDa
Prim2:	DNA primase, p58 subunit
Prss11:	HtrA serine peptidase 1
Prr5:	proline rich 5
Ptpru:	protein tyrosine phosphatase, receptor type, U
Pwwp2:	PWWP domain containing 2B
Pxn:	paxillin
Ralgds:	ral guanine nucleotide dissociation stimulator
Rasd1:	RAS, dexamethasone-induced 1
Rasgeflc:	RasGEF domain family, member 1C (predicted)
Rasgrp3:	RAS, guanyl releasing protein 3 (predicted)
Rassf5:	ras association (RalGDS/AF-6) domain family 5
Rbm3:	RNA binding motif (RNP1, RRM) protein 3
Ret:	ret proto-oncogene
Rimbp2:	RIMS binding protein 2

Rin3:	Ras and Rab interactor 3
Rkhd3:	ring finger and KH domain containing 3 (predicted)
Rnf39:	ring finger protein 39
Rundc1:	RUN domain containing 1 (predicted)
Sbk:	SH3-binding domain kinase 1
Sesn1:	sestrin 1 (predicted)
Sgk:	serum/glucocorticoid regulated kinase
Siat7E:	sialyltransferase 7E
Slc21a14:	solute carrier organic anion transporter family, member 1c1
Slc25a25:	solute carrier family 25 (mitochondrial carrier, phosphate carrier), member 25
Slc2a1:	solute carrier family 2 (facilitated glucose transporter), member 1
Slc39a8:	solute carrier family 39 (zinc transporter), member 8
Slc40a1:	solute carrier family 40 (iron-regulated transporter), member 1
Slc9a3r2:	solute carrier family 9 (sodium/hydrogen exchanger), member 3 regulator 2
Slit2:	slit homolog 2
Smpdl3b:	sphingomyelin phosphodiesterase, acid-like 3B
Snflk:	SNF1-like kinase
Spry4:	sprouty homolog 4 (predicted)
Spsb1:	splA/ryanodine receptor domain and SOCS box containing 1 (predicted)
Srxn1:	sulfiredoxin 1 homolog
Sstr2:	somatostatin receptor 2
Sta2:	stefin A2 (predicted)

Sult1a1:	sulfotransferase family, cytosolic, 1A, phenol-preferring, member 1
Tcfcp2l1:	transcription factor CP2-like 1
Tcfcp2l2:	transcription factor CP2-like 2
Timp3:	tissue inhibitor of metalloproteinase 3
Tiparp:	TCDD-inducible poly(ADP-ribose) polymerase (predicted)
Tmem10:	transmembrane protein 10
Tnfrsf11b:	tumor necrosis factor receptor superfamily, member 11b
Trib1:	tribbles homolog 1
Tsc22d3:	TSC22 domain family, member 3
Uae1:	urinary albumin excretion QTL 1
Usp43:	ubiquitin specific protease 43 (predicted)
Usp54:	ubiquitin specific peptidase 54
Vdac1:	voltage-dependent anion channel 1
Vgll4:	vestigial like 4
Vipr1:	vasoactive intestinal peptide receptor 1
Vwa1:	von Willebrand factor A domain containing 1
Wnt-2:	wingless-related MMTV integration site 2
Wrnip1:	Werner helicase interacting protein 1
Xkr6:	X Kell blood group precursor related family member 6 homolog
Xdh:	xanthine dehydrogenase
Zcch8:	zinc finger, CCHC domain containing 8 (predicted)
Zfp189:	zinc finger protein 189 (predicted)

Effect of Pyrethroid Insecticides on Gene Expression in the Mammalian Central Nervous System

Introductory Chapter

Joshua A. Harrill[1]

[1]University of North Carolina at Chapel Hill, Curriculum in Toxicology, CB 7270, Chapel Hill, NC 27599

I. Overview

Pyrethroids are neurotoxicants that disrupt nervous system function by interacting with membrane bound ion channels in neuronal plasma membranes. Pyrethroid induced alterations in ion channel function result in changes in neuronal firing patterns. These altered firing patterns underlie the acute symptoms of pyrethroid intoxication observed *in vivo*. At the molecular level, changes in the frequency or pattern of neuronal firing results in transcriptional induction or repression of activity-regulated genes. Changes in the expression of activity-regulated genes are an immediate response of neurons to excitatory or inhibitory stimuli and may lead to adaptive changes in the form or function of mature and developing neurons. Transient changes in gene expression can result in longer-lasting alterations in neuronal function that persist even when the excitatory stimulus (such as pharmacological excitotoxicants, i.e. a pyrethroid) is eliminated from the target tissue. To date, there is a paucity of data concerning alterations in gene expression and adaptive changes in neuronal form or function that occur downstream of the pharmacological action of pyrethroids at the neuronal membrane.

The present research was designed to test the hypothesis that *in vivo* pyrethroid exposures alter activity-regulated gene expression in neurons of the central nervous system. There were two specific aims in this research project. **Specific Aim 1 determined whether gene transcription in the rat cortex is affected by pyrethroids *in vivo*, at doses that do not produce profound symptoms of pyrethroid poisoning.** The goals of this specific aim included: 1) identifying genes that are transcriptionally induced or repressed by acute pyrethroid exposure, 2) characterization of the time course of gene expression following acute exposures, and 3) comparison of the similarities and differences in dose-

dependent gene expression patterns between a model Type I and Type II pyrethroid. A corollary hypothesis that pyrethroid exposures result in alterations in neuronal morphogenesis was also tested in light of the findings from the first phase of experimentation. Furthermore, a gene candidate believed to be driven by the pharmacological actions of pyrethroids at the neuronal membrane and linked to pyrethroid effects on neurite branching morphogenesis was further examined in the second chapter of this work**. Specific Aim 2 tested whether acute exposure to equipotent doses of multiple Type I and Type II pyrethroids *in vivo* resulted in similar alterations in gene expression patterns: i.e., is there a structure-activity relationship for the transcriptional effects of pyrethroids?** The goals under this specific aim included: 1) identification of suites of up- and down-regulated genes for each of six pyrethroids tested in an acute time course model, 2) cross compound enrichment analysis and qRT-PCR analysis of genes altered by the individual pyrethroids, and 3) exploration of gene networks commonly affected by the pyrethroid test panel.

The present data contribute to the development of a comprehensive mode-of-action model for the pyrethroids and provide insight into an aspect of pyrethroid neurotoxicology that to date remain poorly characterized.

II. Pyrethroid usage

Pyrethroids are a class of insecticides used in both agricultural and domestic applications including crop protection, household pest control, public health (i.e. head louse treatment), protection of textiles and in the control of contagious disease vectors, such as mosquitoes (Heudorf & Angerer 2001; Yanez et al. 2002). Usage of pyrethroids has increased in recent years due to the phase out of other insecticides such as organophosphates

and organochlorines (Amweg et al. 2005). Pyrethroids are now offered in a variety of commercial formulations available to ordinary consumers for use in the home. It is now estimated that approximately 80-90% percent of households in the United States use pesticides with pyrethroids comprising a considerable percentage of total use (Whyatt et al. 2003).

Increasing usage of pyrethroids, both in agricultural and domestic sectors, yields an increased likelihood of human exposure. Pyrethroids and pyrethroid metabolites have been detected in the blood of pregnant urban mothers, the urine of pesticide applicators, agricultural soil run-off, residential carpet dust, and, perhaps most importantly, in wipe samples from child-care centers (Leng et al. 1997; Whyatt et al. 2003; Colt et al. 2004; Weston et al. 2004; Tulve et al. 2006). The Food Quality Protection Act of 1996 mandates that the United States Environmental Protection Agency reexamine the established tolerances for various pesticide usages and, where necessary, consider the cumulative risk posed by exposure to multiple pesticides with same mechanism-of-action. As result, a variety of research efforts have been focused on examining the molecular mechanisms of pyrethroid toxicity and addressing data gaps critical to the establishment of a comprehensive mode-of-action model for these compounds (Soderlund et al. 2002).

III. Pyrethroid toxicity

Pyrethroids are neurotoxicants that pharmacologically alter the function of voltage-sensitive (and perhaps ligand-gated) ion channels located in the plasma membrane of neurons (Narahashi et al. 1996; Ray 2001; Soderlund et al. 2002). Figure 1.1 outlines the hypothesized mode-of-action for the acute effects of pyrethroids. Classically, pyrethroids have been divided into two types, Type I and Type II, based on chemical structure (Figure

1.2) and the acute poisoning syndromes observed in non-target species at near-lethal dose levels (Vijverberg and Van den Bercken 1990; Soderlund et al. 2002). Structurally, pyrethroids are esters of cyclopropane carboxylic acids linked to aromatic alcohols through a central ester bond (Kaneko and Miyamoto 2001). The difference in chemical structure between the two pyrethroid types is that Type II pyrethroids have an α-cyano group added to the alcohol moiety (Figure 1.2, arrow); Type I pyrethroids lack this group (Coats 1990). At high doses, the signs of acute Type I pyrethroid poisoning in the rat progress from episodes of aggressive sparring behavior and increased sensitivity to external stimuli to fine tremors followed by whole body tremors and prostration. This is known at the T-syndrome of pyrethroid poisoning. Type II pyrethroids produce a CS-syndrome characterized by increased pawing and burrowing behavior followed by profuse salivation, course whole body tremor and a 'sinuous writhing' motion known as choreoathetosis (Verschoyle and Aldridge 1980; Lawrence and Casida 1982). Acute disruption of neuronal firing within the nervous system is the underlying cause of both the Type I and Type II poisoning syndromes (Soderlund et al. 2002; Ray and Fry 2006). However, at this time the precise molecular mechanisms that underlie the divergent signs of poisoning across the two pyrethroid types are unknown.

Pharmacokinetic studies indicate that pyrethroids selectively partition into nervous system tissue from the blood due to their high lipophilicity (Ladowski 2002; Mirfazaelian et al. 2006). Accumulation of target tissue concentrations following oral exposure is rapid: i.e. brain concentrations of deltamethrin peak ~3 hr and elimination half-lives of pyrethroids range from approximately 10 – 30 hr (Ruzo et al. 1978; Anadon et al. 1991; Anadon et al. 1996; Anadon et al. 2006; Mirfazaelian et al. 2006). Metabolism of pyrethroids occurs via

oxidative cleavage of the central ester bond followed by hydroxylation of aromatic moieties (or vice versa) followed by phase II conjugation of hydroxylated products and elimination from the body (Soderlund et al. 2002). Cleavage of the central ester bound is the critical event in the deactivation of pyrethroids. Onset of the acute symptoms of pyrethroid poisoning correlate well with the accumulation of these compounds in nervous system tissue, and recover upon elimination of pyrethroid from the target tissues (Gray et al. 1980; Gray and Rickard 1982; Rickard and Brodie 1985; Kim et al. 2007).

There is no concrete evidence that pyrethroids produce significant toxicities apart from their actions in the nervous system. Some pyrethroids have been shown to have genotoxic effects in *in vitro* carcinogenesis assays (Villarini et al. 1998; Naravaneni and Jamil 2005; Undeger and Basaran 2005; Patel et al. 2006). However several two-year carcinogenicity studies in rats and mice provide little evidence of increased cancer incidence following chronic pyrethroid exposure (Parker et al. 1983; Cabral et al. 1990; Cabral and Galendo 1990). The International Agency for Research in Cancer (IARC) has concluded that there is insufficient evidence to classify pyrethroids as carcinogens (IARC 1991a, 1991b, 1991c). Nerve degeneration or the development of gross lesions either in the central or peripheral nervous system was not reported in studies of chronic pyrethroid exposures, however pyrethroid effects on neuronal microstructure (i.e. dendritic branching, number of synaptic contacts, myelination, etc.,) have not been examined.

Early research in the 1970's that characterized the T- and CS- syndromes was all conducted at extremely high (i.e. lethal) dose-levels. At administered doses below those that induce frank signs of poisoning, pyrethroids affect a number of neurobehavioral endpoints. Reviews of these behavioral effects is available in Soderlund et al. (2002) and Wolansky and

Harrill (2008). Much like the acute signs of pyrethroid poisoning, induction of these acute behavioral effects is rapid, occurring within minutes to hours following oral exposure. Currently, motor activity is the most extensively characterized behavioral endpoint affected by pyrethroids. All pyrethroids, regardless of type, produce a decrease in ambulatory motor activity (Wolansky et al. 2006). Motor activity is an apical behavior shown to be a reliable and sensitive endpoint for measuring the neurotoxicological effects of pyrethroids (Crofton and Reiter 1984; Crofton and Reiter 1988; Crofton et al. 1991; Wolansky et al. 2006; Wolansky and Harrill, 2008). Administered doses required to reach the threshold for effects on motor activity range from ~0.5 to ~120 mg/kg (depending upon the compound) and are 1.5 to 2 orders of magnitude less than reported LD_{50}'s (Wolansky et al. 2006). Effects on motor function (and other behavioral endpoints) following acute pyrethroid exposures are transient. Full recovery to control performance levels is observed in a matter of hours following an acute dose (Crofton and Reiter 1984; Peele and Crofton 1987; McDaniel and Moser, 1993).

There is a paucity of data regarding repeated low-level pyrethroid exposures on neurobehavioral endpoints. The available data argue both for and against the development of deficits in nervous system function and cognition. A thirty day repeated exposure to 6 mg/kg cismethrin and 2 mg/kg deltamethrin did not detect any cumulative effects on ambulatory motor activity in adult rats (Crofton and Reiter 1984). Likewise, Hornychova et al. (1995) did not detect any cumulative effects of supermethrin on learning and memory. On the other hand, Glowa (1986) demonstrated that a repeated exposure to 3 mg/kg deltamethrin (once a day for ten days) reduces daily pre-exposure response rates in an operant responding task and that response rates fail to return to controls levels after cessation of repeated dosing.

Additional studies are needed to clarify the effects of repeated pyrethroid exposures on nervous system function and cognition.

The actions of pyrethroids at the nerve membrane likely produce biological responses secondary to the neurotoxic effects observed in acute behavioral tests, one of which likely being changes in gene expression. In neurons, depolarizing excitatory stimuli activate intracellular signaling pathways that can trigger waves of *de novo* gene expression in the nucleus which can in turn lead to changes in the form or function of the cell (Bradley and Finkbeiner 2002; Clayton 2002; Adams and Dudek 2005). Transcription-mediated changes in neuronal function in response to excitatory stimulus may be beneficial, such as the induction of late-phase long term potentiation, a molecular correlate of learning and memory (Adams and Dudek 2005). In contrast, hyperexcitation of neuronal circuitry by a xenobiotic can lead to persistent detrimental effects on cell function as a result of *de novo* gene expression, such as during addiction to and withdrawal from drugs of abuse (Mohn et al. 2004; Nestler 2005). The acute behavioral effects of pyrethroids are driven by hyperexcitation of neuronal networks in the CNS. However, very few studies have examined the response of neurons to acute or repeated low-level pyrethroid exposure in terms of altered gene expression and changes in downstream cellular functions. The present experiments are designed to provide information on transcriptional events that occur in the brain in response to the acute pharmacological actions of pyrethroids at neuronal membranes *in vivo.* An additional benefit of this work is insight into pyrethroid-induced gene expression changes that may, in turn, lead to changes in neuronal function. An overview of the molecular mechanisms that control membrane excitability and gene expression in the adult nervous system is given below. In addition, a detailed description of the molecular and cellular

effects of pyrethroids and hypotheses on how the pharmacological actions of pyrethroids may affect adaptive gene expression in neurons is provided.

IV. Ion channel functions in the nervous system.

IVa. Molecular mechanisms of neuronal firing and synaptic communication.

In neurons, the rapid movements of Na^+, K^+ and Ca^{+2} ions across the plasma membrane are used to detect, integrate and transduce excitatory and inhibitory stimuli from post-synaptic regions of the dendritic arbor and cell soma to presynaptic axon terminals (McCormick 2003; Sheperd 2003a). Differential concentrations of ions on opposite sides of the plasma membrane establish a membrane potential, which is the molecular basis of electrical excitability in neurons (McCormick 2003). The propagation of changes in membrane potential (i.e. electrical activity) from the area of incoming dendritic synapses to outgoing axonal terminals is known as the action potential and is a key mechanism for intercellular communication in the nervous system (Sheperd 2003b). Initiation of the action potential is controlled by the selective conductance of ions through post-synaptic ionotropic neurotransmitter receptors in the dendrite or cell soma. Ion permeability through ionotropic receptors is increased by binding of their cognate neurotransmitters that are released from the pre-synaptic terminal of a neighboring neuron in response to an excitatory stimulus. The result is either an excitatory (EPSP) or inhibitory (IPSP) post-synaptic membrane potential intracellularly localized to the activated receptor complex (Byrne 2003). Two of the predominant ionotropic receptors present in neuronal networks of the cortex are excitatory glutamate receptors (both NMDA- and AMPA- subtypes) and inhibitory γ-amino butyric acid ($GABA_A$) receptor, which produce EPSPs and IPSPs, respectively (Waxham 2003). In the

dendritic tree of a single neuron, EPSPs and IPSPs are both temporally and spatially integrated to produce a change in the neuronal membrane potential (Sheperd 2003b).

Changes in membrane potential in the positive direction that reach the threshold for action potential firing result in the opening of axonal voltage-sensitive sodium channels (VSSCs), thereby allowing Na^+ to rapidly flow through the neuronal membrane and depolarize the cell. As the cell becomes more depolarized, VSSCs deactivate (terminating Na^+ conductance into the cell) and voltage-sensitive K^+ channels ("delayed rectifier channels") open. K^+ flows out of the cell to offset the net effect of Na^+ ion movement on the membrane potential. The action potential is propagated down the axon by clusters of voltage-sensitive Na^+ and K^+ channels sub-cellularly localized to patches of unmyelinated neuronal membrane (McCormick 2003). Voltage-sensitive Ca^{+2} channels (VSSCs) found in the dendrites, soma and axon terminals of neurons also contribute to changes in membrane potential with different sub-types (L-, N- and P/Q) mediating divergent intracellular events secondary to the action potential (see next section). When the action potential reaches the axon terminals, neurotransmitter filled intracellular vesicles fuse with the plasma membrane. This process is dependent upon the entry of Ca^{+2} into the cell cytoplasm via N-Type VSCCs (Schwarz 2003). Neurotransmitters then diffuse across the synaptic cleft, interact with post-synaptic receptors in neighboring cells and elicit responses such as increases in excitatory (glutamate) or inhibitory (GABA) tone in post-synaptic neurons or movement in innervated muscle cells (Deutch and Roth 2003).

The rapid, transient increases in ionic conductance that control the membrane potential and trigger neurotransmitter release are the molecular basis for intercellular communication in the CNS, both between neighboring neurons and between neurons and

innervated tissues (McCormick 2003). There is ample experimental evidence that pyrethroid insecticides interfere with the function of at least one key molecular mediator of this process, namely VSSCs. There is limited evidence that Ca^{+2} and Cl^{-} channels that contribute to the maintenance of the membrane potential are sensitive to pyrethroids (Narahashi et al. 1996; Soderlund et al. 2002; Ray et al. 2006). There is also evidence that pyrethroids may interfere with the mechanisms of neurotransmitter release independent of their actions on action potential firing. All these effects likely contribute to the neurotoxic actions of pyrethroids.

IVb. Influence of neuronal activity on gene expression.

Electrical activity at the neuronal plasma membrane is not only a mechanism of rapid intercellular communication in the nervous system but also serves as the initiating event in a number of intracellular signaling cascades that control both transient and persistent responses of the neuron to excitatory and inhibitory stimuli (Finkbeiner and Greenberg 1998; Zhang and Poo 2001; Wong and Ghosh 2002). A critical event mediating these adaptive responses is *de novo* gene expression. Gene expression leads to increased translation of effector proteins which can then modulate cell function (Clayton 2000). Gene transcription in the cell nucleus is coupled to changes in the function of membrane bound ion channels and neurotransmitter receptors through increases in the intracellular concentrations of second messenger molecules. These second messengers activate or inhibit signaling transduction pathways that terminate in the cell nucleus and affect the activity of constitutively-expressed transcription factors (Schulman and Roberts 2003; Fields et al 2005). A critical second messenger that activates such signal transduction pathways is Ca^{+2} (Schulman and Roberts 2003). Increases in intracellular Ca^{+2} concentrations ($[Ca^{+2}]_i$)can occur through a variety of mechanisms in response to changes in neuronal excitation. These include opening of

voltage-sensitive Ca^{+2} channels (VSCC) during depolarization, activation of NMDA and AMPA-type glutamate receptors in response to pre-synaptic neurotransmitter release and activation of metabotropic glutamate receptors that increase intracellular inositol-1,4,5-triphosphate (IP_3) and trigger Ca^{+2} release from intracellular stores (Larea et al. 1997; Finkbeiner and Greenberg 1998; Verkratsky 2002; Wang et al. 2004). Movement of Na^+, K^+ and Cl^- ions across the plasma membrane regulate changes in the membrane potential which controls activation of VSCCs, the release of neurotransmitters and subsequent activation of second messenger systems. Thus, even though these ions do not act directly to activate signaling cascades in the neuronal cytoplasm, they do influence the concentration of intracellular second messengers through electrical coupling of ion channels and neurotransmitter release systems.

Activity-dependent neuronal gene expression occurs regularly under normal physiological conditions in response to stimuli from the surrounding environment (Cancedda et al. 2003; Majdan and Shatz 2006; Tropea et al. 2006). However, changes in the frequency, amplitude and type of neuronal stimulation differentially affect the activation pattern of intracellular second messenger systems and may result in unique patterns of gene expression. For example, the frequency and not the duration, of increases in $[Ca^{+2}]_i$ controls the expression of the immediate-early transcription factor *c-fos* (Fields et al. 1997), some neural cell adhesion molecules (Itoh et al. 1997) and a variety of genes related to synaptic transmission, cell growth and motility (Xiang et al. 2007).

Given that alterations in neuronal firing patterns mediate the transcriptional expression of a variety of downstream effectors, it is reasonable to assume that pharmacological agents or toxicants that alter neuronal firing patterns and the excitability of

neuronal networks may, in turn, trigger alterations in gene expression. This abnormal wave of gene expression could then result in a detrimental alteration in cellular microstructure or function. As detailed below, pyrethroids interact with one (and perhaps more than one) type of membrane-bound ion channel that regulates neuronal firing patterns and excitability. Therefore, the pharmacological actions of pyrethroids may be capable of inducing alterations in cell function via the abnormal induction of activity-dependent genes. The transcriptional response of nervous system tissue, downstream of the pharmacological interactions of pyrethroids at their molecular target sites, to date, has not been thoroughly explored.

V. Molecular targets of pyrethroids.

Va. Voltage-sensitive Na^+ channels and pyrethroid effects on neuronal firing rates.

Voltage sensitive Na^+ channels (VSSCs) are considered to be the principal molecular target of pyrethroids in both target and non-target species and are the most extensively characterized sites of pyrethroid action (Narahashi 2000; Soderlund and Knipple 2003). As noted above, VSSCs open in response to changes in the neuronal membrane potential toward more positive values and deactivate as the neuron becomes depolarized. Pyrethroids affect VSSC gating kinetics by slowing inactivation. The result is increased conductance of Na^+ through VSSCs during membrane depolarization, a time when unmodified VSSCs are normally impermeable to Na^+ (Narahashi 2000). This period of abnormal Na^+ conductance is known as a Na^+ tail current. The effect of pyrethroids on Na^+ currents was first examined in invertebrate and amphibian nerve preparations (Lund and Narahashi 1981; Vijverberg et al. 1982). Further studies using heterologous expression systems (Choi and Soderlund 2006), NE-115 neuroblastoma cells (Chinn and Narahashi 1986) and primary cultures of rat dorsal root ganglia (Tatebayashi and Narahashi 1994), cerebellar Purkinje cells (Song and

Narahashi 1996) and hippocampal neurons (Motomura and Narahashi 2001) confirmed that pyrethroids induce prolonged Na^+ tail currents in mammalian VSSCs. In the mammalian CNS, seven VSSC isoforms (α-subunits) are expressed in complex overlapping patterns both with each other and with a variety of accessory proteins (β-subunits, Ogata and Ohishi 2002; Catterall 2003). The sensitivity of different VSSC α-subunits to different pyrethroids may vary and the presence of β-subunits has been demonstrated to modify pyrethroid effects on Na^+ conductance through the α-subunit channel protein (Smith & Soderlund 1998; Soderlund et al. 2002; Choi & Soderlund 2006). A comprehensive characterization of the effects of different pyrethroids on VSSCs in the brain is not available. However, the available data from different labs using a variety of cellular preparations indicate that the qualitative characteristics of VSSC modification are similar for all pyrethroids: i.e. persistent inward Na^+ tail currents occur during the period of normal channel deactivation. The duration of Na^+ tail currents (defined as a time constant of decay, τ) are variable for different compounds within the pyrethroid class, sometimes dramatically so. Typically, VSSC modification by Type I pyrethroids results in a Na^+ tail current that lasts on the order of milliseconds while Type II pyrethroids produce Na^+ tail currents that last on the order hundreds of milliseconds (Vijverberg and Van den Bercken 1990; Choi and Soderlund 2006).

The persistent Na^+ tail currents produced by pyrethroids cause the membrane potential to be slightly more positive (i.e. closer to the threshold potential for neuronal firing) than what would be observed under normal physiological conditions. A consequence of this perturbation is an increase in the frequency of neuronal depolarization in the form of repetitive firing of action potentials following an excitatory stimulus. Multiple Type I and Type II pyrethroids have been shown to induce repetitive action potentials following a single

stimulus in the *X. laevis* peripheral nervous system (Vijverberg 1982) and invertebrate giant axons (Lund and Narahashi 1981, Lund and Narahashi 1982). In mammals, repetitive firing of spinal and trigeminal reflex arcs as well as caudate nuclei of the brain has been observed in response to an excitatory stimulus (Ray 1980; Forshaw and Ray 1986). In addition, neurons from a variety of brain regions have been shown to be sensitive to pyrethroids (Tatebayashi and Narahashi 1994; Song and Narahashi 1996a; 1996b; Motomura and Narahashi 2001; Ginsburg and Narahashi 2005; Meyer et al. 2007; Shafer et al. 2008). It is likely that the acute manifestations of pyrethroid toxicity are the result of the summated effect of disrupted firing patterns at multiple neural substrates throughout the CNS. Hyperexcitation of these brain regions could also conceivably result in the induction of activity-regulated genes that affect downstream neuronal functions.

There is also evidence that the rate of spontaneous neuronal firing (action potentials that occur in the absence of stimulus) is also affected by pyrethroids. Increased rates of spontaneous action potential firing have been observed in *X. laevis* lateral-line sense organs (Vijverberg and Van den Bercken 1990). An increase in spontaneous firing is also observed in unstimulated hippocampal and cortical networks, *in vitro* (Meyer et al. 2007, Shafer – personal communication). In contrast, *in vitro* studies by Meyer et al. (2007) and Shafer et al. (2008) observe decreases in the spontaneous firing rate of glutaminergic neuronal networks derived from the rat hippocampus, cerebrocortex and spinal cord when the influence of inhibitory GABAergic inputs is removed.

The development of persistent Na^+ tail currents and subsequent changes in neuronal firing patterns is the hypothesized molecular mechanism-of-action for acute pyrethroid toxicity (Figure 1.1). As detailed above, neurons respond to increases in neuronal excitation

through the induction of *de novo* gene expression. These gene expression changes in the adult brain are meant to augment the function of specifically activated neuronal circuits in response to a sensory stimulus (Watanabe et al. 1995; Singh et al. 1997; Hendry et al. 2003; Harwell et al. 2005). Acute exposure to pyrethroids could result in non-specific, global hyperexcitability of neuronal circuits within the brain and result in the abnormal over-expression of activity-dependent adaptive gene transcripts.

While the role of changes in spontaneous firing patterns in the development of acute pyrethroid poisoning symptoms in adult animals is unknown, it is highly likely that changes in the spontaneous activity of neurons in the developing nervous system would lead to detrimental alterations in interneuronal connectivity and cell function. Early in development, neurons rely on spontaneous electrical activity to mediate the outgrowth of neuronal processes and the formation of functional synapses (Wong and Ghosh 2002). Pyrethroid-induced disruption of spontaneous activity would likely have a detrimental effect on these developmental events. It is difficult to predict the nature of these effects given the contradictory reports on spontaneous activity in developed neurons and an incomplete knowledge of how pyrethroids interact with developing neurons.

Vb. Pyrethroid effects on voltage-sensitive Ca^{+2} channels.

Pyrethroids have also been shown to interact with a number of voltage-sensitive Ca^{+2} channel (VSCC) isoforms expressed in the nervous system, however pyrethroid mediated effects on these channels are not as well characterized as effects on VSSCs and remain controversial (Shafer and Meyer 2004). VSCC effects are observed *in vitro* at pyrethroid concentrations similar to those that produce effects on Na^+ channel function (Symington et al. 2007a; 2007b). Much like VSSCs, multiple isoforms of VSCCs are expressed in the

mammalian nervous system. Different VSCC isoforms mediate different neuronal functions. $Ca_v1.3$ (L-Type) channels present on neuronal cell bodies and in dendrites mediate the neuronal membrane potential and are linked to downstream intracellular signaling cascades that mediate activity-regulated gene transcription. $Ca_v2.1$ (P/Q-Type) and $Ca_v2.2$ (N-type) mediate neurotransmitter release of axon terminals and may also influence gene transcription. The function of $Ca_v3.1$-$Ca_v3.3$ (T-Type) channels is less well known but is thought to mediate oscillatory bursts in pace-maker cells of the thalamus (Catterall et al. 2005). The pharmacological effects of only a small number of pyrethroids on VSCCs have been reported. Hildebrand et al. (2004) demonstrated that allethrin (a Type I pyrethroid) inhibited Ca^{+2} currents through rat $Ca_v1.3$ (L-Type), $Ca_v2.1$ (P/Q-Type) and $Ca_v3.1$ (T-Type) VSCCs expressed in human embryonic kidney cells. Hagiwara et al. (1988) also noted an inhibition of L- and T-Type VSCCs in cardiac node cells. More recent studies (Symington and Clark 2005; Symington and Clark 2007) have demonstrated that deltamethrin either inhibits or enhances Ca^{+2} influx through N-Type VSCCs depending on the phosphorylation state of the neuron. Shafer and Meyer (2004) have criticized this body of research and suggest a number of serious limitations, including: only *in vitro* observations, lack of concentration-response relationships, the use of indirect measures of VSCC function, and contradictory results from different laboratories/preparations. The role of VSCCs in pyrethroid toxicity is clearly controversial at this time.

As neurotransmitter release is dependent upon entry of Ca^{+2} into the neuron, indirect evaluations of VSCC function can be made based on studies of pyrethroid-induced neurotransmitter release. Previous reports using a variety of experimental models consistently demonstrate that neurotransmitter release is increased in the presence of

pyrethroids. Studies using synaptosomal preparations demonstrated increased neurotransmitter release in the presence of pyrethroids following a depolarizing stimulus (for review, see Shafer & Meyer 2004). These studies, however, did not examine the mechanisms of increased neurotransmitter release. More recent work (Symington and Clark 2005; Symington et al. 2007) also report increased Ca^{+2} entry into, and NT-release from, synaptosomes treated with deltamethrin. These effects on neurotransmitter release were abolished in the presence of ω-conotoxin MVIIC, a $Ca_v2.2$ (N-type VSCC) channel blocker, indicating that this channel mediated the effect. However, in these same studies the Type I pyrethroid cismethrin also caused increased internal Ca^{+2} concentrations, with no effects on neurotransmitter release. The authors attribute this observation to differences in the route of Ca^{+2} entry into the synaptosomes enhanced by the two compounds These observations suggest that the effects of different pyrethroids on Ca^{+2} entry may not be equivalent.

Pyrethroids have also been shown to have heterogeneous effects on neurotransmitter release *in vivo*. A series of microdialysis studies sampled the extracellular milieu of various brain regions of conscious rats treated with a variety of pyrethroids and demonstrates that: 1) different pyrethroids produce non-homologous increases or decreases in neurotransmitter-release, 2) pyrethroid-mediated effects on neurotransmitter release differ depending on brain region and type of neurotransmitter, 3) dose-dependent, biphasic effects on neurotransmitter release may occur and 4) some high dose effects on neurotransmitter release are eliminated by treatment with VSCC antagonists independent of pyrethroid actions at sodium channels (Hossain et al. 2004; Hossain et al. 2006; Hossain et al. 2008). Finally, Meyer and Shafer (2006) have reported that permethrin (a Type I pyrethroid) and not deltamethrin (a Type II pyrethroid) caused increases in neurotransmitter release independent of pyrethroid actions at

VSSCs in cultured hippocampal neurons. In total, these observations indicate that neurotransmitter release is sensitive to pyrethroids. However, the specific effects of different pyrethroids on VSCCs and neurotransmitter release are difficult to predict, may differ between compounds, and may result in divergent patterns of activity-dependent gene expression between pyrethroids following an acute exposure *in vivo*.

Vc. Pyrethroid effects on voltage-sensitive Cl^- channels.

The role of voltage-sensitive Cl^- channels in the toxicity of pyrethroids is not well understood. A decrease in the probability of opening of a Cl^- permeable, Ca^{+2}-independent voltage-sensitive anion channel has been reported for several Type II pyrethroids in NE-115 neuroblastoma cells (Burrr and Ray 2004). Entry of Cl^- into neurons through a voltage-sensitive anion channel could antagonize the effect of prolonged Na^+ entry (through VSSCs) on the membrane potential. Therefore, inhibition of Cl^- conductance by pyrethroids would enhance VSSC-mediated pyrethroid effects on membrane excitability. Type II pyrethroid actions at this channel occur *in vitro* at concentrations comparable to those that produce effects on VSSC function (Ray and Fry 2006) However, the molecular composition, physiological properties and *in vivo* expression patterns of the pyrethroid sensitive anion channel identified in NE-115 cells has not been fully characterized. Therefore, the relevance of pyrethroid effects at this molecular target *in vivo* is yet to be established. There are no known instances where Cl^- acts directly as a second messenger in the neuronal cytoplasm. It is unlikely that Cl^- entry into neurons directly activates signaling networks that control gene expression. However, Cl^- entry may antagonize activity-dependent gene expression by maintaining the membrane potential at values lower than those needed to induce entry of Ca^{+2} into the cell through voltage-sensitive Ca^{+2} channels. Antagonizing Cl^- entry, in turn,

could lead to increased activation Ca^{+2}-dependent signaling networks that control activity-dependent gene expression.

Vd. Pyrethroid effects on GABAergic receptors.

A possible role for a direct effect of pyrethroids on $GABA_A$ receptors has been vigorously investigated over the past 30 years. Inhibitory GABAergic interneurons are expressed throughout the mammalian cerebrocortex (Hof et al. 2003). These interneurons have synaptic contacts on the dendrites and cell soma of excitatory glutaminergic pyramidal neurons in the cortex. The neurotransmitter γ-amino butyric acid (GABA) is released from presynaptic terminals of interneurons, diffuses across the synaptic cleft, binds to postsynaptic $GABA_A$ receptors and triggers Cl^- entry into the postsynaptic neuron. This leads to hyperpolarization of the postsynaptic neuron and an overall decrease in neuronal excitability.

Radioligand binding experiments have demonstrated that Type II pyrethroids displace [^{35}S]TBPS from the picrotoxin binding site of $GABA_A$ receptors *in vitro* (Lawrence and Casida, 1983; Lawrence et al. 1985; Crofton et al. 1987; Lummis et al. 1987; Olsen et al. 1989). Type I pyrethroids do not display this activity (Crofton et al. 1987). Displacement of $GABA_A$ receptor ligands by Type II pyrethroids occurs at concentrations much higher (> 3 orders of magnitude) than those required to produce effects on VSSC-mediated Na^+ currents and actual blockade of Cl^- influx was observed at even higher concentrations (Lawrence et al. 1985; Abalis 1986; Ray and Fry 2006). In contrast, some studies did not detect any modification of $GABA_A$-mediated chloride conductance in the presence of Type II pyrethroids (Ogata et al. 1988). An argument against $GABA_A$ receptor antagonism as a mechanism of pyrethroid toxicity *in vivo* is demonstrated by the studies of Gilbert et al. (1989), Joy et al. (1990) and Joy and Albertson (1991). These studies did not detect any

pyrethroid-mediated modulation of $GABA_A$ function in a pair-pulsed stimulus paradigm at high doses, but in fact observed the opposite of the predicted effect (i.e., reduced inhibition of neuronal activity) for only some high doses of the pyrethroids tested. All of these data indicate that an alteration in $GABA_A$ receptor function by pyrethroids does not occur at tissue concentrations comparable to those that produce effects on VSSC function. However, they do not exclude the possibility that antagonism (or agonism) of $GABA_A$ receptor function occurs at high administered doses of pyrethroids and contributes the divergent poisoning symptoms produced by the two different pyrethroid classes (Crofton and Reiter 1987). Given these findings, it is equally unlikely that a direct pharmacological action of pyrethroids at the $GABA_A$ receptor complex would contribute to alterations in activity-dependent gene expression patterns *in vivo* at administered doses that do not cause profound signs of pyrethroid poisoning.

VI. Pyrethroid effects on gene expression.

As noted above, modulation of VSSC or VSCC function and neurotransmitter release by pyrethroids provides several mechanisms whereby these compounds may influence activity-regulated gene expression in a neuron. Based on the pharmacological actions of pyrethroids, it can be hypothesized that these compounds cause changes in activity-regulated gene expression by altering the intracellular concentration of second messengers (i.e. Ca^{+2}) that initiate and mediate activity-regulated transcription in the nucleus. This may occur via three distinct mechanisms. First, pyrethroids may interact with a molecular target site, such as VSCCs, that directly controls the pattern and duration of transient intracellular Ca^{+2} concentrations. Second, pyrethroids may indirectly increase the intracellular levels of Ca^{+2} by enhancing Na^+ influx (or blocking Cl^- influx), which depolarizes the membrane potential

and triggers activation of Ca^{+2} channels and Ca^{+2} entry. Lastly, pyrethroids may increase neurotransmitter release by producing repetitive firing patterns in presynaptic neurons, thereby simulating or inhibiting the excitatory state of post-synaptic neurons and activating multiple intracellular second messenger systems via neurotransmitter receptor stimulation. Based on the available data, the concentrations required to pharmacologically alter the function of the VSSC, VSCC and Cl- channel types are very similar (Ray and Fry 2006). This means that all of the pharmacological actions may be occurring simultaneously in an integrated neuronal circuit affected by pyrethroids.

This multitude of pharmacological actions, combined with the inherent complexity of intracellular signaling pathways known to control activity-regulated gene expression and an incomplete knowledge of the genes that may be affected by alterations in neuronal activity, make predictions regarding the effects of pyrethroids on gene expression and intracellular signaling extremely difficult. An experimental approach that empirically identifies and characterizes the transcriptional response of the nervous system to pyrethroids *in vivo* serves as a starting point for the systematic examination the complex intracellular events affected by the integrated pharmacological actions of pyrethroids at the neuronal membrane. The overall framework for this molecular approach is to define gene expression changes that occur in response to pyrethroids *in vivo*, validate these changes in an *in vitro* model of functioning neuronal networks, and use pharmacological tools and biochemical manipulations to determine which molecular actions of the pyrethroids are mediating the response. **The experiments conducted in the present study are designed to address the first component of this frame-work: i.e. the identification of activity-regulated gene expression changes**

***in vivo*.** An additional benefit of this work is insight into potential changes in neuronal form or function that may occur downstream of pyrethroid effects on neuronal activity.

Previous research provides limited evidence that acute pyrethroid exposure alters the expression of some genes in the central nervous system. Hassouna et al. (1996) observed increases in *c-fos* and *JunB* immunoreactivity in multiple brain regions of Sprague-Dawley rats several hours after a single i.p. treatment with either permethrin or cypermethrin. In addition, Imamura et al. (2006) reported increased expression of brain-derived neurotrophic factor (*Bdnf*) in the cortex of rats acutely exposed to deltamethrin. *Bdnf, c-fos* and *JunB* are all immediate early genes (IEGs) whose expression is known to correlate with excitatory activation of neuronal circuits (Herdegen and Leah 1998; Fukuchi et al. 2005). Together, these data provide evidence that one of the responses of nervous system tissue *in vivo* to pyrethroid exposure is an upregulation in the expression of genes controled by neuronal activity.

In addition, changes in the expression of neurotransmitter synthesis and transport machinery have been observed following pyrethroid exposure. Studies by Gillette et al. (2003) and Elwan et al. (2006) report an upregulation of the striatal dopamine transporter following repeated i.p. exposure to permethrin and deltamethrin. In the Elwan et al. (2006) study increased expression was coupled with increased transporter activity. Furthermore, Liu et al. (2006) report decreases in tyrosine hydroxylase, the penultimate enzyme in monoaminergic NT synthesis, following ten days of deltamethrin exposure. This change in expression was coupled with a decrease in dopamine content. The relationship of these gene expression changes to pyrethroid-induced effects on neuronal firing is unknown. However, these data demonstrate that gene expression changes in response to pyrethroids can lead to

persistent alterations in neuronal function. Given these data, gene expression changes induced by pyrethroids should be included in a comprehensive mode-of-action model describing the toxicity of these compounds. However, there is currently a lack of data concerning this aspect of pyrethroid neurotoxicity.

VII. Hypothesis and goals.

The present research was designed to test **the hypothesis that *in vivo* pyrethroid exposures result in changes in activity-regulated gene expression in neurons of the central nervous system.** There were two specific aims in this research project. **Specific Aim 1 determined whether gene transcription in the rat cortex is affected by pyrethroids *in vivo*, at doses that do not produce profound symptoms of pyrethroid poisoning.** The goals of this specific aim included: 1) identifying genes that are transcriptionally induced or repressed by acute pyrethroid exposure, 2) characterization of the time course of gene expression following acute exposures, and 3) comparison of the similarities and differences in dose-dependent gene expression patterns between a representative Type I and Type II pyrethroid.

A corollary hypothesis that pyrethroid exposures result in alterations in neuronal morphogenesis was also tested in light of the findings from the first phase of experimentation. Furthermore, a gene candidate believed to be driven by the pharmacological actions of pyrethroids at the neuronal membrane and linked to pyrethroid effects on neurite branching morphogenesis was further examined in the second chapter of this work**.**

Specific Aim 2 tested whether acute exposure to equipotent doses of multiple Type I and Type II pyrethroids *in vivo* resulted in similar alterations in gene expression

patterns: i.e., is there a structure-activity relationship for the transcriptional effects of pyrethroids? The goals under this specific aim included: 1) identification of suites of up- and down-regulated genes for each of six pyrethroids tested in an acute time course model, 2) cross compound enrichment analysis and qRT-PCR analysis of genes altered by the individual pyrethroids, and 3) exploration of gene networks commonly affected by the pyrethroid test panel.

The present data contribute to the development of a comprehensive mode-of-action model for the pyrethroids and provide insight into an aspect of pyrethroid neurotoxicology that to date remain poorly characterized.

VIII. Experimental design.

Throughout the duration of this work an acute *in vivo* dosing paradigm was used to examine pyrethroid effects on gene expression. The acute exposure model was selected for a variety of reasons. First, the most extensively characterized, quantitative measures of pyrethroid toxicity are behaviors that have been examined using an acute dosing paradigm (see section 1 above and Wolansky et al. 2006). The present studies use exactly the same dosing conditions (species, strain, sex, age, route, vehicle and delivery volume) as used in these evaluations of acute toxicity in order to provide a reliable dose-metric with which to compare equipotent doses of pyrethroids and neurotoxic effect thresholds. In addition, extensive pharmacokinetic models for the test compounds used in the first chapter of this work (i.e. deltamethrin and permethrin) have been developed based in acute oral dosing studies (Mirfazaelian et al. 2006; Tornero-Velez et al. 2007). Estimates of the time-to-peak tissue concentrations and elimination half-lives in the brain helped guide the selection of time points used in the *in vivo* portion of these studies. Estimates of brain concentrations from

these models were also used to compare *in vivo* results to *in vitro* functional assays. Toxicological and pharmacokinetic profiles for sub-chronic or repeated dosing schedules with pyrethroids are not as extensively characterized as the acute dosing paradigms. Therefore, comparisons of relative potency or estimations of tissue dosimetry could not be made with a great deal of confidence if a repeated dosing schedule was used.

In the second chapter of this work high-throughput oligonucleotide microarrays are used for the identification of pyrethroid-sensitive genes and comparison of the global transcriptional responses of the rat frontal cortex between two "model" pyrethroids, deltamethrin (Type II) and permethrin (Type I). The frontal cortex was selected as the tissue of interest as previous studies have demonstrated increases in activity-regulated gene transcripts and disruption of neuronal firing patterns *in vivo* in this region of the brain following acute pyrethroid exposure (Ray 1980; Hassouna et al. 1996; Wu and Liu 2003). Linear and isotonic regression models (Tusher et al. 2002; Hu et al. 2005) were used to identify dose-dependent gene expression changes and thresholds for effects. For a select number of transcripts, gene expression changes are confirmed by qRT-PCR. In addition, an *in vitro* growth assay is used to examine a potentially neurotoxic effect of pyrethroids on neuronal morphology that was identified during functional category level analysis of microarray data. These *in vitro* data demonstrate that exposure to pyrethroids can stimulate abnormal changes in neuronal morphology, and also indicates that pyrethroids may act as developmental neurotoxicants.

Chapter Three focused on characterizing transcriptional and translational upregulation of Ca^{+2}/calmodulin-dependent protein kinase 1-gamma (*Camk1g*) by pyrethroids. *Camk1g* was identified in Chapter Two as a reliable indicator of pyrethroid exposure. Previous

studies in the literature indicated that this protein can mediate neuronal branching and growth and is transcriptionally regulated by changes in neuronal excitability. Increased expression of *Camk1g* was identified and confirmed in the initial dose-response microarray study. Subsequent qRT-PCR analysis demonstrates that the Ca^{+2}-sensitive splice variant of *Camk1g* (i.e. *Camk1g1*) is upregulated by pyrethroids whereas the Ca^{+2}-insensitive splice variant of *Camk1g* (*Camk1g2*) is not. These results support a role for Ca^{+2} in the acute toxicity of pyrethroids.

Chapter Four expands upon the results of Chapter Two by comparing global gene expression profiles from the cortex of rats exposed to equipotent doses of either permethrin, bifenthrin or tefluthrin (Type I pyrethroids) or deltamethrin, cypermethrin or cyfluthrin (Type II compounds). Equipotent doses were once again based on the results of Wolansky et al. (2006). The LIMMA (Linear Models for Microarray Data) analysis method was used to detect treatment related changes in gene expression for each of the individual compounds (Smyth 2005). Suites of altered transcripts for each individual compound were then tested for enrichment in the expression profiles of other pyrethroids in the test panel using the SAFE algorithm (Barry et al. 2005). SAFE was also used to examine enrichment of GO categories and KEGG pathways in each compound in the test panel. Finally Igenuity® pathway analysis was used to construct a gene regulatory network commonly affected by the Type II pyrethroids in the test panel. Chapter Five summarizes the major findings, implications, and future directions of this work.

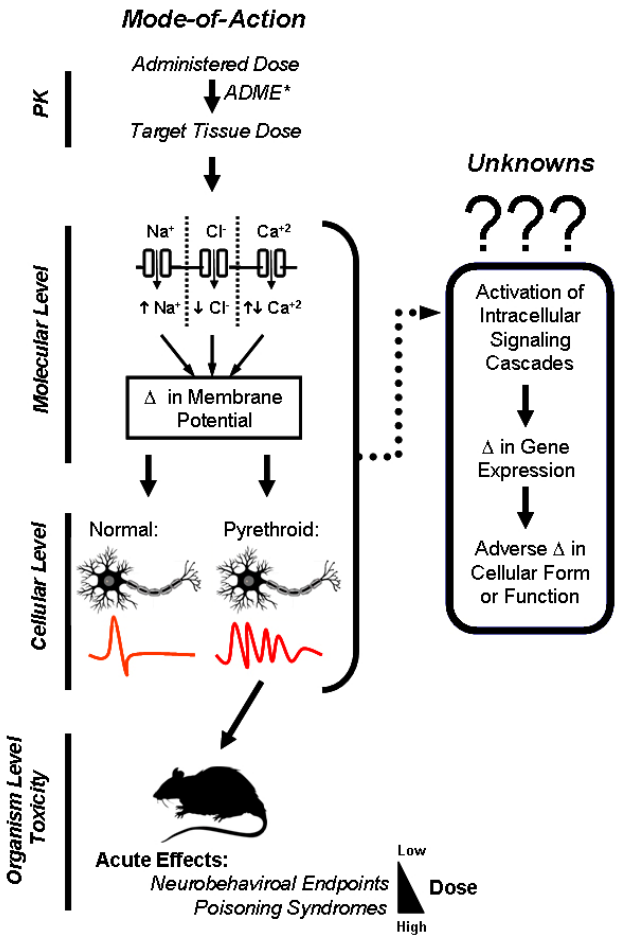

Figure 1.1. ***Mode-of-action for the acute effects of pyrethroids.*** The sequence outlined on the left of the figure corresponds to the sequential events leading from pyrethroid exposure to acute toxicity. Following an administered dose of pyrethroids accumulation of a target tissue (i.e. brain) dose occurs and is controlled by absorption, distribution, metabolism and elimination rates intrinsic to the system. In the target tissue, pyrethroids interact with a variety of voltage-sensitive ion channels, primarily voltage-sensitive sodium channels, which impact the membrane potential. Under normal physiological conditions an excitatory stimulus results in the firing of a single action potential as a means of intracellular communication in the nervous system. In presence of pyrethroids, a repetitive firing of the action potential is produced which leads to acute adverse effects at the behavioral level. These adverse effects range from mild effects on neurobehavioral endpoints such as ambulatory motor activity at low doses to profound signs of poisoning at high doses. The right side of the figure lists data gaps in the comprehensive mode-of-action of pyrethroids. Changes in voltage-sensitive ion channel function and membrane excitability can lead to subsequent changes in gene expression and adaptive or adverse changes in cellular form or function. To date, these types of effects have not been extensively characterized for pyrethroids.

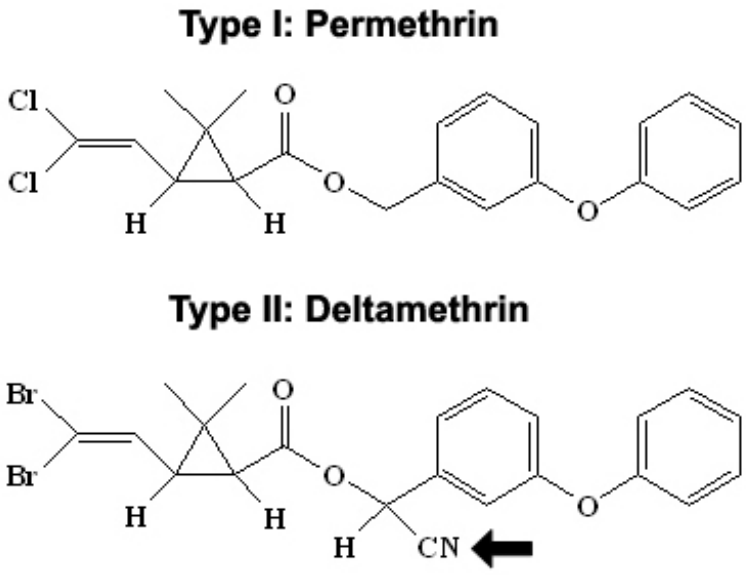

Figure 1.2. ***Examples of pyrethroid chemical structures.*** Chemical structures of the Type I pyrethroid permethrin (top) and the Type II pyrethroid deltamethrin (bottom). A primary structural difference between the two types is the presence or absence of an α-cyano group on the alcohol moiety of the compound (arrow). The two compounds are used in Chapters 2 and 3 of the present work.

Works Cited

Abalis I. M., Eldefrawi M. E. and Eldefrawi A. T. (1986) Effects of insecticides on GABA-induced chloride influx into rat brain microsacs. *J Toxicol Environ Health* **18**, 13-23.

Adams J. P. and Dudek S. M. (2005) Late-phase long-term potentiation: getting to the nucleus. *Nat Rev Neurosci* **6**, 737-43.

Amweg E. L., Weston D. P. and Ureda N. M. (2005) Use and toxicity of pyrethroid pesticides in the Central Valley, California, USA. *Environ Toxicol Chem* **24**, 966-72.

Anadon A., Martinez-Larranaga M. R., Diaz M. J. and Bringas P. (1991) Toxicokinetics of permethrin in the rat. *Toxicol Appl Pharmacol* **110**, 1-8.

Anadon A., Martinez-Larranaga M. R., Fernandez-Cruz M. L., Diaz M. J., Fernandez M. C. and Martinez M. A. (1996) Toxicokinetics of deltamethrin and its 4'-HO-metabolite in the rat. *Toxicol Appl Pharmacol* **141**, 8-16.

Anadon A., Martinez M., Martinez M. A., Diaz M. J. and Martinez-Larranaga M. R. (2006) Toxicokinetics of lambda-cyhalothrin in rats. *Toxicol Lett* **165**, 47-56.

Bradley J. and Finkbeiner S. (2002) An evaluation of specificity in activity-dependent gene expression in neurons. *Prog Neurobiol* **67**, 469-77.

Burr S. A. and Ray D. E. (2004) Structure-activity and interaction effects of 14 different pyrethroids on voltage-gated chloride ion channels. *Toxicol Sci* **77**, 341-6.

Byrne J. H. (2003) Postsynaptic potentials and synaptic intergration. In *Fundamental Neuroscience, Second Edition* (Edited by Squire L. R., Bloom F. E., McConnell S. K., Roberts J. L., Spitzer N. C. and Zigmond M. J.), p. 299-317. Academic Press, New York.

Cancedda L., Putignano E., Impey S., Maffei L., Ratto G. M. and Pizzorusso T. (2003) Patterned vision causes CRE-mediated gene expression in the visual cortex through PKA and ERK. *J Neurosci* **23**, 7012-20.

Catterall W. A., Perez-Reyes E., Snutch T. P. and Striessnig J. (2005) International Union of Pharmacology. XLVIII. Nomenclature and structure-function relationships of voltage-gated calcium channels. *Pharmacol Rev* **57**, 411-25.

Catterall W. A., Striessnig J., Snutch T. P. and Perez-Reyes E. (2003) International Union of Pharmacology. XL. Compendium of voltage-gated ion channels: calcium channels. *Pharmacol Rev* **55**, 579-81.

Chinn K. and Narahashi T. (1986) Stabilization of sodium channel states by deltamethrin in mouse neuroblastoma cells. *J Physiol* **380**, 191-207.

Choi J. S. and Soderlund D. M. (2006) Structure-activity relationships for the action of 11 pyrethroid insecticides on rat Na v 1.8 sodium channels expressed in Xenopus oocytes. *Toxicol Appl Pharmacol* **211**, 233-44.

Clayton D. F. (2000) The genomic action potential. *Neurobiol Learn Mem* **74**, 185-216.

Coats J. R. (1990) Mechanisms of toxic action and structure-activity relationships for organochlorine and synthetic pyrethroid insecticides. *Environ Health Perspect* **87**, 255-62.

Colt J. S., Lubin J., Camann D., Davis S., Cerhan J., Severson R. K., Cozen W. and Hartge P. (2004) Comparison of pesticide levels in carpet dust and self-reported pest treatment practices in four US sites. *J Expo Anal Environ Epidemiol* **14**, 74-83.

Crofton K. M., Howard J. L., Moser V. C., Gill M. W., Reiter L. W., Tilson H. A. and MacPhail R. C. (1991) Interlaboratory comparison of motor activity experiments: implications for neurotoxicological assessments. *Neurotoxicol Teratol* **13**, 599-609.

Crofton K. M. and Reiter L. W. (1984) Effects of two pyrethroid insecticides on motor activity and the acoustic startle response in the rat. *Toxicol Appl Pharmacol* **75**, 318-28.

Crofton K. M. and Reiter L. W. (1987) Pyrethroid insecticides and the gamma-aminobutyric acidA receptor complex: motor activity and the acoustic startle response in the rat. *J Pharmacol Exp Ther* **243**, 946-54.

Crofton K. M. and Reiter L. W. (1988) The effects of type I and II pyrethroids on motor activity and the acoustic startle response in the rat. *Fundam Appl Toxicol* **10**, 624-34.

Crofton K. M., Reiter L. W. and Mailman R. B. (1987) Pyrethroid insecticides and radioligand displacement from the GABA receptor chloride ionophore complex. *Toxicol Lett* **35**, 183-90.

Deutch A. Y. and Roth R. H. (2003) Neurotransmitters. In *Fundamental Neuroscience, Second Edition* (Edited by Squire L. R., Bloom F. E., McConnell S. K., Roberts J. L., Spitzer N. C. and Zigmond M. J.), p. 163-196. Academic Press, New York.

Elwan M. A., Richardson J. R., Guillot T. S., Caudle W. M. and Miller G. W. (2005) Pyrethroid pesticide-induced alterations in dopamine transporter function. *Toxicol Appl Pharmacol*.

Fields R. D., Eshete F., Stevens B. and Itoh K. (1997) Action potential-dependent regulation of gene expression: temporal specificity in ca2+, cAMP-responsive element binding proteins, and mitogen-activated protein kinase signaling. *J Neurosci* **17**, 7252-66.

Fields R. D., Lee P. R. and Cohen J. E. (2005) Temporal integration of intracellular Ca2+ signaling networks in regulating gene expression by action potentials. *Cell Calcium* **37**, 433-42.

Finkbeiner S. and Greenberg M. E. (1998) Ca2+ channel-regulated neuronal gene expression. *J Neurobiol* **37**, 171-89.

Fukuchi M., Tabuchi A. and Tsuda M. (2005) Transcriptional regulation of neuronal genes and its effect on neural functions: cumulative mRNA expression of PACAP and BDNF genes controlled by calcium and cAMP signals in neurons. *J Pharmacol Sci* **98**, 212-8.

Gilbert M. E., Mack C. M. and Crofton K. M. (1989) Pyrethroids and enhanced inhibition in the hippocampus of the rat. *Brain Res* **477**, 314-21.

Gillette J. S. and Bloomquist J. R. (2003) Differential up-regulation of striatal dopamine transporter and alpha-synuclein by the pyrethroid insecticide permethrin. *Toxicol Appl Pharmacol* **192**, 287-93.

Glowa J. R. (1986) Acute and sub-acute effects of deltamethrin and chlordimeform on schedule-controlled responding in the mouse. *Neurobehav Toxicol Teratol* **8**, 97-102.

Harwell C., Burbach B., Svoboda K. and Nedivi E. (2005) Regulation of cpg15 expression during single whisker experience in the barrel cortex of adult mice. *J Neurobiol* **65**, 85-96.

Hassouna I., Wickert H., el-Elaimy I., Zimmermann M. and Herdegen T. (1996) Systemic application of pyrethroid insecticides evokes differential expression of c-Fos and c-Jun proteins in rat brain. *Neurotoxicology* **17**, 415-31.

Hendry S. H., Hsiao S. S. and Brown M. C. (2003) Fundamentals of sensory systems. In *Fundamental Neuroscience, Second Edition* (Edited by Squire L. R., Bloom F. E., McConnell S. K., Roberts J. L., Spitzer N. C. and Zigmond M. J.), p. 577-589. Academic Press, New York.

Herdegen T. and Leah J. D. (1998) Inducible and constitutive transcription factors in the mammalian nervous system: control of gene expression by Jun, Fos and Krox, and CREB/ATF proteins. *Brain Res Brain Res Rev* **28**, 370-490.

Heudorf U., Angerer J. and Drexler H. (2004) Current internal exposure to pesticides in children and adolescents in Germany: urinary levels of metabolites of pyrethroid and organophosphorus insecticides. *Int Arch Occup Environ Health* **77**, 67-72.

Hildebrand M. E., McRory J. E., Snutch T. P. and Stea A. (2004) Mammalian voltage-gated calcium channels are potently blocked by the pyrethroid insecticide allethrin. *J Pharmacol Exp Ther* **308**, 805-13.

Hof P. R., Trapp B. D., De Vellis J., Claudio L. and Colman D. R. (2003) Cellular Components of Nervous Tissue. In *Fundamental Neuroscience, Second Edition* (Edited by Squire L. R., Bloom F. E., McConnell S. K., Roberts J. L., Spitzer N. C. and Zigmond M. J.), p. 49-75. Academic Press, New York.

Hornychova M., Frantik E., Kubat J. and Formanek J. (1995) Neurotoxicity profile of supermethrin, a new pyrethroid insecticide. *Cent Eur J Public Health* **3**, 210-8.

Hossain M. M., Suzuki T., Sato I., Takewaki T., Suzuki K. and Kobayashi H. (2004) The modulatory effect of pyrethroids on acetylcholine release in the hippocampus of freely moving rats. *Neurotoxicology* **25**, 825-33.

Hossain M. M., Suzuki T., Sato I., Takewaki T., Suzuki K. and Kobayashi H. (2005) Neuromechanical effects of pyrethroids, allethrin, cyhalothrin and deltamethrin on the cholinergic processes in rat brain. *Life Sci* **77**, 795-807.

Hossain M. M., Suzuki T., Unno T., Komori S. and Kobayashi H. (2008) Differential presynaptic actions of pyrethroid insecticides on glutamatergic and GABAergic neurons in the hippocampus. *Toxicology* **243**, 155-63.

Hu J., Kapoor, M., Zhang, W., Hamilton, S.R., Coombes, K.R. (2005) Analysis of dose-response effects on gene expression data with comparison of two microarray platforms. *Bioinformatics* **21**, 3524-3529.

Imamura L., Yasuda M., Kuramitsu K., Hara D., Tabuchi A. and Tsuda M. (2006) Deltamethrin, a pyrethroid insecticide, is a potent inducer for the activity-dependent gene expression of brain-derived neurotrophic factor in neurons. *J Pharmacol Exp Ther* **316**, 136-43.

Itoh K., Ozaki M., Stevens B. and Fields R. D. (1997) Activity-dependent regulation of N-cadherin in DRG neurons: differential regulation of N-cadherin, NCAM, and L1 by distinct patterns of action potentials. *J Neurobiol* **33**, 735-48.

Joy R. M. and Albertson T. E. (1991) Interactions of GABAA antagonists with deltamethrin, diazepam, pentobarbital, and SKF100330A in the rat dentate gyrus. *Toxicol Appl Pharmacol* **109**, 251-62.

Joy R. M., Lister T., Ray D. E. and Seville M. P. (1990) Characteristics of the prolonged inhibition produced by a range of pyrethroids in the rat hippocampus. *Toxicol Appl Pharmacol* **103**, 528-38.

Kaneko H. (2001) Pyrethroid Chemistry and Metabolism. In *Handbook of Pesticide Toxicology* (Edited by Krieger R. I.), Vol. 2, p. 1263-1288. Academic Press, San Diego, CA.

Kim K. B., Anand S. S., Muralidhara S., Kim H. J. and Bruckner J. V. (2007) Formulation-dependent toxicokinetics explains differences in the GI absorption, bioavailability and acute neurotoxicity of deltamethrin in rats. *Toxicology* **234**, 194-202.

Laskowski D. A. (2002) Physical and chemical properties of pyrethroids. *Rev Environ Contam Toxicol* **174**, 49-170.

Lawrence L. J. (1982) Pyrethroid toxicology: mouse intracerebral structure-toxicity relationships. *Pesticide Biochemistry and Physiology* **18**, 9-14.

Lawrence L. J. and Casida J. E. (1983) Stereospecific action of pyrethroid insecticides on the gamma-aminobutyric acid receptor-ionophore complex. *Science* **221**, 1399-401.

Lawrence L. J., Gee K. W. and Yamamura H. I. (1985) Interactions of pyrethroid insecticides with chloride ionophore-associated binding sites. *Neurotoxicology* **6**, 87-98.

Leng G., Kuhn K. H. and Idel H. (1997) Biological monitoring of pyrethroids in blood and pyrethroid metabolites in urine: applications and limitations. *Sci Total Environ* **199**, 173-81.

Lerea L. S. (1997) Glutamate receptors and gene induction: signalling from receptor to nucleus. *Cell Signal* **9**, 219-26.

Liu G. P., Ma Q. and Shi N. (2006) Tyrosine hydroxylase as a target for deltamethrin in the nigrostriatal dopaminergic pathway. *Biomed Environ Sci* **19**, 27-34.

Liu G. P. and Shi N. (2006) The inhibitory effects of deltamethrin on dopamine biosynthesis in rat PC12 cells. *Toxicol Lett* **161**, 195-9.

Lummis S. C., Chow S. C., Holan G. and Johnston G. A. (1987) gamma-Aminobutyric acid receptor ionophore complexes: differential effects of deltamethrin, dichlorodiphenyltrichloroethane, and some novel insecticides in a rat brain membrane preparation. *J Neurochem* **48**, 689-94.

Lund A. E. and Narahashi T. (1981) Modification of sodium channel kinetics by the insecticide tetramethrin in crayfish giant axons. *Neurotoxicology* **2**, 213-29.

Lund A. E. and Narahashi T. (1982) Dose-dependent interaction of the pyrethroid isomers with sodium channels of squid axon membranes. *Neurotoxicology* **3**, 11-24.

Majdan M. and Shatz C. J. (2006) Effects of visual experience on activity-dependent gene regulation in cortex. *Nat Neurosci* **9**, 650-9.

McCormick D. A. (2003) Membrane potential and action potential. In *Fundamental Neuroscience, Second Edition* (Edited by Squire L. R., Bloom F. E., McConnell S. K., Roberts J. L., Spitzer N. C. and Zigmond M. J.). Academic Press, New York.

McDaniel K. L. and Moser V. C. (1993) Utility of a neurobehavioral screening battery for differentiating the effects of two pyrethroids, permethrin and cypermethrin. *Neurotoxicol Teratol* **15**, 71-83.

Meyer D. A. and Shafer T. J. (2006) Permethrin, but not deltamethrin, increases spontaneous glutamate release from hippocampal neurons in culture. *Neurotoxicology* **27**, 594-603.

Meyer, D. A., Carter, J. M., Johnstone, A. F., and Shafer, T. J. (2008). Pyrethroid modulation of spontaneous neuronal excitability and neurotransmission in hippocampal neurons in culture. *Neurotoxicology* **29**, 213-25.

Mirfazaelian A., Kim K. B., Anand S. S., Kim H. J., Tornero-Velez R., Bruckner J. V. and Fisher J. W. (2006) Development of a physiologically based pharmacokinetic model for deltamethrin in the adult male Sprague-Dawley rat. *Toxicol Sci* **93**, 432-42.

Mohn A. R., Yao W. D. and Caron M. G. (2004) Genetic and genomic approaches to reward and addiction. *Neuropharmacology* **47 Suppl 1**, 101-10.

Motomura H. and Narahashi T. (2001) Interaction of tetramethrin and deltamethrin at the single sodium channel in rat hippocampal neurons. *Neurotoxicology* **22**, 329-39.

Narahashi T. (1996) Neuronal ion channels as the target sites of insecticides. *Pharmacol Toxicol* **79**, 1-14.

Narahashi T. (2000) Neuroreceptors and ion channels as the basis for drug action: past, present, and future. *J Pharmacol Exp Ther* **294**, 1-26.

Nestler E. J. (2005) Is there a common molecular pathway for addiction? *Nat Neurosci* **8**, 1445-9.

Ogata N. and Ohishi Y. (2002) Molecular diversity of structure and function of the voltage-gated Na+ channels. *Jpn J Pharmacol* **88**, 365-77.

Ogata N., Vogel S. M. and Narahashi T. (1988) Lindane but not deltamethrin blocks a component of GABA-activated chloride channels. *Faseb J* **2**, 2895-900.

Olsen R. W., Szamraj O. and Miller T. (1989) t-[35S]butylbicyclophosphorothionate binding sites in invertebrate tissues. *J Neurochem* **52**, 1311-8.

Peele D. B. and Crofton K. M. (1987) Pyrethroid effects on schedule-controlled behavior: time and dosage relationships. *Neurotoxicol Teratol* **9**, 387-94.

Ray D. E. (1980) An EEG investigation of decamethrin-induced choreoathetosis in the rat. *Exp Brain Res* **38**, 221-7.

Ray D. E. (2001) Pyrethroid Insecticides: Mechanisms of Toxicity, Systematic Poisoning Syndromes, Parethesia, and Therapy. In *Handbook of Pesticide Toxicology* (Edited by Krieger R. I.), Vol. 2, p. 1289-1303. Academic Press, San Diego, CA.

Ray D. E. and Fry J. R. (2006) A reassessment of the neurotoxicity of pyrethroid insecticides. *Pharmacol Ther* **111**, 174-93.

Ruzo L. O., Unai T. and Casida J. E. (1978) Decamethrin metabolism in rats. *J Agric Food Chem* **26**, 918-25.

Schulman H. and Roberts J. L. (2003) Intracellular Signaling. In *Fundamental Neuroscience, Second Edition* (Edited by Squire L. R., Bloom F. E., McConnell S. K., Roberts J. L., Spitzer N. C. and Zigmond M. J.), p. 259-297. Academic Press, New York.

Shafer T. J. and Meyer D. A. (2004) Effects of pyrethroids on voltage-sensitive calcium channels: a critical evaluation of strengths, weaknesses, data needs, and relationship to assessment of cumulative neurotoxicity. *Toxicol Appl Pharmacol* **196**, 303-18.

Shafer, T. J., Rijal, S. O., and Gross, G. W. (2008). Complete inhibition of spontaneous activity in neuronal networks in vitro by deltamethrin and permethrin. *Neurotoxicology* **29**, 203-12.

Shepard G. M. (2003a) Electrotonic properties of axons and dendrites. In *Fundamental Neuroscience, Second Edition* (Edited by Squire L. R., Roberts J. L., Spitzer N. C., Zigmond M. J., McConnell S. K. and Bloom F. E.), p. 115-137. Academic Press, New York.

Shepard G. M. (2003b) Information processing in complex dendrites. In *Fundamental Neuroscience, Second Edition* (Edited by Squire L. R., Roberts J. L., Spitzer N. C., Zigmond M. J., McConnell S. K. and Bloom F. E.), p. 319-337. Academic Press, New York.

Singh T. D., Mizuno K., Kohno T. and Nakamura S. (1997) BDNF and trkB mRNA expression in neurons of the neonatal mouse barrel field cortex: normal development and plasticity after cauterizing facial vibrissae. *Neurochem Res* **22**, 791-7.

Smith T. J. and Soderlund D. M. (1998) Action of the pyrethroid insecticide cypermethrin on rat brain IIa sodium channels expressed in xenopus oocytes. *Neurotoxicology* **19**, 823-32.

Soderlund D. M., Clark J. M., Sheets L. P., Mullin L. S., Piccirillo V. J., Sargent D., Stevens J. T. and Weiner M. L. (2002) Mechanisms of pyrethroid neurotoxicity: implications for cumulative risk assessment. *Toxicology* **171**, 3-59.

Soderlund D. M. and Knipple D. C. (2003) The molecular biology of knockdown resistance to pyrethroid insecticides. *Insect Biochem Mol Biol* **33**, 563-77.

Song J. H., Nagata K., Tatebayashi H. and Narahashi T. (1996) Interactions of tetramethrin, fenvalerate and DDT at the sodium channel in rat dorsal root ganglion neurons. *Brain Res* **708**, 29-37.

Song J. H. and Narahashi T. (1996) Modulation of sodium channels of rat cerebellar Purkinje neurons by the pyrethroid tetramethrin. *J Pharmacol Exp Ther* **277**, 445-53.

Symington S. B. and Clark J. M. (2003) Pyrethroid Effects on Voltage-Sensitive Calcium Channels. *Intenerary Planner for Society for Neuroscience* **Program No. 166.9**.

Symington S. B. and Clark J. M. (2005) Action of deltamethrin on N-Type (Cav2.2) voltage-sensitive calcium channels in rat brain. *Pesticide Biochemistry and Physiology* **82**, 1-15.

Symington S. B., Frisbie R. K., Kim H.-J. and Clark J. M. (2007a) Mutation of threonine 422 to glutamic acid mimics the phosphorylation state and alters the action of deltamethrin on Cav2.2. *Pesticide Biochemistry and Physiology* **88**, 312-320.

Symington S. B., Frisbie R. K., Lu K. D. and Marshall Clark J. (2007b) Action of cismethrin and deltamethrin on functional attributes of isolated presynaptic nerve terminals from rat brain. *Pesticide Biochemistry and Physiology* **87**, 172-181.

Tatebayashi H. and Narahashi T. (1994) Differential mechanism of action of the pyrethroid tetramethrin on tetrodotoxin-sensitive and tetrodotoxin-resistant sodium channels. *J Pharmacol Exp Ther* **270**, 595-603.

Tornero-Velez R., Scollon E. J., Starr J., Hughes M. F., DeVito M. J. and Dary C. C. (2007) Pharmacokinetic/Pharmacodynamic Modeling of Permethrin in the Rat. *The Toxicologist* **96**, 81.

Tropea D., Kreiman G., Lyckman A., Mukherjee S., Yu H., Horng S. and Sur M. (2006) Gene expression changes and molecular pathways mediating activity-dependent plasticity in visual cortex. *Nat Neurosci* **9**, 660-8.

Tulve N. S., Jones P. A., Nishioka M. G., Fortmann R. C., Croghan C. W., Zhou J. Y., Fraser A., Cavel C. and Friedman W. (2006) Pesticide measurements from the first national environmental health survey of child care centers using a multi-residue GC/MS analysis method. *Environ Sci Technol* **40**, 6269-74.

Tusher V. G., Tibshirani R. and Chu G. (2001) Significance analysis of microarrays applied to the ionizing radiation response. *Proc Natl Acad Sci U S A* **98**, 5116-21.

Verkhratsky A. (2002) The endoplasmic reticulum and neuronal calcium signalling. *Cell Calcium* **32**, 393-404.

Verschoyle R. D. and Aldridge W. N. (1980) Structure-activity relationships of some pyrethroids in rats. *Arch Toxicol* **45**, 325-9.

Vijverberg H. P. (1982) Structure-related effects of pyrethroid insecticides on the lateral-line sense organ on peripheral nerves of the clawed frog, Xenopus laevis. *Pesticide Biochemistry and Physiology* **18**, 315-324.

Vijverberg H. P. and van den Bercken J. (1990) Neurotoxicological effects and the mode of action of pyrethroid insecticides. *Crit Rev Toxicol* **21**, 105-26.

Wang J. Q., Tang Q., Parelkar N. K., Liu Z., Samdani S., Choe E. S., Yang L. and Mao L. (2004) Glutamate signaling to Ras-MAPK in striatal neurons: mechanisms for inducible gene expression and plasticity. *Mol Neurobiol* **29**, 1-14.

Watanabe E., Aono S., Matsui F., Yamada Y., Naruse I. and Oohira A. (1995) Distribution of a brain-specific proteoglycan, neurocan, and the corresponding mRNA during the formation of barrels in the rat somatosensory cortex. *Eur J Neurosci* **7**, 547-54.

Waxham M. N. (2003) Neurotransmitter receptors. In *Fundamental Neuroscience, Second Edition* (Edited by Squire L. R., Bloom F. E., McConnell S. K., Roberts J. L., Spitzer N. C. and Zigmond M. J.), p. 225-258. Academic Press, New York.

Weston D. P., You J. and Lydy M. J. (2004) Distribution and toxicity of sediment-associated pesticides in agriculture-dominated water bodies of California's Central Valley. *Environ Sci Technol* **38**, 2752-9.

Whyatt R. M., Barr D. B., Camann D. E., Kinney P. L., Barr J. R., Andrews H. F., Hoepner L. A., Garfinkel R., Hazi Y., Reyes A., Ramirez J., Cosme Y. and Perera F. P. (2003) Contemporary-use pesticides in personal air samples during pregnancy and blood samples at delivery among urban minority mothers and newborns. *Environ Health Perspect* **111**, 749-56.

Wolansky M. J., Gennings C. and Crofton K. M. (2006) Relative potencies for acute effects of pyrethroids on motor function in rats. *Toxicol Sci* **89**, 271-7.

Wolansky M. J. and Harrill J. A. (2007) Neurobehavioral toxicology of pyrethroid insecticides in adult animals: A critical review. *Neurotoxicol Teratol*.

Wong R. O. and Ghosh A. (2002) Activity-dependent regulation of dendritic growth and patterning. *Nat Rev Neurosci* **3**, 803-12.

Wu A. and Liu Y. (2003) Prolonged expression of c-Fos and c-Jun in the cerebral cortex of rats after deltamethrin treatment. *Brain Res Mol Brain Res* **110**, 147-51.

Xiang G., Pan L., Xing W., Zhang L., Huang L., Yu J., Zhang R., Wu J., Cheng J. and Zhou Y. (2007) Identification of activity-dependent gene expression profiles reveals specific subsets of genes induced by different routes of Ca(2+) entry in cultured rat cortical neurons. *J Cell Physiol* **212**, 126-36.

Yanez L., Ortiz-Perez D., Batres L. E., Borja-Aburto V. H. and Diaz-Barriga F. (2002) Levels of dichlorodiphenyltrichloroethane and deltamethrin in humans and environmental samples in malarious areas of Mexico. *Environ Res* **88**, 174-81.

Zhang L. I. and Poo M. M. (2001) Electrical activity and development of neural circuits. *Nat Neurosci* **4 Suppl**, 1207-14.

Transcriptional Response of Rat Frontal Cortex following Acute In Vivo Exposure to the Pyrethroid Insecticides Permethrin and Deltamethrin

Chapter 2

Joshua A. Harrill[*], Zhen Li[†], Fred A. Wright[†], Nicholas M. Radio[‡], William R Mundy[‡], Rogelio Tornero-Valez**, Kevin M. Crofton[‡]

[*]Curriculum in Toxicology, University of North Carolina at Chapel Hill, Chapel Hill, NC, 27599; [†]Department of Biostatistics and the Carolina Environmental Bioinformatics Research Center, University of North Carolina at Chapel Hill Chapel Hill, NC 27599; [‡]Neurotoxicology Division, NHEERL, ORD, USEPA, RTP, NC, 27711; [**] Human Exposure and Atmospheric Sciences Division, NERL, ORD, USEPA, RTP, NC 27711

Correspondence:
Kevin M. Crofton, Ph.D., USEPA, Neurotoxicology Division, B105-04, Research Triangle Park, NC 27711; Phone: 919-541-2672; E-mail: crofton.kevin@epa.gov

Abstract.

Pyrethroids are neurotoxic pesticides that interact with membrane bound ion channels in neurons and disrupt nerve function. The purpose of this study was to characterize and explore changes in gene expression that occur in the nervous system subsequent to the pharmacological actions of pyrethroids at the neuronal membrane. Rats were acutely exposed to either deltamethrin (0.3 – 3 mg/kg) or permethrin (1 – 100 mg/kg) followed by collection of cortical tissue at 6 hours. The doses used range from those that cause minimal signs of intoxication in a behavioral test to doses well below apparent no effect levels. Affymetrix GeneChips® were used to obtain global gene expression profiles and detect changes in gene expression. A group of dose-responsive transcripts were identified using penalized linear (SAM) and isotonic (PIR) regression methods. A sub-set of these genes were confirmed by qRT-PCR. A separate set of rats were used to characterize the time course of transcript expression. Both differences and similarities in the transcriptional response were observed when comparing permethrin and deltamethrin. Changes in *Camk1g*, *Ddc, Gpd3, c-fos and Egr1* mRNA levels were consistently observed across multiple test cohorts for both compounds. In addition, Significance Analysis of Function and Expression (SAFE) identified significantly enriched gene categories common for both pyrethroids including some related to branching morphogenesis and intracellular Ca^{+2} signaling. *In vitro* exposure of primary cortical cell cultures to both deltamethrin and permethrin resulted in an increase in the number of neurite branch points without effects on total neurite length. The effects on neuronal branching and gene expression identified here may represent novel aspects of pyrethroid neurotoxicity.

Introduction.

Pyrethroid insecticides are structural analogs of pyrethrum, a natural constituent of extracts from flowers of *Chrysanthemum cinerariaefolium*. Pyrethroids now represent a significant percentage of the world insecticide market (Amweg et al. 2005). This usage results in an increased potential for human exposure. Pyrethroid residues have been detected in sediments from agricultural run-off (Qin et al. 2006), residential dust samples (Colt et al. 2004), child-care centers (Tulve et al. 2006) and pyrethroid metabolites have been detected in human urine (Leng et al. 1997). A current focus in the field of pyrethroid research is examining the diverse neurotoxic mechanisms-of-action proposed for these compounds and determining if compounds belonging to this chemical class act through the same or similar mechanisms-of-action to produce similar adverse health outcomes (Soderlund et al. 2002).

Pyrethroids are neurotoxicants that disrupt nervous system function by interacting with membrane bound ion channels and altering their normal gating kinetics (Narahashi 1996). The primary molecular targets of pyrethroids are neuronal voltage-sensitive sodium channels (VSSCs, Catterall 1992; Ogata and Ohishi 2002). Prolongation of whole-cell Na^+ currents has been observed in a variety of cultured nervous system tissues exposed to pyrethroids (Song et al. 1996; Motomura and Narahashi 2001; Spencer et al. 2001; Ginsburg and Narahashi 2005). Furthermore, i*n vitro* studies utilizing heterologous expression systems have demonstrated that pyrethroids increase sodium current through some mammalian VSSC isoforms ($Na_v1.2$, $Na_v1.4$ & $Na_v1.8$) although the complete complement of mammalian VSSCs have not been examined for pyrethroid sensitivity (Smith and Soderlund 1998; Choi and Soderlund 2005; Shafer et al. 2005). Pyrethroids may also alter the gating kinetics of both neuronal voltage-sensitive Ca^{+2} (VGCCs, Shafer et al. 2005; Symington and Clark 2005)

and voltage-sensitive Cl^- channels (Burr and Ray 2004) at nominal concentrations similar to those that cause effects on VSSCs (Ray and Fry 2006). Isoforms of all of the aforementioned molecular targets are expressed in the plasma membrane of mammalian neuronal cells.

Pyrethroids affect mammalian nervous system function by producing hyperexcitability in neurons and increasing neuronal firing rates (Ray 1980; Wright et al. 1988; Vijverberg and van den Bercken 1990; Ray 2001). The acute manifestations of neurotoxicity observed in mammals following pyrethroid exposure are driven by this increased neuronal hyperexcitability which is in turn a result of the pharmacological actions of pyrethroids at their molecular target sties, primarily VSSCs (Ray 2001). Under normal conditions, neuronal membrane depolarization results in the activation of intracellular Ca^{+2}-dependent signaling pathways that control the induction of gene expression (Fields et al. 2005). In some cases, these transcriptional responses lead to persistent adaptive changes in cellular functions (i.e. neuronal plasticity; Bading 2000; McClung and Nestler 2008). Some neuroactive chemicals that are known to alter neuronal firing patterns or disrupt neurotransmission can trigger the induction of unique groups of gene transcripts which may in turn impact neuronal function (Bahi and Dreyer 2005; Cai et al. 2006; Xiang et al. 2007). While alterations in neuronal excitability is considered a critical event in the toxiciological mechanism(s)-of-action for pyrethroids, to date, the impact of pyrethroid-induced neuronal hyperexcitability on intracellular signaling pathways and inducible gene-regulatory networks have not been extensively examined.

In the present study Affymetrix GeneChip® microarrays were used to characterize the global transcriptional response of mammalian nervous system tissue following an acute oral exposure to two model pyrethroids: permethrin and deltamethrin. The dose ranges used

in this study include doses that cause minimal neurotoxic signs to doses well below apparent 'no effect' levels in *in vivo* behavioral tests (Wolansky et al. 2006). Low doses were used to minimize any potential transcriptional changes which may be due solely to excessive systemic toxicity at high pyrethroid doses. The goals of this study were to: 1) identify significant dose-dependent alterations in gene transcription, 2) determine at what point significant alterations in gene transcription occur along the dose-effect curve for pyrethroids and 3) determine if any of the dose-responsive genes are components of biological processes that may be sensitive to pyrethroids based on the hypothesized neurotoxic mechanisms-of-action for these compounds. Penalized linear (Significant Analysis of Microarrays, SAM) and isotonic (PIR) regression models (Tusher et al. 2001; Hu et al. 2005) as well as Significant Analysis of Function and Expression (SAFE, Barry et al. 2005) were used, respectively, to: 1) identify dose-responsive alterations in gene transcription and 2) identify Gene Ontology categories (Harris et al. 2004) and canonical cellular signaling networks (Kanehisha et al. 2004) that may be altered by pyrethroids. Alterations in transcript expression detected using microarrays were confirmed by qRT-PCR for a subset of pyrethroid-responsive genes. In addition, the time course of expression was characterized for a limited number of dose-responsive transcripts by qRT-PCR. Data from the *in vivo* gene expression studies lead to an investigation of pyrethroid effects on neuronal morphogenesis. Both permethrin and deltamethrin increased the number of branch points in a primary cortical cell culture with no effects on total neurite length or cell viability.

Methods.

Chemicals. Permethrin (3-phenoxybenzyl (1*R,S*)-*cis-trans*-3-(2,2-dichlorovinyl)-2,2-dimethyl-cyclopropanecarboxylate, 92.0% purity, isomer composition: 40 % *cis*, 60 % *trans*, 1:1 ratio of 1*R* & 1*S*) and deltamethrin ((*S*)-cyano-(3-phenoxyphenyl)methyl (1*R*)-*cis*-3-(2,2-dibromovinyl)-2,2-dimethylcyclopropane carboxylate, 98.9 % purity, isomer composition: 100% 1*R*, 3*R*, α*S*) were generously donated by FMC Corporation (Philadelphia, PA) and Bayer Cropscience (Research Triangle Park, NC), respectively. Pyrethroids were dissolved in corn oil (Sigma-Aldrich, St. Louis, MO) at 1, 10, 40 & 100 mg/mL permethrin and 0.3, 1 & 3 mg/mL deltamethrin. Dosing volume was 1mL/kg.

Animal Care and Treatment. Male Long-Evans rats (49-62 days of age) were obtained from Charles River Laboratories (Wilmington, MA) and housed two per cage in standard polycarbonate hanging cages (45 cm X 24 cm X 20 cm) with heat sterilized pine shavings for bedding (Beta Chips, Northeastern Products, Inc., Warrensburg, NY). Animals were maintained on 12h:12h photoperiod (lighted hours: 06:00-18:00) and allowed a 5-7 day period of acclimation to the colony prior to dosing. Colony rooms were maintained at 22.0 ± 2.0°C with a relative humidity of 55 ± 20%. Food (Purina 5001 Rat Chow) and tap water were provided *ad libitum*. The facility was approved by the American Association for Accreditation of Laboratory Animal Care (AAALAC) and all experimental procedures were approved in advance by the by the US EPA, National Health and Environmental Effects Research Laboratory Animal Care and Use Committee.

Four cohorts of animals were used in this study (Table 2.1). Cohort 1 was used for preliminary data collection to demonstrate that the selected doses of the two compounds

would alter gene transcription. Cohort 2 replicated these findings and expanded group sizes. Cohorts 1 & 2 were combined for microarray data analyses. Dose-response Cohort 3 was examined exclusively by quantitative real-time RT-PCR (qRT-PCR). Individual dose-response cohorts were exposed on separate days. All dosing occurred between 06:30 and 07:00 hours and the last test subject was euthanized before 18:00 hours. Dosing and euthanasia times for individuals were counterbalanced across time of day. Cohort 4 was used in qRT-PCR time course studies. In the time course studies rats were treated via oral gavage with 3 mg/kg deltamethrin, 100 mg/kg permethrin or vehicle. Each time point contained pyrethroid-treated and time-matched vehicle controls. All test subjects were dosed and euthanized between 07:30 & 17:30 hours. In every experimental cohort, test subjects were removed from the colony suite one hour prior to dosing and allowed to acclimate in a quiet holding room maintained under similar environmental conditions. Subjects were administered a single oral dose of test compound by gavage (1 mL/kg delivery volume), and allowed to recover in their home cage prior to euthanasia at 6 hours (dose-response studies) or 1, 3, 6 or 9 hours (time course studies). Subjects were then individually removed to an adjoining suite with a separate HVAC system for euthanasia by decapitation.

Whole brains were rapidly removed and placed on a cold plate (4°C). The cerebral cortex was removed by making a vertical incision at the anterior edge of the optic tract with a stainless steel razor, and rapidly frozen on a bed of dry ice. Cortical samples, without striatal tissue, were then bisected into contralateral hemispheres, weighed, frozen in liquid nitrogen and stored at -80°C.

RNA Extraction. Cortical samples were homogenized in 1 mL of TRI Reagent (Molecular Research Center, Inc., Cincinnati, OH) per 50-100 mg of tissue using a Polytron® PT-K homogenizer (Kinematica, Lucerne, Switzerland) and total RNA was isolated per manufacturer's instructions. Total RNA pellets suspended in DEPC-treated H_2O were then subject to DNase I treatment and re-extracted with acid:phenol chloroform, pH = 4.7 (Ambion Inc., Austin, TX) and chloroform according to manufacturer's protocol and re-suspended in DEPC-treated H_2O until use. The total RNA concentration of each sample was determined (absorbance @ 260 nm) on a Beckman-Coulter DU® 800 spectrophotometer (Fullerton, CA) and adjusted to 1.0 µg/µL prior to sample storage at -80ºC. The ratio of absorbance values at 260 nm and 280 nm (Ab 260/280) was used to assess purity of total RNA samples. All samples used in these studies had Ab 260/280 ratios > 1.6 (data not shown). Preliminary PCR experiments using primers for rat β-actin genomic DNA (outlined in Tully et al. 2006) demonstrated that the above protocol adequately prevents genomic DNA contamination of total RNA samples (data not shown). In addition, the RNA integrity of each sample was determined using an Agilent 2100 Bioanalyzer and RNA 6000 Nano LabChip Kit (Waldbron, Germany) according to manufacturer's instructions. All samples used in microarray and qRT-PCR experiments had 18S:28S rRNA ratios > 1.6 (data not shown). Following the RNA purity and integrity screens, aliquots of each total RNA sample (1 µg/µL for microarray hybridization or 25 ng/µL for qRT-PCR assays) were stored at -80°C until use.

Microarray design, sample preparation and data collection. All protocols for microarray sample preparation (except total RNA extraction, as above), GeneChip® hybridization, array

scanning and data collection were performed by Expression Analysis, Inc., (Durham, NC). Affymetrix Rat Genome 230 2.0 GeneChip® oligonucleotide microarrays (Santa Clara, CA) were used in this experiment. These microarrays contain 31,042 probe sets that represent ~28,000 unique *Rattus norvegicus* genes and expressed sequence tags (ESTs). First and second strand cDNA synthesis, RNase H digestion and (ds)cDNA isolation for each sample were performed according to manufacturer's protocol (Affymetrix 2004). Synthesis and clean-up of biotin-labeled cRNA was performed using a BioArray™ High Yield™ RNA transcript labeling kit (Enzo Life Sciences, Farmingdale, NY) and Qiagen RNeasy spin columns (Spoorstraat, Netherlands), respectively, according to manufacturer's instructions. Biotin-labeled cRNA was fragmented using Affymetrix 5X fragmentation buffer (200mM Tris acetate pH=8.1, 100 mM KOAc, 150 mM MgOAc).

Fragmentation of biotin-labeled cRNA, GeneChip® hybridizations, washes and staining were performed according to standard Affymetrix protocols (Affymetrix 2004). Hybridizations were performed in an Affymetrix Hybridization Oven 640. Washes were performed on an Affymetrix Fluidics Station 450 using the EukGE-WS2v4-450 fluidics script. GeneChips® were scanned using an Affymetrix GeneChip® 3000 Scanner with the GCOS v1.2 software package. Target intensity was set to a value of 500 with all other scanning parameters set at the factory defaults. The 3`/5` ratios for GAPDH and β-actin internal controls genes ranged between 0.93 – 1.11 and 1.2 – 2.01, respectively, indicating that degradation of RNA did not occur during sample preparation for hybridization. The intensity of hybridization controls (*BioB*, *BioC*, *BioD* and *Cre)* increased linearly on all arrays. Gene expression profiles for this experiment have been archived in the NCBI Gene Expression Omnibus (GEO) repository with the series accession number GSE7955.

Microarray Data Analysis. Two methods for the calculation of probe set expression summaries were compared: GeneChip® Operating Software v1.2 signal algorithm (GCOS, Affymetrix 2002) and Robust Multiarray Average (RMA, Irizarry et al. 2003). RMA expression summaries were calculated using RMAExpress© v.4.7 (University of California at Berkeley). RMA provided less within group variation in expression summary values as compared to GCOS v1.2, especially with probe sets with low fluorescent intensities (see Appendix A, Table 1). This is consistent with previous comparisons of the two methods (Millenaar et al. 2006) RMA expression summaries were used for the remainder of microarray data analysis. Microarray data from Cohorts 1 & 2 were combined for statistical analysis providing sample sizes of twelve for the control group and eight for each dose condition.

Analysis of dose-response relationships were performed using Significance Analysis of Microarrays (SAM, Tusher et al. 2001, version 2.21), with the quantitative/linear regression modeling component (SAM User's Manual, Chu et al. 2005). In addition to identifying dose-responsive genes, SAM provides permutation-based estimates of the false-discovery rate (*FDR*) associated with lists of genes for which the null hypothesis is rejected. The SAM statistic (d_i) penalizes lowly expressed genes, and is most powerful when the dose-response function is nearly linear in the range examined. To potentially increase power and account for non-linearity in dose-response relationships, the SAM analyses were supplemented by penalized isotonic regression (PIR) according to the method of (Hu et al. 2005) which was specifically designed for microarray analysis. Similar to SAM, PIR penalizes lowly expressed genes and provides a permutation-based estimate of the false

discovery rate. In contrast to SAM, PIR allows for the dose-response relationship to be nonlinear, but assumes the relationship is increasing or decreasing as a function of increasing dose, and not the reverse direction. This method results in a score (the *M*-statistic) for each probe set that quantifies the evidence for an increasing or decreasing dose-response relationship.

To ensure that the rigorously conservative, permutation-based approaches for controlling Type I error did not exclude probe sets with dose-dependent increases or decreases in expression, an additional analysis was conducted with each regression model. Empirical *p*-values from the PIR analysis or SAM analysis were used to filter out probe sets with no apparent dose-related changes in expression (threshold p-value < 0.01). The reduced group of probe sets were then analyzed using a one-way analysis of variance (ANOVA) followed by a Benjamini-Hochberg correction for control of multiple comparisons. Dose was used as the independent factor. Probe sets meeting the Benjamini-Hochberg correction at an $FDR < 0.05$ were included in the gene lists of interest for each compound (Tables 2.2 & 2.3), analysis of dose thresholds for transcriptional changes (Figure 2.2) and the comparison of effects between compounds (Figure 2.3). Genes of interest for qRT-PCR confirmation were ranked based on the results of the SAM and PIR analyses in conjunction with the results of the one-way ANOVA. For probe sets that passed the one-way ANOVA significance threshold, a Dunnett's multiple-comparison mean contrast test (Dunnett, 1955) was performed comparing the means of the respectively dose groups to the mean of the control group. Regression analysis were performed using R© version 2.3.0 statistical computing analysis software. Dunnett's tests were performed using SAS v8.1 (SAS Institute, Inc., Cary, NC).

Quantitative real-time RT-PCR. qRT-PCR for each transcript of interest was performed using TaqMan® One-Step RT-PCR Master Mix Reagent Kits and TaqMan® Gene Expression Assays on a ABI 7900HT Sequence Detection System (Applied Biosystems, Foster City, CA). AmpliTaq Gold® DNA Polymerase / dNTP mix, Multiscribe™ reverse transcriptase / RNA inhibitor mix and TaqMan® Gene expression primer-probe mix specific for the transcript of interest were combined according to manufacturer's specifications (Applied Biosystems 2005). The reaction mixture was then dispensed into the reaction plate (15 µL / well) and 125 ng of total RNA (5 µL) was added. Each sample was measured in triplicate for each transcript of interest and an internal reference gene. Reaction plates were maintained at 5°C during loading procedure. During data collection, reactions were incubated at 48°C for 45 min followed by incubation at 95°C for 10 min and 40 cycles of 94°C for 25 sec and 60°C for 1 min.

qRT-PCR assays were designed via the Applied Biosystems (ABI) primer / probe selection algorithm and bioinformatics pipeline (Applied Biosystems 2006). The amplification efficiency of each assay utilized in this experiment was examined using a serial dilution of pooled total RNA from rat frontal cortex. Efficiencies were calculated as: $E_x = 10^{(-1/m)} - 1$, where E is the amplification efficiency of target transcript *x* and *m* is the slope of threshold cycles vs log [total RNA concentration] across the range of dilutions (Applied Biosystems 2004). Assay identification numbers, context sequences, amplicon lengths and calculated amplification efficiencies are listed in Appendix A, Table 2.

Nine transcripts identified as being up- or down-regulated were examined by qRT-PCR to confirm the dose-responsive trends observed during microarray analysis (see arrows,

Tables 2.2 & 2.3). The time course of expression for a number of transcripts identified as dose-responsive was also examined in Cohort 4. qRT-PCR data from deltamethrin and permethrin dose-response and time course studies were analyzed according to the $2^{-\Delta\Delta C}{}_T$ method as described by (Livak and Schmittgen 2001). β-actin expression did not change as a function of time or dose for either compound (data not shown) and was used at the internal reference for all $2^{-\Delta\Delta C}{}_T$ calculations. For dose-response studies, the mean $\Delta\Delta^C{}_T$ of vehicle treated controls were used as the $2^{-\Delta\Delta C}{}_T$ calibrator (Livak and Schmittgen 2001) to obtain approximations of fold-change from control. For time course studies, the mean $\Delta\Delta^{CT}$ of vehicle treated controls were used as the $2^{-\Delta\Delta C}{}_T$ calibrator for each time-matched treatment group.

Data from Wolansky et al. (2006) were used to assign equipotent dose-levels (EDL) to the administered doses used in the present study to provide a comparative dose-metric between the two test compounds (see Table 2.1). Statistical analysis of qRT-PCR dose response data was performed using a two-way ANOVA with compound and equipotent dose level (EDL) as independent variables and $2^{-\Delta\Delta C}{}_T$ as the dependent variable followed by Dunnett's mean contrast test. Transcripts with a significant compound by EDL interaction were further analyzed using a one-way ANOVA with dose as the independent variable followed by Dunnett's mean contrast test. Statistical analysis of time course data was performed using a two-way ANOVA with time and treatment as independent variables and $2^{-\Delta\Delta C}{}_T$ as the dependent variable. Transcripts with a significant time*treatment interaction ($p < 0.05$) were additionally analyzed with a one-way ANOVA at each time point with treatment as the independent variable ($p < 0.05$)

Significance Analysis of Function and Expression (SAFE). The SAFE method (Barry et al. 2005) was used to identify pathways/functional categories whose genes are coordinately regulated in a dose-dependent manner. SAFE is similar to other pathway enrichment procedures (e.g. DAVID, Dennis et al. 2003), but accounts for correlation in gene expression within pathways using array permutation to rigorously control error rates. SAFE and accompanying array annotation were loaded from Bioconductor (v.1.8, Gentleman et al. 2004), which includes 126 KEGG pathways, 700 GO-BP (Gene Ontology biological processes) pathways, 142 GO-CC (Gene Ontology cellular component) pathways and 307 GO-MF (Gene Ontology molecular functions) pathways. SAFE tests for enrichment of significant dose-response relationships for genes within each pathway, and accordingly we first calculated the linear regression dose-response *p*-value for each gene. Genes with a nominal p-value < 0.05 formed the gene list to which the enrichment analysis was performed. SAFE (SAFE manual, Barry 2006) enables the user to define a pathway enrichment statistic and a Pearson test of binomial proportions (Pearson 1911) was then implemented. The Pearson statistics is similar to Fisher's exact test commonly employed in pathway enrichment testing (GSEA, Mootha et al. 2003), but does not consider the number of significant genes to have been fixed *a priori* (Barry et al. submitted). 10,000 permutations of dose levels were used by SAFE to assess the significance of the entire procedure, using the (Yekutieli and Benjamini 1999) procedure to control the *FDR* while accounting for the multiple pathways/categories. All categories with an estimated $FDR < 0.1$ are reported in Table 2.4, Part I.

Combining pathway evidence for the two pyrethroids. One aim of using these statistical methods in this study was to identify gene categories showing enrichment for dose-responsiveness for both permethrin and deltamethrin. The Fisher combined *p*-value method (Fisher 1930) allows accrual of evidence across multiple hypotheses, and thus is ideal for testing combined evidence for enrichment of each pathway for both chemicals. Under the null hypothesis that neither chemical shows enrichment for the pathway, each of the two *p*-values is uniform [0,1], and the Fisher statistic

$$S = -2(\ln(p_{delta})+\ln(p_{norm}))$$

is distributed as χ^2_2. The Fisher approach has favorable optimality properties (Littell and Folks 1973) and results in a new (combined) *p*-value for each pathway. For the multiple pathways tested, the Benjamini-Hochberg (1995) method was applied to control the false discovery rate ($FDR < 0.1$).

Fisher's statistic can be asymmetrically sensitive to very small *p*-values for a single chemical, even if the results for the other chemical are not significant. Thus, among pathways with a significant Fisher statistic, the focus was placed on those which showed SAFE *p*-values < 0.05 for both chemicals.

Cell culture and treatment. Cortical cultures containing neurons and glia were prepared from neocortices of newborn rat pups according to the protocol used by Chandler et al. (1993) with modifications. Neocortices were harvested under sterile conditions in a buffer solution containing 137 mM NaCl, 5 mM KCl, 170 µM Na_2HPO_4, 205 µM KH_2PO_4, 5 mM glucose, 59 mM sucrose, 100 U/ml penicillin and 0.1 mg/ml streptomycin, pH 7.4. The cortices were minced with scissors and digested using 0.25% trypsin for 5 minutes, then with

addition of 0.016% DNase for a further 5 minutes at 37°C and mixed at 30 rpm. The cortices were centrifuged (400xg, 1600 rpm) for 5 minutes at room temperature, the supernatant was aspirated and the tissue pellet was re-suspended in Gibco® DMEM/GlutaMAX-1 (Invitrogen Corp, Carlsbad, CA) containing 10 mM HEPES, 100 U/ml penicillin, 0.1 mg/ml streptomycin and 10% horse serum, pH = 7.4. The tissue was dissociated by trituration and filtered through a 100-µm Nitex screen. Cells were plated at a density of 50,000 cells/well in 96-well polystyrene plates (Corning, Inc., Corning, NY) that had been pre-coated with poly-L-lysine. Cells were incubated at 37°C in a humidified atmosphere of 5% CO_2 and 95% air.

Multi-compartment pharmacokinetic models for the disposition of deltamethrin and permethrin (Tornero-Velez et al. 2007, Mirfazaelian et al. 2006) were used to predict tissue concentrations of deltamethrin and permethrin in the brain at 6 h following the acute administered doses used in this study. Predictions are listed in Table 2.7. These estimated brain concentrations were then used to select nominal media concentrations of pyrethroids for use in the functional neurite morphogenesis cell model.

For *in vitro* exposure of cells, pyrethroids were prepared in DMSO using semi-logarithmic serial dilutions of concentrated stock solutions to yield working solutions ranging from 0.001 – 0.03 mM and 0.01 – 3 mM for deltamethrin and permethrin, respectively. On the day of use, working solutions were diluted 1/1000 into the cortical media to produce a final chemical concentration range of 0.001 – 0.03 µM and 0.01 – 3 µM for deltamethrin and permethrin respectively. The final DMSO concentration in the cortical media was 0.1%. Chemicals were added to the cells 2 hours after plating to ensure the cells adhered to the poly-L-lysine and incubated for a 96-hour exposure period.

Evaluation of neurite outgrowth. A Neurite Outgrowth Hitkit (Thermo-Fisher Scientific, Waltham, MA) was used to evaluate cortical cell neurite outgrowth and branching. Cortical cells were fixed for 20 min using a 4% paraformaldyde solution dissolved in PBS at 37^{o} C. Hoechst 33258 dye was included in the fixative to label cell nuclei. Cell bodies and processes were labeled using an anti-β_{III} tubulin primary antibody, followed by an Alexa Fluor 488-conjugated secondary antibody. Plates were evaluated using a Cellomics ArrayScan V^{TI} high content imaging platform for automated image capture and analysis. A multiple bandpass emission filter and matched excitation filters were used to acquire fluorescence images of the nuclei (blue) and cell body/processes (green) using a high-resolution charge-coupled device (CCD) camera. The acquired images were analyzed using the Neuronal Profiling bioapplication (Thermo Fisher Scientific) to measure cell-based changes in neuronal morphology (i.e., total neurite length, neurite count, branch points, and cell body area). Using a 10X objective, a sufficient number of fields were acquired for the analysis of at least 200 cells per well.

Cell viability. Cellular viability was determined in cortical cell cultures grown as described above in opaque 96 well plates using the CellTiter-Glo Viability Assay (Promega Corp., Madison, WI). The number of viable cells in each well was determined through quantification of ATP, an indication of metabolically active cells. Addition of the CellTiter-Glo reagent (100 µl/well) caused cells to lyse and induced a luciferase-catalyzed reaction of ATP with luciferin that produced a luminescent signal proportional to the amount of ATP present. Luminescence in each well was measured thirty minutes after adding the reagent using a FLUOstar Optima plate reader (BMG LABTECH, Durham, NC). Preliminary

experiments verified that ATP content was proportional to the number of live cells in a well (data not shown).

Results.

Microarray dose-response analyses. Both the PIR (isotonic) and SAM (linear) penalized regression methods identified dose dependent increases and decreases in mRNA expression in the cerebrocortex 6 h after an acute, oral exposure to both deltamethrin and permethrin. A comparison the PIR and SAM regression models demonstrate that the two methods yield similar results in terms of identifying dose-responsive probe sets in both the deltamethrin and permethrin treated dose-response cohorts (Figure 2.1A & 2.1B). The rank order of statistical significance was similar between the two methods in that probe sets with test-statistics in the higher end of the observed PIR *M*-statistic range also had test-statistics in the higher end of the observed SAM d_i-statistic range. The same trend was observed in the lower end of the test-statistic ranges.

The SAM analyses identified a small number of probe sets with dose-dependent increases in expression following either deltamethrin (n = 7) or permethrin (n = 10) exposure using the permutation-based false discovery rate values as the significance criteria (*FDR*: $q < 0.10$, see Figure 2.1A & 2.1B). The PIR analyses did not identify any probe sets for either pyrethroid with dose-dependent changes in expression at this $q < 0.10$ *FDR* significance threshold. However, the probe sets with $q < 0.10$ in the deltamethrin and permethrin SAM analyses also had *M*-statistics in the extreme upper portion of the observed PIR test-statistic range. Therefore, these methods yield comparable results in that a rank-ordered list of dose-dependent changes in expression constructed using either the PIR or SAM test-statistics

identifies the same groups of probe sets as being the most significantly changed in the deltamethrin and permethrin test cohorts.

A less statistically conservative method of identifying dose-related changes in probe set expression identified a larger number significantly altered probe sets than that observed using the *FDR* criteria. Both PIR and SAM also calculate an empirical *p*-value associated with the regression model for each probe set on the microarray. Using a threshold of $p < 0.01$ the SAM analysis identified 70 and 61 probe sets with dose-dependent changes in expression for deltamethrin and permethrin, respectively, while the PIR analysis identified 93 and 85, respectively (Figure 2.1A-B). In the deltamethrin analyses, 49.5 % of all the probe sets identified had $p < 0.01$ for both the SAM and PIR methods (Figure 2.1A, green points). Likewise, in the permethrin analyses, 53.7 % of all the probe sets identified had $p < 0.01$ for both the SAM and PIR methods (Figure 2.1B, green points). Therefore, the overlap between probe sets identified as dose-responsive using the empirical *p*-value thresholds is incomplete. Similar to what is observed using the *FDR q*-value significance criteria, use of the empirical *p*-value significance criteria also demonstrates that probe sets commonly identified using either the PIR or SAM method tend to appear at the top of a rank ordered list of significance, as indicated by the convergence of green points in the upper-right and lower-left hand corners of Figures 2.1A and 2.1B.

To provide a measure of multiple-comparison Type I error control, all the probe sets for each compound that had empirical *p*-values < 0.01 in either the SAM or PIR regression methods were additionally analyzed with a one-way ANOVA with dose as the independent factor, followed by a Benjamini-Hochberg multiple testing correction (significance threshold, $p < 0.05$). For deltamethrin and permethrin, 95 of 109 (87.1 %) and 53 of 89 (59.5 %) probe

sets passed the ANOVA significance threshold. A larger percentage of probe sets (deltamethrin: 12.9 %, permethrin: 44.3 %) identified in the SAM analyses did not pass the ANOVA significance threshold as compared to those identified in the PIR analyses (deltamethrin: 8.7 %, permethrin: 23.8 %). The full list of probe sets considered significantly dose-responsive for deltamethrin (n = 95) and permethrin (n = 53) are given in Tables 2.2 and 2.3. Probe sets listed on these tables that correspond to known protein-coding RefSeq database entries were considered candidates for qRT-PCR confirmation in dose-response Cohorts 3 and 4.

The dose-dependent changes in mRNA expression identified with the above analyses are relatively small in magnitude, < 2-fold change from control. Figure 2.2 illustrates the dose-response patterns detected by the SAM and PIR analyses in terms of fold-change from control. For deltamethrin, the magnitude of fold-changes in expression ranged from 0.51 to 1.96 (Figure 2.2A-C). Similarly for permethrin, fold-change values ranged from 0.54 to 1.56-fold (Figure 2.2D-F). No fold-change exclusion criteria were used to filter gene expression changes in the present study.

Further analysis of the dose-response functions illustrated in Figure 2.2 indicate that significant alterations in mRNA expression occur at doses below those needed to produce acute behavioral effects. For each probe set included in the gene-of-interest lists for deltamethrin (Table 2.2) and permethrin (Table 2.3) a Dunnett's mean contrast test was performed comparing the mean of each dose condition with the mean of the vehicle treated control group. The cumulative results of these tests are illustrated in the inset panels of Figure 2.2. A majority of the probe sets identified as dose-responsive had mean expression values in the 3 mg/kg deltamethrin and 100 mg/kg permethrin dose groups different from

those in the vehicle treated control group (78.9 % and 77.3 %, respectively). Of those probe sets, 25.3 % and 19.5 % also had mean expression values in the 1 mg/kg deltamethrin and 10 mg/kg permethrin dose groups different from controls. These doses are below those needed to produce acute neurotoxic effects on behavior. In addition, these data demonstrate that the PIR analyses detected a greater number of probe sets with mean expression values in the behavioral "NOAEL level" dose groups (see Table 2.1) as being different from control as compared to the SAM analyses (Figure 2.2B & E, insets).

Comparison of transcriptional effects across compounds. A comparison of the probe sets identified as dose-responsive in the PIR and SAM regression analyses demonstrates that the transcriptional response elicited by the two pyrethroids has some common characteristics. The panels in Figures 2.3 plot the $-\log_{10}$ of the empirical *p*-values associated with the PIR regression (2.3A) or SAM regression (2.3B) for each probe set identified as dose-responsive for either deltamethrin or permethrin. Data from the PIR regression analyses demonstrate that expression of 27.2 % of all probe sets identified as dose-responsive for either pyrethroid are significantly altered by both compounds at an empirical *p*-value threshold of $p < 0.05$ (Figure 2.3A). Likewise, SAM analyses demonstrated that 27.8 % of all dose-responsive transcripts are altered by both pyrethroids (Figure 2.3B). Differences in the transcriptional response profiles between pyrethroids are also apparent and may represent divergent biological actions elicited by the different pyrethroids.

Quantitative real-time RT-PCR. Measurement of transcript expression by qRT-PCR confirmed the dose-related trends in expression observed during microarray analysis in a

group of nine transcripts taken from Tables 2.2 and 2.3. Table 2.4 summarized the results of these assays and compares them to the fold-change expression values derived from the microarray study. To confirm dose-related changes in transcript expression from the microarray study, a separate cohort of test subjects was dosed under the same conditions as those used previously. This provides both a technical and biological replication of the results observed in the microarray analyses. Given the similarities observed in the transcriptional responses elicited by deltamethrin and permethrin, qRT-PCR data were analyzed with a two-way ANOVA with compound and equipotent dose-level (EDL) as the independent factors ($p < 0.05$ significance threshold). Where a significant interaction of compound and EDL or a significant main effect of compound was observed, data were subsequently analyzed by a one-way ANOVA within compound with dose as the independent factor.

Of the nine transcripts examined by qRT-PCR, Ca^{+2}/calmodulin dependent protein kinase 1γ (*Camk1g*) and dopa decarboxylase (*Ddc*), were commonly affected by both compounds, indicating that for these genes there was no differences in the changes in expression elicited by equipotent doses of either pyrethroid. *Camk1g* mRNA expression was significantly increased with both compounds with expression levels different from control at the three highest equipotent dose levels examined (Dunnett's test, $p < 0.05$). *Camk1g* qRT-PCR expression values closely resembled those observed in the microarray study. *Ddc* mRNA expression was significantly decreased with both compounds in the qRT-PCR assays with significant decreases in expression at the ED_{30} and ED_{50} dose levels (Dunnett's test, $p < 0.05$). In contrast to *Camk1g*, the microarray dose-response cohort demonstrated a dose-related change in *Ddc* expression for deltamethrin only even though a clear dose-dependent

decrease in *Ddc* mRNA expression was observed in both the deltamethrin and permethrin qRT-PCR cohorts.

A significant interaction between compound and EDL was observed for glycerol-3-phosphate dehydrogenase 1 (*Gpd1*) and FK506-binding protein 5 (*Fkbp51*), indicating that equipotent doses of the two pyrethroids did not elicit similar changes in expression at 6 hours post-exposure. A main effect of dose was observed for *Gpd1* and *Fkbp51* mRNA only for deltamethrin (Table 2.4). For both *Gpd1* and *Fkbp51* the mean expression level in the 3 mg/kg deltamethrin dose groups was different from control (Dunnett's test, $p < 0.05$). In addition, the qRT-PCR expression values for *Gpd1* and *Fkbp51* closely match those observed in the microarray study.

The immediate early genes, FBJ murine osteosarcoma viral oncogene homolog (*c-fos*) and early growth response 1 (*Egr1*) were differentially affected by the two pyrethroids at 6 h post-exposure, however, no significant main effect of dose (EDL) was observed for either compound. For deltamethrin, the direction of fold-change for *c-fos* and *Egr1* is down in most dose groups measured by qRT-PCR. The expression of *c-fos* was significantly decreased from control values for 3 mg/kg deltamethrin only. In contrast, for permethrin no change in the expression of *c-fos* and *Egr1* mRNA across dose groups in the qRT-PCR cohort. While *c-fos* and *Egr1* expression at 3 mg/kg deltamethrin and 100 mg/kg permethrin reflect the direction of fold-change observed in the microarray study, very little similarity is apparent between qRT-PCR and microarray expression values at the lower dose levels (Table 2.4).

There were no effects of pyrethroid exposure on mRNA expression for heat shock 27kDa protein (*Hsp27*), brain derived neurotrophic factor (*BDNF*) or Ras association (RalGAS/AF-6) domain family 6 (*Rassf5*). In the case of *BDNF*, qRT-PCR expression

values closely approximate the expression values observed in a second probe set not identified as dose-responsive in the microarray analyses.

Characterization of the time course of mRNA expression for *Camk1g*, *Gpd1*, *c-fos* and *Egr1* demonstrates that altered expression of these transcripts also occurs at times earlier than 6 h following acute, oral pyrethroid exposure. Figure 2.4 illustrates the time course of gene expression changes following exposure to either 3 mg/kg deltamethrin or 100 mg/kg permethrin. A summary of the statistical analyses performed on these data is provided in Table 2.5. Treatment-related increases in *Camk1g* and *Gpd1* mRNA expression were observed for both deltamethrin and permethrin. For deltamethrin, both *Camk1g* and *Gpd1* mRNA had maximally induced expression at 3 h followed by persistent elevations at 6 h (Figure 2.4). Both of these changes reached statistical significance in the time course cohorts (Table 2.5). For permethrin, both *Camk1g* and *Gpd1* had maximal induction at 6 h preceded by slight elevations at 3 h. Permethrin-mediated *Gpd1* induction was statistically significant while *Camk1g* induction reflected the trends observed in the dose-response cohorts but did not reach statistical significance. *Ddc* mRNA expression was decreased following both deltamethrin and permethrin exposure. For deltamethrin decreased expression began at 6 h and persisted through 9 h while for permethrin, expression decreased at 6 h only.

In the qRT-PCR time course cohorts both deltamethrin and permethrin exposure results in the induction of the immediate early genes *c-fos* and *Egr1*, albeit with different temporal characteristics. This is contrary to the trends in *c-fos* and *Egr1* expression observed in the deltamethrin and permethrin dose-response cohorts, where the former pyrethroid produced a trend toward decreased expression while the latter produced a trend toward increased expression. Expression of *c-fos* and *Egr1* increases at 3 h for both deltamethrin

and returns to control levels at 6 h. For permethrin, expression of *c-fos* and *Egr1* increases at 3 h, remains persistently elevated at 6 h and returns to control levels by 9 h. Even though the microarray data at 6 h demonstrates opposite trends in *c-fos* and *Egr1* expression for deltamethrin and permethrin, the data in Figure 2.4 demonstrate that the two pyrethroids, in fact, elicit similar responses in the expression of some immediate early genes. The expression of other immediate early genes, such as *BDNF*, is apparently not affected by pyrethroids under the dosing paradigm used in this study.

In summary, the mRNA expression levels measured using microarray compared favorably with those observed using qRT-PCR in most cases. In addition, the dose-dependent trends and time course profiles examined in these qRT-PCR studies for *Camk1g*, *Gpd1*, *Ddc*, *c-fos* and *Egr1* are qualitatively similar for both deltamethrin and permethrin.

Significant Analysis of Function and Expression (SAFE). Seven GO categories were identified as commonly enriched for both pyrethroids using SAFE analysis and Fisher's χ^2 method (Table 2.6, part I). The composition of the commonly enriched categories for both chemicals included genes involved in neuronal morphogenesis, intracellular Ca^{+2} signaling and small molecule transport. In addition, five GO-BP categories and two canonical KEGG pathways were identified as enriched in the individual SAFE analyses of permethrin and deltamethrin, respectively (Table 2.6, part II). For permethrin, the SAFE findings include enriched gene categories related to neuronal morphogenesis and developmental patterning. For deltamethrin the SAFE findings include two KEGG metabolic pathways, one of which involves synthesis of the precursor molecules for monoamine neurotransmitters.

SAFE plots of the GO categories 'morphogenesis of a branching structure' and 'Ca+2/calmodulin dependent protein kinase complex' demonstrated significant category enrichment for both permethrin and deltamethrin (Figure 2.5). This is evidenced by the divergence of the stair step line from the unity line near the far left of Figure 2.5, panels A-D. A SAFE plot of a GO category not significantly enriched for either compound is given in Figure 2.5, panels E-F for comparison purposes. The most significantly dose-responsive transcripts for each of the enriched GO categories are illustrated in the heatmaps to the right of Figure 2.5, panels A-D. These heatmaps demonstrate that appreciable dose-dependent increases in the expression of probe sets contained within the enriched GO categories occurs following pyrethroid exposure. The functional category level analysis of the microarray data provided the basis for testing the hypothesis that pyrethroids affect neuronal branching morphogenesis.

Pyrethroid effects on neurite length and branching in primary mixed cortical cell cultures. Both deltamethrin and permethrin produce an increase in the number of neurite branch points following a 96 h exposure (Figure 2.6A & D). The range of predicted tissue concentrations (in μM) from the PK predictions (Table 2.7) are marked near the *x*-axes and correspond well to areas along the *in vitro* dose-response curve where changes in branching were observed. An average increase of ~25% above control in the number of neurite branch points was observed at nominal media concentrations ranging from 0.01 - 0.03μM deltamethrin and 0.01 – 3μM permethrin. No significant increase in total neurite length was observed for either compound save at the 0.01μM exposure level for permethrin. Changes in cell viability were not apparent in the concentration ranges tested.

Discussion.

A principal finding of the present study was that acute, oral pyrethroid exposure caused dose-dependent alterations in gene transcription in the cortex at doses of deltamethrin and permethrin that were below those required to elicit acute neurotoxic effects in the whole animal (Wolansky et al. 2006). Both similarities and differences in the overall transcriptional response were observed when comparing the two pyrethroids. Quantitative real-time RT-PCR analysis in additional cohorts of animals provided an independent biological and technical replicate of the findings from the microarray data set. In addition, transcripts for which the time course of gene expression was characterized demonstrated qualitative similarities in the response for both pyrethroids. Finally, SAFE analysis of the microarray data identified several GO categories jointly enriched by both deltamethrin and permethrin including some related to branching morphogenesis. Subsequently, a significant increase in the number of neurite branch points was observed in a primary cortical cell culture model. The transcriptional and functional changes observed in this study are consistent with the downstream responses expected to occur following perturbation of normal neuronal firing patterns (Majdan and Shatz 2006; Xiang et al. 2007) such as those that may be produced by pyrethroid-mediated effects on ion channel function.

The following sections include interpretations of the microarray analysis findings, the data analysis framework, a discussion of how some of the individual transcripts identified in this study may be regulated by the pharmacological actions of pyrethroids, some hypothesis of how changes in the expression of these genes may contribute to pyrethroid neurotoxicity and finally a discussion of the pyrethroid effects on neuronal morphology.

Microarray dose response analyses. Dose-dependent alterations in transcript expression were observed in the frontal cortex at 6 h following acute exposure to pyrethroids. In the present study Affymetrix GeneChips® were used as a discovery tool for identifying dose-dependent changes in gene transcription. The PIR and SAM penalized regression models used in this study provided qualitatively similar outcomes in terms of identifying dose-related alterations in gene expression. The two penalized regression analyses demonstrated that both methods ranked a similar sub-set of transcripts as being the most dose-responsive for each compound (Figure 2.1A & 2.1B). Prior to experimentation, the shape of the dose-response curve for any potential alterations in gene transcription was unknown. The SAM regression model, which was designed to test if dose-response curves are fitted by a linear function, detected a number of dose-dependent changes in gene transcription. However, Figure 2.2 clearly illustrates the heterogeneity of the transcriptional dose-response functions observed in the present study. Not all of these functions are adequately fitted by a linear model. A penalized isotonic regression (PIR) analysis developed from Hu et al. (2005) that searches for monotonic increases or decreases in expression without testing the fit to a particular dose-response function, identified dose-related changes in expression that were not detected by SAM. A majority of these had significant increases in expression from control at the "NOAEL" dose of the test compounds. While both SAM and PIR identified the same subset of transcripts as being the most-significantly dose-responsive within each compound (Figure 2.1A & B), the PIR method provided superior detection of probe sets with treatment related changes in expression that did not fit a linear model.

Collectively, these data indicate that the pyrethroid dose thresholds required to elicit changes in gene expression vary from gene to gene and that the regulation of some genes

occur at lower pyrethroid doses than others. For some transcripts, appreciable alterations in mRNA expression occurred exclusively at the highest administered dose of either pyrethroid compound. For other transcripts, changes were observed at doses not associated with any observable neurotoxic effects (Figure 1.2 insets and Table 2.4). The biological factors mediating the heterogeneity in dose-response functions for different pyrethroid-sensitive transcripts are unclear but could be due to several factors. In neurons, induction or repression of gene expression is controlled by a large and diverse network of intracellular signaling cascades that control the activity of numerous transcription factors in the cell nucleus. These neuronal signaling pathways are activated by either: 1) changes in cytoplasmic second messenger levels in response to activation of voltage-sensitive ion channels, ionotropic or metabotropic neurotransmitter receptors or membrane bound receptor complexes or 2) exogenous ligands that are transported into the cell (such as glucocorticoids) to directly enhance transcription factor activity (de Kloet 1998; West et al. 2002; Schulman and Roberts 2003; Schoneveld 2004). Some of these signal transduction pathways may become activated at lower administered doses of pyrethroids than others, thereby causing the transcripts they control to become induced or repressed at different points along the administered dose range. Alternatively, the use of only one time point in the dose-response study may have contributed to the differences in dose-responsive expression patterns between genes. Differences in the duration of signaling pathway stimulation or transcription factor activation and the rate of mRNA synthesis and degradation may result in variable temporal expression patterns between pyrethroid-sensitive genes.

Time course data demonstrate that pyrethroid-sensitive genes have varying temporal profiles of expression (Figure 2.4). The sampling time of 6 h in the initial phase of this study

was selected to capture both 'early' and 'late' transcriptional changes in response to pyrethroid exposure. The time course data at 6 hr are consistent with the data from the dose-response study which was collected 6 h after exposure. In addition, the available time course data implies that additional alterations in gene expression not detected in the dose-response study may occur at time points other than the one sampled. The qRT-PCR data shown here support this conclusion (Figure 2.4).

In the present experiment, the cortex was selected as the tissue-of-interest based on previous studies demonstrating rapid accumulation of both deltamethrin and permethrin following an acute oral dose, disruption of cortical neuronal firing patterns, and induction of gene products known to be upregulated following neuronal excitation (Ray 1980; Anadon 1991; Hassouna et al. 1996; Anadon 1996; Condes-Lara 1999). However, the use of a brain tissue that is a heterogenous mixture of neuronal sub-types (e.g. glutaminergic, GABAergic), glial cells and vascular endothelia (Hof et al. 2003) presented a particular challenge in analysis of the microarray data: namely, analysis of transcripts with low relative abundance in the total RNA sample. One result of this cellular heterogeneity is lower relative fluorescent signal intensities (and therefore lower expression summaries) of neuron-specific transcripts in the microarray data set than what would be observed using a total RNA sample from an exclusively neuronal cell population (c.f. Ginsberg and Che 2005). Effectively, the neuronal mRNA is diluted by mRNA from other cell types. Arbitrary exclusion of lowly expressed mRNAs from the analysis based on a fluorescence threshold may unduly discard probe sets that have biologically relevant changes in expression. To control for lowly expressed genes without excluding potentially meaningful data from the analysis, both the SAM and PIR penalized regression methods use an adjustment factor in the calculation of the

test-statistics to force probe sets with very low signal intensities to change more dramatically to be considered significant (Tusher et al. 2001; Hu et al. 2005). In the present study the penalized regression analyses reduced the number of lowly-expressed, and potentially unreliable, probe sets included in the dose-responsive gene-of-interest list (Appendix A, Figure 1) while also provided a means of surveying the entire data set for pyrethroid-responsive genes.

The magnitude of the transcriptional alterations (expressed as fold-change from control) observed in the present study are comparable to those observed in other microarray studies that examine the acute effects of pharmacological agents on gene transcription in the brain (Li et al 2004; Xie et al. 2004; Dow et al. 2005; Bowyer et al 2007). The relatively small number of significant changes in expression was not unexpected given the nature of the pyrethroid exposures used: i.e. even the highest doses used in this study were only slightly above the threshold needed to elicit acute behavioral effects (Bloom et al. 1983; Peele and Crofton 1987; McDaniel and Moser 1993; Wolansky et al. 2006). The low doses and resulting small magnitude transcriptional changes observed in this study are likely the reasons why only a very small number of transcripts were identified as dose-responsive using the permutation based *FDR* estimates as the significance criteria ($q < 0.01$). In analyses of training data sets, it has been demonstrated that the SAM analyses can efficiently detect treatment related effects in transcripts with changes in expression (> ~1.5-fold) by using the permutation-based *FDR*s as a significance threshold (Tusher et al. 2001; Larsson et al. 2005). However a systematic analysis of how well these permutation methods perform in picking up small magnitude gene expression changes has not been performed.

Comparison across compounds. The present data demonstrate both similarities and differences in the global transcriptional response in rat cortex to acute, low-dose deltamethrin and permethrin exposure (Figure 2.3). Of the transcripts examined by qRT-PCR (Table 2.4 and Figure 2.4), *Camk1g, Ddc, Gpd1, c-fos* and *Egr1* all had similar expression profiles for both deltamethrin and permethrin. These similarities were not readily apparent upon examination of the microarray probe set data (Cohorts 1 & 2) or 6 h qRT-PCR data (Cohorts 3 & 4). For instance, the immediate early genes *c-fos* and *Egr1* were identified as dose-responsive for permethrin during microarray analysis and had opposite trends in expression at 6 h for the two pyrethroids. Similarly, *Camk1g* and *Gpd1* were identified during microarray analysis for deltamethrin, but not permethrin, even though a similar trend in the direction of change is observed across compounds. Characterization of the time course of mRNA expression for these genes clearly demonstrates a commonality in the transcription responses elicited by the two compounds. The results of the SAFE functional category level analysis support the conclusion that the biological activities of the two pyrethroids overlap. Several categories were found to be commonly upregulated between the two compounds. How many of these individual gene changes or impacted functional categories are relevant to the neurotoxicology of pyrethroids remains yet to be determined. These data provide guidance on some novel cellular functions affected by pyrethroids.

Biological significance of experimental findings. Interestingly, probe sets corresponding to the primary molecular targets for pyrethroids were not altered for either pyrethroid tested in the microarray study. Specifically, there were no treatment related changes in any of the VSSC or VSCC isoforms / subunits or any subunits that comprise neurotransmitter receptors

complexes (Cull-Candy et al. 2001; Ogata and Ohishi 2002; Catteral et al. 2003; Farrant and Kalia 2007). This finding is supported by an *in vitro* study by Xiang et al. (2007) that used a variety of pharmacological manipulations to increase the firing rates of cultured neuronal networks from rat cortex and examined the global transcriptional response of those neurons following stimuli. No changes in the expression of VSSC or VSCC isoforms / sub-units or neurotransmitter receptors were identified in that study in response to increases in neuronal firing rates. The Xiang et al. (2007) study did detect increases in the expression some voltage-sensitive K^+ channels: *Kcna1* and *Kcnk12*. These particular K^+ channel sub-types were not altered in the present study, however *Kcnf1* was upregulated following pyrethroid exposures. The present data do not rule out the possibility that pyrethroids cause transcription-independent changes in the expression or functional state of ion channels or neurotransmitter receptor complexes. Such responses are known to occur in neurons in response to excitatory or depolarizing stimuli (Paillant et al. 1996; Giraud et al. 1998; Shiraishi et al. 2001; Kim et al. 2007). The present data do not support transcriptional induction or repression of VSSCs, VSCCs or neurotransmitter receptor subunits as a neuronal response to pyrethroids.

The immediate early transcription factors *c-fos* and *Egr1* were upregulated following both deltamethrin and permethrin exposure and are in agreement with previous studies of IEG expression in the cortex following acute pyrethroid exposure (Hassouna et al. 1996; Liu and Wu 2001). Increased *Egr1* and *c-fos* expression supports the conclusion that neurons in the cortex were activated by deltamethrin and permethrin in the present study. *Egr1* and *c-fos* are among the genes induced by increased neuronal firing in the Xiang et al. (2007) study as well as in other paradigms for studying neuronal activity (Zangenehpour et al. 2002; Patra

et al. 2004). Immediate early gene (IEG) induction is known to be the most rapid transcriptional response of neurons following increased activity (Steward et al. 1998; Dassesse et al. 1999; Guzowski et al. 1999; Clayton 2000). The time course for the expression of the IEGs *c-fos* and *Egr1* does not support *de novo* gene transcription as being responsible for mediating the acute behavioral effects of pyrethroids. The earliest time that increased IEG expression is observed in the present study is at 3 h. IEG expression is at control levels at 1 h. Onset of behavioral effects occurs prior to the onset of increased IEG expression (i.e. 30 min – 1 h, Crofton and Reiter 1984). Therefore, the novel gene expression changes described herein can not mediate the acute neurotoxic signs of pyrethroid intoxication.

An increase in the expression Ca^{+2}/calmodulin dependent protein kinase 1g (*Camk1g*) mRNA was also observed following deltamethrin and permethrin exposure *in vivo.* There is evidence in the literature that *Camk1g* mRNA expression is regulated by changes in neuronal firing patterns similar to IEGs. In the Xiang et al. (2007) study increases and decreases in the expression of *Camk1g* mRNA matches nearly perfectly with increases and decreases in neuronal burst firing rates. Increases in *Camk1g* mRNA expression have been reported in response to acute or chronic exposure to the opiod analgesic morphine in mouse striatum and chronic exposure to the atypical antipsychotic olanzipine in the rat frontal cortex (Fatemi et al. 2006; Korostynski et al. 2007). Both of these agents are known to increase spontaneous and / or stimulus evoked bursting activity in some brain regions *in vivo* (Stanzione et al.1988; Gronier and Rasmussen 2005) further supporting that *Camk1g* mRNA expression is correlated with changes in neuronal activity. Therefore, increased *Camk1g* mRNA

expression observed in the present study is most likely due to pyrethroid-induced alterations in neuronal firing rates within the frontal cortex.

Increased expression of *Camk1g* may impact on the structure and function of pyrethroid affected neurons. This is consistent with recent data from *in vitro* models of developmental neurite and dendrite morphogenesis. Wayman et al. (2006) demonstrated that *Camk1g* plays a specific role in the activity-dependent growth of hippocampal neurons between 7-9DIV by mediating activation of a Ras/MEK/ERK signaling cascade in response to excitatory stimuli and triggering CREB-mediated transcription of *Wnt-2*, a soluble autocrine factor that promotes dendritic growth. Takemoto-Kimura et al. (2007) demonstrated that *Camk1g* is covalently modified, inserted into lipid rafts and targeted to neuronal dendrites where it activates a Rac signaling pathway that mediates the morphogenesis of cortical neurons. In both the Wayman et al. (2006) and Takemoto-Kimura et al. (2007) studies, knockdown or overexpression of *Camk1g* altered depolarization and neurotrophin-stimulated outgrowth of neuronal processes, respectively. Takemoto-Kimura et al. (2007) also demonstrated that *Camk1g*-mediated effects are restricted to dendrites (axons were not affected). The role of *Camk1g* in maintenance and activity-regulated plasticity of dendritic arbors in adults (Sin et al. 2002) is currently unknown. Given this knowledge of *Camk1g* activity *in vivo*, it is plausible that pyrethroid-mediated increases in *Camk1g* expression (especially in a developmental context) could result in changes in neuronal morphology. In the present study, *in vitro* exposure of developing cortical neurons to both deltamethrin and permethrin resulted in an increase in the number of neurite branch points. The role of *Camk1g* induction in mediating these effects remains unknown.

The transcriptional upregulation of glycerol-3-phosphate dehydrogenase 1 (*Gpd1*) and FK506-binding protein (*Fkbp51*) mRNA in the present study has two major implications: 1) that *in vivo* pyrethroid exposure results in the activation of hypothalamic-pituitary-adrenal (HPA) axis and 2) that the non-neuronal cell populations in the brain are sensitive to pyrethroids, most likely through an indirect activation of the HPA axis. The expression of *Gpd1* mRNA was transiently increased following deltamethrin and permethrin exposure (Table 2.4 and Figure 2.4). Similarly, expression of *Fkbp51* mRNA dose-dependently increased at 6 h following deltamethrin exposure only (Table 2.4), although this transcript was not examined in the time course cohort. These changes in *Gpd1* and *Fkbp51* mRNA expression suggest that pyrethroids can have effects on glial cell populations as the proteins encoded by these transcripts are expressed in the brain exclusively in oligodendrocytes (Leveille et al. 1980) and T-cell lymphocytes (Baughman et al. 1995). However, the induction of these mRNAs is likely an indirect action of pyrethroids via activation of the HPA axis (de Kloet et al. 1998). Both the *Gpd1* and *Fkbp51* genes contain glucocorticoid receptor binding motifs either in the upstream promoter region (*Gpd1,* Cheng and de Vellis 2000) or in an intronic region (*Fkbp5,*; Hubler and Scammell 2004) and increased expression of both is dependent upon glucocorticoid hormone stimulation (Nicols et al. 1996; Baughman et al. 1997). Glucocorticoids are release in the circulation from the adrenals in response to a variety of stressors. Interestingly, increased circulating corticosterone levels were reported in the rat following deltamethrin exposures; albeit at very high, intravenous doses (de Boer et al. 1998). Increases in *Gpd1* and *Fkbp51* expression may be considered to be components of a generalized, non-specific stress response brought about by overstimulation of the HPA axis

by pyrethroids. The potential impact of increased *Gpd1* and *Fkbp51* expression the health and function of affected glia, to date, is unclear.

Data from the present study suggest that the pathways controlling monoaminergic neurotransmitter synthesis may be affected by pyrethroids. Both deltamethrin and permethrin caused decreases in the expression aromatic L-amino acid decarboxylase (*Ddc*) mRNA in the frontal cortex at 6 h (Table 2.4). Small differences in the time course of *Ddc* mRNA expression between the compouds were observed with deltamethrin causing a more persistent decrease than permethrin. *Ddc* is the final enzyme in the synthesis pathways of dopamine and serotonin, neurotransmitters derived from the amino acids tyrosine and tryptophan, respectively (Deutch and Roth 2003). This is consistent with previous reports noting a depletion of dopamine and serotonin in a variety of brain regions following repeated exposure to deltamethrin (Martinez-Larranaga et al. 2003; Liu et al. 2006; Liu and Shi 2006). In the case of dopamine depletion, two of these studies demonstrate concurrent decreases in the expression of tyrosine hydroxylase, the penultimate enzyme in dopamine synthesis (Liu et al. 2006; Liu and Shi 2006). Expression of *Ddc* was not examined in these studies.

The increased expression of *c-fos*, *Egr1* and *Camk1g* in the present study are most likely regulated by pyrethroid-induced changes in the neuronal firing patterns of cortical neurons. In contrast, the increased expression of *Gpd1* and *Fkbp51* mRNA indicates that the HPA-axis was activated by pyrethroid exposure indicating an excitatory effect of these compounds on the sympathetic nervous system. Previous studies have utilized transient activity-dependent alterations in gene expression to map out activated neuronal circuits in response to excitatory or neurotoxic stimuli (Carvajal et al. 2005; Guzowski et al. 2005; Guzowski 2006) essentially using the expression of these mRNA species as biomarkers of

pharmacological or excitatory actions at the neuronal membrane. The data from this study indicate that *c-fos*, *Egr1* and *Camk1g* may be appropriate for use in this type of functional mapping in examination of the pharmacological actions of pyrethroids.

Pyrethroid effects on branching morphogenesis. Both deltamethrin and permethrin increased the number of neurite branch points in an *in vitro* model of cortical neuronal development with no effects on total neurite length. The pharmacokinetic modeling data show these effects occurred at media concentration ranges comparable to tissue concentrations predicted to be present in the brain following an acute exposure *in vivo* (Table 2.7, Figure 2.6). This confirms the results from the functional category (SAFE) analysis which predicted that branching morphogenesis would be affected by pyrethroids. This was based on dose-dependent patterns of gene expression for mRNA transcripts that code proteins which have been shown to control neurite branching and morphogenesis in the nervous system. These genes include *Cxcl12, Notch1,* β-catenin and *Camk1g* (Redmond et al. 2000; Yu and Malenka 2003; Pujol et al. 2005; Wayman et al. 2006; Takemoto-Kimura et al. 2007). A majority of the studies concerning the function of this group of genes focused on their role in developmental neuronal morphogenesis. Therefore, a development model of neurite growth was used to assess pyrethroid effects on neuronal branching. The gene expression data from the present study support that pyrethroid effects on neurite branching and not length may be due to increased expression of a suite of genes that shifts the growth pattern of neurons away from extension of neuronal processes and more towards neurite branching. Overexpression of *Notch1* in rat cortical neurons results in an increase in neuronal branching and an antagonism of neurite extension (Redmond et al. 2000).

Likewise, overexpression of β-catenin and *Cxcl12* results in increased dendritic and axonal branch tip number, respectively and has no or opposite effects on measures of length (Yu and Malenka 2003; Pujol et al. 2005). All of these transcripts are upregulated following pyrethroid exposure *in vivo* (see Figure 2.5 heatmaps). The exact cellular mechanisms that mediate pyrethroid-induced increases in branching are currently unknown.

The present data support that pyrethroids affect the developmental morphogenesis of neurons. However, these data are not consistent with the results of previous studies of pyrethroid effects on developmental neuronal outgrowth. Treatment of developing *X. laevis* neurons with 10 nM deltamethrin resulted in an increase in total neurite length in the presence of extracellular Ca^{+2} (Lautermilch and Spitzer 2000). In contrast, exposure of N2A neuroblastoma or C6 glioma cells the pyrethroid cypermethrin resulted in no effect on morphology (Flaskos et. al 2007). The disparity between the results from these studies and the present study could be due to differences in the compounds tested, exposure conditions and cell types. Preliminary experiments in PC-12 neuroblastoma cells (*data not shown*) did not demonstrate any effects on neurite branching or length. This supports the observations of Flaskos et al. (2007) and indicates a disparity between different cell culture models for detecting pyrethroid effects on neuronal morphology. The present data is the first to demonstrate an effect of pyrethroids on the branching morphology of primary cultured neurons.

Disruption of neuronal morphogenesis in the developing nervous system by pyrethroids could result in detrimental effects on neurological function later in life. Intermittent exposure to stimulant drugs such as amphetamine can produce an increase in dendritic branching *in vivo* in both juvenile and adult rats (Robinson and Kolb 2004; Diaz

Heijtz et al. 2003; Robinson and Kolb 1999). These morphological changes are thought to underlie some of the adverse neurological effects associated with abuse of stimulant drugs (e.g., learning deficits) (see Robinson and Kolb 2004; Gonzalez et al. 2005). In addition, lead exposure during development results in neurological deficits that have been associated with changes in neuronal morphology (Petit and LeBoutillier 1979; McConnell and Berry 1979; Costa et al. 2004). Both lead and stimulant drugs facilitate neurite outgrowth in *in vitro* cell culture models that is similar, but not identical, to the increased branching observed with pyrethroids in the present study (Kern et al. 1993; Audesirk and Cabell 1999; Crumpton et al. 2001; Park et al. 2002; Park et al. 2003). Collectively, these works demonstrate that *in vitro* models of neuronal outgrowth are sensitive to neurotoxic agents that produce neurological deficits and consequent changes in neuronal morphology *in vivo*. Several questions remain to be addressed before definitive conclusions regarding pyrethroid effects on neuronal morphogenesis can be made, including: 1) whether or not pyrethroid-induced changes in morphology occur *in vivo*, 2) are effects on morphogenesis specific to cortical neurons, and 3) do all compounds in the pyrethroid class produce the same types of effects on neuronal branching morphogenesis?

In conclusion, the present study has identified a group of genes whose transcription is altered in a dose-dependent manner in the rat cortex following *in vivo* pyrethroid exposure. A majority of the gene expression changes observed in this study are consistent with the induction of neuronal hyperexcitability by pyrethroids. The gene expression changes observed are transient, comparable between the two pyrethroids tested and provide insight into the cellular response of the neurons downstream of the pharmacological effects of these compounds at the neuronal membrane. Most importantly, this study provides evidence that

branching of cortical neurons is increased by pyrethroids, suggesting that neurotoxic action of these compounds includes effects on neuronal morphology.

Supplementary Data.

Appendix A, Table 1 compares coefficients of variation for probe set expression summaries using either GCOSv1.2 or RMA. Appendix A, Table 2 provides assay identification numbers, context sequences, amplicon lengths and calculated amplification efficiencies for Applied Biosystems TaqMan® qRT-PCR assays used in this study. Appendix A, Figure 1 is a comparison of rank order of significance between SAM-based linear regression and Benjamini-Hochberg adjusted ANOVA analysis methods.

Funding.

J.A. Harrill was currently funded through the EPA/UNC Toxicology Research Program, Training Agreement (CR833237) during this work and previously funded through National Institute of Environmental Health Science Training Grant (T32-ES07126).

Acknowledgements.

This document has been reviewed by the National Health and Environmental Effects Research Laboratory and approved for publication. Approval does not signify that the contents reflect the views of the agency, nor does mention of trade names or commercial products constitute endorsement or recommendation for use. The authors would like to thank Drs. Susan Hester and Ram Ramabhadran for comments on a previous version of this manuscript.

Table 2.1. *Group sizes of cohorts used in this study.*

		Permethrin				Deltamethrin		
Dose (mg/kg) :	**Vehicle**	**1.0**	**10.0**	**40.0**	**100.0**	**0.3**	**1.0**	**3.0**
EDL :	**Control**	**<NOAEL**	**NOAEL**	**ED_{30}**	**ED_{50}**	**<NOAEL**	**NOAEL**	**ED_{30}**
Microarray Dose Response [a]								
Cohort 1	6	3	3		3	3	3	3
Cohort 2	6	5	5		5	5	5	5
qRT-PCR Dose-Response [b]								
Cohort 3	7	7	7	7	7			
	7					7	7	7
qRT-PCR Time Course [c]								
Cohort 4	8_4				8_4			
	8_4							8_4

[a] Microarray data from Cohorts 1 & 2 were combined (n=8 / treatment group) with control values from cohorts 1 & 2 (n=12) for dose-response analysis of permethrin and deltamethrin mediated effects, respectively. [b] Test animals in Cohort 3 were split into two dose-response studies for permethrin and deltamethrin, respectively, for qRT-PCR confirmation of gene expression changes observed during the microarray study. [C] Test animals in Cohort 4 were used for qRT-PCR time course studies. Four time points (1,3,6,9 hours: n = 8 / treatment group) per compound with time matched controls (n = 8 / control group).

Table 2.2. ***List of probe sets with dose-dependent changes in expression for deltamethrin.*** Affymetrix probe set IDs without a gene symbol are expressed sequence tags (ESTs). Probe sets with arrows correspond to genes examined by qRT-PCR. Positive SAM d_i or PIR *M* scores denote upregulated probe sets. Negative SAM d_i or PIR *M* scores denote downregulated probe sets.

	Affymetrix			Linear Regression (SAM)			Isotonic Regression (PIR)			ANOVA
	Gene ID	GenBank	Gene Symbol	Score(d_i)	*p*-value	*q*-value	*M*	*p*-value	*q*-value	*p*-value
➡	1371363_at	BI277042	Gpd1	5.63	0.0000	0.00	2.34	0.0000	0.24	0.0032
➡	1388901_at	AW534837	Fkpb51	5.46	0.0000	0.00	2.21	0.0000	0.42	0.0051
➡	1367577_at	NM_031970	Hsp27	4.60	0.0001	0.00	1.90	0.0002	0.97	0.0195
➡	1369560_at	NM_022215	Gpd1	4.53	0.0001	0.00	1.91	0.0002	1.00	0.0134
	1373415_at	AI407050		4.37	0.0001	0.00	1.80	0.0004	1.00	0.0195
➡	1368064_a_at	U31884	Ddc	-4.35	0.0001	0.14	-1.95	0.0002	1.00	0.0195
➡	1391229_at	BG381458	Camk1g	4.22	0.0002	0.00	2.11	0.0000	0.51	0.0063
➡	1393128_at	BI288424	RGD1311086	4.13	0.0002	0.00	1.76	0.0005	1.00	0.0205
➡	1380611_at	BI284255	Fkpb51	3.90	0.0004	0.11	1.62	0.0012	1.00	0.0276
	1390659_at	BI302830		3.82	0.0005	0.11	1.49	0.0028	1.00	0.0276
	1392492_at	AA956982		3.70	0.0007	0.11	1.66	0.0009	1.00	0.0276
	1369303_at	NM_031019	Crh	3.62	0.0009	0.11	1.73	0.0006	1.00	0.0276
	1389159_at	BM385437		3.56	0.0011	0.18	1.47	0.0031	1.00	0.0319
	1375199_at	BG378641		3.54	0.0011	0.18	1.41	0.0045	1.00	0.0295
	1390449_at	BI289132		3.48	0.0013	0.19	1.64	0.0011	1.00	0.0295
	1388271_at	BM383531	LOC689415	3.48	0.0013	0.19	1.44	0.0037	1.00	0.0300
	1384396_at	AI144852		3.45	0.0014	0.19	1.62	0.0012	1.00	0.0276
	1390606_at	BI289052	RGD1564108_predicted	-3.42	0.0015	0.14	-1.82	0.0004	1.00	0.0276
	1382619_at	AI072460		3.39	0.0017	0.19	1.60	0.0013	1.00	0.0276
	1370989_at	AI639318	Ret	3.38	0.0017	0.19	1.49	0.0028	1.00	0.0300
	1391805_at	BE096676	RGD1310364_predicted	3.29	0.0022	0.29	1.50	0.0027	1.00	0.0300
	1370026_at	NM_012935	Cryab	3.28	0.0022	0.29	1.46	0.0032	1.00	0.0364
	1381693_at	AW526413		-3.24	0.0024	0.14	-1.39	0.0046	1.00	0.0364
	1374626_at	BG371585	Lrg1	3.23	0.0025	0.33	1.45	0.0036	1.00	0.0323
	1378261_at	BE102806		3.15	0.0030	0.41	1.29	0.0089	1.00	0.0429
	1373354_at	BF418347		3.14	0.0031	0.41	1.51	0.0025	1.00	0.0299
	1372761_at	AI228076		3.09	0.0035	0.41	1.29	0.0088	1.00	0.0467
	1378008_at	BF417386		3.08	0.0037	0.51	1.60	0.0014	1.00	0.0276

1376709_at	BM388442	Slc39a8	-3.07	0.0038	0.14	-1.49	0.0026	1.00	0.0364
1368650_at	NM_031135	Klf10	-3.07	0.0038	0.14	-1.30	0.0077	1.00	0.0356
1368891_at	AI014001		3.03	0.0041	0.51	1.34	0.0066	1.00	0.0460
1380329_at	AI717253	Tmem10	-3.03	0.0041	0.14	-1.28	0.0086	1.00	0.0496
1373298_at	BI288011		3.03	0.0042	0.51	1.49	0.0027	1.00	0.0351
1376928_at	BE106737		3.03	0.0042	0.51	1.41	0.0045	1.00	0.0295
1372564_at	AI411375	Ets2	3.03	0.0042	0.51	1.41	0.0045	1.00	0.0396
1382188_at	BF397703	RGD1311086	3.02	0.0042	0.51	1.40	0.0048	1.00	0.0345
1380682_at	BF396302	Rkhd3_predicted	2.99	0.0045	0.51	1.45	0.0035	1.00	0.0329
1370454_at	AB003726		2.99	0.0046	0.51	1.32	0.0075	1.00	0.0369
1388522_at	AI170820	RGD1310383_predicted	2.97	0.0048	0.51	1.40	0.0047	1.00	0.0356
1389507_at	AI072446	Nedd4l	2.97	0.0048	0.51	1.42	0.0043	1.00	0.0306
1372491_at	AI229647	RGD1565591_predicted	2.92	0.0054	0.56	1.19	0.0159	1.00	0.0442
1375138_at	AA893169	Timp3	2.92	0.0054	0.56	1.22	0.0134	1.00	0.0319
1371922_at	AI169140		2.91	0.0056	0.56	1.28	0.0098	1.00	0.0402
1374419_at	AI044435		2.90	0.0057	0.56	1.53	0.0021	1.00	0.0306
1372966_at	AI178784	RGD1310174_predicted	2.89	0.0059	0.56	1.23	0.0128	1.00	0.0476
1383665_at	BE096055	Lpin2_predicted	2.86	0.0063	0.59	1.21	0.0142	1.00	0.0496
1384841_at	AA858815		-2.86	0.0064	0.14	-1.46	0.0031	1.00	0.0421
1385892_at	AA900322		2.84	0.0067	1.15	1.40	0.0046	1.00	0.0276
1390163_at	BF282174		2.83	0.0068	1.15	1.38	0.0052	1.00	0.0440
1370530_a_at	AB000779	Pld1	-2.81	0.0071	0.14	-1.34	0.0062	1.00	0.0493
1385778_at	BF409913	Siat7E	2.79	0.0075	1.15	1.38	0.0055	1.00	0.0276
1388401_at	BI296155	Finb_predicted	2.79	0.0076	1.15	1.17	0.0180	1.00	0.0429
1395986_at	BF391439	Slit2	-2.78	0.0077	0.14	-1.27	0.0094	1.00	0.0419
1382186_a_at	AI136314	RGD1311086	2.77	0.0078	1.15	1.15	0.0204	1.00	0.0442
1369973_at	NM_017154	Xdh	2.76	0.0080	1.15	1.18	0.0167	1.00	0.0472
1393337_at	AW524476	Tcfcp2l1_predicted	2.73	0.0088	1.16	1.37	0.0056	1.00	0.0276
1382225_at	BF284510		2.72	0.0090	1.16	1.28	0.0095	1.00	0.0427
1368438_at	NM_022236	Pde10a	2.70	0.0094	1.16	1.11	0.0255	1.00	0.0496
1387260_at	NM_053713	Klf4	-2.69	0.0096	0.14	-1.49	0.0026	1.00	0.0429
1372356_at	BI285307	Usp54	2.69	0.0097	1.16	1.12	0.0240	1.00	0.0442
1371442_at	BI282904	Hyou1	2.68	0.0099	1.16	1.03	0.0384	1.00	0.0467

	1375296_at	AI407178	LOC684097	2.66	0.0105	1.16	1.40	0.0047	1.00	0.0427
	1398899_at	AI170414	Polr2c	2.64	0.0110	1.16	1.67	0.0009	1.00	0.0195
	1380835_at	BF389476	RGD1565346_predicted	2.62	0.0115	1.16	1.38	0.0053	1.00	0.0467
➡	1377518_at	AW251224	Camk1g	2.59	0.0123	1.16	1.29	0.0090	1.00	0.0315
	1375761_at	AW532391		2.57	0.0128	1.16	1.36	0.0061	1.00	0.0356
	1383861_at	BF394135		2.57	0.0129	1.16	1.35	0.0065	1.00	0.0306
	1392321_at	BE120641		2.57	0.0130	1.16	1.29	0.0092	1.00	0.0467
	1372090_at	AI231566	Max	2.53	0.0143	1.16	1.31	0.0080	1.00	0.0306
	1397261_at	AI547508	Max	-2.50	0.0152	0.14	-1.42	0.0040	1.00	0.0295
	1376768_at	BM386807		2.40	0.0191	1.16	1.52	0.0023	1.00	0.0276
	1381557_at	BI289045	Gna14	2.35	0.0216	1.16	1.29	0.0087	1.00	0.0442
	1397677_at	AI501069		-2.30	0.0243	0.14	-1.42	0.0039	1.00	0.0467
	1398373_at	AA799400	B3galt3	2.29	0.0248	1.16	1.29	0.0091	1.00	0.0396
	1395253_at	BE107893		-2.25	0.0273	0.14	-1.39	0.0046	1.00	0.0388
	1372037_at	AI104117	Pdlm7	2.18	0.0319	1.16	1.28	0.0098	1.00	0.0351
	1382112_at	BM385698	LOC682926	-2.16	0.0333	1.15	-1.26	0.0096	1.00	0.0344
	1397229_at	BF565781		-2.15	0.0342	1.15	-1.26	0.0095	1.00	0.0295
	1391147_at	BF404398		-2.13	0.0354	1.15	-1.36	0.0056	1.00	0.0427
	1397198_at	BE111113		-2.13	0.0361	1.15	-1.26	0.0096	1.00	0.0427
	1396401_at	AW433899		2.11	0.0377	1.16	1.47	0.0031	1.00	0.0319
	1385821_at	BF392004		-2.09	0.0390	1.15	-1.55	0.0019	1.00	0.0300
	1384959_at	BI295935		2.03	0.0449	1.16	1.41	0.0045	1.00	0.0295
	1372448_at	D86711	Medl19_predicted	2.01	0.0467	1.16	1.36	0.0060	1.00	0.0276
	1376463_at	AA955579		-1.97	0.0510	1.15	-1.33	0.0067	1.00	0.0402
	1386344_at	BG662519		1.97	0.0511	1.16	1.29	0.0089	1.00	0.0295
	1395169_at	BF388779	Zcch8_predicted	1.96	0.0516	1.16	1.29	0.0092	1.00	0.0442
	1375752_at	AI577874	Bves	-1.96	0.0519	1.15	-1.41	0.0042	1.00	0.0376
	1370869_at	AI102790	Bcat1	1.92	0.0561	1.16	1.28	0.0096	1.00	0.0345
	1367706_at	NM_031353	Vdac1	1.74	0.0820	1.16	1.29	0.0090	1.00	0.0295
	1385645_at	AA875088		-1.73	0.0827	1.15	-1.32	0.0069	1.00	0.0295
	1377514_at	BF413478		-1.59	0.1087	1.15	-1.30	0.0079	1.00	0.0295
	1380905_at	AA893260		-1.56	0.1162	1.15	-1.72	0.0007	1.00	0.0276
	1393978_at	BF415134	Stfa2_predicted	1.40	0.1564	1.16	1.32	0.0077	1.00	0.0223
	1396505_at	BE113909		-0.64	0.5102	1.15	-1.27	0.0090	1.00	0.0254

Table 2.3. ***List of probe sets with dose-dependent changes in expression for permethrin.*** Affymetrix probe set IDs without a gene symbol are expressed sequence tags (ESTs). Probe sets with arrows correspond to genes examined by qRT-PCR. Positive SAM d_i or PIR *M* scores denote upregulated probe sets. Negative SAM d_i or PIR *M* scores denote downregulated probe sets.

	Affymetrix			Linear Regression (SAM)			Isotonic Regression (PIR)			ANOVA
	Gene ID	**GenBank**	**Gene Symbol**	**Score(d_i)**	***p*-value**	***q*-value**	***M***	***p*-value**	***q*-value**	***p*-value**
	1393119_at	BM388725		5.20	0.0000	0.00	2.22	0.0000	0.96	0.0050
	1373415_at	AI407050		4.89	0.0001	0.00	2.06	0.0001	1.00	0.0050
	1390412_at	AI229664	Slc40a1	-3.50	0.0006	0.18	-1.70	0.0016	1.00	0.0050
	1373035_at	AI031032		4.76	0.0001	0.00	1.96	0.0002	1.00	0.0078
	1373298_at	BI288011		4.22	0.0001	0.00	2.08	0.0001	1.00	0.0078
	1369303_at	NM_031019	Crh	4.26	0.0001	0.00	1.92	0.0003	1.00	0.0113
	1391901_at	AA956085		4.19	0.0002	0.00	1.84	0.0005	1.00	0.0139
	1374610_at	AI599365		4.06	0.0002	0.00	1.91	0.0003	1.00	0.0139
	1395303_at	BF397734		-0.80	0.3465	0.69	-1.48	0.0041	1.00	0.0139
	1396401_at	AW433899		0.71	0.4017	1.32	1.44	0.0038	1.00	0.0139
	1392791_at	AA964492		3.88	0.0003	0.00	1.65	0.0012	1.00	0.0170
➡	1368677_at	NM_012513	Bdnf	3.85	0.0003	0.00	1.52	0.0025	1.00	0.0170
➡	1370415_at	AF002251	Rassf5	3.37	0.0008	0.12	1.85	0.0004	1.00	0.0170
	1393389_at	BF396237		3.25	0.0011	0.18	1.39	0.0049	1.00	0.0170
➡	1375043_at	BF415939	c-fos	3.23	0.0012	0.18	1.41	0.0045	1.00	0.0170
	1379910_at	AI136097	RGD1561967_predicted	2.79	0.0037	0.55	1.42	0.0043	1.00	0.0170
	1398464_at	AI575255		-2.58	0.0066	0.69	-1.38	0.0067	1.00	0.0170
	1389090_at	BI284350	Wrnip1	1.32	0.1319	0.79	1.30	0.0079	1.00	0.0170
	1381557_at	BI289045	Gna14	2.67	0.0052	0.61	1.87	0.0004	1.00	0.0176
	1376602_a_at	AI030899	Fbxo22	0.89	0.2974	1.32	1.27	0.0096	1.00	0.0186
	1387025_at	NM_019234	Dync1i1	2.76	0.0041	0.55	1.29	0.0085	1.00	0.0208
	1370454_at	AB003726		3.85	0.0003	0.00	1.15	0.0185	1.00	0.0215
	1395197_at	BI293027		-3.61	0.0005	0.18	-1.75	0.0013	1.00	0.0230
➡	1368321_at	NM_012551	Egr1	2.87	0.0030	0.50	1.21	0.0132	1.00	0.0230
	1375986_at	AI103155		2.83	0.0034	0.50	1.59	0.0017	1.00	0.0230
	1372019_at	AI231789	RGD1310128_predicted	2.62	0.0059	0.69	1.35	0.0061	1.00	0.0230
	1390716_at	BE098148		-1.87	0.0401	0.69	-1.55	0.0031	1.00	0.0230

	1397745_at	BF414336		-0.91	0.2860	0.69	-1.43	0.0051	1.00	0.0230
	1387024_at	NM_053883	Dusp6	2.59	0.0064	0.75	1.01	0.0398	1.00	0.0230
	1372363_at	BF404414	RGD1561203_predicted	2.54	0.0073	0.79	1.33	0.0067	1.00	0.0230
	1374787_at	BI282169		2.50	0.0081	0.79	1.34	0.0064	1.00	0.0230
	1382275_at	AI236989	MGC125015	2.24	0.0158	0.79	1.46	0.0034	1.00	0.0230
	1383685_at	BI276972	Heatr1_predicted	1.54	0.0836	0.79	1.32	0.0072	1.00	0.0230
	1381400_at	AI137973		1.42	0.1080	0.79	1.33	0.0068	1.00	0.0230
	1380509_at	AW253985		1.37	0.1193	0.79	1.40	0.0047	1.00	0.0230
	1369067_at	NM_031628	Nr4a3	2.77	0.0040	0.55	1.15	0.0187	1.00	0.0270
	1395272_at	BF394456	LOC682937	-1.88	0.0394	0.69	-1.33	0.0084	1.00	0.0305
	1385778_at	BF409913	Siat7E	2.36	0.0116	0.79	1.43	0.0041	1.00	0.0305
	1391301_at	AA997499	LOC682355	0.51	0.5404	1.32	1.35	0.0062	1.00	0.0305
	1371731_at	AI408151	RGD1566215_predicted	3.13	0.0015	0.28	1.44	0.0038	1.00	0.0315
	1378407_at	BF401415		2.28	0.0145	0.79	1.29	0.0083	1.00	0.0315
	1392108_at	BF390648		2.85	0.0032	0.50	1.34	0.0064	1.00	0.0347
	1382225_at	BF284510		3.29	0.0010	0.12	1.50	0.0028	1.00	0.0349
	1381070_at	AI233106		2.01	0.0286	0.79	1.51	0.0026	1.00	0.0351
	1367652_at	AI713966	Igfpb3	1.38	0.1190	0.79	1.35	0.0063	1.00	0.0358
	1395991_at	BE107556	Rimbp2	3.11	0.0016	0.28	1.39	0.0050	1.00	0.0400
	1372998_at	BG381555		2.45	0.0094	0.79	1.20	0.0144	1.00	0.0405
	1384884_at	AW528484	RGD1307595_predicted	1.18	0.1755	1.32	1.35	0.0060	1.00	0.0405
	1382613_at	AW144049		-2.68	0.0051	0.69	-1.50	0.0039	1.00	0.0408
	1388911_at	AI177134	Prim2	2.50	0.0082	0.79	1.45	0.0036	1.00	0.0408
	1396747_at	BE121159		2.33	0.0128	0.79	1.32	0.0071	1.00	0.0428
	1376616_at	BF551036		-2.40	0.0107	0.69	-1.36	0.0071	1.00	0.0429
	1388583_at	BF283398	Cxcl12	2.92	0.0027	0.42	1.36	0.0057	1.00	0.0477

Table 2.4. *qRT-PCR confirmation of transcripts identified as dose-responsive.*

	Deltamethrin				Permethrin				
Dose (mg/kg) :	**V[a]**	**0.3**	**1**	**3**	**V[a]**	**1**	**10**	**40**	**100**
[b]EDL:	**Control**	**sub-NOAEL**	**NOAEL**	**ED_{30}**	**Control**	**sub-NOAEL**	**NOAEL**	**ED_{30}**	**ED_{50}**
Camk1g	**1.03 ± 0.10**	**1.23 ± 0.18**	**1.40 ± 0.18***	**1.57 ± 0.14***	**1.04 ± 0.13**	**1.05 ± 0.14**	**1.97 ± 0.28***	**1.76 ± 0.32***	**1.72 ± 0.30***
1391229_at	*1.00 ± 0.04*	*1.10 ± 0.03*	*1.26 ± 0.07*	*1.31 ± 0.06*	*1.00 ± 0.04*	*1.16 ± 0.10*	*1.09 ± 0.05*		*1.25 ± 0.09*
1377518_at	*1.00 ± 0.05*	*1.07 ± 0.08*	*1.40 ± 0.12*	*1.36 ± 0.16*	*1.00 ± 0.05*	*1.20 ± 0.13*	*1.09 ± 0.09*		*1.45 ± 0.17*
Ddc	**1.01 ± 0.06**	**0.79 ± 0.06**	**0.89 ± 0.07**	**0.70 ± 0.05***	**1.04 ± 0.12**	**0.97 ± 0.10**	**0.91 ± 0.10**	**0.81 ± 0.11***	**0.71 ± 0.09***
1368064_a_at	*1.00 ± 0.03*	*0.96 ± 0.04*	*0.90 ± 0.05*	*0.80 ± 0.03*	*1.00 ± 0.03*	*1.04 ± 0.04*	*1.01 ± 0.04*		*1.00 ± 0.05*
Gpd1	**1.06 ± 0.13**	**1.16 ± 0.13**	**1.04 ± 0.12**	**2.04 ± 0.28***	**1.04 ± 0.14**	**0.94 ± 0.07**	**0.97 ± 0.06**	**1.24 ± 0.15**	**1.23 ± 0.13**
1371363_at	*1.00 ± 0.11*	*0.88 ± 0.07*	*1.42 ± 0.17*	*1.94 ± 0.19*	*1.00 ± 0.11*	*1.03 ± 0.10*	*1.03 ± 0.09*		*1.19 ± 0.18*
1369560_at	*1.00 ± 0.08*	*0.88 ± 0.05*	*1.25 ± 0.13*	*1.55 ± 0.14*	*1.00 ± 0.08*	*0.98 ± 0.09*	*0.95 ± 0.10*		*1.12 ± 0.16*
Fkbp51	**1.01 ± 0.06**	**0.92 ± 0.06**	**1.02 ± 0.07**	**1.52 ± 0.14***	**1.02 ± 0.09**	**1.03 ± 0.09**	**1.00 ± 0.06**	**0.95 ± 0.07**	**1.03 ± 0.12**
1388901_at	*1.00 ± 0.05*	*1.00 ± 0.03*	*1.17 ± 0.05*	*1.41 ± 0.09*	*1.00 ± 0.05*	*0.92 ± 0.05*	*1.06 ± 0.03*		*1.07 ± 0.05*
1380611_at	*1.00 ± 0.04*	*1.04 ± 0.07*	*1.16 ± 0.08*	*1.35 ± 0.10*	*1.00 ± 0.04*	*0.96 ± 0.07*	*0.99 ± 0.06*		*1.07 ± 0.09*
c-fos	**1.19 ± 0.27**	**0.63 ± 0.14**	**1.09 ± 0.43**	**0.54 ± 0.08***	**1.09 ± 0.21**	**1.49 ± 0.25**	**1.30 ± 0.22**	**0.91 ± 0.11**	**1.25 ± 0.27**
1375043_at	*1.00 ± 0.16*	*1.01 ± 0.31*	*0.72 ± 0.12*	*0.69 ± 0.06*	*1.00 ± 0.16*	*0.54 ± 0.07*	*0.57 ± 0.08*		*1.56 ± 0.34*
Egr1	**1.04 ± 0.12**	**0.81 ± 0.05**	**0.90 ± 0.16**	**0.87 ± 0.07**	**1.01 ± 0.07**	**1.10 ± 0.10**	**1.10 ± 0.11**	**1.09 ± 0.08**	**1.12 ± 0.10**
1368321_at	*1.00 ± 0.08*	*0.93 ± 0.09*	*0.95 ± 0.08*	*0.98 ± 0.06*	*1.00 ± 0.08*	*0.77 ± 0.02*	*0.89 ± 0.09*		*1.19 ± 0.08*
BDNF	**1.07 ± 0.18**	**0.78 ± 0.12**	**0.91 ± 0.11**	**1.02 ± 0.10**	**1.08 ± 0.17**	**1.06 ± 0.14**	**1.27 ± 0.22**	**0.83 ± 0.12**	**1.09 ± 0.11**
1368678_at	*1.00 ± 0.02*	*1.00 ± 0.02*	*0.98 ± 0.01*	*0.99 ± 0.02*	*1.00 ± 0.02*	*0.99 ± 0.01*	*0.96 ± 0.02*		*1.04 ± 0.03*
1368677_at	*1.00 ± 0.06*	*1.16 ± 0.10*	*1.09 ± 0.07*	*1.16 ± 0.06*	*1.00 ± 0.06*	*0.91 ± 0.08*	*0.91 ± 0.06*		*1.39 ± 0.14*
Hsp27	**1.06 ± 0.17**	**0.77 ± 0.06**	**0.96 ± 0.12**	**1.12 ± 0.12**	**1.01 ± 0.05**	**0.95 ± 0.13**	**0.96 ± 0.10**	**1.14 ± 0.13**	**1.19 ± 0.24**
1367577_at	*1.00 ± 0.09*	*1.00 ± 0.07*	*1.15 ± 0.05*	*1.41 ± 0.05*	*1.00 ± 0.09*	*1.14 ± 0.12*	*1.10 ± 0.06*		*1.31 ± 0.19*
Rassf5	**1.00 ± 0.02**	**0.90 ± 0.06**	**0.98 ± 0.05**	**1.08 ± 0.07**	**1.02 ± 0.08**	**1.00 ± 0.06**	**0.95 ± 0.04**	**0.92 ± 0.06**	**1.08 ± 0.05**
1370415_at	*1.00 ± 0.02*	*1.11 ± 0.06*	*1.11 ± 0.06*	*1.15 ± 0.05*	*1.00 ± 0.02*	*1.11 ± 0.06*	*1.11 ± 0.04*		*1.23 ± 0.05*

Bold values are $2^{-\Delta\Delta CT}$ values (± SE) from qRT-PCR Cohorts 3 (DLT) & 4 (PERM). Values in italics are fold-change from control (± SE) for microarray probe sets (Cohorts 1 & 2) corresponding to the transcript of interest. All gene expression measurements were at 6 h following pyrethroid exposure. [a]V = Vehicle control. [b]EDL = Equipotent Dose Level, defined from Wolansky et al (2006) – see methods section. Main effects in two-way ANOVA: **RED** = EDL (p <0.05) and COMPOUND*EDL (p > 0.05), **GREEN** = COMPOUND (p < 0.05) and COMPOUND*EDL (p > 0.05), **BLUE** = COMPOUND*EDL (p <0.05) and main effect of DOSE in a one-way ANOVA for deltamethrin. *= Significant difference from vehicle control in a Dunnett's mean contrast test (p <0.05).

Table 2.5. ***Two-way analysis of variance (ANOVA) for qRT-PCR time course data.***

Gene Name	Factor	3 mg/kg Deltamethrin *F*	*p*-value	Pair Wise	100 mg/kg Permethrin *F*	*p*-value	Pair Wise
Camk1g	TRT	4.56	0.0371**	3 h	2.16	0.1472	n.e.
	TIME	1.75	0.1665		1.14	0.3391	
	TRT*TIME	2.07	0.1140		0.54	0.6586	
Gpd1	TRT	17.56	n/a	3,6 h	12.76	0.0007**	6 h
	TIME	4.05	n/a		1.55	0.2126	
	TRT*TIME	4.44	0.0072**		1.42	0.2465	
Ddc	TRT	4.48	0.0387	6,9 h	0.01	0.9419	n.e.
	TIME	1.78	0.1620		1.01	0.3970	
	TRT*TIME	2.17	0.1025		0.91	0.4438	
c-fos	TRT	5.78	n/a	3 h	10.66	0.0019**	3 h
	TIME	6.35	n/a		2.99	0.0386**	
	TRT*TIME	6.26	0.0010**		1.56	0.2014	
Egr1	TRT	7.63	n/a	3 h	26.12	n/a	3,6 h
	TIME	10.43	n/a		8.26	n/a	
	TRT*TIME	7.62	0.0002**		8.40	0.0001**	
BDNF	TRT	0.14	0.7110	n.e.	2.04	0.1587	n.e.
	TIME	0.29	0.8358		1.24	0.3052	
	TRT*TIME	0.22	0.8814		0.69	0.5633	

Two-way ANOVA factors are: TIME, TRT, TIME*TRT. Analysis of $2^{-\Delta\Delta CT}$ values is presented. n.e. = no effect. n/a = not applicable. ** = significant effect at $p < 0.05$. Pair-wise comparisons are within time for a main effect of treatment ($p < 0.05$).

Table 2.6. *Significant Analysis of Function and Expression (SAFE).*

Category I.D. and name	size*	DLT *p*-value	PERM *p*-value
Part I. Commonly enriched gene categories for both permethrin and deltamethrin‡			
GO Biological Process			
GO:0048754, 'branching morophogenesis of a tube'	66	0.0171	2.00E-04
GO:0001763, 'morphogenesis of a branching structure'	67	0.0172	2.00E-04
GO:0007162, 'negative regulation of cell adhesion'	27	0.0175	0.0025
GO:0015718, 'monocarboxylic acid transport'	30	0.0051	0.0125
GO:0007498, 'mesoderm development'	57	0.0105	0.0067
GO Cellular Component			
GO:0005954, 'calcium- and calmodulin-dependent protein kinase complex'	25	0.0053	0.0146
GO Molecular Function			
GO:0046915, 'transition metal ion transporter activity'	44	0.0026	0.0348

Category I.D. and name	size*	*p*-value**
Part II. Enriched gene categories identified by SAFE.		
Deltamethrin		
KEGG Pathway		
KEGG:00564, 'Glycerophospholipid metabolism'	73	0.0404
KEGG:00400, 'Phenylalanine, tyrosine and tryptophan biosynthesis	12	0.0928
Permethrin		
GO Biological Process		
GO:0048754, 'branching morphogenesis of a tube'	66	0.0349
GO:0001763, 'morphogenesis of a branching structure'	67	0.0349
GO:0001569, 'patterning of blood vessels'	31	0.0406
GO:0009880, 'embryonic pattern specification'	49	0.0554
GO:0045655, 'regulation of monocyte differentiation'	32	0.0932

‡ = GO catergories or KEGG pathways with $p < 0.1$ for both test compounds using SAFE & Fisher's χ^2 method. * = number of Affymetrix probe sets included in GO category or KEGG pathway groupings.
** = GO categories or KEGG pathways with an adjusted $p < 0.1$ for SAFE method.

Table 2.7. ***Pharmacokinetic estimates of pyrethroid brain concentrations.***

	Administered Dose (mg/kg)	Time (h)	Brain Concentration (μM)
Deltamethrin[a]	0.3	6	0.005
	1	6	0.0169
	3	6	0.050
Permethrin[b]	1	6	0.060
	10	6	0.582
	100	6	5.940

[a] Estimates based on Mirfazaelian et al. (2006).
[b] Estimates based on Tornero-Velez et al. (2007).

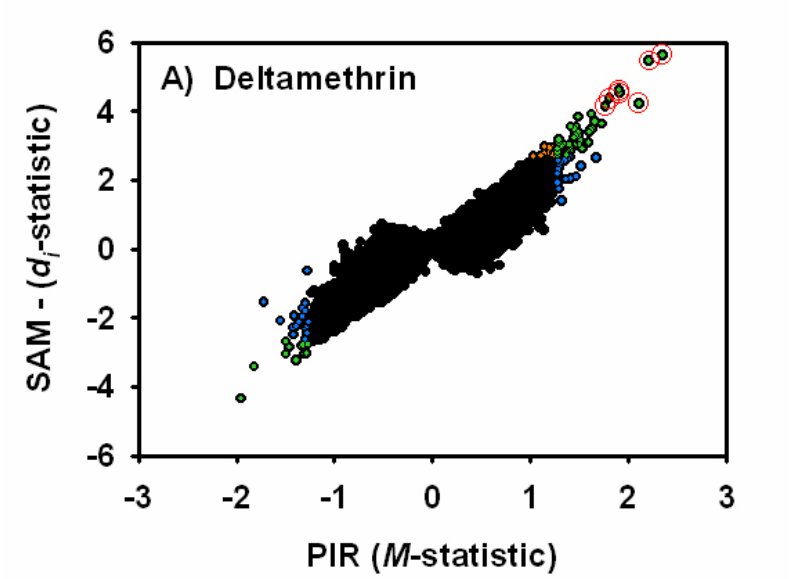

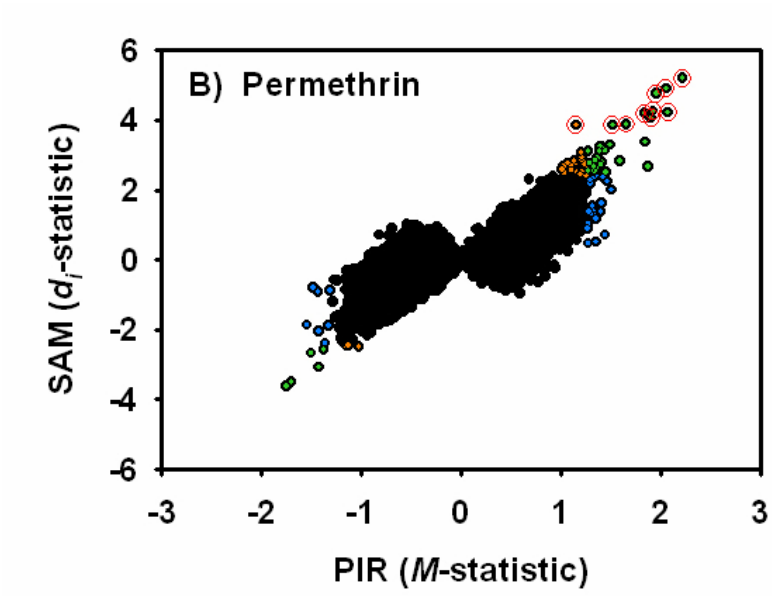

Figure 2.1. ***Comparison of PIR and SAM regression methods.*** Panels A & B plot the penalized isotonic regression (PIR) test statistic (*M*, *x*-axis) against the penalized linear regression (SAM) test statistic (d_i, *y*-axis) for deltamethrin and permethrin, respectively. All 31,042 probe sets present on the Affymetrix Rat 230 2.0 array are shown. Data points in green have an empirical *p*-value < 0.01 for both the PIR and SAM methods. Data points in blue have an empirical *p*-value < 0.01 for the PIR regression only. Data points in orange have an empirical *p*-value < 0.01 for the SAM regression only. Data points circled in red have a *q*-value < 0.10 in permutation-based *FDR* calculations employed in the SAM algorithm.

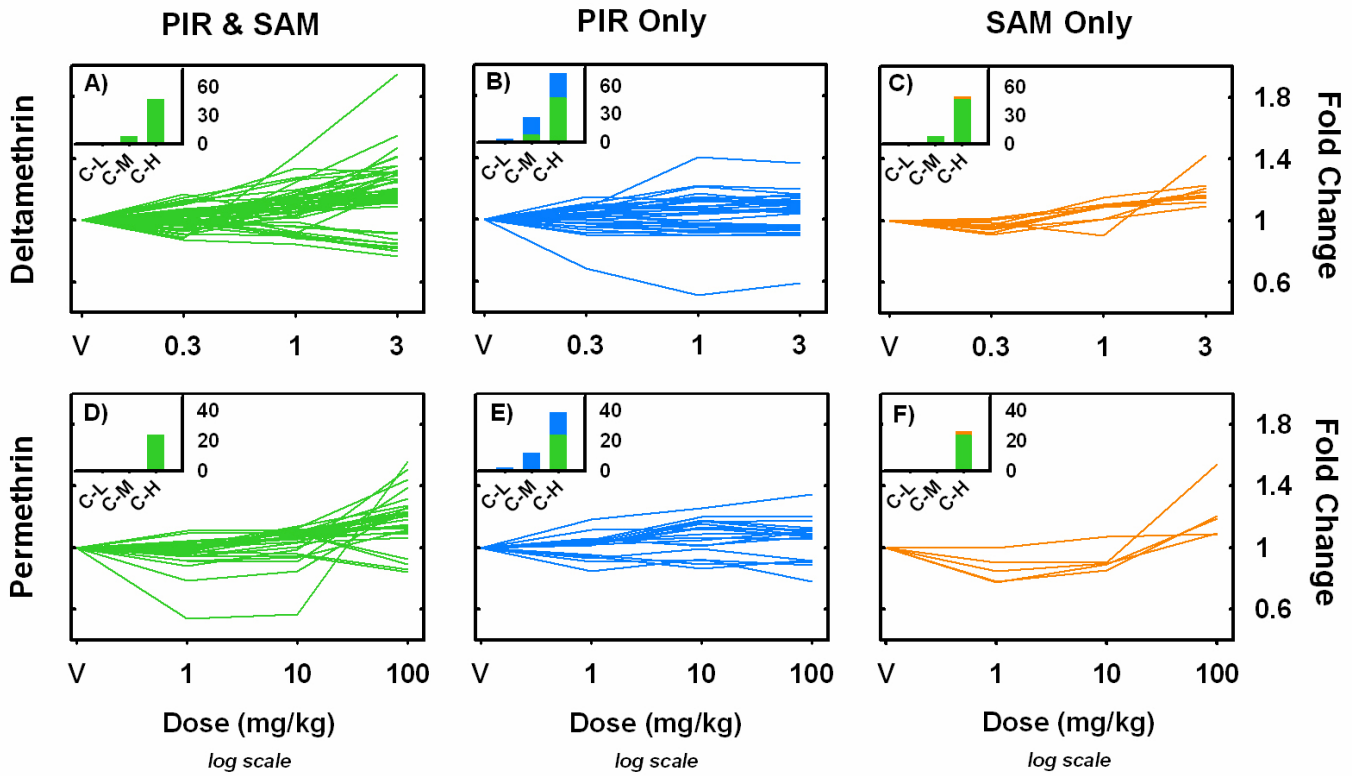

Figure 2.2. ***Dose-response functions identified by PIR and SAM regression methods.*** Panels A-F plot dose-response functions for probe sets identified by PIR (B & E), SAM (C & F) or both regression methods (A & D) for deltamethrin (A-C) and permethrin (D-F). Only probe sets that had a Benjamini-Hochberg adjusted *p*-value < 0.05 for a main effect of dose in a one-way ANOVA are shown. For each probe set expression summaries for each treatment group were normalized to vehicle control and plotted as fold-change from control. The color scheme corresponds to that used in Figure 1, with green curves being detected by both PIR and SAM regression methods, blue curves being detected exclusively with the PIR method and orange curves being detected exclusively with the SAM method. Insets on each panel are the summated results of a Dunnett's many-to-one mean contrast test performed within each probe set comparing the means of the lowest (C-L), middle (C-M) and highest (C-H) doses to the mean of vehicle treated control. *y*-axis is number of probe sets identified under each comparison at a significance level of $p < 0.05$. Note the green portion of the stacked bars in the insets are the same values for panels A-C and D-E, respectively.

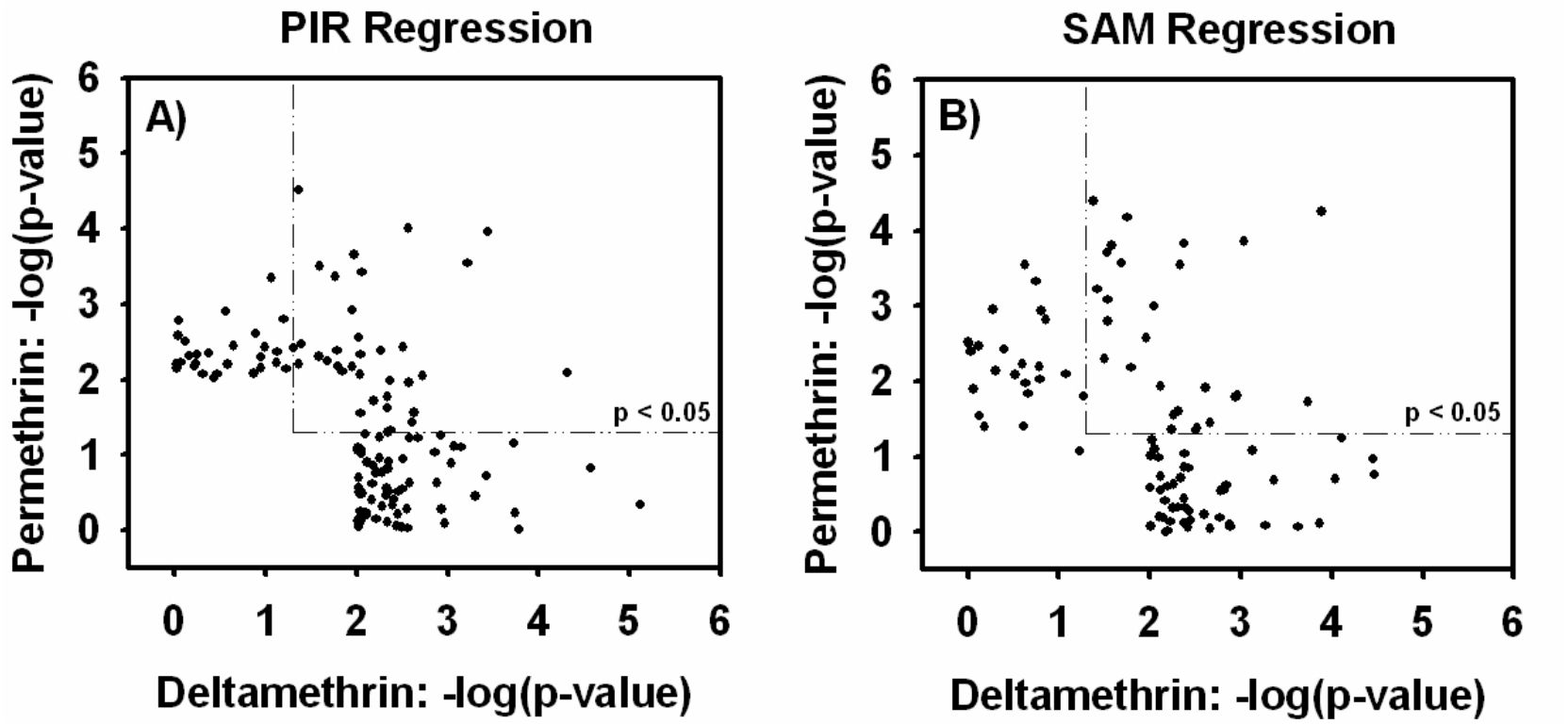

Figure 2.3. ***Comparison of probe sets identified by PIR or SAM between pyrethroids.*** Panels A and B plot the $-\log_{10}$ (empirical *p*-value) for deltamethrin (*x*-axis) against the $-\log_{10}$ (empirical *p*-value) for permethrin (*y*-axis) for probe sets identified during PIR or SAM regression analyses, respectively. All probe sets that had a Benjamini-Hochberg adjusted *p*-value <0.05 for a one-way ANOVA for either permethrin or deltamethrin are included in the plot. Dashed boxes represent $p < 0.05$, $p < 0.005$, and $p < 0.0005$ empirical *p*-value thresholds. All points in the upper right of the figures, within the dashed boxes, meet the respective *p*-value criteria for both pyrethroids. 27.2% and 27.8% of all probe sets identified during PIR or SAM analysis, respectively, had empirical *p*-values of $p < 0.05$ for both compounds.

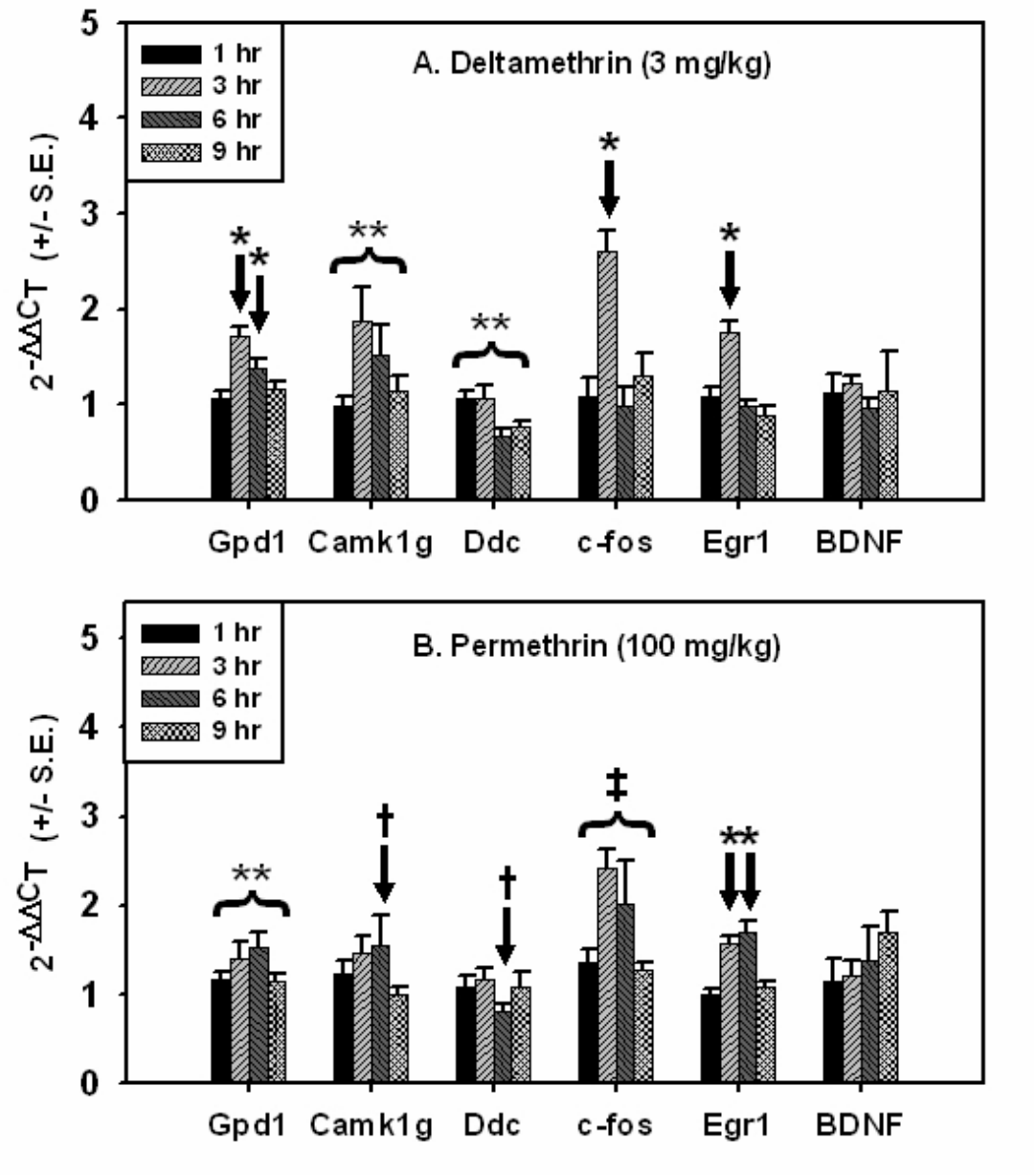

Figure 2.4. ***qRT-PCR time course results.*** Transcript expression over time following a single acute dose of 3 mg/kg deltamethrin (top) or 100 mg/kg permethrin (bottom). Gene symbols are listed on the *y*-axis. Data were analyzed using two-way ANOVA followed by one-way ANOVA within time points were interaction was observed. (**) denotes no interaction of time and treatment and a main effect of treatment ($p < 0.05$). (‡) denotes no interaction of time and treatment and a main effect of both time and treatment ($p < 0.05$). (*) denotes a significant effect of treatment for that time point ($p < 0.05$). (†) denotes a significant main effect of dose from qRT-PCR dose-response analysis (Table 2.4). Values for time-matched vehicle controls are not shown.

Figure 2.5. ***Composition and expression patterns of significantly enriched GO categories from SAFE analysis.*** Panels A-D are SAFE plots for two commonly enriched categories for both deltamethrin (A & C) and permethrin (B & D). Panels E & F are SAFE plots for a category not enriched for either deltamethrin (E) or permethrin (F). The *x*-axis of each plot denotes the position of all probe set in a rank ordered list of significance (from left to right) according to the empirical *p*-value from a linear regression across dose. The *y*-axis is a cumulative percentage calculated by taking the rank position of a given probe set either within the entire data set (solid unity line) or the interrogated Gene Ontology sub-category (solid stair-step line) and dividing them by the total number of probe sets contained within the entire data set or interrogated category, respectively. The degree of deviation of the stair-step line from the unity line indicates enrichment. The probe sets (excluding ESTs) that are ranked highest in significance for each GO category for both compounds in panels A-B and C-D are denoted at the top of each panel and included in a heatmap to the side of the respective panels. In the heatmaps, each row of tiles is a probe set and each column of tiles represents the mean fold-change from control with increasing doses of each compound running from right to left. Colorbar for heatmaps is given in panel G.

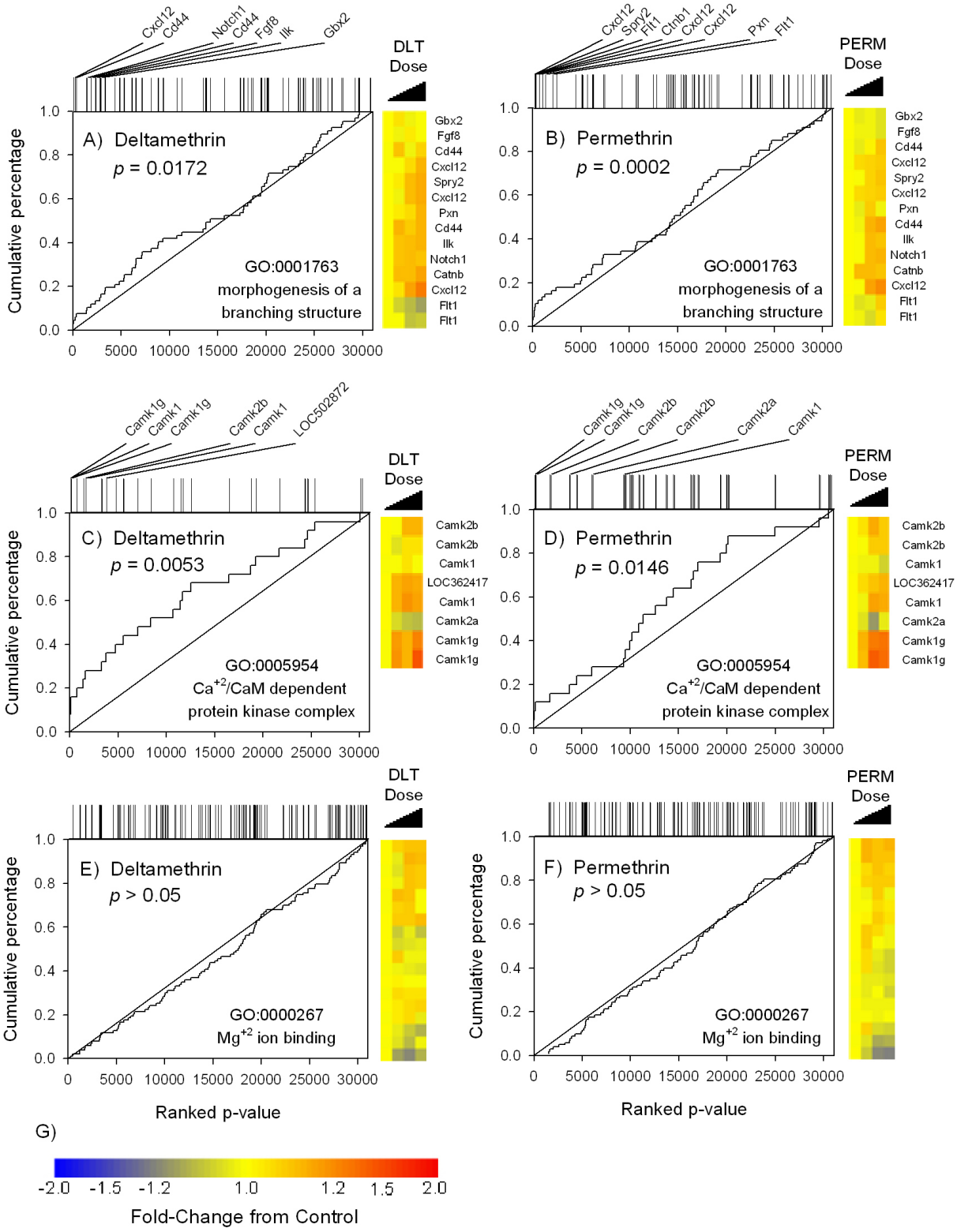
A) Deltamethrin
p = 0.0172
GO:0001763
morphogenesis of a
branching structure
B) Permethrin
p = 0.0002
GO:0001763
morphogenesis of a
branching structure
C) Deltamethrin
p = 0.0053
GO:0005954
Ca+2/CaM dependent
protein kinase complex
D) Permethrin
p = 0.0146
GO:0005954
Ca+2/CaM dependent
protein kinase complex
E) Deltamethrin
p > 0.05
GO:0000267
Mg+2 ion binding
F) Permethrin
p > 0.05
GO:0000267
Mg+2 ion binding
DLT Dose
PERM Dose
Cumulative percentage
Ranked p-value
G)
-2.0 -1.5 -1.2 1.0 1.2 1.5 2.0
Fold-Change from Control

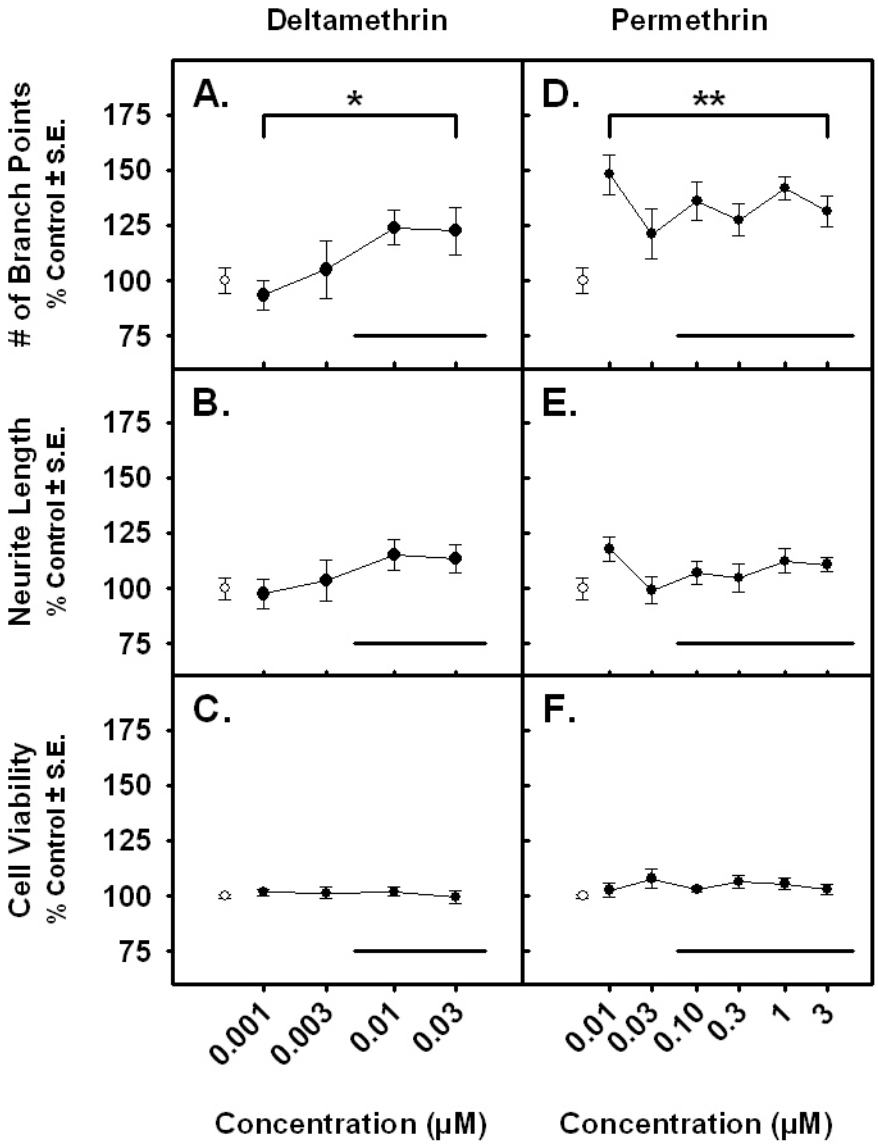

Figure 2.6. ***Pyrethroid effects on branching and neurite length in primary cortical cell cultures.*** Changes in the total number neurite of branch points (A & D), total neurite length (B & E) and cell viability using an ATP-luciferase assay (C & F) in primary cortical cell cultures exposed to deltamethrin (A-C) or permethrin (D-F). n = 3 different cultures. Values for each end point are normalized to untreated controls (± standard error). Untreated control values are shown in white. The bold lines underneath each curve represent the range of estimated brain concentrations expected to occur during the *in vivo* exposures used in the present study (Mirfazaelian et al. 2006 and Tornero-Velez et al. 2007). Significance was determined using a One-way ANOVA, * = $p < 0.10$, ** = $p < 0.05$.

Works Cited

Affymetrix Inc. (2002) *GeneChip Expression Analysis: Data Analysis Fundamentals (Part No. 701190).* Affymetrix Inc., Santa Clara, CA.

Affymetrix Inc. (2004) *GeneChip Expression Analysis Technical Manual (Pub 701021).* Affymetrix Inc.,, Santa Clara, CA.

Amweg E. L., Weston D. P. and Ureda N. M. (2005) Use and toxicity of pyrethroid pesticides in the Central Valley, California, USA. *Environ Toxicol Chem* **24**, 966-72.

Anadon A., Martinez-Larranaga M. R., Diaz M. J. and Bringas P. (1991) Toxicokinetics of permethrin in the rat. *Toxicol Appl Pharmacol* **110**, 1-8.

Anadon A., Martinez-Larranaga M. R., Fernandez-Cruz M. L., Diaz M. J., Fernandez M. C. and Martinez M. A. (1996) Toxicokinetics of deltamethrin and its 4'-HO-metabolite in the rat. *Toxicol Appl Pharmacol* **141**, 8-16.

Applied Biosystems Inc. (2004) *Amplification Efficiency of Taqman Assays-on-Demand Gene Expression Products (Publication 127AP05-01).* Applied Biosystems Inc., Foster City, CA.

Applied Biosystems Inc. (2005) *TaqMan Gene Expression Assays Protocol (Part Number 4333458).* Applied Biosystems Inc., Foster City, CA.

Applied Biosystems Inc. (2006) *The Design Process for a New Generation of Quantitative Gene Expression Analysis Tools (Publication 127WP02-02).* Applied Biosystems Inc., Foster City, CA.

Audesirk, T., and Cabell, L. (1999). Nanomolar concentrations of nicotine and cotinine alter the development of cultured hippocampal neurons via non-acetylcholine receptor-mediated mechanisms. *Neurotoxicology* **20**, 639-46.

Bading H. (2000) Transcription-dependent neuronal plasticity the nuclear calcium hypothesis. *Eur J Biochem* **267**, 5280-3.

Bahi A. and Dreyer J. L. (2005) Cocaine-induced expression changes of axon guidance molecules in the adult rat brain. *Mol Cell Neurosci* **28**, 275-91.

Barry W. T. (2007) Signifcance Analysis of Function and Expression, User's Guide. http://bioconductor.org/packages/1.8/bioc/vignettes/safe/inst/doc/SAFEmanual.pdf.

Barry W. T., Nobel A. B. and Wright F. A. (2005) Significance analysis of functional categories in gene expression studies: a structured permutation approach. *Bioinformatics* **21**, 1943-9.

Barry W. T., Nobel A. B. and Wright F. A. (2007) A statistical framework for testing functional categories in microarray data. *Annals of Applied Statistics* **(submitted)**.

Baughman G., Wiederrecht G. J., Campbell N. F., Martin M. M. and Bourgeois S. (1995) FKBP51, a novel T-cell-specific immunophilin capable of calcineurin inhibition. *Mol Cell Biol* **15**, 4395-402.

Baughman G., Wiederrecht G. J., Chang F., Martin M. M. and Bourgeois S. (1997) Tissue distribution and abundance of human FKBP51, and FK506-binding protein that can mediate calcineurin inhibition. *Biochem Biophys Res Commun* **232**, 437-43.

Benjamini Y. and Hochberg Y. (1995) Controlling the false discovery rate: a practical and powerful approach to multiple testing. *J. Roy. Statist. Soc. Ser. B* **232**, 437-443.

Bloom A. S., Staatz C. G. and Dieringer T. (1983) Pyrethroid effects on operant responding and feeding. *Neurobehav Toxicol Teratol* **5**, 321-4.

Bowyer J. F., Pogge A. R., Delongchamp R. R., O'Callaghan J. P., Patel K. M., Vrana K. E. and Freeman W. M. (2007) A threshold neurotoxic amphetamine exposure inhibits parietal cortex expression of synaptic plasticity-related genes. *Neuroscience* **144**, 66-76.

Burr S. A. and Ray D. E. (2004) Structure-activity and interaction effects of 14 different pyrethroids on voltage-gated chloride ion channels. *Toxicol Sci* **77**, 341-6.

Cai N. S., McCoy M. T., Ladenheim B., Lyles J., Ali S. F. and Cadet J. L. (2006) Serial analysis of gene expression in the rat striatum following methamphetamine administration. *Ann N Y Acad Sci* **1074**, 13-30.

Carvajal F., Sanchez-Amate M. C., Sanchez-Santed F. and Cubero I. (2005) Neuroanatomical targets of the organophosphate chlorpyrifos by c-fos immunolabeling. *Toxicol Sci* **84**, 360-7.

Catterall W. A. (1992) Cellular and molecular biology of voltage-gated sodium channels. *Physiol Rev* **72**, S15-48.

Catterall W. A., Striessnig J., Snutch T. P. and Perez-Reyes E. (2003) International Union of Pharmacology. XL. Compendium of voltage-gated ion channels: calcium channels. *Pharmacol Rev* **55**, 579-81.

Chandler L. J., Newsom H., Sumners C. and Crews F. (1993) Chronic ethanol exposure potentiates NMDA excitotoxicity in cerebral cortical neurons. *J Neurochem* **60**, 1578-81.

Cheng J. D. and de Vellis J. (2000) Oligodendrocytes as glucocorticoids target cells: functional analysis of the glycerol phosphate dehydrogenase gene. *J Neurosci Res* **59**, 436-45.

Choi J. S. and Soderlund D. M. (2006) Structure-activity relationships for the action of 11 pyrethroid insecticides on rat Na v 1.8 sodium channels expressed in Xenopus oocytes. *Toxicol Appl Pharmacol* **211**, 233-44.

Chu G., Balasubramanian N., Tibshirani R. and Tusher V. G. (2005) *SAM "Significance Analysis of Microarrays" Users guide and technical document.* Stanford University, Palo Alto, CA.

Clayton D. F. (2000) The genomic action potential. *Neurobiol Learn Mem* **74**, 185-216.

Colt J. S., Lubin J., Camann D., Davis S., Cerhan J., Severson R. K., Cozen W. and Hartge P. (2004) Comparison of pesticide levels in carpet dust and self-reported pest treatment practices in four US sites. *J Expo Anal Environ Epidemiol* **14**, 74-83.

Condes-Lara M., Graff-Guerrero A. and Vega-Riveroll L. (1999) Effects of cypermethrin on the electroencephalographic activity of the rat: a model of chemically induced seizures. *Neurotoxicol Teratol* **21**, 293-8.

Costa, L. G., Aschner, M., Vitalone, A., Syversen, T., and Soldin, O. P. (2004). Developmental neuropathology of environmental agents. *Annu Rev Pharmacol Toxicol* **44**, 87-110.

Crofton K. M. and Reiter L. W. (1984) Effects of two pyrethroid insecticides on motor activity and the acoustic startle response in the rat. *Toxicol Appl Pharmacol* **75**, 318-28.

Crumpton, T., Atkins, D. S., Zawia, N. H., and Barone, S., Jr. (2001). Lead exposure in pheochromocytoma (PC12) cells alters neural differentiation and Sp1 DNA-binding. *Neurotoxicology* **22**, 49-62.

Cull-Candy S., Brickley S. and Farrant M. (2001) NMDA receptor subunits: diversity, development and disease. *Curr Opin Neurobiol* **11**, 327-35.

Dassesse D., Vanderwinden J. M., Goldberg I., Vanderhaeghen J. J. and Schiffmann S. N. (1999) Caffeine-mediated induction of c-fos, zif-268 and arc expression through A1 receptors in the striatum: different interactions with the dopaminergic system. *Eur J Neurosci* **11**, 3101-14.

de Boer S. F., van der Gugten J., Slangen J. L. and Hijzen T. H. (1988) Changes in plasma corticosterone and catecholamine contents induced by low doses of deltamethrin in rats. *Toxicology* **49**, 263-70.

De Kloet E. R., Vreugdenhil E., Oitzl M. S. and Joels M. (1998) Brain corticosteroid receptor balance in health and disease. *Endocr Rev* **19**, 269-301.

Dennis G., Jr., Sherman B. T., Hosack D. A., Yang J., Gao W., Lane H. C. and Lempicki R. A. (2003) DAVID: Database for Annotation, Visualization, and Integrated Discovery. *Genome Biol* **4**, P3.

Deutch A. Y. and Roth R. H. (2003) Cellular and Molecular Neuroscience, Section 7. Neurotransmitters. In *Fundamental Neuroscience* (Edited by Squire L. R., Bloom F.

E., McConnell S. K., Roberts J. L., Spitzer N. C. and Zigmond M. J.), p. 163-196. Academic Press, San Diego, CA.

Diaz Heijtz, R., Kolb, B., and Forssberg, H. (2003). Can a therapeutic dose of amphetamine during pre-adolescence modify the pattern of synaptic organization in the brain? *Eur J Neurosci* **18**, 3394-9.

Dierssen M. and Ramakers G. J. (2006) Dendritic pathology in mental retardation: from molecular genetics to neurobiology. *Genes Brain Behav* **5 Suppl 2**, 48-60.

Dow G. S., Caridha D., Goldberg M., Wolf L., Koenig M. L., Yourick D. L. and Wang Z. (2005) Transcriptional profiling of mefloquine-induced disruption of calcium homeostasis in neurons in vitro. *Genomics* **86**, 539-50.

Dunnett C. W. (1950) A multiple comparison procedure for comparing several treatments with a control. *Journal of the American Statistical Association* **50**, 1096-1121.

Farrant M. and Kaila K. (2007) The cellular, molecular and ionic basis of GABA(A) receptor signalling. *Prog Brain Res* **160**, 59-87.

Fatemi S. H., Reutiman T. J., Folsom T. D., Bell C., Nos L., Fried P., Pearce D. A., Singh S., Siderovski D. P., Willard F. S. and Fukuda M. (2006) Chronic olanzapine treatment causes differential expression of genes in frontal cortex of rats as revealed by DNA microarray technique. *Neuropsychopharmacology* **31**, 1888-99.

Fields R. D., Lee P. R. and Cohen J. E. (2005) Temporal integration of intracellular Ca2+ signaling networks in regulating gene expression by action potentials. *Cell Calcium* **37**, 433-42.

Fisher R. A. (1930) *Statistical Methods for Research Workers, Third Edition*, Oliver and Boyd, London. 283 p.

Flaskos J., Harris W., Sachana M., Munoz D., Tack J. and Hargreaves A. J. (2007) The effects of diazinon and cypermethrin on the differentiation of neuronal and glial cell lines. *Toxicol Appl Pharmacol* **219**, 172-80.

Gentleman R. C., Carey V. J., Bates D. M., Bolstad B., Dettling M., Dudoit S., Ellis B., Gautier L., Ge Y., Gentry J., Hornik K., Hothorn T., Huber W., Iacus S., Irizarry R., Leisch F., Li C., Maechler M., Rossini A. J., Sawitzki G., Smith C., Smyth G., Tierney L., Yang J. Y. and Zhang J. (2004) Bioconductor: open software development for computational biology and bioinformatics. *Genome Biol* **5**, R80.

Ginsberg S. D. and Che S. (2005) Expression profile analysis within the human hippocampus: comparison of CA1 and CA3 pyramidal neurons. *J Comp Neurol* **487**, 107-18.

Ginsburg K. S. and Narahashi T. (1993) Differential sensitivity of tetrodotoxin-sensitive and tetrodotoxin-resistant sodium channels to the insecticide allethrin in rat dorsal root ganglion neurons. *Brain Res* **627**, 239-48.

Giraud P., Alcaraz G., Jullien F., Sampo B., Jover E., Couraud F. and Dargent B. (1998) Multiple pathways regulate the expression of genes encoding sodium channel subunits in developing neurons. *Brain Res Mol Brain Res* **56**, 238-55.

Gonzalez, C. L., Gharbawie, O. A., Whishaw, I. Q., and Kolb, B. (2005). Nicotine stimulates dendritic arborization in motor cortex and improves concurrent motor skill but impairs subsequent motor learning. *Synapse* **55**, 183-91.

Gronier B. S. and Rasmussen K. (2003) Electrophysiological effects of acute and chronic olanzapine and fluoxetine in the rat prefrontal cortex. *Neurosci Lett* **349**, 196-200.

Guzowski J. F., McNaughton B. L., Barnes C. A. and Worley P. F. (1999) Environment-specific expression of the immediate-early gene Arc in hippocampal neuronal ensembles. *Nat Neurosci* **2**, 1120-4.

Guzowski J. F., Miyashita T., Chawla M. K., Sanderson J., Maes L. I., Houston F. P., Lipa P., McNaughton B. L., Worley P. F. and Barnes C. A. (2006) Recent behavioral history modifies coupling between cell activity and Arc gene transcription in hippocampal CA1 neurons. *Proc Natl Acad Sci U S A* **103**, 1077-82.

Guzowski J. F., Timlin J. A., Roysam B., McNaughton B. L., Worley P. F. and Barnes C. A. (2005) Mapping behaviorally relevant neural circuits with immediate-early gene expression. *Curr Opin Neurobiol* **15**, 599-606.

Harris M. A., Clark J., Ireland A., Lomax J., Ashburner M., Foulger R., Eilbeck K., Lewis S., Marshall B., Mungall C., Richter J., Rubin G. M., Blake J. A., Bult C., Dolan M., Drabkin H., Eppig J. T., Hill D. P., Ni L., Ringwald M., Balakrishnan R., Cherry J. M., Christie K. R., Costanzo M. C., Dwight S. S., Engel S., Fisk D. G., Hirschman J. E., Hong E. L., Nash R. S., Sethuraman A., Theesfeld C. L., Botstein D., Dolinski K., Feierbach B., Berardini T., Mundodi S., Rhee S. Y., Apweiler R., Barrell D., Camon E., Dimmer E., Lee V., Chisholm R., Gaudet P., Kibbe W., Kishore R., Schwarz E. M., Sternberg P., Gwinn M., Hannick L., Wortman J., Berriman M., Wood V., de la Cruz N., Tonellato P., Jaiswal P., Seigfried T. and White R. (2004) The Gene Ontology (GO) database and informatics resource. *Nucleic Acids Res* **32**, D258-61.

Hassouna I., Wickert H., el-Elaimy I., Zimmermann M. and Herdegen T. (1996) Systemic application of pyrethroid insecticides evokes differential expression of c-Fos and c-Jun proteins in rat brain. *Neurotoxicology* **17**, 415-31.

Hof P. R., Trapp, B.D., De Vellis, J., Claudio, L., Colman, D.R. (2003) Cellular Components of Nervous Tisse. In *Fundamental Neuroscience* (Edited by Squire L. R., Bloom, F.E., McConnell, S.K., Roberts, J.L., Spitzer, N.C., Zigmond, M.J.), p. 49-75. Academic Press, Amsterdam.

Hu J., Kapoor, M., Zhang, W., Hamilton, S.R., Coombes, K.R. (2005) Analysis of dose-response effects on gene expression data with comparison of two microarray platforms. *Bioinformatics* **21**, 3524-3529.

Hubler T. R. and Scammell J. G. (2004) Intronic hormone response elements mediate regulation of FKBP51 by progestins and glucocorticoids. *Cell Stress Chaperones* **9**, 243-52.

Irizarry R. A., Hobbs B., Collin F., Beazer-Barclay Y. D., Antonellis K. J., Scherf U. and Speed T. P. (2003) Exploration, normalization, and summaries of high density oligonucleotide array probe level data. *Biostatistics* **4**, 249-64.

Kanehisa M., Goto S., Kawashima S., Okuno Y. and Hattori M. (2004) The KEGG resource for deciphering the genome. *Nucleic Acids Res* **32**, D277-80.

Kern, M., Audesirk, T., and Audesirk, G. (1993). Effects of inorganic lead on the differentiation and growth of cortical neurons in culture. *Neurotoxicology* **14**, 319-27.

Kim J., Jung S. C., Clemens A. M., Petralia R. S. and Hoffman D. A. (2007) Regulation of dendritic excitability by activity-dependent trafficking of the A-type K+ channel subunit Kv4.2 in hippocampal neurons. *Neuron* **54**, 933-47.

Korostynski M., Piechota M., Kaminska D., Solecki W. and Przewlocki R. (2007) Morphine effects on striatal transcriptome in mice. *Genome Biol* **8**, R128.

Larsson O., Wahlestedt C. and Timmons J. A. (2005) Considerations when using the significance analysis of microarrays (SAM) algorithm. *BMC Bioinformatics* **6**, 129.

Lautermilch N. J. and Spitzer N. C. (2000) Regulation of calcineurin by growth cone calcium waves controls neurite extension. *J Neurosci* **20**, 315-25.

Leng G., Kuhn K. H. and Idel H. (1997) Biological monitoring of pyrethroids in blood and pyrethroid metabolites in urine: applications and limitations. *Sci Total Environ* **199**, 173-81.

Leveille P. J., McGinnis J. F., Maxwell D. S. and de Vellis J. (1980) Immunocytochemical localization of glycerol-3-phosphate dehydrogenase in rat oligodendrocytes. *Brain Res* **196**, 287-305.

Li M. D., Kane J. K., Wang J. and Ma J. Z. (2004) Time-dependent changes in transcriptional profiles within five rat brain regions in response to nicotine treatment. *Brain Res Mol Brain Res* **132**, 168-80.

Littell R. C. and Folks J. L. (1973) Asymptotic optimality of Fisher's method of combining tests II. *Journal of the American Statistical Association* **68**, 193-194.

Liu G. P., Ma Q. and Shi N. (2006) Tyrosine hydroxylase as a target for deltamethrin in the nigrostriatal dopaminergic pathway. *Biomed Environ Sci* **19**, 27-34.

Liu G. P. and Shi N. (2006) The inhibitory effects of deltamethrin on dopamine biosynthesis in rat PC12 cells. *Toxicol Lett* **161**, 195-9.

Livak K. J. and Schmittgen T. D. (2001) Analysis of relative gene expression data using real-time quantitative PCR and the 2(-Delta Delta C(T)) Method. *Methods* **25**, 402-8.

Majdan M. and Shatz C. J. (2006) Effects of visual experience on activity-dependent gene regulation in cortex. *Nat Neurosci* **9**, 650-9.

Martinez-Larranaga M. R., Anadon A., Martinez M. A., Martinez M., Castellano V. J. and Diaz M. J. (2003) 5-HT loss in rat brain by type II pyrethroid insecticides. *Toxicol Ind Health* **19**, 147-55.

McConnell, P., and Berry, M. (1979). The effects of postnatal lead exposure on Purkinje cell dendritic development in the rat. *Neuropathol Appl Neurobiol* **5**, 115-32.

McClung C. A. and Nestler E. J. (2008) Neuroplasticity mediated by altered gene expression. *Neuropsychopharmacology* **33**, 3-17.

McDaniel K. L. and Moser V. C. (1993) Utility of a neurobehavioral screening battery for differentiating the effects of two pyrethroids, permethrin and cypermethrin. *Neurotoxicol Teratol* **15**, 71-83.

Millenaar F. F., Okyere J., May S. T., van Zanten M., Voesenek L. A. and Peeters A. J. (2006) How to decide? Different methods of calculating gene expression from short oligonucleotide array data will give different results. *BMC Bioinformatics* **7**, 137.

Mirfazaelian A., Kim K. B., Anand S. S., Kim H. J., Tornero-Velez R., Bruckner J. V. and Fisher J. W. (2006) Development of a physiologically based pharmacokinetic model for deltamethrin in the adult male Sprague-Dawley rat. *Toxicol Sci* **93**, 432-42.

Motomura H. and Narahashi T. (2001) Interaction of tetramethrin and deltamethrin at the single sodium channel in rat hippocampal neurons. *Neurotoxicology* **22**, 329-39.

Narahashi T. (1996) Neuronal ion channels as the target sites of insecticides. *Pharmacol Toxicol* **79**, 1-14.

Nicols N. R., Dokas L., Ting S. M., Kumar S., de Vellis J., Shors T. J., Uenishi N., Thompson R. F. and Finch C. E. (1996) Hippocampal responses to corticosterone and stress, one of which is the 35,000 M(r) protein, glycerol phosphate dehydrogenase. *J Neuroendocrinol* **8**, 867-76.

Ogata N. and Ohishi Y. (2002) Molecular diversity of structure and function of the voltage-gated Na+ channels. *Jpn J Pharmacol* **88**, 365-77.

Paillart C., Boudier J. L., Boudier J. A., Rochat H., Couraud F. and Dargent B. (1996) Activity-induced internalization and rapid degradation of sodium channels in cultured fetal neurons. *J Cell Biol* **134**, 499-509.

Park, Y. H., Kantor, L., Guptaroy, B., Zhang, M., Wang, K. K., and Gnegy, M. E. (2003). Repeated amphetamine treatment induces neurite outgrowth and enhanced amphetamine-stimulated dopamine release in rat pheochromocytoma cells (PC12 cells) via a protein kinase C- and mitogen activated protein kinase-dependent mechanism. *J Neurochem* **87**, 1546-57.

Park, Y. H., Kantor, L., Wang, K. K., and Gnegy, M. E. (2002). Repeated, intermittent treatment with amphetamine induces neurite outgrowth in rat pheochromocytoma cells (PC12 cells). *Brain Res* **951**, 43-52.

Patra R. C., Blue M. E., Johnston M. V., Bressler J. and Wilson M. A. (2004) Activity-dependent expression of Egr1 mRNA in somatosensory cortex of developing rats. *J Neurosci Res* **78**, 235-44.

Pearson K. (1911) On the probability that two independent distributions of frequency are really samples from the same population. *Biometrika* **8**, 250-254.

Peele D. B. and Crofton K. M. (1987) Pyrethroid effects on schedule-controlled behavior: time and dosage relationships. *Neurotoxicol Teratol* **9**, 387-94.

Petit, T. L., and LeBoutillier, J. C. (1979). Effects of lead exposure during development on neocortical dendritic and synaptic structure. *Exp Neurol* **64**, 482-92.

Pujol F., Kitabgi P. and Boudin H. (2005) The chemokine SDF-1 differentially regulates axonal elongation and branching in hippocampal neurons. *J Cell Sci* **118**, 1071-80.

Qin S., Budd R., Bondarenko S., Liu W. and Gan J. (2006) Enantioselective degradation and chiral stability of pyrethroids in soil and sediment. *J Agric Food Chem* **54**, 5040-5.

Ray D. E. (1980) An EEG investigation of decamethrin-induced choreoathetosis in the rat. *Exp Brain Res* **38**, 221-7.

Ray D. E. (2001) Pyrethroid Insecticides: Mechanisms of Toxicity, Systematic Poisoning Syndromes, Parethesia, and Therapy. In *Handbook of Pesticide Toxicology* (Edited by Krieger R. I.), Vol. 2, p. 1289-1303. Academic Press, San Diego, CA.

Ray D. E. and Fry J. R. (2006) A reassessment of the neurotoxicity of pyrethroid insecticides. *Pharmacol Ther* **111**, 174-93.

Redmond L., Oh S. R., Hicks C., Weinmaster G. and Ghosh A. (2000) Nuclear Notch1 signaling and the regulation of dendritic development. *Nat Neurosci* **3**, 30-40.

Robinson T. E., Gorny G., Mitton E. and Kolb B. (2001) Cocaine self-administration alters the morphology of dendrites and dendritic spines in the nucleus accumbens and neocortex. *Synapse* **39**, 257-66.

Robinson T. E. and Kolb B. (1999) Alterations in the morphology of dendrites and dendritic spines in the nucleus accumbens and prefrontal cortex following repeated treatment with amphetamine or cocaine. *Eur J Neurosci* **11**, 1598-604.

Robinson, T. E., and Kolb, B. (2004). Structural plasticity associated with exposure to drugs of abuse. *Neuropharmacology* **47 Suppl 1**, 33-46.

Schoneveld O. J., Gaemers I. C. and Lamers W. H. (2004) Mechanisms of glucocorticoid signalling. *Biochim Biophys Acta* **1680**, 114-28.

Schulman H. and Roberts J. L. (2003) Cellular and Molecular Neuroscience, Section 10. Intracellular Signaling. In *Fundamental Neuroscience* (Edited by Squire L. R., Bloom F. E., McConnell S. K., Roberts J. L., Spitzer N. C. and Zigmond M. J.), p. 259-297. Academic Press, San Diego, CA.

Shafer T. J., Meyer D. A. and Crofton K. M. (2005) Developmental neurotoxicity of pyrethroid insecticides: critical review and future research needs. *Environ Health Perspect* **113**, 123-36.

Shiraishi S., Yanagita T., Kobayashi H., Uezono Y., Yokoo H., Minami S. I., Takasaki M. and Wada A. (2001) Up-regulation of cell surface sodium channels by cyclosporin A, FK506, and rapamycin in adrenal chromaffin cells. *J Pharmacol Exp Ther* **297**, 657-65.

Sin W. C., Haas K., Ruthazer E. S. and Cline H. T. (2002) Dendrite growth increased by visual activity requires NMDA receptor and Rho GTPases. *Nature* **419**, 475-80.

Smith T. J. and Soderlund D. M. (1998) Action of the pyrethroid insecticide cypermethrin on rat brain IIa sodium channels expressed in xenopus oocytes. *Neurotoxicology* **19**, 823-32.

Soderlund D. M., Clark J. M., Sheets L. P., Mullin L. S., Piccirillo V. J., Sargent D., Stevens J. T. and Weiner M. L. (2002) Mechanisms of pyrethroid neurotoxicity: implications for cumulative risk assessment. *Toxicology* **171**, 3-59.

Song J. H. and Narahashi T. (1996) Modulation of sodium channels of rat cerebellar Purkinje neurons by the pyrethroid tetramethrin. *J Pharmacol Exp Ther* **277**, 445-53.

Spencer C. I., Yuill K. H., Borg J. J., Hancox J. C. and Kozlowski R. Z. (2001) Actions of pyrethroid insecticides on sodium currents, action potentials, and contractile rhythm in isolated mammalian ventricular myocytes and perfused hearts. *J Pharmacol Exp Ther* **298**, 1067-82.

Stanzione P., Stefani A. and Bernardi G. (1988) Morphine induces a spontaneous and evoked bursting activity in rat cortical neurons by adding a postsynaptic active mechanism to the synaptic input: an intracellular study in vivo. *Neuroscience* **26**, 45-53.

Steward O., Wallace C. S., Lyford G. L. and Worley P. F. (1998) Synaptic activation causes the mRNA for the IEG Arc to localize selectively near activated postsynaptic sites on dendrites. *Neuron* **21**, 741-51.

Symington S. B. and Clark J. M. (2005) Action of deltamethrin on N-Type (Cav2.2) voltage-sensitive calcium channels in rat brain. *Pesticide Biochemistry and Physiology* **82**, 1-15.

Takemoto-Kimura S., Ageta-Ishihara N., Nonaka M., Adachi-Morishima A., Mano T., Okamura M., Fujii H., Fuse T., Hoshino M., Suzuki S., Kojima M., Mishina M., Okuno H. and Bito H. (2007) Regulation of dendritogenesis via a lipid-raft-associated Ca2+/calmodulin-dependent protein kinase CLICK-III/CaMKIgamma. *Neuron* **54**, 755-70.

Tornero-Velez R., Scollon E. J., Starr J., Hughes M. F., DeVito M. J. and Dary C. C. (2007) Pharmacokinetic/Pharmacodynamic Modeling of Permethrin in the Rat. *The Toxicologist* **96**, 81.

Tully D. B., Bao W., Goetz A. K., Blystone C. R., Ren H., Schmid J. E., Strader L. F., Wood C. R., Best D. S., Narotsky M. G., Wolf D. C., Rockett J. C. and Dix D. J. (2006) Gene expression profiling in liver and testis of rats to characterize the toxicity of triazole fungicides. *Toxicol Appl Pharmacol* **215**, 260-73.

Tulve N. S., Jones P. A., Nishioka M. G., Fortmann R. C., Croghan C. W., Zhou J. Y., Fraser A., Cavel C. and Friedman W. (2006) Pesticide measurements from the first national environmental health survey of child care centers using a multi-residue GC/MS analysis method. *Environ Sci Technol* **40**, 6269-74.

Tusher V. G., Tibshirani R. and Chu G. (2001) Significance analysis of microarrays applied to the ionizing radiation response. *Proc Natl Acad Sci U S A* **98**, 5116-21.

Vijverberg H. P. and van den Bercken J. (1990) Neurotoxicological effects and the mode of action of pyrethroid insecticides. *Crit Rev Toxicol* **21**, 105-26.

Wayman G. A., Impey S., Marks D., Saneyoshi T., Grant W. F., Derkach V. and Soderling T. R. (2006) Activity-dependent dendritic arborization mediated by CaM-kinase I activation and enhanced CREB-dependent transcription of Wnt-2. *Neuron* **50**, 897-909.

West A. E., Griffith E. C. and Greenberg M. E. (2002) Regulation of transcription factors by neuronal activity. *Nat Rev Neurosci* **3**, 921-31.

Wolansky M. J., Gennings C. and Crofton K. M. (2006) Relative potencies for acute effects of pyrethroids on motor function in rats. *Toxicol Sci* **89**, 271-7.

Wright C. D. P., Forshaw P. J. and Ray D. E. (1988) Classification of the actions of ten pyrethroid insecticides in the rat, using the trigeminal reflex and skeletal muscle as test systems. *Pesticide Biochemistry and Physiology* **30**, 79-86.

Wu A. and Liu Y. (2003) Prolonged expression of c-Fos and c-Jun in the cerebral cortex of rats after deltamethrin treatment. *Brain Res Mol Brain Res* **110**, 147-51.

Xiang G., Pan L., Xing W., Zhang L., Huang L., Yu J., Zhang R., Wu J., Cheng J. and Zhou Y. (2007) Identification of activity-dependent gene expression profiles reveals specific subsets of genes induced by different routes of Ca(2+) entry in cultured rat cortical neurons. *J Cell Physiol* **212**, 126-36.

Xie T., Tong L., Barrett T., Yuan J., Hatzidimitriou G., McCann U. D., Becker K. G., Donovan D. M. and Ricaurte G. A. (2002) Changes in gene expression linked to methamphetamine-induced dopaminergic neurotoxicity. *J Neurosci* **22**, 274-83.

Yekutieli D. and Benjamini Y. (1999) Resampling-based false discovery rate controlling multiple test procedures for correlated test statistics. *J Statist Plann Inference* **82**, 171-196.

Yu X. and Malenka R. C. (2003) Beta-catenin is critical for dendritic morphogenesis. *Nat Neurosci* **6**, 1169-77.

Zangenehpour S. and Chaudhuri A. (2002) Differential induction and decay curves of c-fos and zif268 revealed through dual activity maps. *Brain Res Mol Brain Res* **109**, 221-5.

Splice Variant Specific Induction of Ca^{+2}/calmodulin Dependent Protein Kinase 1-gamma mRNA in Response to Pyrethroid Exposure.

Chapter 3

Joshua A. Harrill[1], Kevin M. Crofton[2]

[1]University of North Carolina at Chapel Hill, Curriculum in Toxicology, CB 7270, Chapel Hill, NC 27599, [2]Neurotoxicology Division, National Health and Environmental Effects Research Laboratory, Office of Research and Development, U.S. Environmental Protections Agency, B105-06, Research Triangle Park, NC 27711

Correspondence:
[‡]Kevin M. Crofton, Ph.D., USEPA, Neurotoxicology Division, B105-04, Research Triangle Park, NC 27711; Phone: 919-541-2672; E-mail: crofton.kevin@epa.gov

Abstract.

Pyrethroid insecticides induce neurotoxicity in mammals by interfering with ion channel function in excitable neuronal membranes. Previous work demonstrated dose-dependent increases in the expression of Ca^{+2}/calmodulin dependent protein kinase (*Camk1g*) mRNA following acute deltamethrin (DLT) and permethrin (PERM) exposure. The present study tests the hypothesis that changes in *Camk1g* expression in the rat following acute pyrethroid exposure are due to a specific increase in the *Camk1g1* (Ca^{+2}-sensitive) splice variant and not the Ca^{+2}-insensitive splice variant *Camk1g2*. Long-Evans rats (n = 8 / group) were acutely exposed (p.o.) to PERM (1, 10, 40, 100 mg/kg), DLT (0.3, 1, 3 mg/kg) or corn oil vehicle. Frontal cortex was collected at 6 h post-dosing. In addition, rats were exposed to PERM (100 mg/kg) or DLT (3 mg/kg) and frontal cortex was collected at 1, 3, 6 or 9 hours along with time matched vehicle controls. Expression of *Camk1g1* and *Camk1g2* mRNA was measured by quantitative real-time RT-PCR and quantified with the $2^{-\Delta\Delta CT}$ method. Dose-dependent increases in *Camk1g1* mRNA expression were observed for DLT and PERM at 6 h. In addition, a dose-dependent increase in *Camk1g2* was also observed at 6 h with DLT only, although it was very small in magnitude (<1.2-fold). The increases in *Camk1g1* expression for DLT and PERM peak between 3 & 6 h post-exposure and return to control levels by 9 h. There was no detectable increase in *Camk1g1* protein as assessed with Western blots. This study demonstrates that following an acute *in vivo* exposure, deltamethrin and permethrin increase expression of *Camk1g1* mRNA in rat cortex. These changes in *Camk1g1* mRNA expression may be caused by the actions of pyrethroids at the neuronal membrane.

Introduction.

Pyrethroids are insecticides commonly used in a variety of agricultural, veterinary, domestic and human healthcare related applications (Heudorf and Angerer 2003). As the use of other insecticide classes such as organophosphates and organochlorines has declined, pyrethroid usage has risen. It is estimated that pyrethroids comprise ~25% of the world insecticide market (Amweg et al. 2003). Exposure assessments have detected pyrethroids and pyrethroid residues in the urine of pesticide applicators, blood samples of pregnant urban mothers, residential carpet dust, and in surface wipe samples from U.S. child-care centers (Leng et al. 1997; Whyatt et al. 2003; Colt et al. 2004; Weston et al. 2004; Tulve et al. 2006). These data indicate that the potential for human pyrethroid exposure is present in a variety of settings.

Pyrethroids are neurotoxicants that interact with voltage-sensitive ion channels expressed in nerve membranes (Narahashi 1996). The primary molecular targets of pyrethroids are voltage-sensitive Na^+ channels (VSSCs) expressed in neuronal axons. Pyrethroids slow the deactivation of these channels and induce persistent Na^+ currents that occur at membrane potentials when VSSCs are normally impermeable to Na^+ (Na^+ tail currents, see Narahashi 2001). Voltage sensitive Ca^{+2} channels and voltage-sensitive Cl^- channels have also been shown to be affected by pyrethroids (Burr and Ray 2004; Shafer and Meyer 2004; Symington and Clark 2005). The net effect of the pharmacological actions of pyrethroids at these channels is an alteration in neuronal firing patterns that is thought to underlie the poisoning symptoms and transient effects on behavior observed following acute *in vivo* pyrethroid exposures (for review see Ray 2001; Soderlund et al. 2002; Wolansky and Harrill 2008). Alterations in neuronal firing patterns from pharmacological or sensory

stimuli have also been shown to trigger *de novo* gene expression that contributes to long-lasting adaptive changes in neuronal form and function, such as late-phase long term potentiation and synaptic terminal remodeling (Bading 2000; West et al. 2002; Fields et al. 2005). To date, alterations in the expression of activity-regulated genes downstream of the pharmacological interactions of pyrethroids with molecular targets at the neuronal membrane remain poorly characterized.

Previous work in this laboratory on the acute *in vivo* actions of pyrethroids revealed a dose-dependent increase in the expression of Ca^{+2}/calmodulin dependent protein kinase 1g (*Camk1g*) mRNA in the frontal cortex of the rat following exposure to two pyrethroids: deltamethrin and permethrin (Harrill et al, *submitted*). Treatment of *in vitro* cultures of interconnected cortical neurons to pharmacological agents that increase spontaneous firing rates also results in an increase in *Camk1g* mRNA expression (Xiang et. al 2007). Likewise, sub-chronic *in vivo* exposure of laboratory animals to pharmacological agents known to increase spontaneous and sensory evoked neuronal firing patterns also results in an increase in *Camk1g* mRNA expression (Lampl et al. 1998; Gronier and Rasmussen 1998; Dingledine 2005; Fatemi et al. 2006). Thus, the increase in *Camk1g* mRNA expression following *in vivo* pyrethroid exposure is consistent with increases in neuronal excitability elicited by these compounds

In the rat brain, *Camk1g* is expressed in two alternative mRNA splice variants that are transcribed from the same chromosomal locus (13q27). These splice variants are termed *Camk1g1* and *Camk1g2* and contain 13 and 12 exons, respectively (Nishimura et al. 2003). The domain structure of the protein encoded by the rat *Camk1g1* splice variant includes a kinase catalytic domain, overlapping Ca^{+2}/calmodulin-binding and autoinhibitory domains,

C-terminal prenylation and palmitoylation motifs, and has 99% amino acid homology with the *Camk1g1* protein expressed in mice (Nishimura et al. 2003; Takemoto-Kimura et al. 2003; Takemoto-Kimura et al. 2007). The activity of the *Camk1g1* protein is dependent upon both the presence of Ca^{+2}-bound calmodulin and activation by an upstream CaM kinase kinase (Nishimura et al. 2003). In contrast, the rat *Camk1g2* mRNA splice variant lacks exon 11 (see Figure 3.1). The transcribed *Camk1g2* protein does not contain a Ca^{+2}/calmodulin-dependent binding domain and the kinase activity of this protein is not enhanced in the presence of Ca^{+2}-bound calmodulin (Nishimura et al. 2003). In addition, a frame shift in the amino-acid coding sequence of *Camk1g2* occurs upon excision of exon 11, resulting in a C-terminal tail that lacks the lipidification sites present in *Camk1g1* and essential to *Camk1g1* function (Nishimura et al. 2003; Takemoto-Kimura et al. 2007). In previous studies that detected pyrethroid-induced increases in the expression of *Camk1g* mRNA in rat cortex, neither the Affymetrix microarray probe sets nor the qRT-PCR assays used distinguished between the expression of the *Camk1g1* and *Camk1g2* splice variants (Harrill et al. *submitted*).

Proteins in the Ca^{+2}/calmodulin dependent protein kinase family act as intracellular signaling molecules that detect transient increases in Ca^{+2} concentrations in the neuronal cytoplasm (such as those that occur in response to an incoming excitatory stimulus) and transduce those signals to downstream effector proteins by means of phosphorylation (Agell et al. 2002). In this manner activation of CaM-kinase cascades can bring about alterations in neuronal function in response to neuronal activity. A specific role of *Camk1g* in regulating activity-dependent outgrowth and branching in developing neurons has recently been described by Wayman et al. (2006) and Takemoto-Kimura et al. (2007). Both of these works

use constitutive overexpression or knock-down of *Camk1g* to demonstrate a role for *Camk1g* in controlling neuronal outgrowth in cultures derived from mouse hippocampus and rat cortex, respectively. In addition, these dendritogenesis studies used constructs based on the mouse and rat *Camk1g1* protein. Wayman et al. (2006) demonstrate a *Camk1g* specific activation of the Ras/MEK/ERK signaling pathway in response to depolarization, a subsequent activation of the transcription factor CREB and transcription of *Wnt-2*, a soluble extracellular autocrine factor that promotes dendritic growth. Takemoto-Kimura et al. (2007) demonstrate that *Camk1g* is lipidified, inserted into membrane rafts that deliver the activated protein to dendritic arbors and controls neurotrophin stimulated dendrite growth and branching through the activation of a STEF/Rac signaling pathway. However, neither of these studies addressed the transcriptional regulation of *Camk1g* expression in response to changes in neuronal membrane excitability.

The highly divergent structure and functions of the proteins encoded by the two *Camk1g* splice variants, makes it important to determine whether pyrethroids alter expression of one or the other splice variants. Differential up-regulation of *Camk1g1* or *Camk1g2* mRNA by pyrethroids would have a different impacts on intraneuronal downstream signaling pathways because of the dissimilar structure and upstream regulatory mechanisms that control the kinase activity of these two proteins (Takemoto-Kimura et al. 2007). The goals of the present study included characterizing the effects of acute pyrethroid exposure on the expression of *Camk1g1* and *Camk1g2* mRNA splice variants in the rat frontal cortex, and determining if acute pyrethroid exposures *in vivo* result in a change in the expression of *Camk1g1* protein. A low dose exposure paradigm was used (i.e. doses that ranged from below to slightly above the threshold for detecting changes in neurobehavioral function,

Wolansky et al. 2006) to prevent possible confounding effects of more highly toxic exposures.

Methods.

Chemicals and dose solutions. Permethrin (3-phenoxybenzyl (1*R,S*)-*cis-trans*-3-(2,2-dichlorovinyl)-2,2-dimethyl-cyclopropanecarboxylate, 92.0% purity, isomer composition: 40 % cis, 60 % trans, 1:1 ratio of 1*R* & 1*S*) and deltamethrin ((*S*)-cyano-(3-phenoxyphenyl)methyl (1R)-*cis*-3-(2,2-dibromovinyl)-2,2-dimethylcyclopropane carboxylate, 98.9 % purity, isomer composition: 100% 1*R*, 3*R*, α*S*) were generously donated by FMC Corporation (Philadelphia, PA) and Bayer Cropscience (Research Triangle Park, NC), respectively. Chemical structures are shown in Figure 3.2. Pyrethroids were dissolved in corn oil (Sigma-Aldrich, St. Louis, MO) at 1, 10, 40 & 100 mg/mL permethrin and 0.3, 1 & 3 mg/mL deltamethrin. Dosing volume was 1mL/kg. qRT-PCR primers, probes and reagents were obtained from Applied Biosystems (Foster City, CA). AP7253b rabbit polyclonal antibody for *Camk1g1* was obtained from Abgent, Inc. (San Deigo, CA). Mouse monoclonal antibody (sc-47751) for βII tubulin was obtained from Santa Cruz Biotechnologies, Inc. (Santa Cruz, CA). HRP-conjugated rabbit and mouse secondary antibodies were obtained from KPL, Inc. (Gaithersburg, MD).

Animal care and treatment. Male Long-Evans rats (49-62 days of age) were obtained from Charles River Laboratories (Wilmington, MA) and housed two per cage in standard polycarbonate hanging cages (45 cm X 24 cm X 20 cm) with heat sterilized pine shavings for bedding (Beta Chips, Northeastern Products, Inc., Warrensburg, NY). Animals were maintained on 12h:12h photoperiod (lighted hours: 06:00-18:00) and allowed a 5-7 day

period of acclimation to the colony prior to dosing. Colony rooms were maintained at 22.0 ± 2.0°C with a relative humidity of 55 ± 20%. Food (Purina 5001 Rat Chow) and tap water were provided *ad libitum*.

For the dose-response studies, rats were treated by oral gavage with 0.3, 1 or 3 mg/kg deltamethrin, 1, 10, 40 or 100 mg/kg permethrin or corn oil vehicle. Dose-effect data from Wolansky et al. (2006) were used to: 1) pick doses that were slightly below, at, and slightly above the threshold for detecting neurotoxic effects, and 2) assign equipotent dose-levels (EDL) to the administered doses to provide a comparative dose-metric between the two test compounds. Dosing for dose-response studies occurred between 06:30 and 07:00 hours and the last test subject was euthanized before 18:00 hours. Dosing and euthanasia times for individuals were counterbalanced across time of day. In the time course studies rats were treated via oral gavage with 3 mg/kg deltamethrin, 100 mg/kg permethrin or vehicle. All test subjects were dosed and euthanized between 07:30 & 17:30 hours. Rats were removed from the colony suite one hour prior to dosing and allowed to acclimate in a quiet holding room maintained under similar environmental conditions. Subjects were administered a single oral dose of test compound by gavage, and allowed to recover in their home cage prior to euthanasia for 6 hours (dose-response studies) or 1, 3, 6, 9, 12 or 24 hours (time course studies). Subjects were then individually removed to an adjoining suite with a separate HVAC system for euthanasia by decapitation. The facility was approved by the American Association for Accreditation of Laboratory Animal Care (AAALAC) and all experimental procedures were approved in advance by the by the US EPA, National Health and Environmental Effects Research Laboratory Animal Care and Use Committee.

Whole brains were rapidly removed and placed on a cold plate (4°C). The frontal cortex was removed by making a vertical incision at the anterior edge of the optic tract with a stainless steel razor, and rapidly frozen on a bed of dry ice. Cortical samples, without striatal tissue, were then bisected into contralateral hemispheres, weighed, frozen in liquid nitrogen and stored at -80°C. In the time course study, one contralateral hemisphere was used for RNA extraction and qRT-PCR assays while the other hemisphere was used to make protein homogenates for Western Blot analysis.

RNA extraction. Frontal cortex samples were homogenized in 1 mL of TRI Reagent (Molecular Research Center, Inc., Cincinnati, OH) per 50-100 mg of tissue using a Polytron® PT-K homogenizer (Kinematica, Lucerne, Switzerland) and total RNA was isolated per manufacturer's instructions. Total RNA pellets suspended in DEPC-treated H_2O were then subject to DNase I treatment and reextracted with acid:phenol chloroform, pH = 4.7 and chloroform according to manufacturer's protocol and resuspended in DEPC-treated H_2O until use (Ambion Inc., Austin, TX). The total RNA concentration of each sample was determined (absorbance @ 260 nm) on a Beckman-Coulter DU® 800 spectrophotometer (Fullerton, CA) and adjusted to 1.0 µg/µL prior to sample storage at -80ºC. The ratio of absorbance values at 260 nm and 280 nm (Ab 260/280) was used to assess purity of total RNA samples. All samples used in these studies had Ab 260/280 ratios > 1.6 (data not shown). Preliminary PCR experiments using primers for rat β-actin genomic DNA (outlined in Tully et al. 2006) demonstrated that the above protocol adequately prevents genomic DNA contamination of total RNA samples (data not shown). In addition, the RNA integrity of each sample was determined using an Agilent 2100 Bioanalyzer and RNA 6000 Nano

LabChip Kit (Waldbron, Germany) according to manufacturer's instructions. All samples used in qRT-PCR experiments had 18S:28S rRNA ratios > 1.6 (data not shown). Following the RNA purity and integrity screens, aliquots of each total RNA sample were stored at -80°C until use.

Quantitative real-time RT-PCR. qRT-PCR assays were performed using TaqMan® One-Step RT-PCR Master Mix Reagent Kits and TaqMan® Gene Expression Assays on a ABI 7900HT Sequence Detection System (Applied Biosystems, Foster City, CA). The custom designed qRT-PCR assays used to distinguish between the *Camk1g1* and *Camk1g2* mRNA splice variants (Applied Biosystems, Foster City, CA) were targeted to exon junctions unique to the respective transcripts (see figure 3.1). AmpliTaq Gold® DNA Polymerase / dNTP mix, Multiscribe^{TM} reverse transcriptase / RNA inhibitor mix and TaqMan® Gene expression primer-probe mix specific for the transcript of interest were combined according to manufacturer's specifications (Applied Biosystems 2005). The reaction mixture was then dispensed into the reaction plate (15 µL / well) and 125 ng of total RNA (5 µL) was added. Each sample was measured in triplicate for each transcript of interest and internal reference gene. Reaction plates were maintained at 5°C during loading procedure. During data collection, reactions were incubated at 48°C for 45 min followed by incubation at 95°C for 10 min and 40 cycles of 94°C for 25 sec and 60°C for 1 min.

Details of the qRT-PCR assays used in this work are listed in Table 3.1. The amplification efficiency of each assay utilized in this experiment was examined using a serial dilution of pooled total RNA from rat cerebrocortex. Efficiencies were calculated as: $E_x = 10^{(-1/m)} - 1$, where E is the amplification efficiency of target transcript *x* and *m* is the slope of

threshold cycles versus $\log_{10}$ [total RNA concentration] across the range of dilutions (Applied Biosystems 2004). All assays used in this experiment had amplification efficiencies in the range of 100 +/- 10% within in the standard operating range of TaqMan assays suggested by the manufacturer (Applied Biosystems 2004). qRT-PCR data from deltamethrin and permethrin dose-response and time course studies were analyzed according to the $2^{-\Delta\Delta C}{}_T$ method as described by (Livak and Schmittgen 2001). β-actin expression did not change as a function of time or dose for either compound (data not shown) and was used at the internal reference for all $2^{-\Delta\Delta C}{}_T$ calculations. For dose-response studies, the mean $\Delta\Delta^C{}_T$ of vehicle treated controls were used as the $2^{-\Delta\Delta C}{}_T$ calibrator (Livak and Schmittgen 2001) to obtain approximations of fold-change from control. For time course studies, the mean $\Delta\Delta^C{}_T$ of vehicle treated controls were used as the $2^{-\Delta\Delta C}{}_T$ calibrator for each time-matched treatment group.

Statistical analysis of qRT-PCR dose response data was performed using a two-way ANOVA with compound and equipotent dose level (EDL) as independent variables and $2^{-\Delta\Delta C}{}_T$ as the dependent variable followed by Dunnett's mean contrast test. EDLs were defined as follows: group 1 (control) – vehicle controls for both compounds, group 2 ("sub-NOAEL") – 0.3 mg/kg DLT & 1 mg/kg PERM, group 3 ("threshold") – 1 mg/kg DLT & 10 mg/kg PERM, group 4 ("ED_{30}") – 3 mg/kg DLT & 40 mg/kg PERM, group 5("ED_{50}") – 100 mg/kg PERM. Statistical analysis of time course data was performed using a two-way ANOVA with time and treatment as independent variables and $2^{-\Delta\Delta C}{}_T$ as the dependent variable. Data were additionally analyzed with a one-way ANOVA at each time point with treatment as the independent variable ($p < 0.05$) to determine times of peak effect.

Western blot analysis. Cortical tissue was homogenized in a buffer containing (in mM): Tris-HCl (50), NaCl (150), EDTA (1), EGTA (1), Na_3VO_4 (1), 1 % Trition X-100, 1% $C_{24}H_{39}NaO_4$, 0.1 % SDS and 5 uL of Protease Inhibitor Cocktail III (Calbiochem, Inc.,) per 5 uL total buffer (pH = 7.4). Protein was homogenized with thirty even up and down strokes with a teflon pestle in a glass tube. Homogenates were then centrifuged at 12,000 x *g* at 4°C for 10 minutes. Supernatant was removed and protein concentrations measured using Pierce BCA™ Protein Assay Kit (Rockford, IL). Proteins were then stained with a 1:1 volume of Laemmli buffer (Bio-Rad, Hercules, CA) and stored at -80°C until use. On day of use, protein samples were boiled for 5 min and allowed to cool to room temperature. 12 µg of total protein for each sample was separated on 10% Precise™ pre-cast polyacrylamide gel (Pierce, Inc., Rockford, IL) with running buffer containing (in mM): Tris-HCl (100), HEPES (3), SDS (3), pH = 8.0. Gels were run at a constant voltage of 100 V for 15 min following by 125 V for 80 min. Proteins were then transferred to a nitrocellulose membrane using a TransBlot SD Semi-Dry Transfer cell (Bio-Rad, Inc., Hercules, CA) using a buffer containing (in mM): Tris-Base (48), Glycine (39), 0.000375% SDS and 20 % methanol. Proteins were transferred at 20 V for 30 min. Membranes were then washed with Tris-buffered saline (TBS, 42.1 mM Tris-HCl, 7.5 mM Tris-Base, 0.9% NaCl, pH=7.5) containing 0.03% Tween-20 and blocked for 1 h in 5% non-fat dry milk (Bio-Rad, Inc., Hercules, CA) diluted in TBS with 0.03% Tween-20. Membranes were then incubated overnight in blocking solution containing 0.03% Tween-20 and a 1:1000 dilution of *Camk1g1* primary antibody at 4°C. Membranes were then washed with TBS contained 0.01% Tween-20 and incubated with at 1:5000 dilution of rabbit HRP-conjugated secondary

antibody in blocking solution at room temperature for 1 h. Membranes were then washed again with TBS, 0.01% Tween-20 and incubated for 5 min at room temperature with SuperSignal® West Dura Extendend Duration Substrate (Pierce, Inc., Rockford, IL) according to manufacturer's instructions. Blots were imaged (400 sec exposure) and optical densities of the stained bands quantified on a Bio-Rad VersaDoc™ Imaging system and Quantity One® 1-D Analysis software (v4.6, Bio-Rad, Inc., Hercules, CA). Membranes were then stripped for 10 min with Restore™ Western Blot Stripping Buffer (Bio-Rad). Membranes were sequentially reprobed with β-II tubulin primary antibody (1:2500) and mouse secondary antibody (1:10,000) and imaged according to the above protocol save that the primary incubation was for 1 h at room temperature and blots were visualized for 200 sec. Western blot expression ratios were calculated by normalizing each *Camk1g* signal to the corresponding β-tubulin signal and divided by the mean *Camk1g*/β-tubulin ratio from the control treated samples. Each time point was examined independently on separate gels.

Results.

Acute oral exposure of rats to 0.3 – 3 mg/kg deltamethrin or 1 – 100 mg/kg permethrin resulted in a dose-dependent increase in the expression of *Camk1g1* in the frontal cortex at 6 h post-exposure (Figure 3.2C and 3.2D). The mRNA expression patterns observed using the *Camk1g1* specific assay (red curve, Figure 3.2C and 3.2D) closely approximates, but does not exactly match, those observed using a qRT-PCR assay that detects both splice variants (blue curve, Figure 3.2A and 3.2B). For deltamethrin, expression of *Camk1g1* was increased compared to control (~1.75-fold) across all doses at approximately the same level of expression. For permethrin, expression of *Camk1g1* increased at 10 mg/kg and higher by ~2-fold greater compared to controls. This closely

matches the results of the *Camk1g* assay that detects both splice variants. A very small yet statistically significant increase in the expression of the *Camk1g2* splice variant was observed at the ED_{30} for motor activity (Wolansky et al. 2006) for each compound tested (Figure 3.2E and 3.2F). Results of the statistical analyses of these data are given in Table 3.2. It is apparent from these data that increased expression of the *Camk1g1* splice variant is the main factor underlying the results obtained in the previous study by Harrill et al. (*submitted*).

The time course of *Camk1g* mRNA splice variant expression following either 3 mg/kg deltamethrin or 100 mg/kg permethrin exposures demonstrates that the increases in *Camk1g1* and *Camk1g2* are transient after an acute *in vivo* exposure (Figure 3.3A and 3.3B). Results of the statistical analyses of these data are given in Table 3.3. An appreciable increase in the expression of *Camk1g1* mRNA is observed at 3 and 6 h with both compounds and returns to control levels by 9 h. The changes in *Camk1g1* mRNA expression are larger in magnitude than those for *Camk1g2* mRNA with both compounds. Similar to the dose-response data, the increases in *Camk1g1* mRNA expression closely match the increases observed using the qRT-PCR assay that detects both splice variants. These data also support that increased expression of the *Camk1g1* splice variant is the main contributor to the results obtained in the previous study (Harrill et al. *submitted*).

Since it was determined that *Camk1g1* mRNA was changing most dramatically in response to pyrethroid exposure, alterations in *Camk1g1* protein expression was examined in the *in vivo* time course samples used in this study. An antibody specific for a region the C-terminal tail of *Camk1g1* (and not *Camk1g2*) was used to detect changes in protein levels. The predicted molecular weight of rat *Camk1g1* protein is ~ 53 kDa. The *Camk1g1* primary antibody detected a protein band with a slightly larger molecular weight (~ 60 kDa, Figure

3.4B). Both antibodies were able to detect linear increases in expression of their respective proteins across a range of diluted protein standards (Figure 3.4C and D). β-tubulin was used as the loading control as treatment had no effect on expression (data not shown). No significant change in the expression of *Camk1g1* protein was observed following treatment with either 3 mg/kg deltamethrin or 100 mg/kg permethrin (Figure 3.5).

Discussion.

The data from the present study demonstrate induction of *Camk1g1* mRNA following acute *in vivo* exposure to both deltamethrin and permethrin. These exposures also resulted in modest and very low magnitude changes in the expression of the *Camk1g2* mRNA splice variant. No changes in the expression of *Camk1g1* protein was observed following acute exposure to either 3 mg/kg deltamethrin or 100 mg/kg permethrin, the highest doses used in this study. These data are consistent with increased *Camk1g* mRNA expression observed in the previous work using both Affymetrix microarray technology and a qRT-PCR assay capable of detecting both mRNA splice variants of this gene (Harrill et al., *submitted*). The present data expand on the previous finding by demonstrating that pyrethroid-induced changes in *Camk1g* are driven mainly by increased expression of the *Camk1g1* splice variant. Furthermore, these data demonstrate that under the dosing conditions used in this study, increased *Camk1g1* mRNA expression is transient, returning to control levels within 9 h, and does not lead to a concurrent increase in *Camk1g1* protein expression.

It appears, at the least in the case of pyrethroid exposure, that expression of the rat *Camk1g1* and *Camk1g2* mRNA splice variants are not similarly regulated. Large treatment related effects on *Camk1g2* mRNA expression are not present even when the expression of *Camk1g1* mRNA is greatly affected. Currently, the intracellular mechanisms that control

inducible *Camk1g1* or *Camk1g2* mRNA expression are not known. Splice variant specific upregulation of activity-dependent mRNA species is not unprecedented in the central nervous system. Brain derived neurotrophic factor (*Bdnf*) mRNA be can expressed in a variety of splice variants in the CNS and different splice variants are expressed in response to different types, or different durations, of neuronal activity (Khundakar and Zetterstrom 2006; Liu et al. 2006). Differential activation of promoter elements upstream of the *Bdnf* untranslated exons controls the specific patterns of splice variant expression for this gene (Tabuchi et al. 2000). The promoter elements upstream of the *Camk1g* coding exons have not been examined. It is possible that differential activation of promoter elements in response to an excitatory stimulus may be the mechanism driving the differential expression observed here in response to pyrethroids. Alternatively, both *Camk1g1* and *Camk1g2* mRNA may be transcribed at the same rate even in the presence of pyrethroids. A pyrethroid-induced increase or decrease in the rate of *Camk1g1* or *Camk1g2* mRNA degradation, respectively, would also explain the differential response. Fukuchi et al. (2005) demonstrate that the half-life of mRNA expression for the pituitary adenylate cyclase-activating polypeptide (PACAP) increases in parallel to increases in the intensity of a depolarizing stimulus. Increased depolarization of neurons affected by pyrethroids may result in a stabilization of the expression of *Camk1g1* mRNA and not *Camk1g2*, therefore resulting in divergent, stimulus-dependent expression patterns. The mechanism of differential *Camk1g1* and *Camk1g2* mRNA expression in the rat brain requires further investigation.

Changes in the expression of *Camk1g* mRNA are consistent with changes in neuronal excitability, such as those produced by pyrethroids (Vijverberg and Van den Bercken 1992; Song and Narahashi 1996; Narahashi 2001). Xiang et al. (2007) correlated firing rates of

cortical neuronal networks maintained in culture with global mRNA expression following stimulation. They reported that patterns of *Camk1g* mRNA expression closely paralleled increases in neuronal firing rates. Increased *Camk1g* mRNA expression (as well as the increased neuronal firing rates) were dependent upon activation of voltage-sensitive sodium channels (VSSC) and the presence of free Ca^{+2}, as the VSSC blocker tetrodotoxin and the Ca^{+2} chelator EGTA abolished both effects (Xiang et al., 2007). In separate studies, sub-chronic dosing of olanzipine results in both increased burst firing in the frontal cortex *in vivo*, and increased expression of *Camk1g* (Fatemi et al. 2005; Gronier and Rasmussen 2006). In addition, *in vivo* exposure of rats to the antiepileptic drug phenytoin decreased *Camk1g* mRNA expression (Dingledine et al. 2005). Phenytoin decreases neuronal firing rates in several brain regions, including cortex (Matthews and Conner 1977; Lampl et al. 1998; Calabresi et al. 1999). It is apparent that *Camk1g* mRNA expression is correlated with alterations in neuronal firing rates. However, this previous research has not provided information on which of the *Camk1g* splice variants is affected by the alterations in firing rates. The present data suggest that in the rat the *Camk1g1* mRNA splice variant may be more sensitive to changes in neuronal excitability given that the pyrethroids produce a more robust increase in *Camk1g1* mRNA as compared to *Camk1g2* mRNA.

The finding that *Camk1g1* mRNA expression and not *Camk1g2* mRNA expression is affected by pyrethroids is significant given that the biological activities of the proteins encoded by these two splice variants are very distinct. *Camk1g1* kinase activity is dependent upon the presence of Ca^{+2}-bound calmodulin and activation by an upstream CaM kinase kinase whose own activity is also regulated by intracellular Ca^{+2} levels. *Camk1g2* kinase activity is not enhanced in the presence of Ca^{+2}-bound calmodulin or affected by the

Camk1g1 upstream activating kinase (Nishimura et al. 2003). More importantly, the ability of *Camk1g1* to regulate neuronal dendritogenesis in developing neurons is dependent upon sequential prenyaltion and palmitoylation of the C-terminal region of this protein (Takemoto-Kimura et al. 2007). *Camk1g2* lacks the lipidification sites present on *Camk1g1* required for mediating these effects. All studies reporting biologically significant effects of *Camk1g* on neuronal morphogenesis used the *Camk1g1* splice variant as the basis for their study (Wayman et al. 2007; Takemoto-Kimura et al. 2007). No role for endogenous *Camk1g2* protein has been identified. The induction of *Camk1g1* mRNA in the present study indicates that pyrethroids may disrupt neuronal processes mediated by *Camk1g1* protein such as dendritogenesis. Indeed, dendritic branching has been shown to be affected by both deltamethrin and permethrin in *in vitro* developmental neurotoxicity assays (Harrill et al. *submitted*). The induction of *Camk1g1* mRNA observed here supports a putative role for the transcriptional induction of *Camk1g1* in the pyrethroid-mediated effects on neurite branching.

The *in vivo* exposures utilized in the present time course study did not result in a significant increase in the expression of *Camk1g1* protein. This is inconsistent with the increased expression of *Camk1g1* mRNA. There are a number of possible explanations for this discrepancy. First, the Western blot assay used may not be detecting *Camk1g1* protein. It is possible that a post-translational modification interferes with the ability of the *Camk1g1* antibody to recognize the protein. The primary antibody used for quantification of *Camk1g1* protein detected a strong protein band at ~ 60 kDa. This is larger than the predicted molecular weight of the rat *Camk1g1* protein (53 kDa). The disparity between the predicted and observed *Camk1g1* molecular weights is likely due to to post-translational prenylation

and palmitoylation of the *Camk1g1* protein (Takemoto-Kimura et al. 2007). This suggests that the 60 kDa band may be modified *Camk1g1*. Alternatively, this band may represent a non-specific recognition of a different protein by the primary antibody. Additional studies with purified *Camk1g1* protein may help resolve this issue.

In contrast, the lack of measurable increases in *Camk1g1* protein could be due to the acute dosing paradigm used in the present research. As demonstrated in Figure 3.3, the pyrethroid-induced increases in *Camk1g1* mRNA expression are transient and recover on a time scale that reflects the pharmacokinetics of these compounds. Acute oral exposure of rats to permethrin and deltamethrin results in a rapid accumulation of these compounds in the brain. Peak concentrations occur between ~1-3 h and these compounds are cleared from the brain with half-lives on the order of tens of hours (Anadon et al. 1991; Anadon et al. 1996; Mirfazaelian et al. 2006; Tornero-Velez et al. 2007). Triggering an appreciable increase in *Camk1g1* protein in adult neurons may require a more sustained increase in *Camk1g1* mRNA then what is observed in the present study. More persistent (i.e., sub-chronic) exposures to pyrethroids that produce a steady-state brain burden of these compounds may be necessary to elevate *Camk1g1* protein, but this is yet to be determined.

In summary, this study demonstrates that following an acute *in vivo* exposure to either deltamethrin or permethrin transiently increased expression *Camk1g1* splice variant mRNA in the rat frontal cortex. The transient increases in *Camk1g1* mRNA did not result in measureable increases in *Camk1g1* protein under the exposure conditions used here. Future research efforts concerning *Camk1g*, neuronal excitability and pyrethroids should focus on determining how pyrethroid actions at the neuronal membrane results in the increased

expression of *Camk1g1* mRNA and whether this response impacts neuronal structure or function.

Funding.

J.A. Harrill is currently funded through the EPA/UNC Toxicology Research Program training agreement (CR833237) and previously funded through National Institute of Environmental Health Science Training Grant (T32-ES07126).

Acknowledgements.

This document has been reviewed by the National Health and Environmental Effects Research Laboratory and approved for publication. Approval does not signify that the contents reflect the views of the agency, nor does mention of trade names or commercial products constitute endorsement or recommendation for use. The authors wish to thank Chris Miller for his help in the design of the *Camk1g1* and *Camk1g2* splice variant specific TaqMan® qRT-PCR assays and Applied Biosystems (Foster City, CA) for graciously supplying these assays for use in this work. We also thank Dr. William Mundy for his help with the Western blots.

Table 3.1. Camk1g *and* Camk1g *splice variant specific TaqMan assays.*

Assay	GenBank Ascension		Nucleotide Sequences	Nucleotide Alignments	Exon Junction	Amplification Efficiency
Camk1g	NM_182842	Reference[a,b]:	5'-GATGACATTTCTGAGTCAGCCAAGG-3'	810 → 834	8-9	96.0 %
	AB101231			810 → 834	8-9	
	AB101232			810 → 834	8-9	
Camk1g1	NM_182842	Forward:	5'-CCTCCAGATTCAGAAGAACTTTGC-3'	956 → 979	10-11	94.2 %
	AB101231	Backward:	5'-CGGCGGCCGCATTG-3'	1017 ← 1004	10-11	
		Reporter:	5'-AAGTGGAGGCAAGCCT-3'	987 → 1002		
Camk1g2	AB101232	Forward:	5'-CCTCCAGATTCAGAAGAACTTTGC-3'	956 → 979	10-12	98.7 %
		Backward:	5'-CCTGCTTTCACTGGTACCATGAC-3'	1034 ← 1012		
		Reporter:	5'-AAGTGGAGGGAACTTCAA-3'	987 → 1004		

[a]Primer and probe sequences of Applied Biosystems pre-designed TaqMan® qRT-PCR assays are proprietary. Reference sequence provided by manufacturer is listed. [b]TaqMan® gene expression assay Rn00788224_m1.

Table 3.2. ***Statistical analysis of qRT-PCR dose-response data.***[a]

Camk1g	EDL	$F(4, 54) = 4.47,\ p = 0.0034$**	3, 4, 5[b]
	COMPOUND	$F(1, 54) = 0.96,\ p = 0.3370$	
	EDL*COMPOUND	$F(3, 54) = 1.16,\ p = 0.3335$	
Camk1g1	EDL	$F(4, 54) = 2.79,\ p = 0.0355$**	4
	COMPOUND	$F(1, 54) = 0.04,\ p = 0.8380$	
	EDL*COMPOUND	$F(3, 54) = 0.78,\ p = 0.5096$	
Camk1g2	EDL	$F(4, 54) = 2.57,\ p = 0.0484$**	4
	COMPOUND	$F(1, 54) = 6.76,\ p = 0.0120$**	
	EDL*COMPOUND	$F(3, 54) = 1.95,\ p = 0.1325$	

[a]Data were analyzed using a two-way ANOVA model with equipotent dose level (EDL) and COMPOUND (deltamethrin, permethrin) as the independent variables. [b]A post-hoc Dunnett's many-to-one mean contrast test was also performed on the data. Numbers represent the EDL with means in expression significantly different from vehicle controls ($p < 0.05$ significance level), 3 = NOAEL, 4 = ED_{30} and 5 = ED_{50} for decreases in ambulatory motor activity. ** = significant at $p < 0.05$ in two-way ANOVA model. Analysis were performed on $2^{-\Delta\Delta C}{}_T$ values (Livak and Schmittgen 2001)

Table 3.3. ***Statistical analysis of qRT-PCR time course data.***[a]

Camk1g	TRT	F (1, 56) = 4.56, p = 0.0371**	3 h[b]	TRT	F (1, 56) = 2.16, p = 0.1472	n.e.
	TIME	F (3, 56) = 1.75, p = 0.1665		TIME	F (3, 56) = 1.14, p = 0.3391	
	TRT*TIME	F (3, 56) = 2.07, p = 0.1140		TRT*TIME	F (3, 56) = 0.54, p = 0.6586	
Camk1g1	TRT	F (1, 56) = 4.76, p = 0.0334**	3 h	TRT	F (1, 56) = 4.65, p = 0.0354**	n.e.
	TIME	F (3, 56) = 3.67, p = 0.0174**		TIME	F (3, 56) = 0.76, p = 0.5225	
	TRT*TIME	F (3, 56) = 3.92, p = 0.0131**		TRT*TIME	F (3, 56) = 0.37, p = 0.7784	
Camk1g2	TRT	F (1, 56) = 6.13, p = 0.0164**	6 h	TRT	F (1, 56) = 6.89, p = 0.0112**	6 h
	TIME	F (3, 56) = 5.25, p = 0.0029**		TIME	F (3, 56) = 4.73, p = 0.0052**	
	TRT*TIME	F (3, 56) = 4.92, p = 0.0042**		TRT*TIME	F (3, 56) = 4.47, p = 0.0069**	

[a]Data were analyzed using a Two-way ANOVA model with treatment (TRT) and TIME as the independent factors. ** = significant at $p < 0.05$. [b]Data were additionally analyzed within time point for each gene using a One-way ANOVA. Times noted on this table were significant at $p < 0.05$.

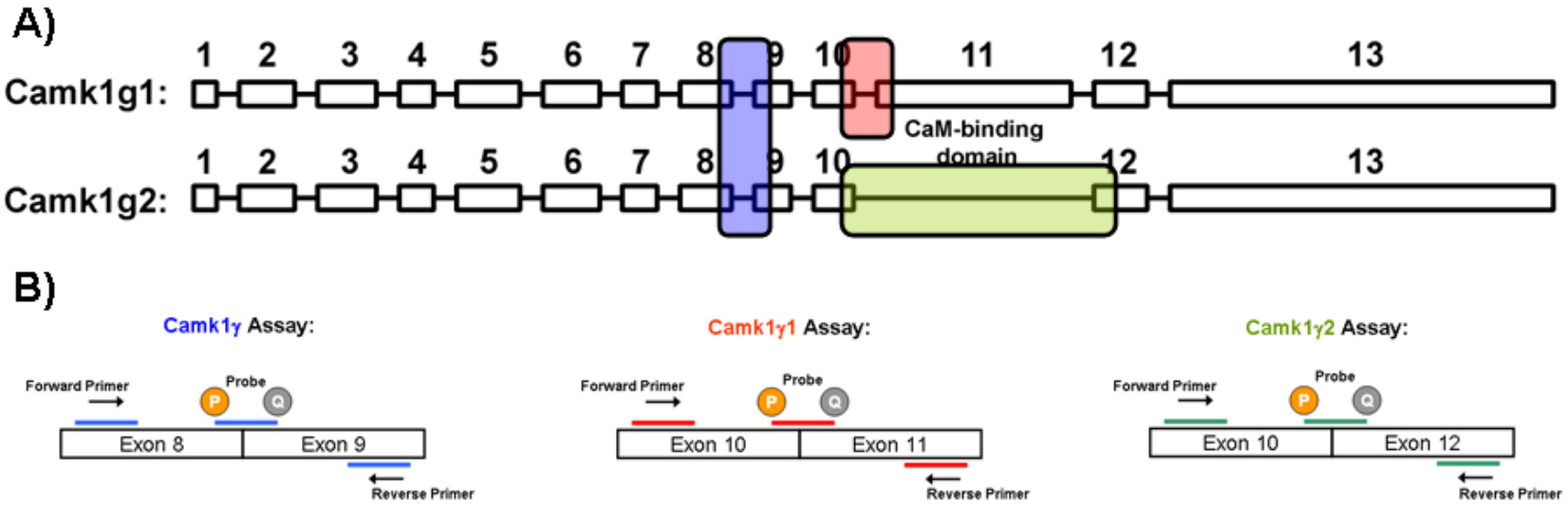

Figure 3.1. ***Exon schematic of rat*** **Camk1g1** ***and*** **Camk1g2.** A) Intron/exon diagram of rat *Camk1g1* and *Camk1g2*. Boxes are exons while lines are introns. *Camk1g1* contains 13 exons while *Camk1g2* contains 12 exons, with the calmodulin-binding domain of *Camk1g1* (exon 11) absent. Highlighted boxes correspond to the exon junctions targeted by the qRT-PCR assays. B) Assay schematics for *Camk1g*, *Camk1g1* and *Camk1g2* assays, respectively. Each assay contains a forward primer, reverse primer and a probe sequence with fluorophone (P) and quencher (Q). Upon primer extension the 5' to 3' nuclease activity of the AmpliTaq Gold DNA polymerase degrades the primer, releases the fluorophore from the quencher and light is emitted which is quantified for calculations of mRNA abundance. Note the probe and reverse primer of the *Camk1g1* and *Camk1g2* assays are unique while the forward primer of each of these two is the same. Assays are described in detail in Table 3.1.

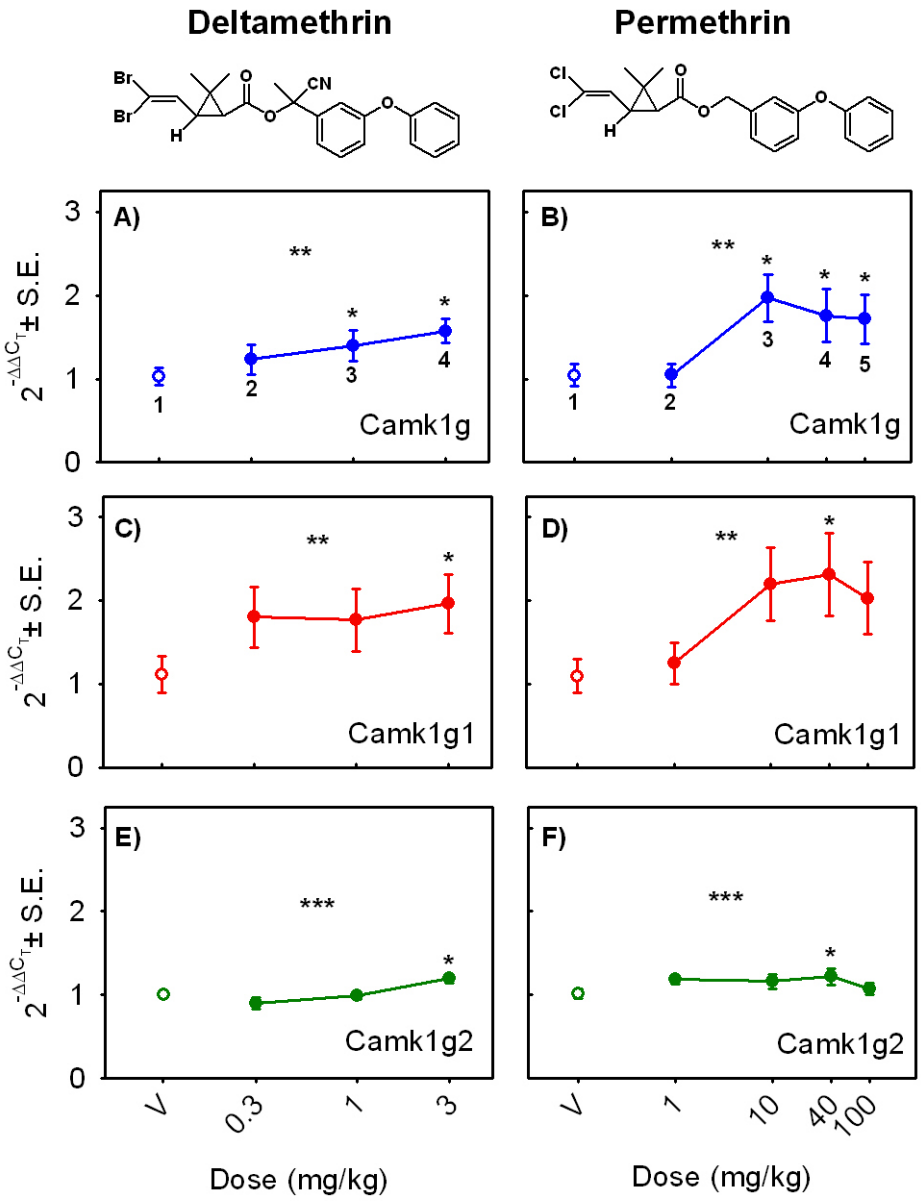

Figure 3.2. ***Dose-response for* Camk1g1 *and* Camk1g2 *mRNA expression.*** Panels A-F show dose-response curves for the *Camk1g* (A-B), *Camk1g1* (C-D) and *Camk1g2* (E-F) qRT-PCR assays in frontal cortex at 6 h following acute exposure to deltamethrin (A,C & E) or permethrin (B,D & F). Data were quantified and analyzed using the $2^{-\Delta\Delta}{}_{CT}$ method and data are expressed as mean $2^{-\Delta\Delta}{}_{CT} \pm$ standard error. Numbers underlying the points in panels A & B demonstrate which equipotent dose level (EDL) groupings each treatment belongs to for statistical analyses of these data: 1 = vehicle control, 2 = sub-NOAEL, 3 = threshold, 4 = ED_{30}, 5 = ED_{50} for decreases in motor activity. Results of statistical analyses of these data are given in Table 3.2. * = treatment group mean is significantly different from vehicle control in a Dunnett's many-to-one mean contrast test ($p < 0.05$) ** = main effect of equipotent dose level with no interaction of EDL & compound in Two way ANOVA ($p < 0.05$). *** = significant interaction of EDL & COMPOUND.

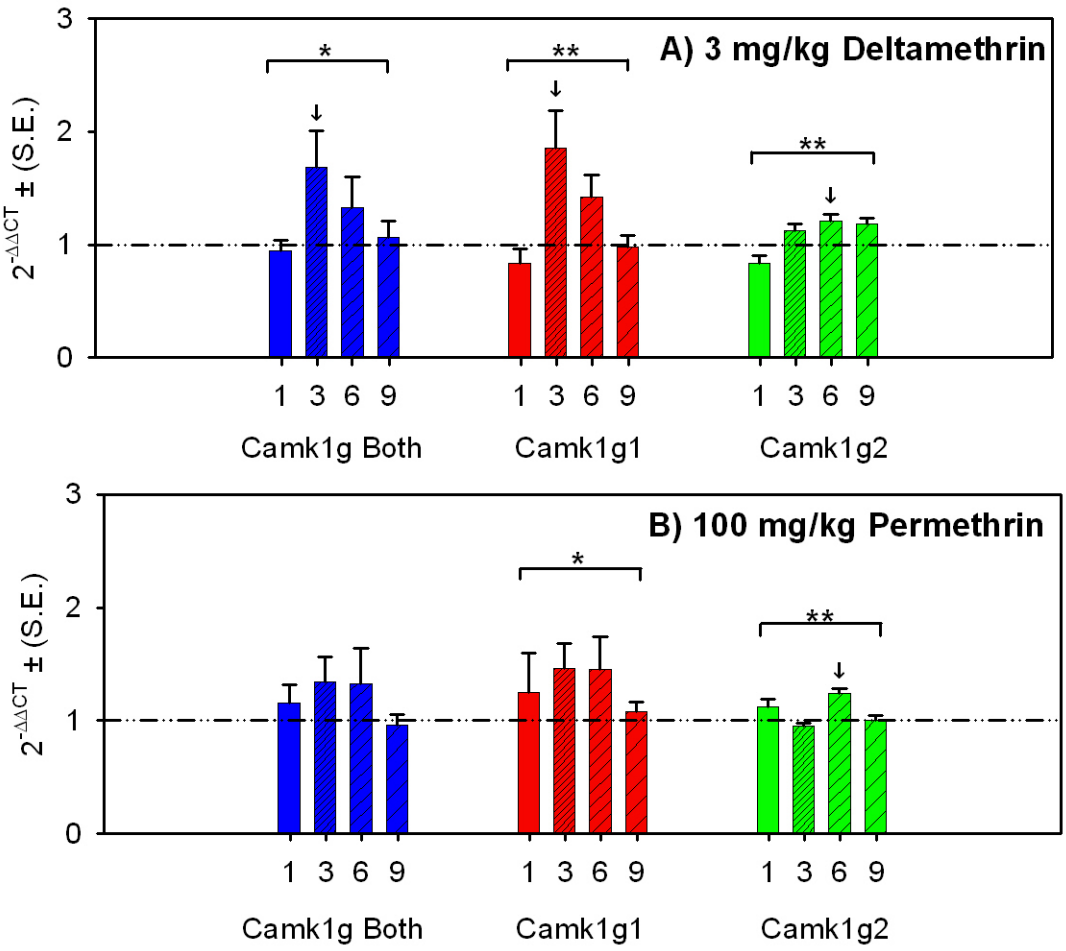

Figure 3.3. ***Time course for*** **Camk1g1** ***and*** **Camk1g2** ***mRNA expression.*** Rats were orally exposed to either 3 mg/kg deltamethrin (A) or 100 mg/kg permethrin (B) and mRNA expression quantified in the frontal cortex at 1,3,6 and 9 h post-exposure. Data within each time point were quantified using the $2^{-\Delta\Delta}{}_{CT}$ method and data are expressed as mean $2^{-\Delta\Delta}{}_{CT} \pm$ standard error. Red bars correspond to the *Camk1g1* specific qRT-PCR assay, green bars to the *Camk1g2* specific qRT-PCR assay and blue bars to the assay that detects both splice variants. Results of statistical analyses of these data is given in Table 3.3. * = main effect of treatment with no interaction of time & treatment in a two-way ANOVA ($p < 0.05$). ** = significant interaction of time & treatment ($p < 0.05$). Arrows denote time points with means in expression significantly different from time-matched vehicle control values in a One-Way ANOVA ($p < 0.05$). Vehicle treated control data not shown.

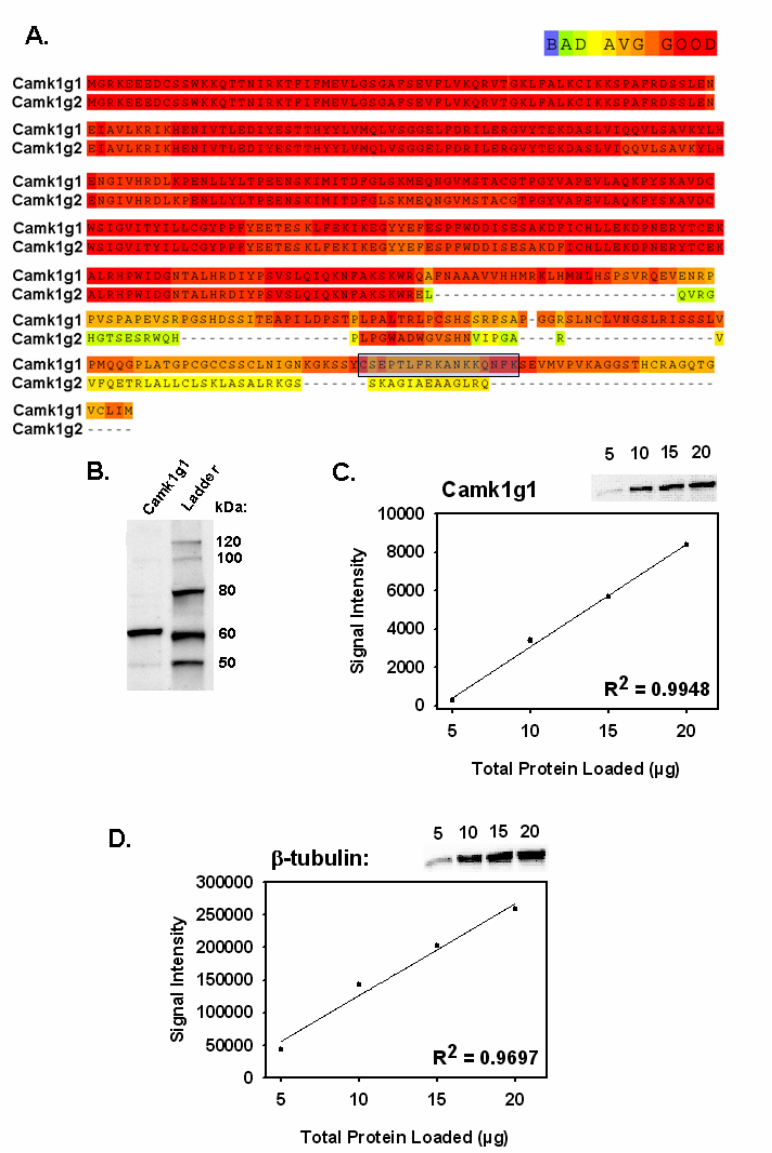

<u>Figure 3.4</u>. ***Rat* Camk1g1 *and* Camk1g2 *protein sequences and Camk1g1 protein assay development.*** A) Alignment of rat *Camk1g1* and *Camk1g2* protein coding sequences. *Camk1g1* is the top line and *Camk1g2* the bottom line in each doublet. Highlighting colors correspond to the strength of identify between the matched amino acids with red being absolute identity and blue being a poor match. Color bar is in top right corner. Protein alignment performed using Swiss Institute for Bioinformatics TCoffee tool. The antigen sequence for the *Camk1g1* primary antibody is marked with a blue box. B) A single strong band at ~ 60 kDa was detected using the *Camk1g1* primary antibody. C) Signal from *Camk1g1* increases linearly as a function of total protein loaded from 5-20 µg. Visualization of Western blot bands given in top right corner of panel. D) Signal from β-tubulin primary antibody increased linearly as a function of total protein loaded from 5-20 µg after stripping of *Camk1g1* primary antibody. Standard curves in C and E were obtained from the same blot.

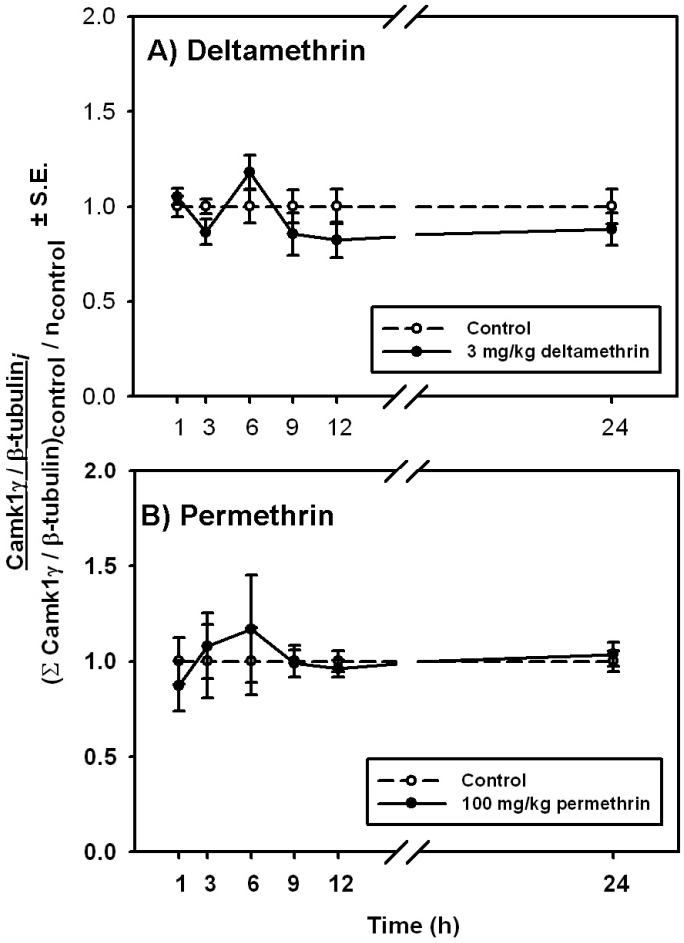

Figure 3.5. Camk1g1 ***protein expression following acute pyrethroid exposure.*** Rats were orally exposed to either 3 mg/kg deltamethrin (A) or 100 mg/kg permethrin (B) and *Camk1g1* protein expression was quantified in frontal cortex via Western blots at 1,3,6,9,12 or 24 h post-exposure. Signal intensities for *Camk1g1* expression were normalized within sample to β-tubulin and expressed as percent change from untreated control within each set of treated and time-matched control samples. Data are expressed as mean fold-change from time matched, vehicle-treated control groups ± S.E.

Works Cited

Amweg, E. L., Weston, D. P., and Ureda, N. M. (2005). Use and toxicity of pyrethroid pesticides in the Central Valley, California, USA. *Environ Toxicol Chem* **24**, 966-72.

Anadon, A., Martinez-Larranaga, M. R., Diaz, M. J., and Bringas, P. (1991). Toxicokinetics of permethrin in the rat. *Toxicol Appl Pharmacol* **110**, 1-8.

Anadon, A., Martinez-Larranaga, M. R., Fernandez-Cruz, M. L., Diaz, M. J., Fernandez, M. C.,and Martinez, M. A. (1996). Toxicokinetics of deltamethrin and its 4'-HO-metabolite in the rat. *Toxicol Appl Pharmacol* **141**, 8-16.

Applied Biosystems Inc. (2004). *Amplification Efficiency of Taqman Assays-on-Demand Gene Expression Products (Publication 127AP05-01).* Applied Biosystems Inc.,, Foster City, CA.

Applied Biosystems Inc. (2005). *TaqMan Gene Expression Assays Protocol (Part Number 4333458).* Applied Biosystems Inc.,, Foster City, CA.

Bading, H. (2000). Transcription-dependent neuronal plasticity the nuclear calcium hypothesis. *Eur J Biochem* **267**, 5280-3.

Burr, S. A., and Ray, D. E. (2004). Structure-activity and interaction effects of 14 different pyrethroids on voltage-gated chloride ion channels. *Toxicol Sci* **77**, 341-6.

Calabresi, P., Centonze, D., Marfia, G. A., Pisani, A., and Bernardi, G. (1999). An in vitro electrophysiological study on the effects of phenytoin, lamotrigine and gabapentin on striatal neurons. *Br J Pharmacol* **126**, 689-96.

Colt, J. S., Lubin, J., Camann, D., Davis, S., Cerhan, J., Severson, R. K., Cozen, W., and Hartge,P. (2004). Comparison of pesticide levels in carpet dust and self-reported pest treatment practices in four US sites. *J Expo Anal Environ Epidemiol* **14**, 74-83.

Dingledine, R. (2004). Antiepileptic drugs levetiracetam and phenytoin effect on the brain. In NIH Neuroscience Microarray Consortium, Vol. 2007. National Institute of Health.

Dunnett, C. W. (1950). A multiple comparison procedure for comparing several treatments with a control. *Journal of the American Statistical Association* **50**, 1096-1121.

Fatemi, S. H., Reutiman, T. J., Folsom, T. D., Bell, C., Nos, L., Fried, P., Pearce, D. A., Singh, S., Siderovski, D. P., Willard, F. S., and Fukuda, M. (2006). Chronic olanzapine treatment causes differential expression of genes in frontal cortex of rats as revealed by DNA microarray technique. *Neuropsychopharmacology* **31**, 1888-99.

Fields, R. D., Lee, P. R., and Cohen, J. E. (2005). Temporal integration of intracellular Ca2+ signaling networks in regulating gene expression by action potentials. *Cell Calcium* **37**, 433-42.

Fukuchi, M., Tabuchi, A., and Tsuda, M. (2005). Transcriptional regulation of neuronal genes and its effect on neural functions: cumulative mRNA expression of PACAP and BDNF genes controlled by calcium and cAMP signals in neurons. *J Pharmacol Sci* **98**, 212-8.

Gronier, B. S., and Rasmussen, K. (2003). Electrophysiological effects of acute and chronic olanzapine and fluoxetine in the rat prefrontal cortex. *Neurosci Lett* **349**, 196-200.

Harrill, J. A., LI, Z., Wright, F. A., Radio, N. M., Mundy, W. R., and Crofton, K. M. (*submitted*). Transcriptional response of rat cerebrocortical tissue following acute in vivo exposure to the pyrethroid insecticides permethrin and deltamethrin. *BMC Genomics*.

Harrill, J. A., Wright, F. A., and Crofton, K. M. (2007). Dose-response modeling of the transcriptional response of rat cerebrocortical tissue after acute pyrethroid exposure *in vivo*. *The Toxicologist* **96**, 186.

Heudorf, U., Angerer, J., and Drexler, H. (2004). Current internal exposure to pesticides in children and adolescents in Germany: urinary levels of metabolites of pyrethroid and organophosphorus insecticides. *Int Arch Occup Environ Health* **77**, 67-72.

Khundakar, A. A., and Zetterstrom, T. S. (2006). Biphasic change in BDNF gene expression following antidepressant drug treatment explained by differential transcript regulation. *Brain Res* **1106**, 12-20.

Lampl, I., Schwindt, P., and Crill, W. (1998). Reduction of cortical pyramidal neuron excitability by the action of phenytoin on persistent Na+ current. *J Pharmacol Exp Ther* **284**, 228-37.

Leng, G., Kuhn, K. H., and Idel, H. (1997). Biological monitoring of pyrethroids in blood and pyrethroid metabolites in urine: applications and limitations. *Sci Total Environ* **199**, 173-81.

Liu, Q. R., Lu, L., Zhu, X. G., Gong, J. P., Shaham, Y., and Uhl, G. R. (2006). Rodent BDNF genes, novel promoters, novel splice variants, and regulation by cocaine. *Brain Res* **1067**, 1-12.

Livak, K. J., and Schmittgen, T. D. (2001). Analysis of relative gene expression data using real-time quantitative PCR and the 2(-Delta Delta C(T)) Method. *Methods* **25**, 402-8.

Matthews, W. D., and Connor, J. D. (1977). Actions of iontophoretic phenytoin and medazepam on hippocampal neurons. *J Pharmacol Exp Ther* **201**, 613-21.

Mirfazaelian, A., Kim, K. B., Anand, S. S., Kim, H. J., Tornero-Velez, R., Bruckner, J. V., and Fisher, J. W. (2006). Development of a physiologically based pharmacokinetic model for deltamethrin in the adult male Sprague-Dawley rat. *Toxicol Sci* **93**, 432-42.

Narahashi, T. (1996). Neuronal ion channels as the target sites of insecticides. *Pharmacol Toxicol* **79**, 1-14.

Narahashi, T. (2001). Neurophysiological Effects of Insecticides. In Handbook of Pesticide Toxicology (R. I. Krieger, ed., Vol. 2, pp. 335-351. Academic Press, San Diego, CA.

Nishimura, H., Sakagami, H., Uezu, A., Fukunaga, K., Watanabe, M., and Kondo, H. (2003). Cloning, characterization and expression of two alternatively splicing isoforms of Ca2+/calmodulin-dependent protein kinase I gamma in the rat brain. *J Neurochem* **85**, 1216-27.

Ray, D. E. (2001). Pyrethroid Insecticdes: Mechanisms of Toxicity, Systematic Poisoning Syndromes, Parethesia, and Therapy. In Handbook of Pesticide Toxicology (R. I. Krieger, ed., Vol. 2, pp. 1289-1303. Academic Press, San Diego, CA.

Shafer, T. J., and Meyer, D. A. (2004). Effects of pyrethroids on voltage-sensitive calcium channels: a critical evaluation of strengths, weaknesses, data needs, and relationship to assessment of cumulative neurotoxicity. *Toxicol Appl Pharmacol* **196**, 303-18.

Soderlund, D. M., Clark, J. M., Sheets, L. P., Mullin, L. S., Piccirillo, V. J., Sargent, D., Stevens, J. T., and Weiner, M. L. (2002). Mechanisms of pyrethroid neurotoxicity: implications for cumulative risk assessment. *Toxicology* **171**, 3-59.

Song, J. H., and Narahashi, T. (1996). Modulation of sodium channels of rat cerebellar Purkinje neurons by the pyrethroid tetramethrin. *J Pharmacol Exp Ther* **277**, 445-53.

Symington, S. B., and Clark, J. M. (2005). Action of deltamethrin on N-Type (Cav2.2) voltage-sensitive calcium channels in rat brain. *Pesticide Biochemistry and Physiology* **82**, 1-15.

Tabuchi, A., Nakaoka, R., Amano, K., Yukimine, M., Andoh, T., Kuraishi, Y., and Tsuda, M. (2000). Differential activation of brain-derived neurotrophic factor gene promoters I and III by Ca2+ signals evoked via L-type voltage-dependent and N-methyl-D-aspartate receptor Ca2+ channels. *J Biol Chem* **275**, 17269-75.

Takemoto-Kimura, S., Ageta-Ishihara, N., Nonaka, M., Adachi-Morishima, A., Mano, T., Okamura, M., Fujii, H., Fuse, T., Hoshino, M., Suzuki, S., Kojima, M., Mishina, M., Okuno, H., and Bito, H. (2007). Regulation of dendritogenesis via a lipid-raft-associated Ca2+/calmodulin-dependent protein kinase CLICK-III/CaMKIgamma. *Neuron* **54**, 755-70.

Takemoto-Kimura, S., Terai, H., Takamoto, M., Ohmae, S., Kikumura, S., Segi, E., Arakawa, Y., Furuyashiki, T., Narumiya, S., and Bito, H. (2003). Molecular cloning and characterization of CLICK-III/CaMKIgamma, a novel membrane-anchored neuronal Ca2+/calmodulin-dependent protein kinase (CaMK). *J Biol Chem* **278**, 18597-605.

Tornero-Velez, R., Scollon, E. J., Starr, J., Hughes, M. F., DeVito, M. J., and Dary, C. C. (2007). Pharmacokinetic/Pharmacodynamic Modeling of Permethrin in the Rat. *The Toxicologist* **96**, 81.

Tulve, N. S., Jones, P. A., Nishioka, M. G., Fortmann, R. C., Croghan, C. W., Zhou, J. Y., Fraser, A., Cavel, C., and Friedman, W. (2006). Pesticide measurements from the first national environmental health survey of child care centers using a multi-residue GC/MS analysis method. *Environ Sci Technol* **40**, 6269-74.

Tully, D. B., Bao, W., Goetz, A. K., Blystone, C. R., Ren, H., Schmid, J. E., Strader, L. F., Wood, C. R., Best, D. S., Narotsky, M. G., Wolf, D. C., Rockett, J. C., and Dix, D. J. (2006). Gene expression profiling in liver and testis of rats to characterize the toxicity of triazole fungicides. *Toxicol Appl Pharmacol* **215**, 260-73.

Vijverberg, H. P., and van den Bercken, J. (1982). Annotation. Action of pyrethroid insecticides on the vertebrate nervous system. *Neuropathol Appl Neurobiol* **8**, 421-40.

Wayman, G. A., Impey, S., Marks, D., Saneyoshi, T., Grant, W. F., Derkach, V., and Soderling, T. R. (2006). Activity-dependent dendritic arborization mediated by CaM-kinase I activation and enhanced CREB-dependent transcription of Wnt-2. *Neuron* **50**, 897-909.

West, A. E., Griffith, E. C., and Greenberg, M. E. (2002). Regulation of transcription factors by neuronal activity. *Nat Rev Neurosci* **3**, 921-31.

Weston, D. P., You, J., and Lydy, M. J. (2004). Distribution and toxicity of sediment-associated pesticides in agriculture-dominated water bodies of California's Central Valley. *Environ Sci Technol* **38**, 2752-9.

Whyatt, R. M., Barr, D. B., Camann, D. E., Kinney, P. L., Barr, J. R., Andrews, H. F., Hoepner, L. A., Garfinkel, R., Hazi, Y., Reyes, A., Ramirez, J., Cosme, Y., and Perera, F. P. (2003). Contemporary-use pesticides in personal air samples during pregnancy and blood samples at delivery among urban minority mothers and newborns. *Environ Health Perspect* **111**, 749-56.

Wolansky, M. J., Gennings, C., and Crofton, K. M. (2006). Relative potencies for acute effects of pyrethroids on motor function in rats. *Toxicol Sci* **89**, 271-7.

Wolansky, M. J., and Harrill, J. A. (2008). Neurobehavioral toxicology of pyrethroid insecticides in adult animals: A critical review. *Neurotoxicol Teratol* **30**, 55-78.

Xiang, G., Pan, L., Xing, W., Zhang, L., Huang, L., Yu, J., Zhang, R., Wu, J., Cheng, J., and Zhou, Y. (2007). Identification of activity-dependent gene expression profiles reveals specific subsets of genes induced by different routes of Ca(2+) entry in cultured rat cortical neurons. *J Cell Physiol* **212**, 126-36.

Transcriptional Response of Rat Frontal Cortex to Acute Pyrethroid Exposure.

Chapter 4

Joshua A. Harrill[*], Hongzu Ren[†], J. Christopher Corton[†], Kevin M. Crofton[‡]

[*]*Curriculum in Toxicology, University of North Carolina at Chapel Hill, NC, 27599,*
[†]*Environmental Carcinogenesis Division and* [‡]*Neurotoxicology Division, NHEERL ORD, USEPA,RTP, NC, 27711*

Correspondence:
[‡]Kevin M. Crofton, Ph.D., USEPA, Neurotoxicology Division, B105-04, Research Triangle Park, NC 27711; Phone: 919-541-2672; E-mail: crofton.kevin@epa.gov

Abstract.

Pyrethroids are pesticides that interact with voltage-sensitive ion channels and disrupt neuronal function. Acute disruption of neuronal function can result in adverse effects on behavior. In addition, change in neuronal firing patterns, such as those produced by pyrethroids, may also lead to changes in activity-regulated gene expression. Previous research demonstrated that permethrin (a Type I pyrethroid) and deltamethrin (a Type II pyrethroid) exposure alters gene expression in the rat cortex. The present study expands upon the previous findings by examining the global transcriptional response of rat cortex for six different pyrethroids. Rats were acutely dosed with a Type I pyrethroid (permethrin, bifenthrin or tefluthrin), a Type II pyrethroid (deltamethrin, cypermethrin or cyfluthrin) or vehicle and cortex was sampled at 3 and 6 h post exposure. Affymetrix GeneChips® were used to obtain global gene expression profiles from the cortical tissue. Analysis of the microarray data demonstrated robust transcriptional responses following exposure to Type II pyrethroids. Type I pyrethroids produced only marginal effects on cortical gene transcription some of which were in common with the effect produced by the Type II pyrethroids. Comparison of gene expression profiles revealed a suite of genes commonly affected by the Type II pyrethroids. Ingenuity® pathway analysis of these transcriptional changes yielded an interconnecting network of gene interactions that is consistent with the excitatory effects of these compounds.

Introduction.

Pyrethroids are neurotoxic pesticides used in a variety of agricultural, household, veterinary and human health applications (Heudorf & Angerer 2001; Yanez et al. 2002). Use of pyrethroids has increased in conjunction with decreased use of insecticides from other chemical classes. There is a potential for human exposures as pyrethroids and pyrethroid residues have been detected in urine samples from pesticide applicators, blood samples of urban mothers, residential house dust and wipe samples from U.S. child care centers (Leng et al. 1997; Whyatt et al. 2003; Colt et al 2004; Weston et al. 2004; Tulve et al. 2006).

Classically, pyrethroids have been divided into different sub-types based chemical structure and the signs of acute poisoning observed in laboratory rodents at near lethal dose levels (Verschoyle and Aldridge 1980; Lawrence and Casida 1982). Pyrethroids containing an α-cyano group (Type II) produce a poisoning syndrome characterized by increased burrowing and digging behavior that progresses to whole body tremor followed by profuse salivation and a sinuous writhing known as choreoathetosis (CS-syndrome, Verschoyle and Aldridge 1980). Pyrethroids that lack an α-cyano group (Type I) produce a poisoning syndrome characterized by episodes of aggressive sparing behavior and increased sensitivity to external stimuli that progresses to fine tremors followed by course whole body tremors and prostration (T-syndrome, Verschoyle and Aldridge 1980). At lower dose levels, the neurotoxic effects of pyrethroids have been detected by a number of neurobehavioral tests. Some behavioral endpoints are commonly affected by all pyrethroids (i.e. motor activity, Wolansky et al. 2006), while others are affected differently across the pyrethroid class (e.g. acoustic startle response and thermoregulation, Crofton and Reiter 1988; Wolansky and Harrill 2007).

The primary molecular targets of pyrethroids are voltage-sensitive sodium channels (VSSCs). Pyrethroids delay VSSC deactivation which results in a prolonged entry of Na^+ into the neuron (Na^+ tail current) during periods when unmodified VSSCs are normally impermeable (Narahashi 2001). Abnormal Na^+ tail currents can persist for as little as milliseconds and as long as hundreds of milliseconds depending upon the structure of the pyrethroid and the isoform of VSSC (Vijverberg and Van den Bercken 1990; Smith and Soderlund 1998; Choi and Soderlund 2006). Type II pyrethroids consistently produce more prolonged Na^+ tail currents than Type I pyrethroids (Vijverberg and Van den Bercken 1990; Song et al. 1996; Choi and Soderlund 2006). The result of increased Na^+ permeability through VSSCs is repetitive neuronal action potential firing following a stimulus and an overall change in neuronal firing rates (Vijverberg and Van den Bercken 1990; Song and Narahashi 1996). Some pyrethroids also affect a number of secondary molecular targets such as voltage-sensitive Ca^{+2} channels, voltage-sensitive Cl^- channels (Burr and Ray 2004; Shafer and Meyer 2004; Symington and Clark 2007). Activation of these channels may or may not contribute to the manifestation of acute neurotoxicity *in vivo* or the difference in the acute signs of poisoning observed with the two pyrethroid types (Soderlund et al. 2002; Ray and Fry 2006).

The accepted mode-of-action for the acute adverse effects of pyrethroids includes disruption of voltage-sensitive ion channel function and subsequent increases in neuronal excitability which, in turn, leads to behavioral effects observed at the whole organism level (Ecobichon 2001; Soderlund et al. 2002; Ray and Fry 2006). Changes in neuronal excitability also triggers changes in gene expression that may result in alterations in neuronal function (Fields et al. 1997; Finkbeiner and Greenberg 1998; Fields et al. 2005; Tropea et al.

2006). To date, the effects of acute pyrethroid exposure on activity-dependent gene expression in the nervous system has not been extensively studied. Questions remain regarding which genes are altered following pyrethroid exposure, whether or not the same sets of genes are affected by different compounds within the pyrethroid class and what intracellular signal transduction mechanisms are activated to trigger pyrethroid-induced changes in gene expression.

Previous work using oligonucleotide microarrays demonstrated that acute pyrethroid exposure, at doses near the threshold for producing behavioral effects in the rat, altered gene expression in the frontal cortex (Harrill et al. *submitted*). The gene expression changes observed in that study were consistent with pyrethroid-induced increases in neuronal excitability *in vivo*. In addition, this study demonstrated both differences and similarities in the overall transcriptional response elicited by permethrin and deltamethrin, the two pyrethroids tested. The present study expands upon these findings by examining global gene expression patterns in the rat frontal cortex across time following acute exposure to six pyrethroids: permethrin, bifenthrin and tefluthrin (Type I) or deltamethrin, cypermethrin or cyfluthrin (Type II). Equipotent dose levels were selected based on the behavioral data of Wolansky et al. (2006). Global gene expression profiles from Affymetrix GeneChips® were compared across compounds and functional gene regulatory networks were constructed from commonly altered genes.

Methods.

Chemicals. All pyrethroids examined in this study were of technical grade. Bifenthrin (BIF: 98.9 % purity), permethrin (PERM: 92 % purity) and cypermethrin (CYP: 88.0 % purity) were donated by FMC Corporation (Philadelphia, PA). Deltamethrin (DLT: 98.9 % purity)

and β-cyfluthrin (CYF: 99.2 % purity) were donated by Bayer Cropscience (Research Triangle Park, NC). Tefluthrin (TEF: 92.6 % purity) was donated by Syngenta Crop Protection (Greensboro, NC). Chemical structures for the six pyrethroids are provided in Figure 4.1. Complete IUPAC nomenclature and isomer ratios of the test material are available in Wolansky et al. (2006). Equipotent dose levels (ED_{30} for decreased motor activity) for each of the pyrethroids were selected based on data from Wolansky et al. (2006) (see Figure 4.2). Pyrethroids were dissolved in corn oil (Sigma-Aldrich, St. Louis, MO) with a dosing volume of 1 mL/kg.

Animal care and treatment. Male Long-Evans rats (58 days of age) were obtained from Charles River Laboratories (Wilmington, MA) and housed two per cage in standard polycarbonate hanging cages (45 cm X 24 cm X 20 cm) with heat sterilized pine shavings for bedding (Beta Chips, Northeastern Products, Inc., Warrensburg, NY). Animals were maintained on 12h:12h photoperiod (lighted hours: 06:00-18:00) and allowed a 5 to 7 day period of acclimation to the colony prior to dosing. Colony rooms were maintained at 22.0 ± 2.0°C with a relative humidity of 55 ± 20%. Food (Purina 5001 Rat Chow) and tap water were provided *ad libitum*. The facility was approved by the American Association for Accreditation of Laboratory Animal Care (AAALAC) and all experimental procedures were approved in advance by the by the US EPA, National Health and Environmental Effects Research Laboratory Animal Care and Use Committee.

Rats received a single, oral dose of either 43 mg/kg PERM, 10.7 mg/kg CYP, 3.2 mg/kg BIF, 3 mg/kg DLT, 2.3 mg/kg TEF, 2.2 mg/kg CYF or corn oil vehicle and allowed to recover for either 3 or 6 h. These doses are an approximate ED_{30} for decreased motor

activity based on the data of Wolansky et al. (2006). Rats were treated and tissues collected in four separate blocks in this study. Blocks 1 and 2 contained rats treated with Type I pyrethroids (PERM, BIF, TEF) or Type II pyrethroids (DLT, CYP, CYF) for 3 h (n = 3 / block, n = 6 / treatment). Blocks 3 and 4 contained rats treated with Type I pyrethroids or Type II pyrethroids for 6 h (n = 3 / block, n = 6 / treatment). Each block also contained time matched vehicle controls (n = 3 / block). Dosing and euthanasia times for pyrethroid and vehicle treated rats was counterbalanced across time of day within each block. All dosing occured between 09:00 and 12:00 hours and the last test subject was euthanized before 18:00 hours. Rats were removed from the colony suite 1 h prior to dosing and allowed to acclimate in a quiet holding room maintained under similar environmental conditions. Subjects were administered a single oral dose of test compounds by gavage and allowed to recover in their home cage prior to tissue sampling. Subjects were then individually removed to an adjoining suite with a separate HVAC system for euthanasia by decapitation.

Whole brains were rapidly removed and placed on a cold plate (4°C). The frontal cortex was dissected by making a vertical incision at the anterior edge of the optic tract with a stainless steel razor, and rapidly frozen on a bed of dry ice. Cortical samples, without striatal tissue, were then bisected into contralateral hemispheres, weighed, frozen in liquid nitrogen and stored at -80°C.

RNA extraction. Cortical samples were homogenized in 1 mL of TRI Reagent (Molecular Research Center, Inc., Cincinnati, OH) per 50-100 mg of tissue using a Polytron® PT-K homogenizer (Kinematica, Lucerne, Switzerland) and total RNA was isolated per manufacturer's instructions. Total RNA pellets suspended in DEPC-treated H_2O were then

subject to DNase I treatment and re-extracted with acid:phenol chloroform, pH = 4.7 (Ambion Inc., Austin, TX) and chloroform according to manufacturer's protocol and resuspended in DEPC-treated H_2O until use. The total RNA concentration of each sample was determined (absorbance @ 260 nm) on a Beckman-Coulter DU® 800 spectrophotometer (Fullerton, CA) and adjusted to 1.0 µg/µL prior to sample storage at -80ºC. The ratio of absorbance values at 260 nm and 280 nm (Ab 260/280) was used to assess purity of total RNA samples. All samples used in these studies had Ab 260/280 ratios > 1.83 (data not shown). Preliminary PCR experiments using primers for rat β-actin genomic DNA (outlined in Tully et al. 2006) demonstrated that the above protocol adequately prevents genomic DNA contamination of total RNA samples (data not shown). In addition, the RNA integrity of each sample was determined using an Agilent 2100 Bioanalyzer and RNA 6000 Series II Nano LabChip Kit (Waldbron, Germany) according to manufacturer's instructions. All samples used in microarray and qRT-PCR experiments had 18S:28S rRNA ratios > 1.8 and RNA Integrity Numbers > 8.8 (data not shown). Following the RNA purity and integrity screens, aliquots of each total RNA sample (1 µg/µL for microarray hybridization or 25 ng/µL for qRT-PCR assays) were stored at -80°C until use.

Microarray sample preparation and data collection. Affymetrix Rat Genome 230 2.0 GeneChip® oligonucleotide microarrays (Santa Clara, CA) were used in this experiment. First and second strand cDNA synthesis, cRNA amplification, clean-up and biotin-labeling of each sample were performed with BioArray^{TM} single-round RNA amplification and biotin labeling system (Enzo Life Sciences, Farmingdale, NY) and Qiagen RNeasy spin columns (Spoorstraat, Netherlands), respectively, according to manufacturer's instructions. Biotin-

labeled cRNA was fragmented using Affymetrix 5X fragmentation buffer (200mM Tris acetate - pH=8.1, 100 mM KOAc, 150 mM MgOAc).

Fragmentation of biotin-labeled cRNA, GeneChip® hybridizations, washes and staining were performed according to standard Affymetrix protocols (Affymetrix 2004). Hybridizations were performed in an Affymetrix Hybridization Oven 640. Washes were performed on an Affymetrix Fluidics Station 450 using the EukGE-WS2v4-450 fluidics script. GeneChips® were scanned using an Affymetrix GeneChip® 3000 Scanner with the GCOS v1.4.0.036 software package. Target intensity was set to a value of 500 with all other scanning parameters set at the factory defaults. The 3`/5` ratios for GAPDH and β-actin internal controls genes were within the range suggested by the manufacturer, indicating that RNA was not degraded during processing. The intensity of hybridization controls (*BioB*, *BioC*, *BioD* and *Cre)* increased linearly on all arrays.

Microarray data analysis. Gene expression profiles for all samples in the study were collapsed across block for data analysis. Gene expression summaries were calculated with RMAExpress© v4.7 (University of California at Berkeley) using the Robust Multiarray Average method (RMA, Irizarry et al. 2003). Paired *t*-tests between treated samples and time-matched controls were performed using Microsoft Excel® to obtain an initial global overview of the data. Treatment-related changes in gene expression were detected using the Linear Models for Microarray Data (LIMMA, Smyth 2005) package in the R statistical computing environment (v2.6.1). Each compound was analyzed separately in conjunction with time-matched vehicle control values according to contrast matrix outlined in Figure 4.4A. The comparisons made for each probe set using LIMMA followed the general model

for a two-way analysis of variance (ANOVA) with time and treatment as the independent factors (Figure 4.4B). Treatment-related changes in expression were determined according to the flowchart in Figure 4.4C. Main effects of time and treatment and the interaction between time and treatment were considered significant at a false discovery rate adjusted *p*-value < 0.10.

The Significant Analysis of Function and Expression (SAFE, Barry et al. 2005) method was used to identify pathways and functional categories whose genes are coordinately regulated in a treatment-related fashion. SAFE and array annotation were loaded from Bioconductor (v2.1, Gentleman et al. 2004). A comparative SAFE analysis was also used to test for enrichment of gene sets with treatment related changes in expression for each of the individual pyrethroids (according to LIMMA) across all the other pyrethroids in the test panel. Prior to implementation of the SAFE analyses data were normalized (or re-centered) to the combined mean of the vehicle treated control groups collapsed across time. This normalization was necessary due to the inability of the SAFE method to simultaneously analyze two independent variables. Normalization removed the main effects of time from the data (Appendix B, Figure 1). A multi-factor one-way ANOVA *F*-statistic was used as the local statistic in the SAFE analyses to assess treatment related change in expression within the four treatment groups for each pyrethroid. The global statistic for enrichment was a Wilcoxon ranked sum test (Ott 2003). 1000 permutations of the treatment groups were used by SAFE to assess the significance of the entire procedure using the Yekutieli and Benjamini (1999) method to control the false discovery rate (FDR) and account for multiple comparisons. Ingenuity® pathway analysis software (Ingenuity Inc., Redwood City, CA)

was also used to construct interactive gene networks from probe sets altered by pyrethroid treatment.

Quantitative real-time RT-PCR. qRT-PCR was performed using TaqMan® One-Step RT-PCR Master Mix Reagent Kits and TaqMan® Gene Expression Assays on a ABI 7900HT Sequence Detection System (Applied Biosystems, Foster City, CA). AmpliTaq Gold® DNA Polymerase / dNTP mix, Multiscribe^{TM} reverse transcriptase / RNA inhibitor mix and TaqMan® Gene expression primer-probe mix specific for the transcript of interest were combined according to manufacturer's specifications (Applied Biosystems, 2005). The reaction mixture was then dispensed into the reaction plate (15 µL / well) and 125 ng of total RNA (5 µL) was added. Each sample was measured in triplicate for each transcript of interest and internal reference gene. Reaction plates were maintained at 5°C during loading procedure. During data collection, reactions were incubated at 48°C for 45 min followed by incubation at 95°C for 10 min and 40 cycles of 94°C for 25 sec and 60°C for 1 min.

qRT-PCR assays were designed via the Applied Biosystems (ABI) primer / probe selection algorithm and bioinformatics pipeline (Applied Biosystems 2006). The amplification efficiency of each assay was examined using a serial dilution of pooled total RNA from rat cortex. Efficiencies were calculated as: $E_x = 10^{(-1/m)} - 1$, where E is the amplification efficiency of target transcript *x* and *m* is the slope of threshold cycles vs log [total RNA concentration] across the range of dilutions (Applied Biosystems 2004). Assay identification numbers, context sequences, amplicon lengths and calculated amplification efficiencies are listed in Appendix B, Table 1.

Six transcripts identified as having treatment related changes in expression were examined by qRT-PCR to confirm results of the microarray data. qRT-PCR data was analyzed according to the $2^{-\Delta\Delta C}{}_T$ method as described by (Livak and Schmittgen 2001). β-actin expression did not change as a function of time or treatment for either compound (data not shown) and was used at the internal reference for all $2^{-\Delta\Delta C}{}_T$ calculations. The mean $\Delta\Delta C_T$ of vehicle treated controls within each time was used as the $2^{-\Delta\Delta C}{}_T$ calibrator for each time-matched treatment group. A two-way ANOVA was used to statistically analyze the qRT-PCR data with time and treatment as independent variables and $2^{-\Delta\Delta C}{}_T$ as the dependent variable ($p < 0.05$ for each contrast). Transcripts with a significant time*treatment interaction were additionally analyzed with a one-way ANOVA at each time point with treatment as the independent variable ($p < 0.05$).

Results.

The type II pyrethroids had a much more dramatic effect on gene expression in the frontal cortex than Type I pyrethroids. Figure 4.3 plots the magnitude of fold change from control versus the empirical *p*-value for pair-wise comparisons of treatment and control samples for each pyrethroid tested at each time point in the study. Note that the statistical test used in this figure is not adjusted for multiple comparisons or low abundance transcripts and was not used in the present study as final indication of significance. Instead, these comparisons were used to examine global trends in the gene expression data. For all the pyrethroids tested, at both 3 h and 6 h post-exposure, the magnitude of fold-change from control was less than 4-fold for genes that met an empirical *p*-value threshold < 0.001 (Figure 4.3, dotted lines). At 3 h the Type II pyrethroids deltamethrin (DLT), cypermethrin (CYP) and cyfluthrin (CYF) had a larger number of probe sets with empirical $p < 0.001$ than at 6 h.

A majority of these probe sets were upregulated following pyrethroid exposure. The degree of change is much more pronounced for the Type II pyrethroids as compared to the Type I pyrethroids. PERM had a very small number of probe sets with an empirical $p < 0.001$ in the paired *t*-test. BIF exposure resulted in alterations in expression mainly at 6 h while TEF exposure resulted in alteration in expression mainly at 3 h. Collectively, these data demonstrate that the overall transcriptional response of the rat frontal cortex to Type II pyrethroids is qualitatively different from the response produced by the Type I pyrethroids at behaviorally equipotent doses.

LIMMA analysis of the microarray gene expression data identified a large number of probe sets with treatment related changes in expression for the Type II pyrethroids. No significant treatment related effects were observed for the Type I pyrethroids using LIMMA. A decision tree for the determination of treatment related effects on expression in the LIMMA analysis framework is given in Figure 4.4C. Unlike the paired *t*-tests shown in Figure 4.3, LIMMA analysis utilizes a false discovery rate multiple comparison correction and an adjustment factor for lowly-expressed probe sets. Figure 4.5 demonstrates three distinct patterns of significant treatment related changes in gene expression for the three type II compounds: 1) probe sets up- or down- regulated predominantly at 3 h, 2) probe sets up- or down- regulated predominantly at 6 h and 3) probe sets up or down-regulated across both time points in the study. The first pattern describes the most dramatic changes in gene expression for each of the Type II compounds. CYP exposure yielded the least number of probe sets with treatment related changes in expression (n = 149) followed by DLT (n = 399) and CYF (n = 3742). In the case of CYF a large number of the identified gene expression

changes (~80 %) were small in magnitude with < 1.25-fold changes from control at either time point.

Comparison of the probe sets with treatment related changes in expression for DLT, CYP and CYF, respectively, revealed a group of probe sets commonly affected by the Type II compounds (Figure 4.6A). Comparative enrichment analysis (SAFE algorithm, Barry et al. 2005) provided a quantitative measure of similarity between the gene expression profiles of the different pyrethroids in the test panel (Table 4.1). Queried lists of probe sets were based on LIMMA analysis of individual Type II compounds in the test panel and zones of similarity in the Venn diagram comparison from Figure 4.6A. Significant enrichment of the group of probe sets identified as being affected by either DLT (n = 399) or CYP (n = 149) was observed in all three Type II compounds in the study (Table 4.1). In contrast the large list of treatment affected probe sets identified for CYF (n = 3742) was not significantly enriched for the other Type II compounds. Gene lists based on the DLT-CYP, DLT-CYF and CYP-CYF unions of the Venn diagram (Figure 4.6A) were also significantly enriched for the other Type II compound not involved in forming the union.

The LIMMA analysis did not detect significant alterations in gene expression for the Type I pyrethroids. This is in contrast to the empirical *t*-tests illustrated in Figure 4.3 that identified a group probe sets as being altered by PERM, BIF and TEF. A heatmap visualization of probe sets commonly altered by the Type II pyrethroids demonstrates that some of the genes within this union are changed by Type I pyrethroids, albeit at lower fold-change magnitudes than observed with the Type II's (Figure 4.6B, arrows and bracket). Results of the comparative SAFE enrichment procedures also demonstrates a similarity in the overall response of the Type I pyrethroids to the Type II pyrethroids (Table 4.1). Probe sets

with treatment related effects for DLT were enriched for PERM. Likewise, probe sets with treatment related effects for DLT and CYP were enriched for BIF. These data demonstrate a degree of similarity is present in the overall transcriptional response for PERM, BIF, DLT and CYP. The large group of probe sets with treatment related effects for CYF was enriched in the TEF treated group but not the PERM and BIF treated groups, demonstrating that the overall transcriptional response of TEF is more similar to CYF than CYP or DLT. All of the gene lists defined from the common overlaps of the Type II pyrethroids had significant enrichment in all of the Type I compounds tested.

Lists of genes commonly altered by any combination of at least two Type II pyrethroids in the microarray data sets are given in Table 4.2. The most pronounced response to the Type II pyrethroids was the induction of a variety immediate early genes encoding transcription factors (*Junb*, *c-fos*, *Egr2*, *Nr4a1*, *Klf4* and *Klf10*), phosphatases (*Dusp1*, *Dusp5* and *Dusp6*) and cellular effectors (*Arc*). Some glucocorticoid responsive gene transcripts were also induced (*Rasd1*, *Gpd1* and *Sgk*). In addition, all three of the Type II pyrethroids induced the expression of a small group of receptors *Cxcr4*, *Il6r*, *Vipr1* and *Tnfrsf11b*. Complete lists of probe sets regulated by each of the Type II pyrethroids in available in the electronic appendices for the present study.

Six transcripts were selected for confirmation of treatment-related changes in expression for all six pyrethroids in the test panel using qRT-PCR: *Nr4a1, Arc, Gpd1, Nedd9, Camk1g* and *Egr1*. The first four are located in the DLT-CYP-CYF union in Figure 4.6A. *Camk1g*, and *Egr1* are located in the DLT-CYF, and CYP-CYF unions, respectively. A summary of statistical analyses of qRT-PCR data for these genes is given in Appendix B, Table 2. Expression of *Nr4a1* mRNA was increased following exposure to all six

pyrethroids in the test panel. *Nr4a1* induction was of much greater magnitude for the Type II pyrethroids (4 to 6-fold at 3 h) than the Type I pyrethroids (< 3-fold at 3 h). The expression pattern of *Arc* mRNA was similar to the expression patterns observed for *Nr4a1* for all pyrethroids except lower in magnitude. *Arc* mRNA expression was increased with all the Type II pyrethroids on the order of 3 to 4-fold at 3 h. In contrast, *Arc* expression was increased only 1.5-fold at 3 h for the Type I pyrethroids. *Gpd1* mRNA expression was increased for all of the Type II pyrethroids with the largest responses observed for DLT, CYF and CYP respectively. Only PERM had a significant effect on *Gpd1* expression and this effect was very low in magnitude (<1.2-fold). *Camk1g* mRNA expression was affected most dramatically by DLT at 6 h. A smaller increase in *Camk1g* expression (~1.3-fold) was observed across both time points in the study for CYP and CYF (main effect of time, see Appendix B, Table 2) however no main effects of treatment were observed at $p < 0.05$. *Nedd9* mRNA expression was increased at 3 h for DLT and CYP only, consistent with its location in the comparison in Figure 4.6A. The Type I pyrethroids had no effects on *Camk1g* or *Nedd9* expression. *Egr1* mRNA expression was increased following exposure to all three Type II pyrethroids similar to the trends in expression observed for the other immediate early genes *Nr4a1* and *Arc*. TEF was the only Type I with significant effects on *Egr1* mRNA expression. Overall, gene expression patterns measured by qRT-PCR had good concordance with the microarray data.

Two methods were implemented to identify biologically meaningful associations between the transcripts regulated by the two Type II pyrethroids: SAFE analysis (Barry et al. 2005) and Ingenuity® pathway analysis. SAFE analysis of Gene Ontology 'molecular function' (GOMF), 'biological process' (GOBP) and 'cellular component' (GOCC)

categories from Bioconductor v1.8 did not detect significant enrichment for any of the pyrethroids in the test panel using the Yekutieli and Benjamini (1999) false discovery rate correction at a threshold of $p < 0.1$ (data not shown). However, the overlapping GOMF categories 'MAP kinase tyrosine/serine/threonine phosphatase activity' (GO:0017017) and 'MAP kinase phosphatase activity' (GO:0044440) had an empirical $p < 0.01$ for all of the Type II pyrethroids in the panel. This is consistent with the numerous phosphatases and kinases demonstrated to be upregulated after Type II exposure (Table 4.2).

Input of genes commonly regulated by all of the Type II pyrethroids into the Ingenuity® pathway analysis software package yielded a complex interconnected network of protein interactions (Figure 4.8C). This network is comprised primarily of inducible transcription factors and protein phosphatases upregulated following Type II pyrethroid exposure and a variety of interconnected kinase complexes, growth factors and transcription factors that are constitutively expressed in neurons and not transcriptionally regulated by pyrethroids in the present study (Figure 4.8A-B). Dissection of this interconnected network into its component parts demonstrates that the phosphatases and kinases upregulated by the Type II pyrethroids primarily act upstream of the constitutively expressed interconnecting kinase complexes (Figure 4.8D). Furthermore, the constitutively expressed kinase complexes and transcription factors (*NFκB*, *STAT*, *CREB*) act primarily upstream of the pyrethroid inducible transcription factors (Figure 4.8E). Other pyrethroid upregulated genes (*Ier2, Gadd45b, Nedd9, Per1* and *Per2*) are downstream of interconnecting transcription factors and growth factors. The peptide receptor *Vipr1* acts upstream of *NFκB* while the chemokine receptor *Cxcr4* has a variety of upstream and downstream interactions with the constitutive kinase complexes (Figure 4.8F). Figure 4.8G-H illustrates the protein

interactions between the constitutive kinase complexes and the transcription factors or growth factors present in the Ingenuity® network, respectively. The constitutive transcription factors are downstream of the kinase complexes (Figure 4.8G, orange arrows) while the kinase complexes are downstream of the growth factors (Figure 4.8H, orange arrows).

Discussion.

The present study demonstrates that Type I and Type II pyrethroids do not produce equivalent effects on gene transcription in the rat frontal cortex following behaviorally equipotent doses. The expression of a large number of transcripts was affected by the Type II pyrethroids with maximal changes in expression on the order of 4-fold from control. The mRNA expression patterns produced by the Type II pyrethroids have features common to DLT, CYP and CYF as well as features unique to each of the respective compounds. The observed gene expression changes are consistent with pyrethroids producing increased excitability of cortical circuits *in vivo*. Ingenuity® pathway analysis modeling yielded a complex network of interconnecting gene expression changes consistent with increases in neuronal excitability by the Type II pyrethroids. In addition, visual inspection of the microarray gene expression data and comparative enrichment analysis indicated that some components of the common Type II transcriptional response were also present in the Type I treatment groups, albeit at lower magnitudes of change. This hypothesis was supported by qRT-PCR analysis of a sub-set of pyrethroid regulated mRNAs.

A principal finding from this study is that Type I and Type II pyrethroids administered at dose levels that produce equivalent effects on an apical behavior (i.e. motor activity) cause dramatically different effects on global gene expression in the rat frontal

cortex. A large number of gene expression changes were detected with the Type II pyrethroids DLT, CYP and CYF using the LIMMA analysis framework (Figure 4.5). In contrast, LIMMA did not detect any gene expression changes with the Type I pyrethroids PERM, BIF and TEF even though empirical pair-wise contrast tests indicated that a small number of low-magnitude gene expression changes occurred following Type I pyrethroid exposure (Figure 4.3). These data are consistent with the differential effects of the two pyrethroid types on voltage-sensitive sodium channel function. Type I pyrethroids produce abnormal Na^+ tail currents with time constants of decay much shorter than those produced by Type II pyrethroids (Song et al. 1996; Tabarean and Narahashi 1998; Narahashi 2000; Choi and Soderlund 2006). The longer duration Na^+ tail currents produced by Type II pyrethroids maintain neurons in a more hyperexcitable state than Type I pyrethroids (Ecobichon 2001; Ray and Fry 2006). Furthermore, Type II pyrethroids produce longer trains of repetitive firing following stimulus than the Type I pyrethroids (Vijverberg and Van den Bercken 1990). The present data suggest that Type II pyrethroids produce a greater degree of neuronal excitation in the cortex than the Type I pyrethroids at the administered doses examined which would in turn produce more dramatic changes in the expression of genes regulated by neuronal activity.

The differences in gene expression profiles between the two pyrethroids types may also reflect differential activation of secondary molecular targets sites that control gene transcription. For example, Ca^{+2} is an intracellular second messenger capable of triggering *de novo* gene transcription (Schulman and Roberts 2003). Symington and Clark (2007) have demonstrated an increase in Ca^{+2} influx into rat brain synaptosomes following both deltamethrin (Type I) and cismethrin (Type II). Cismethrin-stimulated Ca^{+2} influx was

dependent upon Na^+ channel mediated depolarization while deltamethrin-stimulated Ca^{+2} influx was Na^+ channel independent. In addition, the concentration-response curve for deltamethrin-stimulated Ca^{+2} influx is to the left of that for cismethrin, indicating a smaller concentration of the Type II pyrethroid is required to produce the response. It is possible that at the dose levels used in the present study, the Type II pyrethroids are more potent activators of a secondary molecular target(s) that mediate gene transcription than the Type I pyrethroids. These actions could be independent of both pyrethroid effects at VSSCs and the behavioral response (i.e. decreased motor activity), which may explain why the doses used here produce the same magnitude of behavioral change for the two pyrethroid types but do not produce the same magnitude of gene expression changes.

An additional alternative is that pharmacokinetic differences in the distribution or metabolism of Type I and Type II pyrethroids may be contributing to the divergent effects on global gene expression observed here. Comparison of pharmacokinetic (PK) data available in the literature for DLT and PERM do not support this conclusion (PK models for CYP, CYF, BIF and TEF in the rat are not presently available). Both DLT and PERM accumulate in the frontal cortex following an acute oral dose (Anadon 1991; Anadon 1996). Furthermore, brain concentrations of both Type I and Type II pyrethroids correlate with changes in behavior at high doses (Gray et al. 1980; Rickard and Brodie 1985) and doses compatible with those used in this study (Scolon et al. *in preparation*). Lastly, pyrethroids all have different efficacies for interacting with different VSSC isoforms (Soderlund et al. 2000; Choi and Soderlund 2006). In *in vitro* studies of neuronal function, different pyrethroid types produce disparate effects on the excitable properties of the same neuronal cell populations and different neuronal subtypes respond differently to the same pyrethroid

(Tatebayashi and Narahashi 1994; Tabarean and Narahashi 1998; Grosse et al. 2002; Meyer and Shafer 2006; Meyer et al. 2007). Therefore, since different VSSC isoforms and neuronal subtypes are heterogeneously expressed throughout central nervous system tissues, the unique effects of the individual pyrethroid types on channel function may be the critical factor contributing to the differential gene expression patterns.

The transcriptional response of the frontal cortex to the Type II pyrethroids DLT, CYP and CYF contains some genes that are commonly regulated by multiple Type II pyrethroids in the test panel and some genes that are uniquely regulated by the individual Type II pyrethroids (Figure 4.6A). These data support that all three of the Type II pyrethroids in the test panel elicit similar changes in the expression of a sub-set of genes while also producing changes in expression unique to the different Type II compounds. The comparative SAFE enrichment analysis also supported this conclusion and demonstrates that the transcription response of DLT and CYP is the most similar. Differences in chemical structure between the three Type II pyrethroids in the panel may be responsible for mediating the differences in the global transcriptional response of DLT, CYP and CYF. Structurally, DLT and CYP differ only in the identity of halogen groups on the cyclopropane carboxylic acid moiety of the compounds: bromines for DLT and chlorines for CYP (Figure 4.1). CYF differs from CYP only by the addition of a fluorine group to the aromatic alcohol moiety (Figure 4.1). These small differences in chemical structure can have impacts on the duration of VSSC modification and adverse outcomes on the behavioral level (Verschoyle and Aldridge 1980; Choi and Soderlund 2006). Differences in stereoisomer ratios between the Type II pyrethroids may also explain the divergences observed in global gene expression profiles. The preparation of DLT used is composed exclusively of the 'more toxic' *cis*-(α*R*)

stereoisomer whereas CYP and CYF are heterogenous mixtures of *cis*- and *trans*- α-*S* and α-*R* stereoisomers (Soderlund 1985; Ray 2001; Soderlund et al. 2002). Definitive conclusions regarding the impact of chemical modifications or stereochemistry on pyrethroid induced gene expression can not be made without systematic comparison of isomerically pure preparations of the test compounds. However, the present data clearly demonstrate that there is a specific suite of genes commonly regulated by Type II pyrethroid compounds regardless of isomeric composition.

The mechanistic relationship(s) between acute pyrethroid action at ion channels and the genes altered by Type II pyrethroids is currently unclear. However, the present data are consistent with the previous findings (Harrill et al. *submitted*). Both studies failed to detect any changes in gene expression corresponding to the primary molecular targets of pyrethroids (i.e. VSSCs, Ca^{+2} channels, Cl^{-} channels). On the other hand, some of the transcripts within the suite of genes commonly regulated by the Type II pyrethroids are known to be upregulated in response to excitatory stimulation. This supports the hypothesis that the Type II pyrethroids DLT, CYP and CYF produce neuronal excitation within the frontal cortex in the present study. The expression of the immediate early (IEG) transcription factors *c-fos*, *JunB*, *Egr1*and *Nr4a1* have been shown to be upregulated by a variety of excitatory stimuli (Hazel et al. 1991; Morgan and Curran 1991; Fields et al. 1997; Hughes et al. 1999; Patra et al. 2004) and are also upregulated by Type II pyrethroids in the present study. In addition, the expression of the phosphatases *Dusp1*, *Dusp5* and *Dusp6* and the cytoskeletal protein *Arc* that are upregulated by DLT, CYP and CYF in the present study are also induced following neuronal excitation (Gass et al. 1996; Muda et al. 1996; Hevroni et al. 1998; Kodama et al. 2005; Guzowski et al. 2006; Machado et al. 2008). Another component

of the common Type II response are the genes *Rasd1* and *Gpd1* which are both regulated by activation of intracellular glucocorticoid receptors by the hypothalamic-pituitary-adrenal axis (Baughman et al. 1997; de Kloet et al. 1998; Brogan et al. 2001). The upregulation of *Gpd1* indicates that transcriptional responses of glial cells may be included in the overall global expression profiles for pyrethroids in the frontal cortex, given that this protein is expressed exclusively in oligodendrocytes (Leveille et al. 1980). In addition, *Sgk* has been shown to be upregulated following both glucocorticoid receptor activation and activation of post-synaptic excitatory glutamate receptors (Lee et al. 2003; Webster et al. 2003) which supports a role for both neuronal excitation and glucocorticoid stimulation in the transcriptional response of the frontal cortex to pyrethroids. These data are consistent with previous studies that demonstrate induction of activity-regulated genes and increases in circulating corticosterone following acute pyrethroid exposure (Hassouna et al. 1996; de Boer et al. 1998; Wu and Liu 2003). Even though the mechanistic linked between pyrethroid action at the ion channel and the present gene expression is unknown, these data do provide insight into some of the intracellular signaling pathways that may be stimulated by acute pyrethroid action *in vivo.*

Ingenuity® pathway analysis of genes commonly affected by the Type II pyrethroids yielded an interconnected network of protein interactions that is also consistent with the induction of hyperexcitability by pyrethroids in the frontal cortex. This network is comprised of the IEG transcription factors, phosphatases and effector proteins commonly upregulated by the Type II pyrethroids as well as constitutively expressed kinase and transcription factor complexes (Figure 4.8C). Systematic deconstruction of this interactive network supports a model of acute pyrethroid action that includes stimulation of constitutive kinase signaling cascades and subsequent activation of constitutive transcription factors followed by *de novo*

expression of IEG phosphatases and kinases that deactivate the excitatory signaling pathways, effector proteins that may impact cellular function and IEG transcription factors that can regulate subsequent changes in the expression of additional effector proteins (Figure 4.9). Increased neuronal excitation results in the activation of *Akt, Jnk, MAPK, p38 MAP, MEK* and *Pkc* (Rosen et al. 1994; Vanhoutte et al. 1999; Perkinton et al. 2002; Brager et al. 2003; Chen et al. 2003; Vaillant et al. 2003; Corvol et al. 2005; Pezet et al. 2005) which are the connecting nodes of the Ingenuity® network (Figure 4.8C). *Dusp1*, *Dusp5*, *Dusp6* and *Ptpn1* may then act to dephosphorylate and deactivate these kinases, and to turn off the excitatory stimulus in a transcription dependent feedback loop. The activated kinase complexes are also upstream of *de novo* expression of the IEG transcription factors induced by the Type II pyrethroids. The model supports a role for the constitutive transcription factors *STAT*, *CREB* and *NFκB* in connecting the excitatory responses of the kinase networks to the pyrethroid induced *de novo* gene expression changes. These three proteins are downstream of the putatively activated kinase complexes and upstream of the transcriptional responses elicited by the Type II pyrethroids (Figure 4.8D and 4.8E, Wooten 1999; Davis et al. 2000; Kaltschmidt et al. 2002). Ingenuity® also incorporated the growth factors *Fgf, Pdgf* and *Tgfβ* into the network based on upstream effects on the inducible components of the Type II pyrethroid response. However, there are no data available that support a role for these genes in the biological activity of pyrethroids *in vivo*. At this time, the effect of *de novo* gene expression induced by pyrethroids on downstream cellular functions is unclear. Additional studies are needed to investigate the activation of the signaling pathways putatively identified in the present study in response to pyrethroids.

Several lines of evidence within that current study suggest that components of the transcriptional response commonly elicited by the Type II pyrethroids (Table 4.2, far right column) was also be present in the Type I treatment groups, even though LIMMA analysis did not detect them. First, pair-wise comparisons of PERM, BIF and TEF treated groups to vehicle controls indicated that the expression of a small group of probe sets was in fact changed (Figure 4.3). Second, visual inspection of the expression profiles for genes commonly affected by the Type II pyrethroids demonstrated that a small sub-set of genes had qualitatively similar changes in expression between pyrethroid types, although the response produced by the Type I's was lower in magnitude (Figure 4.6B, brackets). Lastly, comparative SAFE enrichment analysis (Table 4.1) demonstrated that gene lists derived from the overlapping portions of the Type II transcriptional responses were significantly enriched in the PERM, BIF and TEF treatment groups. Similarities in the transcriptional response to Type I and II pyrethroids has been previously reported (Harrill et al. *submitted*). These observations support that the multiple-test correction employed by LIMMA may have been too conservative for the purpose of detecting the small number of low-magnitude gene expression changes observed in the Type I treatment groups. Alternatively, the use of motor function data (Wolansky et al. 2006) to define equipotent dose levels may have overestimated the potency of Type I pyrethroids at the neuronal membrane. This latter point is consistent with the smaller effects observed with the Type I pyrethroids in this study. Dose-response data on gene expression for Type I pyrethroids using higher administered doses would test this hypothesis.

Quantitative RT-PCR analysis performed on a group of transcripts commonly regulated by multiple Type II pyrethroids in the microarray experiment are consistent with

the expression patterns observed in the microarray study and also support that a small number activity-regulated genes are regulated in response to the Type I pyrethroids. *Arc* and *Nr4a1* IEG expression was significantly changed by all six pyrethroids in the test panel (Figure 4.7). *Egr1* and *Gpd1* mRNA was upregulated by all the Type II pyrethroids and by PERM and TEF respectively. *Nedd9* expression was upregulated by DLT and CYP while *Camk1g* was significantly increased only by DLT. The changes in *Arc* and *Nr4a1* mRNA expression for the Type I pyrethroids were of smaller magnitude than those observed with the Type II pyrethroids and is consistent with a lesser degree of neuronal activation in the cortex for the doses PERM, BIF and TEF used here as compared to DLT, CYP and CYF. In a previous study (Harrill et al. *submitted*) a dose of 100 mg/kg PERM produced increases in *Egr1, Gpd1* and *Camk1g* comparable to the 3 mg/kg dose of DLT used in the present study. The 100 mg/kg PERM dose examined was slightly more efficacious for decreasing ambulatory motor activity than the 3 mg/kg DLT dose (ED_{50} vs. ED_{30}, Wolansky et al. 2006). This is consistent with the hypothesis stated above that suggests higher doses of Type I pyrethroids will produce similar effects to the Type II pyrethroids observed in the present study. These data do not support that the frontal cortex is insensitive to the effects of Type I pyrethroids in terms of *de novo* gene transcription.

The lack of effect of Type I pyrethroids on *Camk1g* mRNA is inconsistent with previous studies (Harrill et al., *submitted*, Harrill and Crofton, *in preparation*). In those studies an ED_{30} dose of DLT and either an ED_{30} or ED_{50} doses of PERM (based on Wolansky et al. (2006) motor activity data) were sufficient to produce an upregulation of *Camk1g* mRNA. In addition, in these previous studies, the *Camk1g* mRNA response to PERM was less robust that that observed with DLT. In the present study, an ED_{30} dose of

DLT again resulted in an increase in *Camk1g* mRNA expression, whereas an ED_{30} dose of PERM caused no effect. The reason for this disparity is unclear. The PERM used in the present study was taken from the same lot of technical grade product as used in the two previous studies. Therefore, differences in isomer composition and purity can not account for the disparate results. Alternatively, differences in the metabolic rates for PERM between the cohorts of animals used across studies may account for the difference. The rats used in the present study may have had a greater capacity for metabolizing PERM than the rats used in the previous studies, therefore resulting in a lower target tissue concentration at a comparable administered dose level and no appreciable increase in *Camk1g* mRNA.

Collectively, across studies the data indicate that *Camk1g* mRNA expression is affected by pyrethroids with DLT being the most potent for producing this effect. *Camk1g* mRNA expression in cortical neurons is responsive to changes in neuronal firing patterns and internal Ca^{+2} trafficking (Xiang et al. 2007). The greater relative potency of DLT for increasing in *Camk1g* mRNA expression may be due to the longer duration Na^{+} tail currents, and consequently greater increase in neuronal excitability, produced by DLT as compared to other pyrethroids (Vijverberg and Van den Bercken 1990; Choi and Soderlund 2006). Alternatively, DLT may activate a secondary molecular target that controls *Camk1g* expression, such as a voltage-sensitive Ca^{+2} channel, at lower concentrations than other pyrethroids (Symington and Clark 2007). Further work is needed to substantiate these hypothesis as a formal link between pyrethroid action at the neuronal membrane, increased internal Ca^{+2} concentrations and increased *Camk1g* mRNA expression has not been established.

In conclusion, the present data demonstrate that the Type II pyrethroids produce more pronounced changes in activity-regulated gene expression than Type I pyrethroids in the frontal cortex of rats orally exposed to behaviorally equipotent doses. The data also provide predictions for some intracellular signaling pathways that may be affected directly downstream of pyrethroids actions at the neuronal membrane.

Funding.

J.A. Harrill is currently funded through the EPA/UNC Toxicology Research Program training agreement (CR833237) and previously funded through National Institute of Environmental Health Science Training Grant (T32-ES07126).

Acknowledgements.

This document has been reviewed by the National Health and Environmental Effects Research Laboratory and approved for publication. Approval does not signify that the contents reflect the views of the agency, nor does mention of trade names or commercial products constitute endorsement or recommendation for use. The authors wish to thank Chris Corton, Ph.D., Hongzu Ren, Ph.D. and the US EPA National Health and Environmental Effects Research Laboratory Genomics Core Facility for their work with the Affymetrix GeneChip® hybridizations and data collection. Special thanks to Fred Wright, Ph.D. and Dan Gatti for their help with the SAFE enrichment analyses.

Table 4.1. ***Enrichment scores for gene-of-interest lists derived from Venn Diagram comparison.***

		Type II			Type I		
	n	**DLT**	**CYP**	**CYF**	**PERM**	**BIF**	**TEF**
DLT-Limma	399	n/a	**0.0001**	**0.0009**	**0.0345**	**0.0314**	*0.1433*
CYP-Limma	149	**0.0001**	n/a	**0.0022**	*0.0689*	**0.0030**	*0.0854*
CYF-Limma	3742	*0.1246*	*0.3499*	n/a	*0.0874*	*0.1632*	**0.0046**
DLT-CYP Union	91	n/a	n/a	**0.0003**	**0.0345**	**0.0060**	**0.0258**
DLT-CYF Union	216	n/a	**0.0001**	n/a	**0.0345**	**0.0311**	**0.0258**
CYP-CYF Union	85	**0.0001**	n/a	n/a	**0.0348**	**0.0031**	**0.0258**
DLT-CYP-CYF Union	71	n/a	n/a	n/a	**0.0345**	**0.0060**	**0.0107**

Gene lists derived from the LIMMA analysis Venn Diagram (Figure 4.6a) were analyzed for enrichment by SAFE analysis across all six compounds in the study. Prior to analysis microarray expression values were re-centered to the combined mean of 3 h and 6 h controls to eliminate main effects of time (Appendix B, Figure 1). The local statistic for the SAFE analysis is based on a multi-factor ANOVA of mean centered expression values. Global statistics are based on a Wilcoxon rank sum test. The threshold for significant enrichment was set at an FDR < 0.05 (highlighted in bold). n/a = not analyzed: compounds upon which a particular gene-of-interest list is based were not tested for enrichment for that list.

Table 4.2. ***Genes changed by Type II pyrethroid exposure.***

	DLT-CYP Union	DLT-CYF Union	CYP-CYF Union	DLT-CYP-CYF Union
Transcription / Nuclear Factors	Vgll4	Cebpb, Tsc22d3, Ets2, Mybbp1a, Madh3, Mcyn	Egr1, Tcfcp212	Klf10, Junb, Nab2, c-fos, Nr4a1, Id1, Hes1, Klf4, Egr2
Phosphatases	Acpl2	Ptpru		Dusp1, Dusp5, Dusp6, Ptpn1
Kinases	Map2k3	Camk1g, Mertk, Pdk4, Pim3, Uae1		Sgk, Snf1lk, Sbk, Trib1
Cytoskeletal/Structural Proteins		Cryab, Pxn, Pkp2		Arc, Nedd9, Lims2
Metabolic Proteins		Fmo2, Fmo3, Lfng, Xdh, Sult1a1, Hyal2 Usp54		Gpd1, Gfpt2, Hs3st1
Ligands / Receptors	Nppc	Sstr2, Chrm4, Adipor2		Cxcr4, Il6r, Vipr1, Tnfrsf11b
Extracellular Matrix Proteins	Vwa1, Prss11, Lcn7 Fst, Angpt14			
Ion Channels / Ion Transport	Gjb6, Cacng2			
Transporters		Slc21a14, Slc2a1, Slc25a25, Slc39a1		

Table 4.2. *continued*

Cellular Stress Response				
		Hspb1	Bcl2l1, Ndrg1, Rbm3	
Adaptor Proteins [a]				
	Homer1	Ralgds, Mgl1, Errfi1, Lrg1, Rin3, Fkbp51, Slc9a3r2, Cdkn1a, Cnksr3, Nfkbia, Bag3, Arhgap7		Irs2, Gadd45b
Other / Unknown Functions				
	Ctrl, LOC681858, LOC367746, LOC500592	Smpdl3b, Arrdc2, Degs, Clec14a, Prr5, Srxn1, Nid67. LOC684871, LOC690516, LOC683687, RGD1311086, RGD1308276 RGD1359349, RGD1311086, RGD1304790		Rnf39, Xkr6, Per1, Per2, Ier2, Plekhf1, Rasd1, Ier5 Ier5l
Predicted Protein Sequences				
	Cttnbp2nl, Rasgeflc	Rasgrp3, Pnpla2, Sesn1, Cbr3, Mkl1, Asah3l, Spsb1 B3galt5, Cables1, Map3k6 Bcl6, Cd163, Asph, Rundc1, Pla2g3, Usp43, Cdc42ep4, Pwwp2, Mrc1, RGD1310714, RGD1561512, RGD1559797, RGD1306323	Midn, Ephb3, RGD1560818	Dnajb5, Tiparp, Klf2, Zfp189, Rkhd3, Axud1, Spry4
Number of ESTs				
	8	39	9	12

[a]Columns were defined from different zones of similarity shown in Figure 4.6A. [b]Proteins that directly associate with and affect the function of another protein without phosphorylation or dephosphorylation.

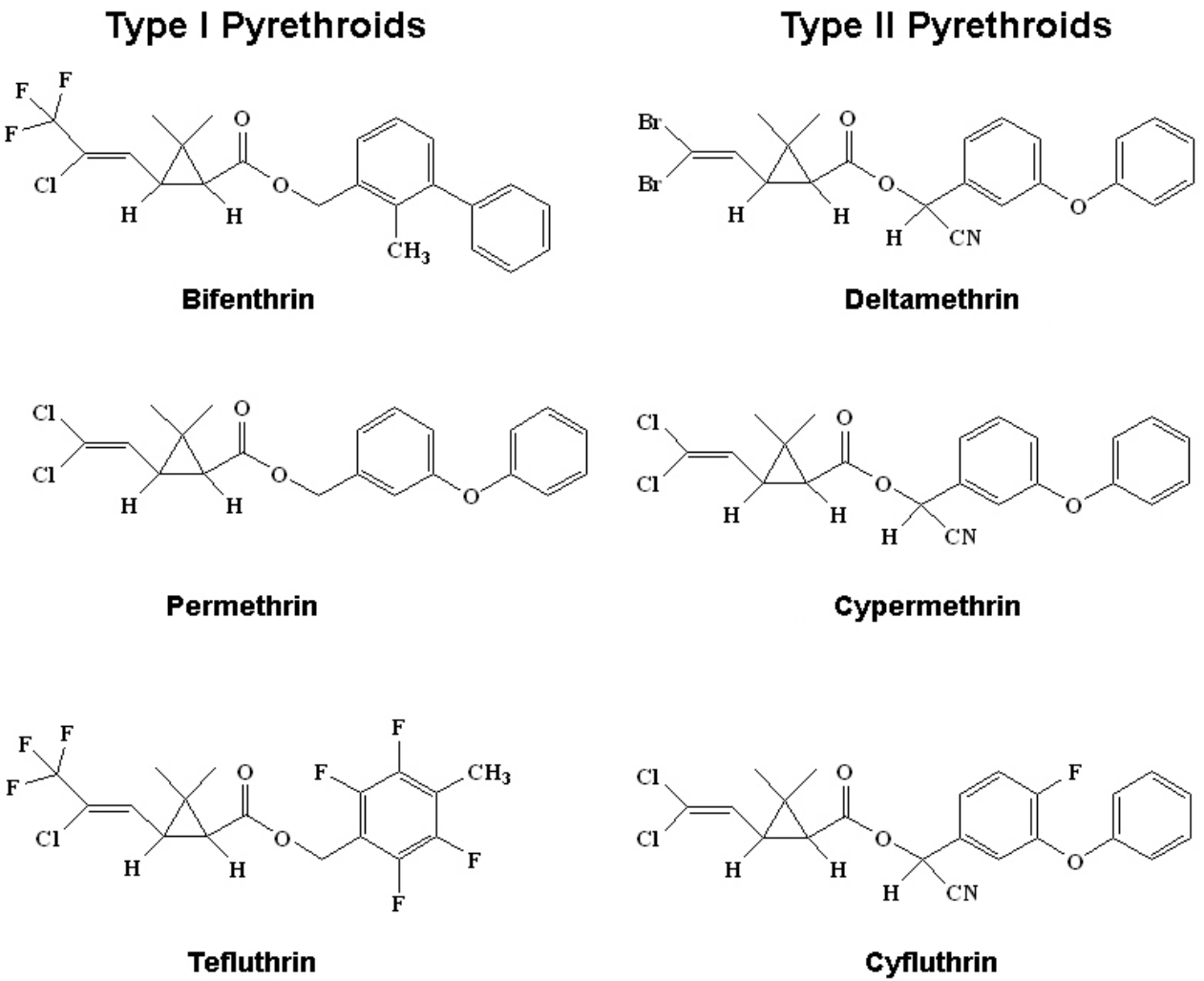

Figure 4.1. Chemical structures of pyrethroids.

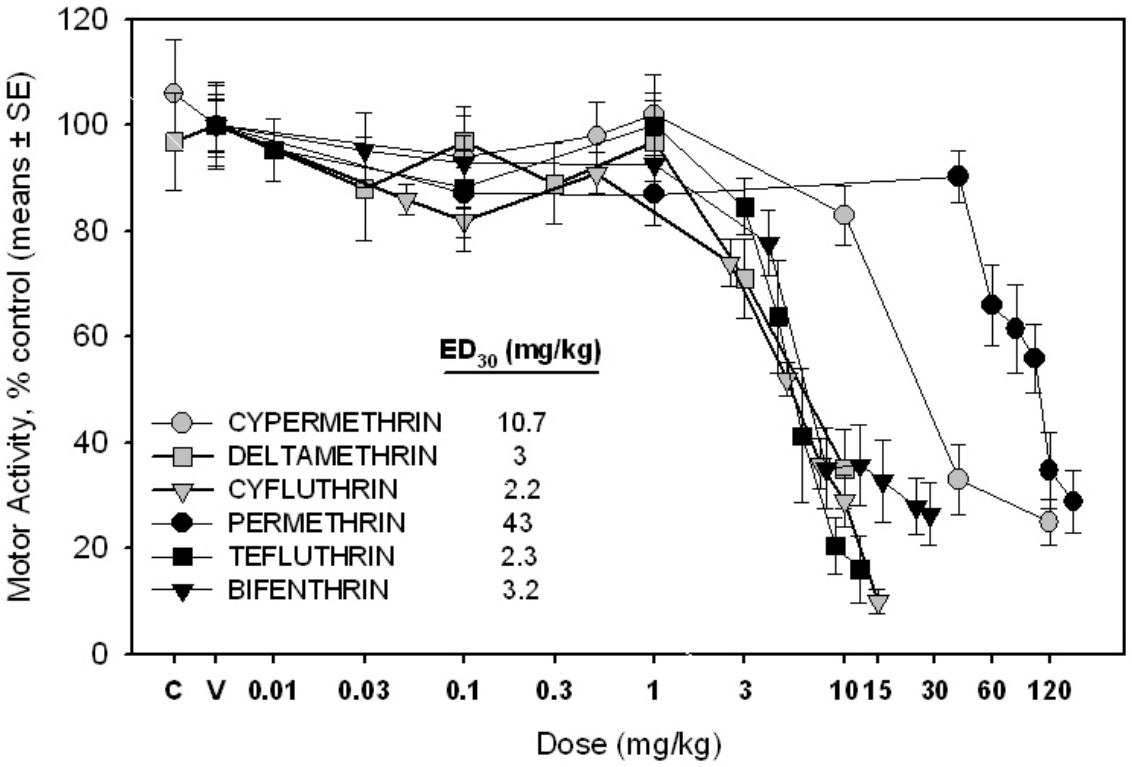

Figure 4.2. ***Pyrethroid effects on motor activity.*** Data replotted from Wolansky et al. (2006). Ambulatory motor activity expressed as percent change from vehicle treated control ± standard error (*y*-axis) versus administered dose of pyrethroids (*x*-axis). Type II pyrethroids plotted in gray, Type I pyrethroids plotted in black. The calculated ED_{30} for decreased motor activity for each compound is given in the inset. These are the administered doses used in the present study.

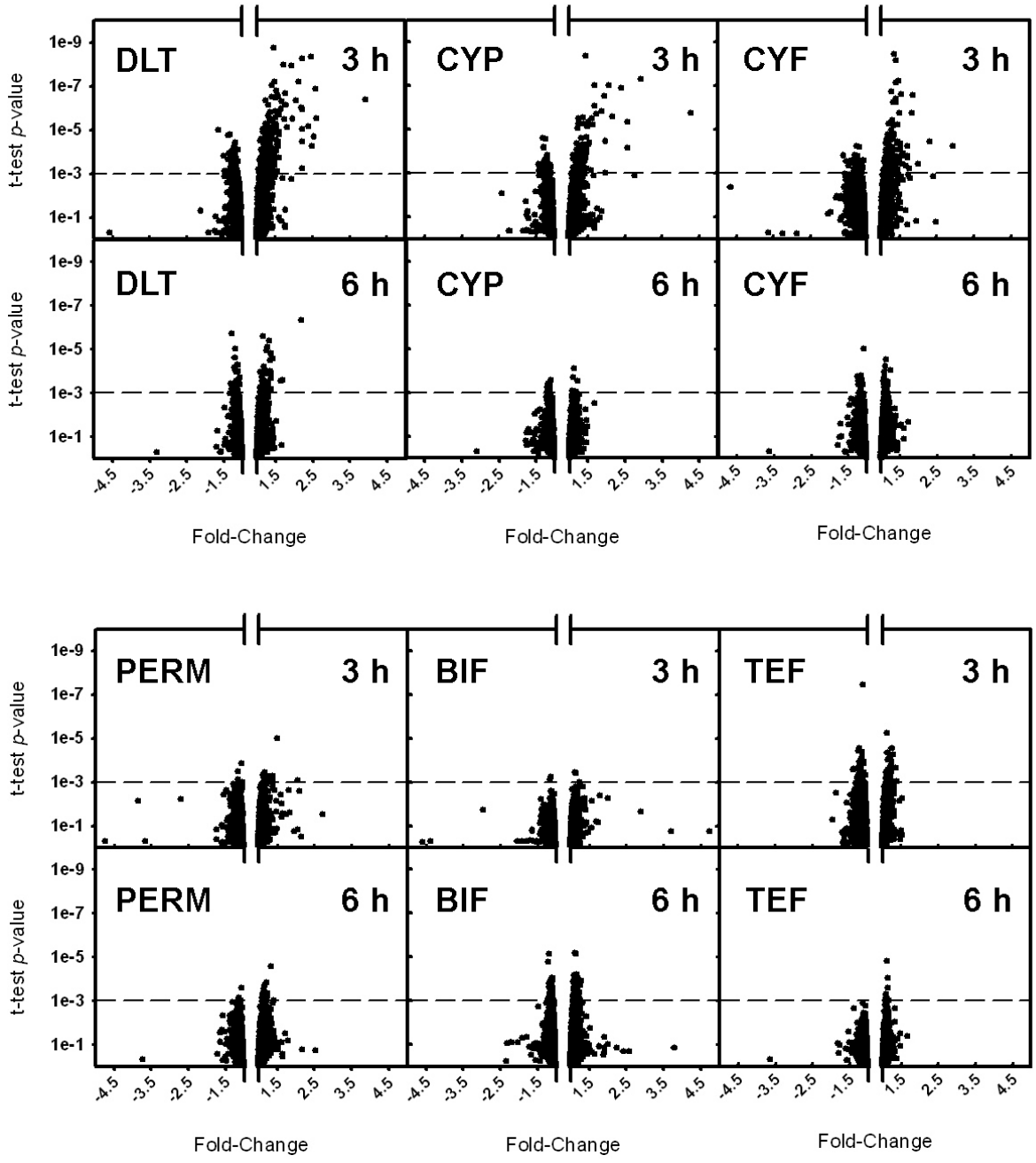

Figure 4.3. ***Volcano plots of pair-wise comparisons of microarray data.*** Each panel plots the empirical *p*-value from a pair-wise *t*-test of treated groups to their corresponding time-matched vehicle controls groups (*y*-axes) versus fold change from control (*x*-axis). Type II pyrethroids are in the upper panels while Type I pyrethroids are in the lower panels. 3 h treatment groups are in rows 1 and 3. 6 h treatment groups are in rows 2 and 4. Dashed lines represent an empirical *p*-value threshold of $p < 0.001$. All probe sets present on the Affymetrix Rat 230_2 array are shown in each panel.

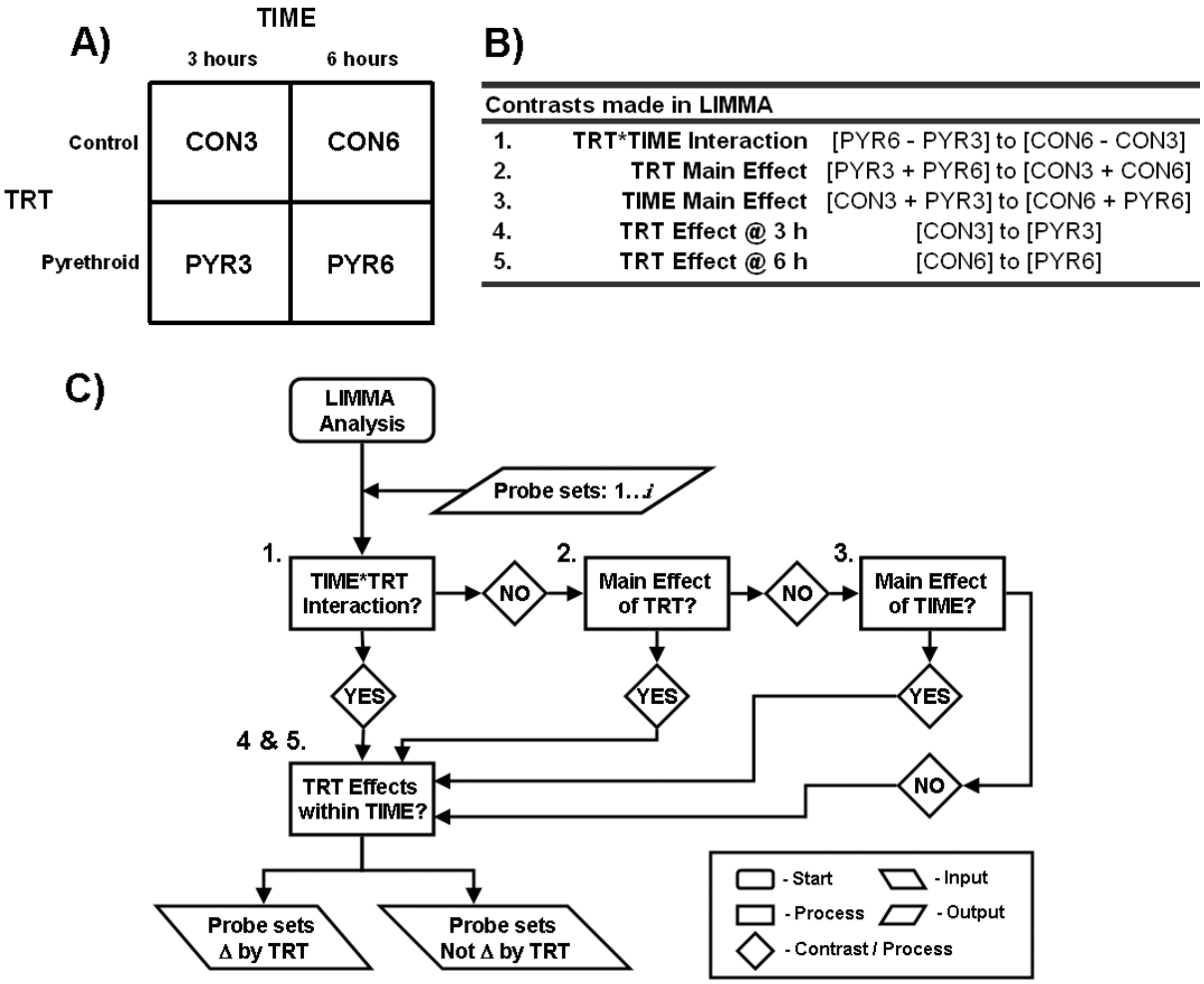

Figure 4.4. ***Linear Models for Microarray Data (LIMMA) analysis scheme.*** (A) Condition matrix for each of the compounds examined in the study. Two treatments (control and pyrethroid) and two times (3 h and 6 h) comprise the 2-by-2 matrix. (B) Contrasts made in the LIMMA analysis for each probe set. Treatment groups involved in each contrast are listed in brackets. The structure is identical to a two-way ANOVA model. (C) Flowchart for the determination of treatment related changes in expression by LIMMA analysis. Decisions for each contrast are made based on a significance threshold of $p < 0.1$ for Yekutieli-Benjamini (1999) adjusted *p*-values. Gene expression values for each pyrethroid were examined individually within this framework.

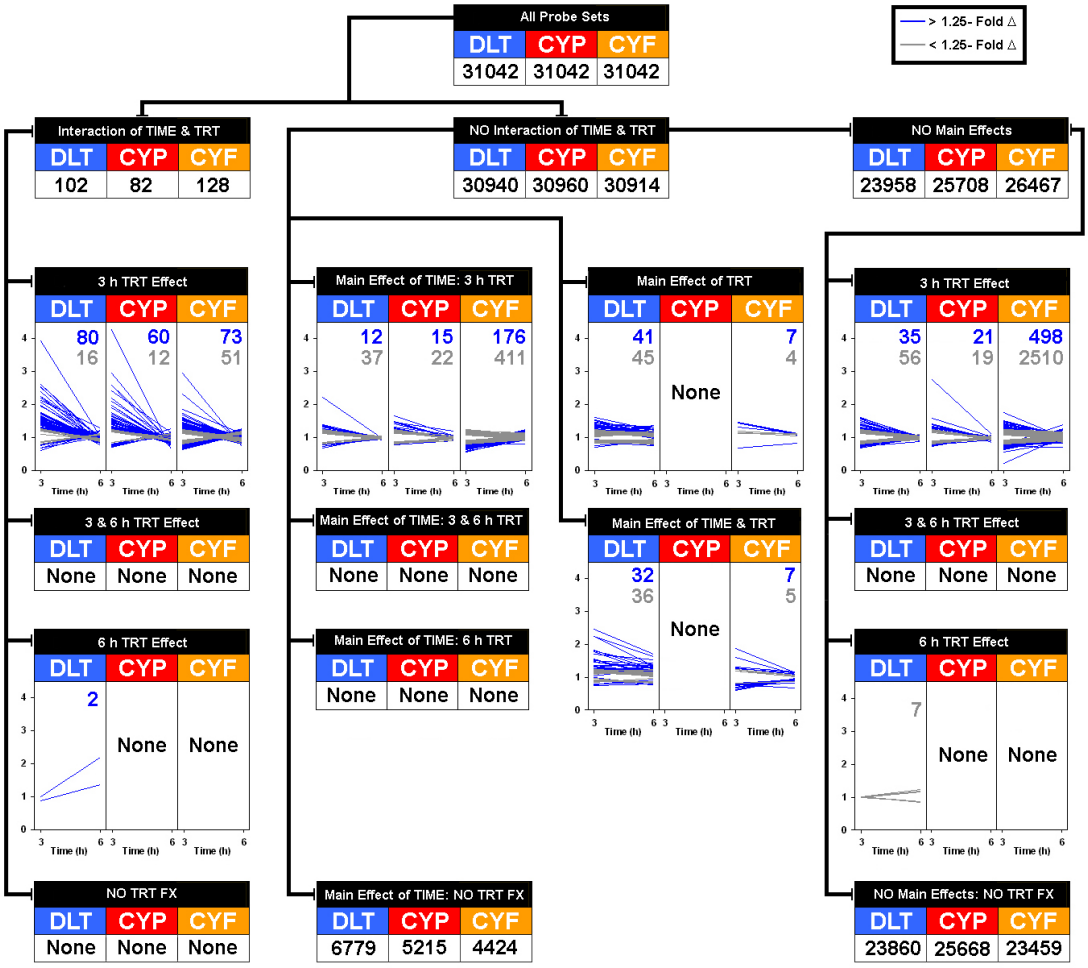

Figure 4.5. ***Results of LIMMA analysis for Type II pyrethroids.*** Each panel shows gene expression changes as a function of fold-change from control (*y*-axes) across time (*x*-axes) for probe sets with treatment related changes in expression for DLT (blue tabbed panels), CYP (red tabbed panels) and CYF (orange tabbed panels). Branches within the diagram correspond to the decisions regarding each contrast outline in the flowchart in Figure 4.4C. Tabs with black numbers in the top two or last row of the diagram represent the number of probe sets that met the particular condition. Probe sets with > 1.25-fold changes in expression for either the 3 h or 6 h condition are shown in blue and correspond to the blue numbers in each panel. Probe sets with no fold changes in expression >1.25 for either the 3 h or 6 h condition are shown in gray and correspond to the gray numbers in each panel.

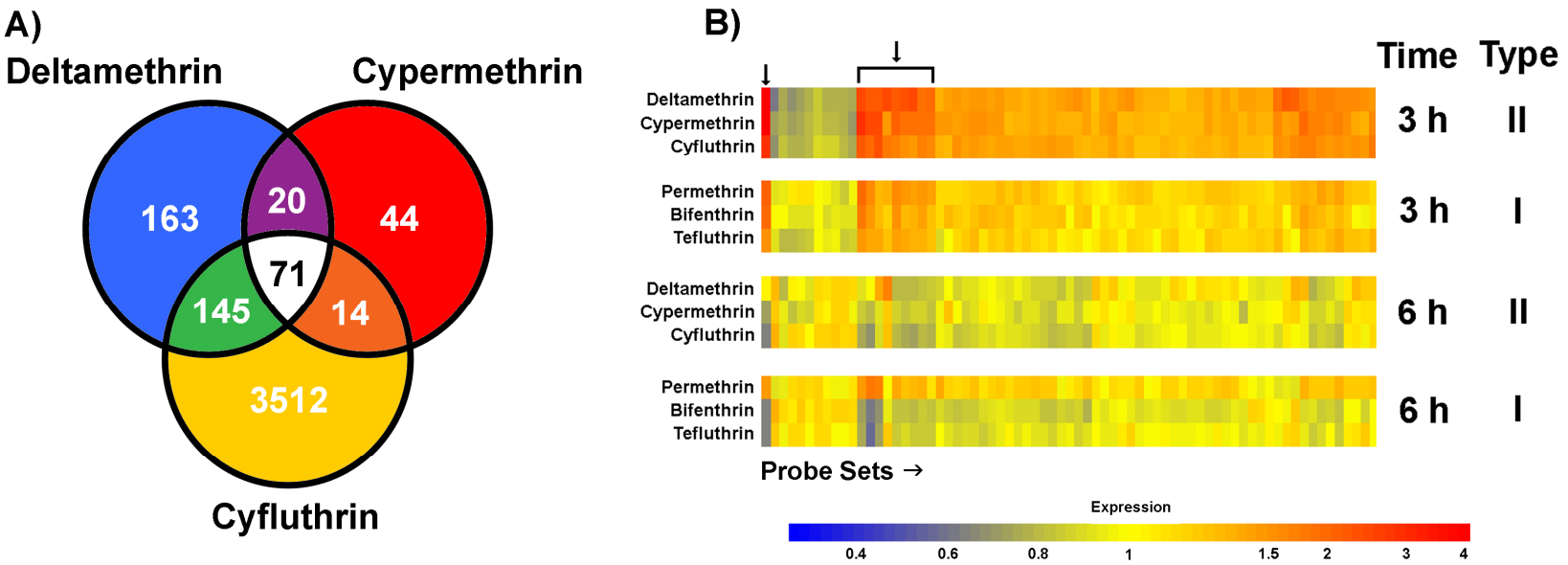

Figure 4.6. ***Comparison of gene expression changes across compounds.*** (A) Venn diagram comparing treatment related changes in gene expression for the Type II pyrethroids deltamethrin, cypermethrin and cyfluthrin. (B) Heatmap displaying patterns of gene expression changes for the 71 probe sets commonly regulated by the Type II pyrethroids. Columns are individual probe sets. Rows are treatment groups. Areas of apparent similarity between the Type II and Type I compounds are marked with arrows and brackets. Tile coloring is based on the mean fold change from control for each of the treatment conditions.

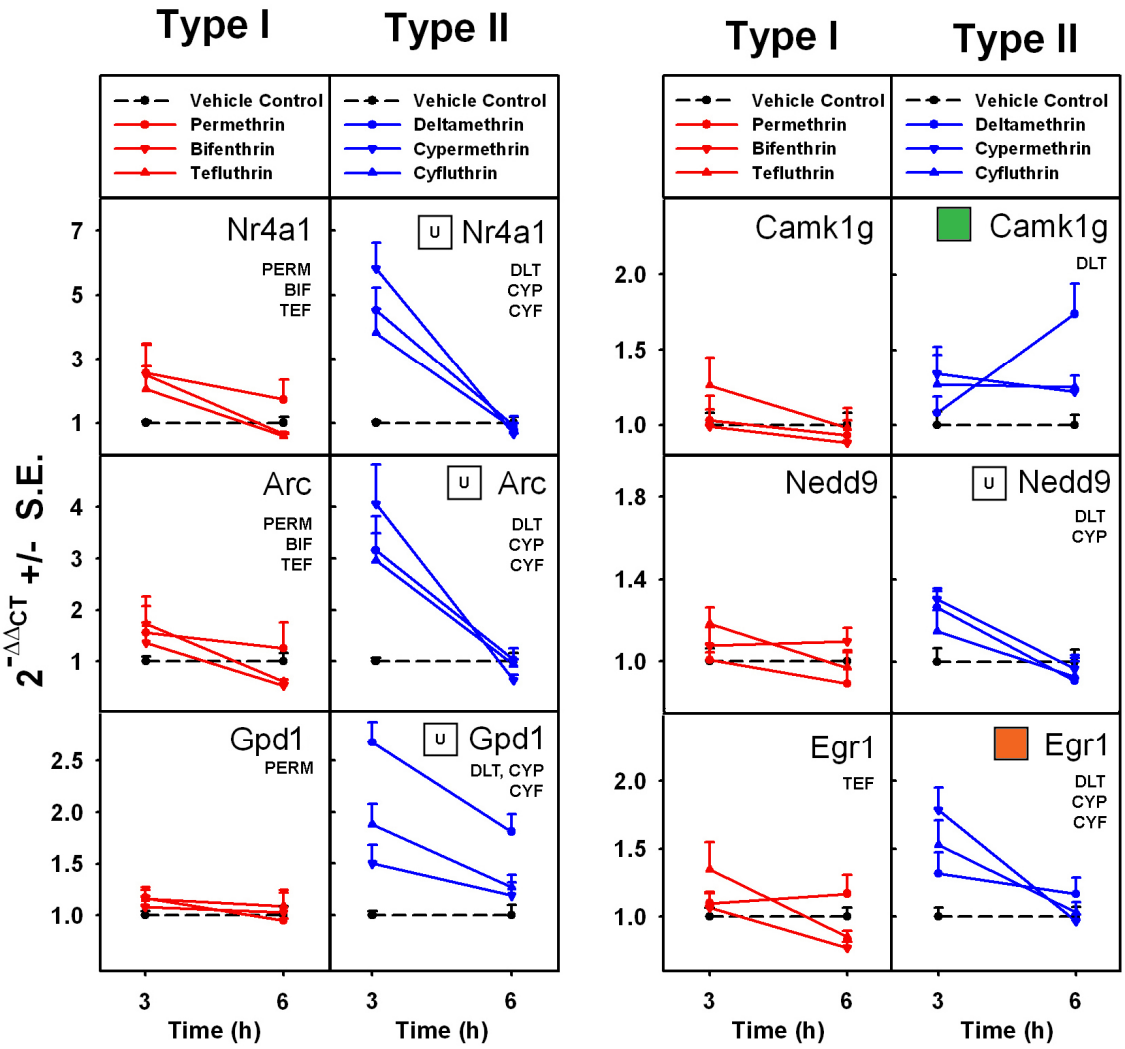

Figure 4.7. ***qRT-PCR results.*** Each panel shows changes in gene expression measured with TaqMan® qRT-PCR for *Nr4a1*, *Arc*, *Gpd1*, *Camk1g*, *Nedd9* and *Egr1*. Each gene of interest was examined for each pyrethroid in the test panel. Data are expressed as $2^{-\Delta\Delta C}{}_T$ values ± standard error (*y*-axes) across time (*x*-axes) as described in the Methods section. Colored boxes beside each gene name correspond to the area of the Venn Diagram in Figure 4.6A in which each transcript is found. Compound abbreviations listed under each gene symbol denote that a significant effect of treatment was observed for that individual pyrethroid ($p < 0.05$). Statistical analyses of these data are described in the Methods section and results are given in Appendix B, Tables 2.

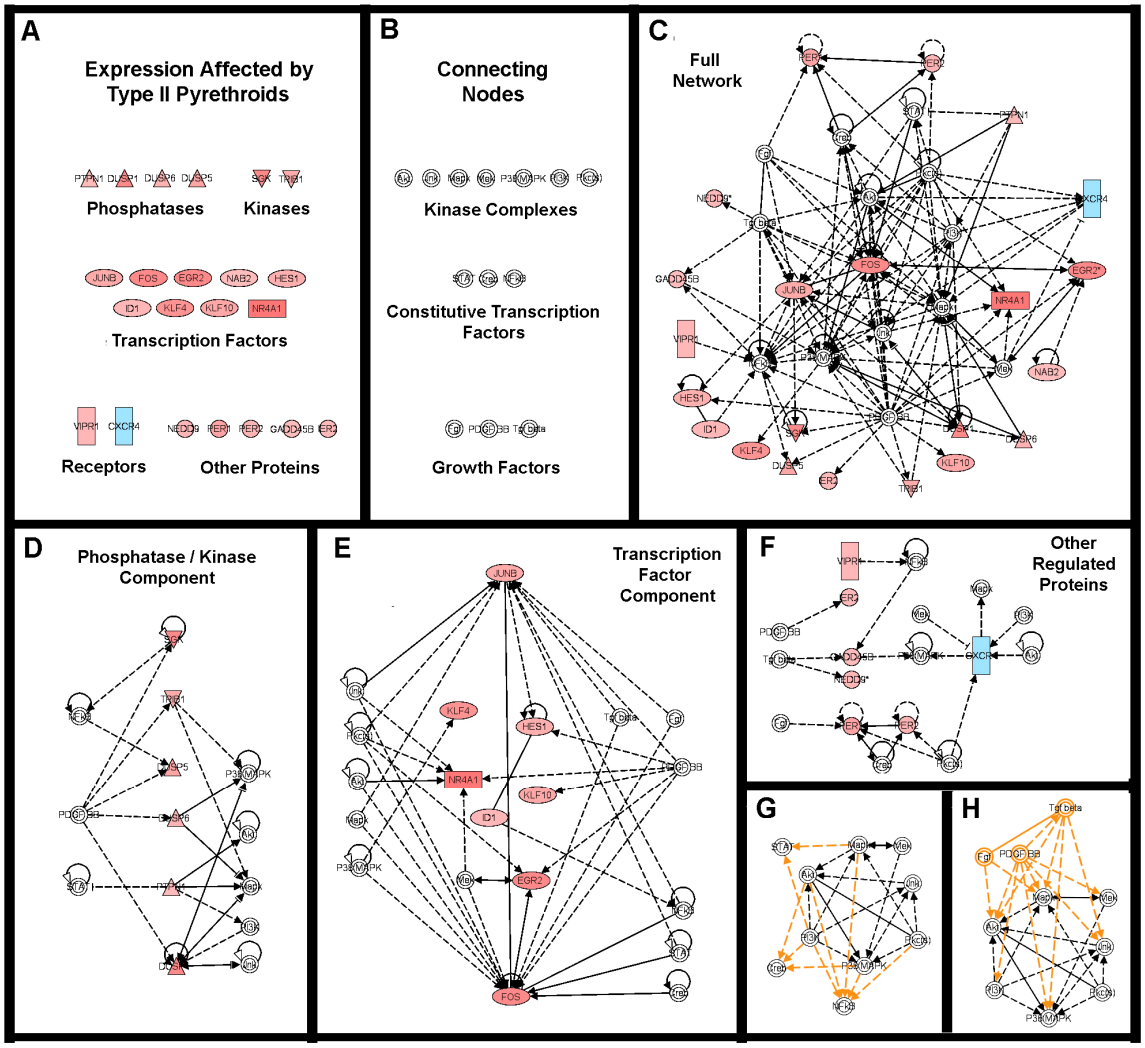

Figure 4.8. ***Ingenuity® pathway analysis of genes commonly affected by Type II pyrethroids.*** The 71 probe sets commonly affected by all the Type II pyrethroids in the microarray data was input into the Ingenuity® pathway analysis software package and yielded the interconnected network shown in panel C. (A) List of the pyrethroid-sensitive genes present in the network. Coloring of these elements is based on the expression pattern observed with deltamethrin: red = upregulated, blue = downregulated. (B) List of connecting nodes present in the network. (D-F) Systematic deconstruction of the interaction network in Figure C. Associations between the connecting nodes of the full network removed for clarity in panels D-F. The network is separated into an inducible phosphatase/kinase component (D), an inducible transcription factor component (E) and other regulated proteins component (F). Note in panel D that inducible phosphatases act upstream of the constitutive kinases (arrows pointed to the right) and in panel E constitutive kinases and transcription factors act upstream of inducible transcription factors (arrows radiating inward). (G-H) The interconnections of the constitutive kinase complexes are given in the absence of pyrethroid-responsive genes for clarity. Interconnections between kinase complexes and transcription factors (orange arrows pointing out) and kinase complexes and growth factors (orange arrows pointing in) are given in panels G and H.

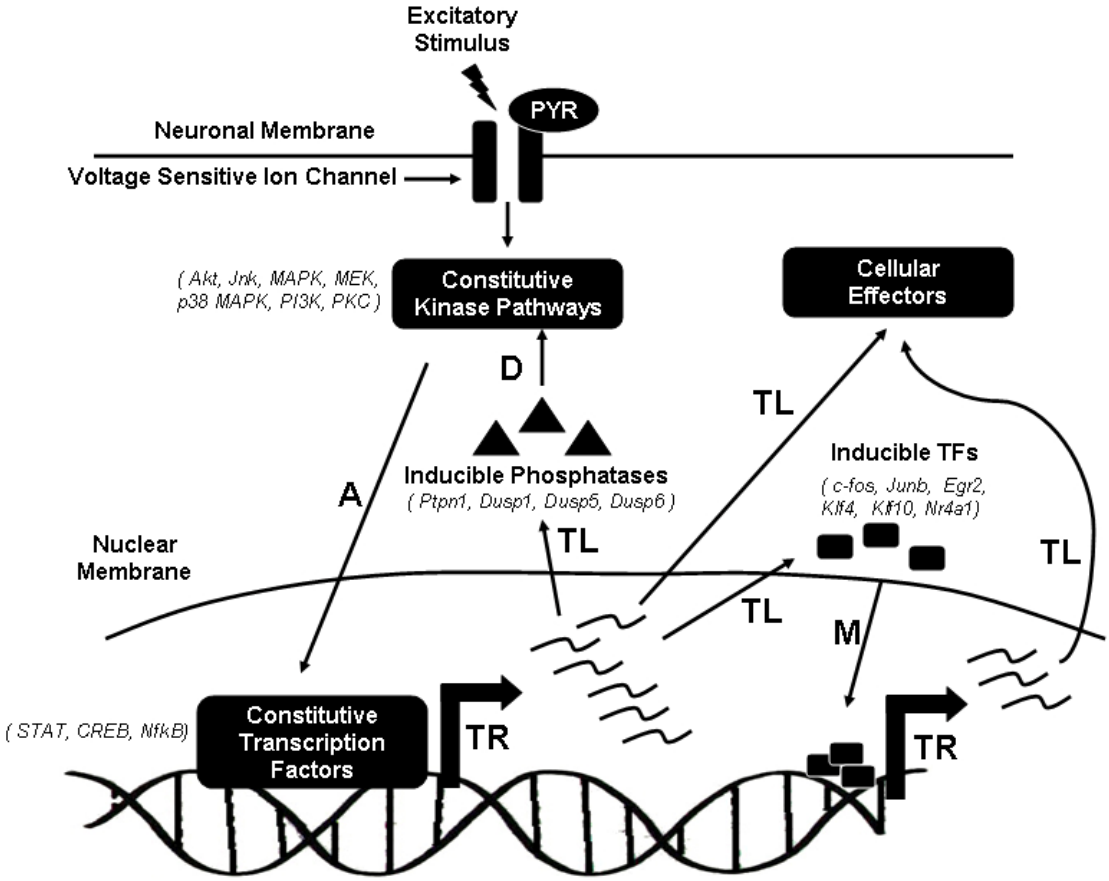

Figure 4.9. ***Schematic of putative pyrethroid gene regulatory network.*** Putative intracellular signaling cascades impacted by pyrethroids as indicted by Ingenuity® analysis. A = activation, TR = transcription, TL = translation, D = deactivation, M = translocation / movement.

Works Cited

Affymetrix Inc. (2002) *GeneChip Expression Analysis: Data Analysis Fundamentals (Part No. 701190).* Affymetrix Inc., Santa Clara, CA.

Affymetrix Inc. (2004) *GeneChip Expression Analysis Technical Manual (Pub 701021).* Affymetrix Inc.,, Santa Clara, CA.

Anadon A., Martinez-Larranaga M. R., Diaz M. J. and Bringas P. (1991) Toxicokinetics of permethrin in the rat. *Toxicol Appl Pharmacol* **110**, 1-8.

Anadon A., Martinez-Larranaga M. R., Fernandez-Cruz M. L., Diaz M. J., Fernandez M. C. and Martinez M. A. (1996) Toxicokinetics of deltamethrin and its 4'-HO-metabolite in the rat. *Toxicol Appl Pharmacol* **141**, 8-16.

Applied Biosystems Inc. (2004) *Amplification Efficiency of Taqman Assays-on-Demand Gene Expression Products (Publication 127AP05-01).* Applied Biosystems Inc.,, Foster City, CA.

Applied Biosystems Inc. (2005) *TaqMan Gene Expression Assays Protocol (Part Number 4333458).* Applied Biosystems Inc.,, Foster City, CA.

Applied Biosystems Inc. (2006) *The Design Process for a New Generation of Quantitative Gene Expression Analysis Tools (Publication 127WP02-02).* Applied Biosystems Inc.,, Foster City, CA.

Barry W. T., Nobel A. B. and Wright F. A. (2005) Significance analysis of functional categories in gene expression studies: a structured permutation approach. *Bioinformatics* **21**, 1943-9.

Baughman G., Wiederrecht G. J., Chang F., Martin M. M. and Bourgeois S. (1997) Tissue distribution and abundance of human FKBP51, and FK506-binding protein that can mediate calcineurin inhibition. *Biochem Biophys Res Commun* **232**, 437-43.

Brager D. H., Cai X. and Thompson S. M. (2003) Activity-dependent activation of presynaptic protein kinase C mediates post-tetanic potentiation. *Nat Neurosci* **6**, 551-2.

Brogan M. D., Behrend E. N. and Kemppainen R. J. (2001) Regulation of Dexras1 expression by endogenous steroids. *Neuroendocrinology* **74**, 244-50.

Burr S. A. and Ray D. E. (2004) Structure-activity and interaction effects of 14 different pyrethroids on voltage-gated chloride ion channels. *Toxicol Sci* **77**, 341-6.

Chen R. W., Qin Z. H., Ren M., Kanai H., Chalecka-Franaszek E., Leeds P. and Chuang D. M. (2003) Regulation of c-Jun N-terminal kinase, p38 kinase and AP-1 DNA binding in cultured brain neurons: roles in glutamate excitotoxicity and lithium neuroprotection. *J Neurochem* **84**, 566-75.

Choi J. S. and Soderlund D. M. (2006) Structure-activity relationships for the action of 11 pyrethroid insecticides on rat Na v 1.8 sodium channels expressed in Xenopus oocytes. *Toxicol Appl Pharmacol* **211**, 233-44.

Colt J. S., Lubin J., Camann D., Davis S., Cerhan J., Severson R. K., Cozen W. and Hartge P. (2004) Comparison of pesticide levels in carpet dust and self-reported pest treatment practices in four US sites. *J Expo Anal Environ Epidemiol* **14**, 74-83.

Corvol J. C., Valjent E., Toutant M., Enslen H., Irinopoulou T., Lev S., Herve D. and Girault J. A. (2005) Depolarization activates ERK and proline-rich tyrosine kinase 2 (PYK2) independently in different cellular compartments in hippocampal slices. *J Biol Chem* **280**, 660-8.

Crofton K. M. and Reiter L. W. (1984) Effects of two pyrethroid insecticides on motor activity and the acoustic startle response in the rat. *Toxicol Appl Pharmacol* **75**, 318-28.

Crofton K. M. and Reiter L. W. (1988) The effects of type I and II pyrethroids on motor activity and the acoustic startle response in the rat. *Fundam Appl Toxicol* **10**, 624-34.

Davis S., Vanhoutte P., Pages C., Caboche J. and Laroche S. (2000) The MAPK/ERK cascade targets both Elk-1 and cAMP response element-binding protein to control long-term potentiation-dependent gene expression in the dentate gyrus in vivo. *J Neurosci* **20**, 4563-72.

de Boer S. F., van der Gugten J., Slangen J. L. and Hijzen T. H. (1988) Changes in plasma corticosterone and catecholamine contents induced by low doses of deltamethrin in rats. *Toxicology* **49**, 263-70.

De Kloet E. R., Vreugdenhil E., Oitzl M. S. and Joels M. (1998) Brain corticosteroid receptor balance in health and disease. *Endocr Rev* **19**, 269-301.

Ecobichon D. J. (2001) Toxic Effects of Pesticides. In *Casarett & Doull's Toxicology: The Basic Science of Poisons* (Edited by Klaassen C. D.), p. 763-810. McGraw-Hill, New York, NY.

Fields R. D., Eshete F., Stevens B. and Itoh K. (1997) Action potential-dependent regulation of gene expression: temporal specificity in ca2+, cAMP-responsive element binding proteins, and mitogen-activated protein kinase signaling. *J Neurosci* **17**, 7252-66.

Fields R. D., Lee P. R. and Cohen J. E. (2005) Temporal integration of intracellular Ca2+ signaling networks in regulating gene expression by action potentials. *Cell Calcium* **37**, 433-42.

Finkbeiner S. and Greenberg M. E. (1998) Ca2+ channel-regulated neuronal gene expression. *J Neurobiol* **37**, 171-89.

Gass P., Eckhardt A., Schroder H., Bravo R. and Herdegen T. (1996) Transient expression of the mitogen-activated protein kinase phosphatase MKP-1 (3CH134/ERP1) in the rat brain after limbic epilepsy. *Brain Res Mol Brain Res* **41**, 74-80.

Gentleman R. C., Carey V. J., Bates D. M., Bolstad B., Dettling M., Dudoit S., Ellis B., Gautier L., Ge Y., Gentry J., Hornik K., Hothorn T., Huber W., Iacus S., Irizarry R., Leisch F., Li C., Maechler M., Rossini A. J., Sawitzki G., Smith C., Smyth G., Tierney L., Yang J. Y. and Zhang J. (2004) Bioconductor: open software development for computational biology and bioinformatics. *Genome Biol* **5**, R80.

Gray A. J., Connors T. A., Hoellinger H. and Nam N. H. (1980) The Relationship between the Pharmacokinetics of Intravenous Cismethrin and Bioresmethrin and their Mammalian Toxicity. *Pesticide Biochemistry and Physiology* **13**, 281-293.

Grosse G., Thiele T., Heuckendorf E., Schopp E., Merder S., Pickert G. and Ahnert-Hilger G. (2002) Deltamethrin differentially affects neuronal subtypes in hippocampal primary culture. *Neuroscience* **112**, 233-41.

Guzowski J. F., Miyashita T., Chawla M. K., Sanderson J., Maes L. I., Houston F. P., Lipa P., McNaughton B. L., Worley P. F. and Barnes C. A. (2006) Recent behavioral history modifies coupling between cell activity and Arc gene transcription in hippocampal CA1 neurons. *Proc Natl Acad Sci U S A* **103**, 1077-82.

Harrill, J. A., LI, Z., Wright, F. A., Radio, N. M., Mundy, W. R., and Crofton, K. M. (*submitted*). Transcriptional response of rat cerebrocortical tissue following acute in vivo exposure to the pyrethroid insecticides permethrin and deltamethrin. *BMC Genomics*.

Harrill, J.A., Crofton K.M. (*in preparation*). Splice variant specific induction of Ca+2/calmodulin dependent protein kinase 1-gamma mRNA in response to pyrethroid exposure.

Harrill J. A., Wright F. A. and Crofton K. M. (2007) Dose-response modeling of the transcriptional response of rat cerebrocortical tissue after acute pyrethroid exposure in vivo. *The Toxicologist* **96**, 186.

Hassouna I., Wickert H., el-Elaimy I., Zimmermann M. and Herdegen T. (1996) Systemic application of pyrethroid insecticides evokes differential expression of c-Fos and c-Jun proteins in rat brain. *Neurotoxicology* **17**, 415-31.

Hazel T. G., Misra R., Davis I. J., Greenberg M. E. and Lau L. F. (1991) Nur77 is differentially modified in PC12 cells upon membrane depolarization and growth factor treatment. *Mol Cell Biol* **11**, 3239-46.

Heudorf U. and Angerer J. (2001) Metabolites of pyrethroid insecticides in urine specimens: current exposure in an urban population in Germany. *Environ Health Perspect* **109**, 213-7.

Hevroni D., Rattner A., Bundman M., Lederfein D., Gabarah A., Mangelus M., Silverman M. A., Kedar H., Naor C., Kornuc M., Hanoch T., Seger R., Theill L. E., Nedivi E., Richter-Levin G. and Citri Y. (1998) Hippocampal plasticity involves extensive gene induction and multiple cellular mechanisms. *J Mol Neurosci* **10**, 75-98.

Hughes P. E., Alexi T., Walton M., Williams C. E., Dragunow M., Clark R. G. and Gluckman P. D. (1999) Activity and injury-dependent expression of inducible transcription factors, growth factors and apoptosis-related genes within the central nervous system. *Prog Neurobiol* **57**, 421-50.

Irizarry R. A., Hobbs B., Collin F., Beazer-Barclay Y. D., Antonellis K. J., Scherf U. and Speed T. P. (2003) Exploration, normalization, and summaries of high density oligonucleotide array probe level data. *Biostatistics* **4**, 249-64.

Kaltschmidt, B., Heinrich, M., and Kaltschmidt, C. (2002). Stimulus-dependent activation of NF-kappaB specifies apoptosis or neuroprotection in cerebellar granule cells. *Neuromolecular Med* **2**, 299-309.

Kodama M., Russell D. S. and Duman R. S. (2005) Electroconvulsive seizures increase the expression of MAP kinase phosphatases in limbic regions of rat brain. *Neuropsychopharmacology* **30**, 360-71.

Lawrence L. J. and Casida J. E. (1982) Pyrethroid toxicology: mouse intracerebral structure-toxicity relationships. *Pesticide Biochemistry and Physiology* **18**, 9-14.

Lee E. H., Hsu W. L., Ma Y. L., Lee P. J. and Chao C. C. (2003) Enrichment enhances the expression of sgk, a glucocorticoid-induced gene, and facilitates spatial learning through glutamate AMPA receptor mediation. *Eur J Neurosci* **18**, 2842-52.

Leng G., Kuhn K. H. and Idel H. (1997) Biological monitoring of pyrethroids in blood and pyrethroid metabolites in urine: applications and limitations. *Sci Total Environ* **199**, 173-81.

Leveille P. J., McGinnis J. F., Maxwell D. S. and de Vellis J. (1980) Immunocytochemical localization of glycerol-3-phosphate dehydrogenase in rat oligodendrocytes. *Brain Res* **196**, 287-305.

Livak K. J. and Schmittgen T. D. (2001) Analysis of relative gene expression data using real-time quantitative PCR and the 2(-Delta Delta C(T)) Method. *Methods* **25**, 402-8.

Machado H. B., Vician L. J. and Herschman H. R. (2008) The MAPK pathway is required for depolarization-induced "promiscuous" immediate-early gene expression but not for depolarization-restricted immediate-early gene expression in neurons. *J Neurosci Res* **86**, 593-602.

Meyer D. A., Carter J. M., Johnstone A. F. and Shafer T. J. (2007) Pyrethroid modulation of spontaneous neuronal excitability and neurotransmission in hippocampal neurons in culture. *Neurotoxicology*.

Meyer D. A. and Shafer T. J. (2006) Permethrin, but not deltamethrin, increases spontaneous glutamate release from hippocampal neurons in culture. *Neurotoxicology* **27**, 594-603.

Morgan J. I. and Curran T. (1986) Role of ion flux in the control of c-fos expression. *Nature* **322**, 552-5.

Muda M., Boschert U., Dickinson R., Martinou J. C., Martinou I., Camps M., Schlegel W. and Arkinstall S. (1996a) MKP-3, a novel cytosolic protein-tyrosine phosphatase that exemplifies a new class of mitogen-activated protein kinase phosphatase. *J Biol Chem* **271**, 4319-26.

Muda M., Theodosiou A., Rodrigues N., Boschert U., Camps M., Gillieron C., Davies K., Ashworth A. and Arkinstall S. (1996b) The dual specificity phosphatases M3/6 and MKP-3 are highly selective for inactivation of distinct mitogen-activated protein kinases. *J Biol Chem* **271**, 27205-8.

Narahashi T. (2000) Neuroreceptors and ion channels as the basis for drug action: past, present, and future. *J Pharmacol Exp Ther* **294**, 1-26.

Narahashi T. (2001) Neurophysiological Effects of Insecticides. In *Handbook of Pesticide Toxicology* (Edited by Krieger R. I.), Vol. 2, p. 335-351. Academic Press, San Diego, CA.

Ott R. L. (1993) *An Introduction to Statistical Methods and Data Analysis*. PWS-Kent Pub. Co.,, Boston, MA.

Patra R. C., Blue M. E., Johnston M. V., Bressler J. and Wilson M. A. (2004) Activity-dependent expression of Egr1 mRNA in somatosensory cortex of developing rats. *J Neurosci Res* **78**, 235-44.

Perkinton M. S., Ip J. K., Wood G. L., Crossthwaite A. J. and Williams R. J. (2002) Phosphatidylinositol 3-kinase is a central mediator of NMDA receptor signalling to MAP kinase (Erk1/2), Akt/PKB and CREB in striatal neurones. *J Neurochem* **80**, 239-54.

Pezet S., Spyropoulos A., Williams R. J. and McMahon S. B. (2005) Activity-dependent phosphorylation of Akt/PKB in adult DRG neurons. *Eur J Neurosci* **21**, 1785-97.

Ray D. E. (2001) Pyrethroid Insecticdes: Mechanisms of Toxicity, Systematic Poisoning Syndromes, Parethesia, and Therapy. In *Handbook of Pesticide Toxicology* (Edited by Krieger R. I.), Vol. 2, p. 1289-1303. Academic Press, San Diego, CA.

Ray D. E. and Fry J. R. (2006) A reassessment of the neurotoxicity of pyrethroid insecticides. *Pharmacol Ther* **111**, 174-93.

Rickard J. and Brodie M. E. (1985) Correlation of Blood and Brain Levels of the Neurotoxic Pyrethroid Deltamethrin with the Onset of Symptoms in Rat. *Pesticide Biochemistry and Physiology* **23**, 143-156.

Rosen L. B., Ginty D. D., Weber M. J. and Greenberg M. E. (1994) Membrane depolarization and calcium influx stimulate MEK and MAP kinase via activation of Ras. *Neuron* **12**, 1207-21.

Shafer T. J. and Meyer D. A. (2004) Effects of pyrethroids on voltage-sensitive calcium channels: a critical evaluation of strengths, weaknesses, data needs, and relationship to assessment of cumulative neurotoxicity. *Toxicol Appl Pharmacol* **196**, 303-18.

Schulman, H., and Roberts, J. L. (2003). Cellular and Molecular Neuroscience, Section 10. Intracellular Signaling. In Fundamental Neuroscience (L. R. Squire, F. E. Bloom, S. K. McConnell, J. L. Roberts, N. C. Spitzer and M. J. Zigmond, eds.), pp. 259-297. Academic Press, San Diego, CA.

Scollon, E.J., Starr,J,M., Hughes, M.F., Crofton,K.M., Wolansky,M.J., and Devito,M.J. (2008) Blood and brain concentrations of bifenthrin correlate with decreased motor activity. (in prep).Smith T. J. and Soderlund D. M. (1998) Action of the pyrethroid insecticide cypermethrin on rat brain IIa sodium channels expressed in xenopus oocytes. *Neurotoxicology* **19**, 823-32.

Smyth G. K. (2005) Limma: linear models for microarray data. In *Bioinformatics and Computational Biology Solutions using R and Bioconductor* (Edited by Gentleman R., Carey V., Dudoit R., Irizarry R. A. and Huber W.), p. 397-420. Springer, New York.

Soderlund D. M. (1985) Pyrethroid-receptor interactions: stereospecific binding and effects on sodium channels in mouse brain preparations. *Neurotoxicology* **6**, 35-46.

Soderlund D. M., Clark J. M., Sheets L. P., Mullin L. S., Piccirillo V. J., Sargent D., Stevens J. T. and Weiner M. L. (2002) Mechanisms of pyrethroid neurotoxicity: implications for cumulative risk assessment. *Toxicology* **171**, 3-59.

Song J. H., Nagata K., Tatebayashi H. and Narahashi T. (1996) Interactions of tetramethrin, fenvalerate and DDT at the sodium channel in rat dorsal root ganglion neurons. *Brain Res* **708**, 29-37.

Song J. H. and Narahashi T. (1996) Modulation of sodium channels of rat cerebellar Purkinje neurons by the pyrethroid tetramethrin. *J Pharmacol Exp Ther* **277**, 445-53.

Symington, S. B., Frisbie, R. K., Lu, K. D., and Clark, J. M. (2007). Action of cismethrin and deltamethrin on functional attributes of isolated presynaptic nerve terminals from rat brain. *Pesticide Biochemistry and Physiology* **87**, 172-181.

Tabarean I. V. and Narahashi T. (1998) Potent modulation of tetrodotoxin-sensitive and tetrodotoxin-resistant sodium channels by the type II pyrethroid deltamethrin. *J Pharmacol Exp Ther* **284**, 958-65.

Tatebayashi H. and Narahashi T. (1994) Differential mechanism of action of the pyrethroid tetramethrin on tetrodotoxin-sensitive and tetrodotoxin-resistant sodium channels. *J Pharmacol Exp Ther* **270**, 595-603.

Tropea D., Kreiman G., Lyckman A., Mukherjee S., Yu H., Horng S. and Sur M. (2006) Gene expression changes and molecular pathways mediating activity-dependent plasticity in visual cortex. *Nat Neurosci* **9**, 660-8.

Tulve N. S., Jones P. A., Nishioka M. G., Fortmann R. C., Croghan C. W., Zhou J. Y., Fraser A., Cavel C. and Friedman W. (2006) Pesticide measurements from the first national environmental health survey of child care centers using a multi-residue GC/MS analysis method. *Environ Sci Technol* **40**, 6269-74.

Vaillant A. R., Mazzoni I., Tudan C., Boudreau M., Kaplan D. R. and Miller F. D. (1999) Depolarization and neurotrophins converge on the phosphatidylinositol 3-kinase-Akt pathway to synergistically regulate neuronal survival. *J Cell Biol* **146**, 955-66.

Vanhoutte P., Barnier J. V., Guibert B., Pages C., Besson M. J., Hipskind R. A. and Caboche J. (1999) Glutamate induces phosphorylation of Elk-1 and CREB, along with c-fos activation, via an extracellular signal-regulated kinase-dependent pathway in brain slices. *Mol Cell Biol* **19**, 136-46.

Verschoyle R. D. and Aldridge W. N. (1980) Structure-activity relationships of some pyrethroids in rats. *Arch Toxicol* **45**, 325-9.

Vijverberg H. P. and van den Bercken J. (1990) Neurotoxicological effects and the mode of action of pyrethroid insecticides. *Crit Rev Toxicol* **21**, 105-26.

Virtaneva K., Wright F. A., Tanner S. M., Yuan B., Lemon W. J., Caligiuri M. A., Bloomfield C. D., de La Chapelle A. and Krahe R. (2001) Expression profiling reveals fundamental biological differences in acute myeloid leukemia with isolated trisomy 8 and normal cytogenetics. *Proc Natl Acad Sci U S A* **98**, 1124-9.

Webster M. K., Goya L., Ge Y., Maiyar A. C. and Firestone G. L. (1993) Characterization of sgk, a novel member of the serine/threonine protein kinase gene family which is transcriptionally induced by glucocorticoids and serum. *Mol Cell Biol* **13**, 2031-40.

Weston D. P., You J. and Lydy M. J. (2004) Distribution and toxicity of sediment-associated pesticides in agriculture-dominated water bodies of California's Central Valley. *Environ Sci Technol* **38**, 2752-9.

Whyatt R. M., Barr D. B., Camann D. E., Kinney P. L., Barr J. R., Andrews H. F., Hoepner L. A., Garfinkel R., Hazi Y., Reyes A., Ramirez J., Cosme Y. and Perera F. P. (2003) Contemporary-use pesticides in personal air samples during pregnancy and blood

samples at delivery among urban minority mothers and newborns. *Environ Health Perspect* **111**, 749-56.

Wolansky M. J., Gennings C. and Crofton K. M. (2006) Relative potencies for acute effects of pyrethroids on motor function in rats. *Toxicol Sci* **89**, 271-7.

Wolansky M. J. and Harrill J. A. (2007) Neurobehavioral toxicology of pyrethroid insecticides in adult animals: A critical review. *Neurotoxicol Teratol*.

Wooten, M. W. (1999). Function for NF-kB in neuronal survival: regulation by atypical protein kinase C. *J Neurosci Res* **58**, 607-11.

Wu A. and Liu Y. (2003) Prolonged expression of c-Fos and c-Jun in the cerebral cortex of rats after deltamethrin treatment. *Brain Res Mol Brain Res* **110**, 147-51.

Yanez L., Ortiz-Perez D., Batres L. E., Borja-Aburto V. H. and Diaz-Barriga F. (2002) Levels of dichlorodiphenyltrichloroethane and deltamethrin in humans and environmental samples in malarious areas of Mexico. *Environ Res* **88**, 174-81.

Yekutieli D. and Benjamini Y. (1999) Resampling-based false discovery rate controlling multiple test procedures for correlated test statistics. *J Statist Plann Inference* **82**, 171-196.

Discussion and Future Directions

Chapter 5

Joshua A. Harrill

[1]University of North Carolina at Chapel Hill, Curriculum in Toxicology, CB 7270, Chapel Hill, NC 27599

The present research project was undertaken to address a fundamental data gap in the toxicological profile of pyrethroid insecticides: i.e. changes in gene expression that occur downstream of the pharmacological interaction of these agents with voltage-sensitive ion channels. The acute neurotoxic effects of pyrethroids manifest at the whole organism level as a result of pharmacological disruption of neuronal firing (Narahashi 2001; Soderlund et al. 2002; Ray et al. 2005). A vast literature in the fields of molecular biology and neuroscience demonstrate that increased neuronal excitability produce changes in gene expression. These changes in gene expression are thought to mediate adaptive responses of neurons to excitatory stimuli in both adult and developing animals (Finkbeiner and Greenberg 1998; Zhang and Poo 2001; Wong and Ghosh 2002; Zito and Svoboda 2002; Miller and Kaplan 2003; Uesaka et al. 2006; Uesaka et al. 2005; Kullman and Lamsa 2007). Yet, the effects of pyrethroids on neuronal gene expression downstream of actions at the neuronal membrane had not been characterized.

The overall goal of the present research was to test the hypothesis that pyrethroids cause changes in the expression of activity-regulated gene transcripts in the central nervous system in dose ranges surrounding the threshold for acute neurotoxic effects. The present studies: 1) identified activity-regulated gene expression changes following acute pyrethroid exposure, 2) identified some intracellular signaling pathways that may be activated by pyrethroids, and 3) demonstrated that neuronal branching morphogenesis is affected by pyrethroid exposure *in vitro*. The latter finding may represent a novel neurotoxic effect of pyrethroids.

The gene expression studies conducted in Chapters 2 and 4 of this work identified a suite of activity-regulated genes as being sensitive to pyrethroids including *c-fos, Arc, Nr4a1,*

Egr1, Dusp1, Dusp5, Dusp6 and *Camk1g*. The majority of these findings are novel to the field of pyrethroid research and consistent with the neuronal hyperexcitability produced by pyrethroids. These changes in gene expression occur at or below doses that produce minimal effects on neurobehavior in the whole animal (Bloom et al 1983; Crofton and Reiter 1984; Peele and Crofton 1987; McDaniel and Moser 1996; Wolansky et al. 2006). The activity-regulated transcripts identified as being responsive to pyrethroids are a 'molecular tool' useful in addressing a critical gap in the field of pyrethroid research; do different pyrethroids activate the same neuronal circuits at doses that produce minimal effects on neurobehavior?

The neurobehavioral endpoints affected by pyrethroids are apical measures of nervous system function and can be affected by a wide variety of chemicals with diverse toxicological mechanisms (Davis 1986; Moser and MacPhail 1990; Crofton et al. 1991; Crofton and MacPhail 1996). It is possible that at moderately effective dose levels, Type I and Type II pyrethroids activate different neuronal circuits or different neuronal sub-types to elicit the same overall effect on apical neurobehavioral endpoints. In support of this, *in vitro* studies have demonstrated that different pyrethroid types produce disparate effects on the same neuronal cell populations and that neurons with different cellular phenotypes respond differently to the same pyrethroid (Tatebayashi and Narahashi 1994; Tabarean and Narahashi 1998; Stucky and Lewin 1999; Grosse et al. 2002; Wu and Pan 2004; Meyer and Shafer 2006; Meyer et al. 2008). In addition, the present data from Chapter 4 demonstrate that activity-regulated gene expression in the rat cortex is less intense following Type I pyrethroid exposure as compared to Type II pyrethroids at low doses that produce the same quantitative effect on motor function. The pyrethroid-regulated gene signatures defined in the present study may be used as cellular 'markers-of-activation' to compare the excitatory effects of

pyrethroids, both across brain regions and across different compounds. Data on activation of specific neuronal circuits in the lower end of the pyrethroid-dose effect range would aid in the mechanistic grouping of different pyrethroids in the context of a cumulative risk assessment framework (EPA 2002).

The mapping of activated neuronal circuits with immediate early genes has been used to study both behavior in untreated animals and neurotoxicity produced by a variety of compounds (Vendrell et al. 1991; Vendrell et al. 1992; Andre et al. 1998; Guzowski et al. 1999; Storey et al. 2002; Caravajel et al. 2005). Guzowski et al. (2005) demonstrated the utility of fluorescent *in situ* hybridization (FISH) in identifying neurons activated by an excitatory stimuli using an immediate early mRNA as the marker of effect. The immediate early genes identified in the present study could be used as markers of effect with the FISH method to examine the neuronal circuitry activated by pyrethroids in an acute dosing model. Future experiments could include a multi-factorial design that examines pyrethroid-induced neuronal activation at several doses surrounding the threshold for acute behavioral effects, several sampling times that match the onset and peak of neurobehavioral effects and several different pyrethroids for comparison of effects across the chemical class. Serial sectioning of whole brains would be used to provide a comprehensive map of neuronal cell bodies activated by pyrethroids throughout the different brain regions at different times and doses. The commercial availability of fluorophores that excite at different wavelengths also allows for multicolor FISH. Different colored flourophores could be used to label the immediate early gene marker and other mRNA species specific to neurons with different molecular phenotypes (such as those coding for specific neurotransmitter receptors or ion channels). This would allow determinations of whether different neuronal populations within the brain

are activated by different pyrethroids or at different pyrethroid doses. The type of approach described here would address potential mechanistic differences in the Type I and Type II action at the cellular level.

From a molecular biology standpoint, the data on pyrethroid-regulated gene expression in the present study support a model for the intracellular effects of these compounds at the protein level. This putative signaling network includes the activation of constitutive kinase pathways (*PI3K/Akt, Jnk, p38 MAPK, ERK/MEK, Pkc*), subsequent activation of *CREB, NFκB* and *STAT* transcription factors and finally induction of immediate early gene phosphatases, transcription factors and effectors. These pyrethroid induced genes terminate stimulation of the kinase pathways, mediate subsequent gene transcription events and may augment downstream neuronal functions, respectively (see Chapter 4, Figure 4.9). The pyrethroid effects on immediate early gene expression are empirically measured in the present studies, however the activation of the constitutive kinase complexes and transcription factors in this network are speculative at this point. Future experiments examining the phosophorylation states, kinase activities and transcriptional activities of these proteins in response to pyrethroids are required to validate the proposed intracellular signaling network.

Predictions regarding the role of immediate early gene expression and the putative intracellular signaling networks as it relates to pyrethroid neurotoxicity are difficult. Some of genes upregulated by pyrethroids in the present studies (*Arc, Egr1*), as well as some components of the predicted pyrethroid signaling network (*MAPK, p38 MAPK, Jnk, CREB, NFκB*) are essential to the process of long-term potentiation and memory consolidation in the brain (Bozon et al. 2003; Li et al. 2005; Miyamoto 2006; O'Mahoney et al. 2006; Plath et al. 2006; Liu et al. 2007; Toyoda et al. 2007). Subsequently, abnormal activation of these

pathways by pyrethroids may interfere with memory formation and cognitive recall. In support of this, a limited number of *in vivo* studies report effects of acute pyrethroid exposure on learned behavior in rats using operant response tasks (Bloom et al. 1983; Peele and Crofton 1987; Stein et al. 1987). A consistent decrease in operant response rates was observed for numerous pyrethroids and indicates that these compounds either interfere with cognitive recall of a learned response or, alternatively, decrease motivation for completing a reward-driven task. If protein phosphorylation and activation studies confirm the putative findings from the gene array pathway analysis, then investigation of low dose pyrethroid-induced effects on working memory (learning) and reference memory (retention) with classical behavioral test paradigms (Eckerman and Bushnell 1992) and correlation of those effects with changes in biochemical endpoints would be a sensible follow-up study.

Of all the findings in the present study, the observation that pyrethroids can affect neuronal branching morphogenesis *in vitro* has the highest potential impact on human health and the field of pyrethroid toxicology. The basis for testing whether or not pyrethroids affected this developmental process came from functional category level analysis of the microarray data presented in Chapter 2 of this work. The *in vitro* model used herein revealed that pyrethroids increased neurite branching but not length. This finding is novel and in contrast to the few available reports of pyrethroid effects on neuronal morphology (Nandi et al. 2006; Tran et al. 2006; Weeks and Perez 2006). The present data predict that pyrethroids may affect neuronal branching *in vivo* in both the adult and developing nervous system. Repeated abuse of the stimulant drugs cocaine and amphetamine have been shown to produce increased dendritic branching in the adult cortex, which has been putatively linked to impairment of cognitive function and development of addiction (Robinson and Kolb 1999;

Robinson et al. 2001). Repeated exposures to pyrethroids may cause the same types of effects. In addition, neurons undergo extensive dendritic branching prior to the formation of synaptic contacts in the developing nervous system (Wong and Ghosh 2002; Jan and Jan 2003; Libersat and Duch 2004; McAllister et al. 2004). Pyrethroids also have the potential to affect this developmental process, based on the present *in vitro* findings.

The potential for pyrethroids to act as developmental neurotoxicants has been recently reviewed (Shafer et al. 2005). To date, the database on pyrethroid developmental neurotoxicology includes investigations of acetylcholine receptor density, neurotransmitter levels and motor behavior in adult rats and mice exposed during gestational or early post-natal life (Eriksson and Nordberg 1990; Eriksson and Fredriksson 1991; Ahlbom et al. 1994; Talts et al. 1998a; Lazarini et al. 2001). The present data argue that changes in neuronal microstructure and network connectivity should also be examined in laboratory animal models exposed to pyrethroids during the critical period of neuronal growth and branching.

Gene expression data provides a number of attractive candidate molecules that may mediate the pyrethroid effects on branching morphogenesis. These include *Camk1g, Cxcl12* and its cognate receptor *Cxcr4*, *Notch* and *β-catenin* all of which control some aspects of neuronal branching (Redmond et al. 2000; Yu and Malenka 2003; Pujol et al. 2005; Wayman et al. 2006; Takemoto-Kimura et al. 2007). An immediate future direction would be to confirm the effects on branching morphology observed *in vitro* in an *in vivo* model. A morphological examination of neuronal dendritic fields following pyrethroid exposure in both early life and in adulthood would serve to confirm or refute the present observations. If pyrethroids are shown to impact neuronal branching *in vivo*, then the gene candidates

identified in the present studies could be used as starting point to examining the molecular mechanisms that control this response

In summary, the present research provides important findings regarding the effects of pyrethroids on gene expression in the brain, an area of pyrethroid research that had not been extensively studied previously. The results of these studies supported the hypothetical model of pyrethroid effects on gene expression outlined prior to experimentation. In addition, these data demonstrated that different pyrethroids induce changes in a similar sub-set of activity regulated genes and facilitated predictions regarding the activation of intracellular signaling cascades and functional effects in neurons downstream of the pharmacological actions of pyrethroids at the neuronal membrane. Finally, one of the functional effects predicted by the gene expression studies was confirmed in an *in vitro* model of neuronal morphogenesis.

Works Cited

Ahlbom, J., Fredriksson, A., and Eriksson, P. (1994). Neonatal exposure to a type-I pyrethroid (bioallethrin) induces dose-response changes in brain muscarinic receptors and behaviour in neonatal and adult mice. *Brain Res* **645**, 318-24.

Andre, V., Pineau, N., Motte, J. E., Marescaux, C., and Nehlig, A. (1998). Mapping of neuronal networks underlying generalized seizures induced by increasing doses of pentylenetetrazol in the immature and adult rat: a c-Fos immunohistochemical study. *Eur J Neurosci* **10**, 2094-106.

Bloom, A. S., Staatz, C. G., and Dieringer, T. (1983). Pyrethroid effects on operant responding and feeding. *Neurobehav Toxicol Teratol* **5**, 321-4.

Bozon, B., Kelly, A., Josselyn, S. A., Silva, A. J., Davis, S., and Laroche, S. (2003). MAPK, CREB and zif268 are all required for the consolidation of recognition memory. *Philos Trans R Soc Lond B Biol Sci* **358**, 805-14.

Carvajal, F., Sanchez-Amate, M. C., Sanchez-Santed, F., and Cubero, I. (2005). Neuroanatomical targets of the organophosphate chlorpyrifos by c-fos immunolabeling. *Toxicol Sci* **84**, 360-7.

Crofton, K. M., Howard, J. L., Moser, V. C., Gill, M. W., Reiter, L. W., Tilson, H. A., and MacPhail, R. C. (1991). Interlaboratory comparison of motor activity experiments: implications for neurotoxicological assessments. *Neurotoxicol Teratol* **13**, 599-609.

Crofton, K. M., and MacPhail, R. C. (1996). Reliability of Motor Activity Assessments. In Measuring Movement and Locomotion: From Invertebrates to Humans (K. P. Ossenkopp, M. Kavaliers and P. R. Sanberg, eds.). R.G. Landes Company, New York.

Crofton, K. M., and Reiter, L. W. (1984). Effects of two pyrethroid insecticides on motor activity and the acoustic startle response in the rat. *Toxicol Appl Pharmacol* **75**, 318-28.

Davis, M. (1986). Pharmacological and anatomical analysis of fear conditioning using the fear-potentiated startle paradigm. *Behav Neurosci* **100**, 814-24.

Eckerman D. A. and Bushnell P. J. (1992) Neurotoxicology of cognition: attention, learning, and memory. In Neurotoxicology (Edited by Tilson H. A. and Mitchell C. L.), Raven Press, New York. p. 213–270.

Eriksson, P., and Fredriksson, A. (1991). Neurotoxic effects of two different pyrethroids, bioallethrin and deltamethrin, on immature and adult mice: changes in behavioral and muscarinic receptor variables. *Toxicol Appl Pharmacol* **108**, 78-85.

Eriksson, P., and Nordberg, A. (1990). Effects of two pyrethroids, bioallethrin and deltamethrin, on subpopulations of muscarinic and nicotinic receptors in the neonatal mouse brain. *Toxicol Appl Pharmacol* **102**, 456-63.

Finkbeiner, S., and Greenberg, M. E. (1998). Ca2+ channel-regulated neuronal gene expression. *J Neurobiol* **37**, 171-89.

Grosse, G., Thiele, T., Heuckendorf, E., Schopp, E., Merder, S., Pickert, G., and Ahnert-Hilger, G. (2002). Deltamethrin differentially affects neuronal subtypes in hippocampal primary culture. *Neuroscience* **112**, 233-41.

Guzowski, J. F., McNaughton, B. L., Barnes, C. A., and Worley, P. F. (1999). Environment-specific expression of the immediate-early gene Arc in hippocampal neuronal ensembles. *Nat Neurosci* **2**, 1120-4.

Jan, Y. N., and Jan, L. Y. (2003). The control of dendrite development. *Neuron* **40**, 229-42.

Kullmann, D. M., and Lamsa, K. P. (2007). Long-term synaptic plasticity in hippocampal interneurons. *Nat Rev Neurosci* **8**, 687-99.

Lazarini, C. A., Florio, J. C., Lemonica, I. P., and Bernardi, M. M. (2001). Effects of prenatal exposure to deltamethrin on forced swimming behavior, motor activity, and striatal dopamine levels in male and female rats. *Neurotoxicol Teratol* **23**, 665-73.

Li, L., Carter, J., Gao, X., Whitehead, J., and Tourtellotte, W. G. (2005). The neuroplasticity-associated arc gene is a direct transcriptional target of early growth response (Egr) transcription factors. *Mol Cell Biol* **25**, 10286-300.

Libersat, F., and Duch, C. (2004). Mechanisms of dendritic maturation. *Mol Neurobiol* **29**, 303-20.

Liu, Y. L., Zhou, L. J., Hu, N. W., Xu, J. T., Wu, C. Y., Zhang, T., Li, Y. Y., and Liu, X. G. (2007). Tumor necrosis factor-alpha induces long-term potentiation of C-fiber evoked field potentials in spinal dorsal horn in rats with nerve injury: the role of NF-kappa B, JNK and p38 MAPK. *Neuropharmacology* **52**, 708-15.

McAllister, A. K., Katz, L. C., and Lo, D. C. (1996). Neurotrophin regulation of cortical dendritic growth requires activity. *Neuron* **17**, 1057-64.

McDaniel, K. L., and Moser, V. C. (1993). Utility of a neurobehavioral screening battery for differentiating the effects of two pyrethroids, permethrin and cypermethrin. *Neurotoxicol Teratol* **15**, 71-83.

Meyer, D. A., Carter, J. M., Johnstone, A. F., and Shafer, T. J. (2008). Pyrethroid modulation of spontaneous neuronal excitability and neurotransmission in hippocampal neurons in culture. *Neurotoxicology*. 29, 213-225

Meyer, D. A., and Shafer, T. J. (2006). Permethrin, but not deltamethrin, increases spontaneous glutamate release from hippocampal neurons in culture. *Neurotoxicology* **27**, 594-603.

Miller, F. D., and Kaplan, D. R. (2003). Signaling mechanisms underlying dendrite formation. *Curr Opin Neurobiol* **13**, 391-8.

Miyamoto, E. (2006). Molecular mechanism of neuronal plasticity: induction and maintenance of long-term potentiation in the hippocampus. *J Pharmacol Sci* **100**, 433-42.

Moser, V. C., and MacPhail, R. C. (1990). Comparative sensitivity of neurobehavioral tests for chemical screening. *Neurotoxicology* **11**, 335-44.

Nandi, A., Chandil, D., Lechesal, R., Pryor, S. C., McLaughlin, A., Bonventre, J. A., Flynnx, K., and Weeks, B. S. (2006). Bifenthrin causes neurite retraction in the absence of cell death: a model for pesticide associated neurodegeneration. *Med Sci Monit* **12**, BR169-73.

Narahashi, T. (2001). Neurophysiological Effects of Insecticides. In Handbook of Pesticide Toxicology (R. I. Krieger, ed., Vol. 2, pp. 335-351. Academic Press, San Diego, CA.

O'Mahony, A., Raber, J., Montano, M., Foehr, E., Han, V., Lu, S. M., Kwon, H., LeFevour, A., Chakraborty-Sett, S., and Greene, W. C. (2006). NF-kappaB/Rel regulates inhibitory and excitatory neuronal function and synaptic plasticity. *Mol Cell Biol* **26**, 7283-98.

Peele, D. B., and Crofton, K. M. (1987). Pyrethroid effects on schedule-controlled behavior: time and dosage relationships. *Neurotoxicol Teratol* **9**, 387-94.

Plath, N., Ohana, O., Dammermann, B., Errington, M. L., Schmitz, D., Gross, C., Mao, X., Engelsberg, A., Mahlke, C., Welzl, H., Kobalz, U., Stawrakakis, A., Fernandez, E., Waltereit, R., Bick-Sander, A., Therstappen, E., Cooke, S. F., Blanquet, V., Wurst, W., Salmen, B., Bosl, M. R., Lipp, H. P., Grant, S. G., Bliss, T. V., Wolfer, D. P., and Kuhl, D. (2006). Arc/Arg3.1 is essential for the consolidation of synaptic plasticity and memories. *Neuron* **52**, 437-44.

Pujol, F., Kitabgi, P., and Boudin, H. (2005). The chemokine SDF-1 differentially regulates axonal elongation and branching in hippocampal neurons. *J Cell Sci* **118**, 1071-80.

Ray, D. E., and Fry, J. R. (2006). A reassessment of the neurotoxicity of pyrethroid insecticides. *Pharmacol Ther* **111**, 174-93.

Redmond, L., Oh, S. R., Hicks, C., Weinmaster, G., and Ghosh, A. (2000). Nuclear Notch1 signaling and the regulation of dendritic development. *Nat Neurosci* **3**, 30-40.

Robinson, T. E., Gorny, G., Mitton, E., and Kolb, B. (2001). Cocaine self-administration alters the morphology of dendrites and dendritic spines in the nucleus accumbens and neocortex. *Synapse* **39**, 257-66.

Robinson, T. E., and Kolb, B. (1999). Alterations in the morphology of dendrites and dendritic spines in the nucleus accumbens and prefrontal cortex following repeated treatment with amphetamine or cocaine. *Eur J Neurosci* **11**, 1598-604.

Shafer, T. J., Meyer, D. A., and Crofton, K. M. (2005). Developmental neurotoxicity of pyrethroid insecticides: critical review and future research needs. *Environ Health Perspect* **113**, 123-36.

Soderlund, D. M., Clark, J. M., Sheets, L. P., Mullin, L. S., Piccirillo, V. J., Sargent, D., Stevens, J. T., and Weiner, M. L. (2002). Mechanisms of pyrethroid neurotoxicity: implications for cumulative risk assessment. *Toxicology* **171**, 3-59.

Stein, E. A., Washburn, M., Walczak, C., and Bloom, A. S. (1987). Effects of pyrethroid insecticides on operant responding maintained by food. *Neurotoxicol Teratol* **9**, 27-31.

Storey, T. W., Rho, J. M., White, S. S., Sankar, R., and Szot, P. (2002). Age-dependent differences in flurothyl-induced c-fos and c-jun mRNA expression in the mouse brain. *Dev Neurosci* **24**, 294-9.

Stucky, C. L., and Lewin, G. R. (1999). Isolectin B(4)-positive and -negative nociceptors are functionally distinct. *J Neurosci* **19**, 6497-505.

Tabarean, I. V., and Narahashi, T. (1998). Potent modulation of tetrodotoxin-sensitive and tetrodotoxin-resistant sodium channels by the type II pyrethroid deltamethrin. *J Pharmacol Exp Ther* **284**, 958-65.

Takemoto-Kimura, S., Ageta-Ishihara, N., Nonaka, M., Adachi-Morishima, A., Mano, T., Okamura, M., Fujii, H., Fuse, T., Hoshino, M., Suzuki, S., Kojima, M., Mishina, M., Okuno, H., and Bito, H. (2007). Regulation of dendritogenesis via a lipid-raft-associated Ca2+/calmodulin-dependent protein kinase CLICK-III/CaMKIgamma. *Neuron* **54**, 755-70.

Talts, U., Fredriksson, A., and Eriksson, P. (1998). Changes in behavior and muscarinic receptor density after neonatal and adult exposure to bioallethrin. *Neurobiol Aging* **19**, 545-52.

Tatebayashi, H., and Narahashi, T. (1994). Differential mechanism of action of the pyrethroid tetramethrin on tetrodotoxin-sensitive and tetrodotoxin-resistant sodium channels. *J Pharmacol Exp Ther* **270**, 595-603.

Toyoda, H., Zhao, M. G., Xu, H., Wu, L. J., Ren, M., and Zhuo, M. (2007). Requirement of extracellular signal-regulated kinase/mitogen-activated protein kinase for long-term potentiation in adult mouse anterior cingulate cortex. *Mol Pain* **3**, 36.

Tran, V., Hoffman, N., Mofunanaya, A., Pryor, S. C., Ojugbele, O., McLaughlin, A., Gibson, L., Bonventre, J. A., Flynn, K., and Weeks, B. S. (2006). Bifenthrin inhibits neurite outgrowth in differentiating PC12 cells. *Med Sci Monit* **12**, BR57-62.

Uesaka, N., Hirai, S., Maruyama, T., Ruthazer, E. S., and Yamamoto, N. (2005). Activity dependence of cortical axon branch formation: a morphological and electrophysiological study using organotypic slice cultures. *J Neurosci* **25**, 1-9.

Uesaka, N., Ruthazer, E. S., and Yamamoto, N. (2006). The role of neural activity in cortical axon branching. *Neuroscientist* **12**, 102-6.

USEPA. (2000) Supplementary Guidance for Conducting Health Risk Assessment of Chemical Mixtures. EPA/630/R-00/002.

Vendrell, M., Pujol, M. J., Tusell, J. M., and Serratosa, J. (1992a). Effect of different convulsants on calmodulin levels and proto-oncogene c-fos expression in the central nervous system. *Brain Res Mol Brain Res* **14**, 285-92.

Vendrell, M., Tusell, J. M., and Serratosa, J. (1992b). c-fos expression as a model for studying the action of hexachlorocyclohexane isomers in the CNS. *J Neurochem* **58**, 862-9.

Wayman, G. A., Impey, S., Marks, D., Saneyoshi, T., Grant, W. F., Derkach, V., and Soderling, T. R. (2006). Activity-dependent dendritic arborization mediated by CaM-kinase I activation and enhanced CREB-dependent transcription of Wnt-2. *Neuron* **50**, 897-909.

Weeks, B. S., and Perez, P. P. (2006). PolicosanolPlus and Neuroprevin ameliorate pesticide-mediated inhibition of neurite outgrowth and neurite degeneration. *Med Sci Monit* **12**, BR379-384.

Wolansky, M. J., Gennings, C., and Crofton, K. M. (2006). Relative potencies for acute effects of pyrethroids on motor function in rats. *Toxicol Sci* **89**, 271-7.

Wong, R. O., and Ghosh, A. (2002). Activity-dependent regulation of dendritic growth and patterning. *Nat Rev Neurosci* **3**, 803-12.

Wu, Z. Z., and Pan, H. L. (2004). Tetrodotoxin-sensitive and -resistant Na+ channel currents in subsets of small sensory neurons of rats. *Brain Res* **1029**, 251-8.

Yu, X., and Malenka, R. C. (2003). Beta-catenin is critical for dendritic morphogenesis. *Nat Neurosci* **6**, 1169-77.

Zhang, L. I., and Poo, M. M. (2001). Electrical activity and development of neural circuits. *Nat Neurosci* **4 Suppl**, 1207-14.

Zito, K., and Svoboda, K. (2002). Activity-dependent synaptogenesis in the adult mammalian cortex. *Neuron* **35**, 1015-7.

Appendix A. Chapter 2 Supplementary Material

Mean coefficients of variation for GCOSv1.2 normalized expression summaries

	1-10%	11-20%	21-30%	31-40%	41-50%	51-60%	61-70%	71-80%	81-90%	91-100%
n	3105	3104	3104	3104	3104	3104	3104	3104	3104	3105
Control	66.52	57.09	40.99	32.80	28.50	26.69	25.29	24.84	24.33	21.21
Permethrin										
1 mg/kg	63.15	55.64	41.30	33.61	29.65	29.05	28.67	28.48	28.24	24.44
10 mg/kg	63.61	55.24	40.35	32.25	27.69	25.73	25.08	24.45	23.72	21.13
100 mg/kg	61.74	55.51	41.06	33.35	28.94	27.03	26.02	25.35	24.78	22.55
Deltamethrin										
0.3 mg/kg	61.29	52.91	37.26	28.68	24.00	21.44	19.17	17.85	16.91	14.91
1.0 mg/kg	61.36	54.54	39.81	31.28	27.01	24.69	23.65	23.00	22.55	19.61
3.0 mg/kg	63.26	55.61	39.18	32.80	25.77	23.49	21.79	20.53	19.52	17.03

Mean coefficients of variation for RMA normalized expression summaries

	1-10%	11-20%	21-30%	31-40%	41-50%	51-60%	61-70%	71-80%	81-90%	91-100%
n	3105	3104	3104	3104	3104	3104	3104	3104	3104	3105
Control	7.08	9.99	11.95	13.65	15.05	16.59	18.07	18.45	19.21	16.86
Permethrin										
1 mg/kg	7.39	10.53	12.77	15.25	17.36	20.03	22.71	23.35	23.80	20.53
10 mg/kg	6.99	9.68	11.66	13.69	15.40	17.47	19.42	20.21	20.72	18.08
100 mg/kg	7.01	10.10	12.27	14.41	16.52	18.68	20.99	21.76	22.43	19.46
Deltamethrin										
0.3 mg/kg	6.08	8.40	9.96	11.42	12.55	13.45	14.33	14.51	14.89	12.84
1.0 mg/kg	6.66	9.49	11.49	13.34	14.95	16.71	18.55	19.16	19.75	17.70
3.0 mg/kg	6.53	8.99	10.84	13.65	13.94	15.37	16.58	17.09	17.27	15.29

Appendix A, Table 1. ***Comparison of mean coefficients of variation (CV) between GCOSv1.2 and RMA microarray expression summaries.*** For each expression summary calculation method, all 31,042 probe sets present on the Affymetrix Rat 230 2.0 GeneChip® array were sorted based on the mean expression summary within the control group and divided into equally sized percentile ranges in ascending order. CV's were calculated for each individual probe set within each dose group. The mean CV for each percentile range was then calculated across probe sets for each dose group. Expression summaries calculated using RMA consistently reduces the variability of the expression summaries across the entire data set when compared to GCOSv1.2. A dramatic decrease in variability is observed in the lower 50% of the data set.

Appendix A, Table 2. ***Taqman® qRT-PCR assay information.***

Gene Symbol	Assay I.D.	Reference Sequence	Assay Position*	Amplicon Length	Amplification Efficiency (%)
β-actin	Rn00667869_m1	CTTCCTTCCTGGGTATGGAATCCTG	4 - 5 exon junction	91	95.2
Gpd1	Rn00573596_m1	GGGCCTCGTGGACAAGTTTCCCTTG	7 - 8 exon junction	79	92.4
Fkpb51	Rn01768371_m1	GAGCAGGATGCCAAGGAAGAGGCCA	10 - 11 exon junction	74	91.8
Camk1g	Rn00788224_m1	CATTTCTGAGTCAGCCAAGGACTTT	8 - 9 exon junction	71	96.0
Hsp27	Rn00583001_g1	TCACCCGGAAATACACGCTCCCTCC	2 - 3 exon junction	136	94.4
Ddc	Rn01401187_m1	TCCGGCTAAAGGGCTCCAACCAGTT	13 - 14 exon junction	102	92.5
BDNF	Rn02531967_s1	AAATTCTTGCTGTGGTCTCTTTTTG	exon VIII**	142	97.5
Rassf5	Rn00571287_m1	GGAGACGTAGAGTGGGATGCCTTTT	5 - 6 exon junction	75	92.4
c-fos	Rn02105433_s1	CTTCAGCGTCCATGTTCATTGTCAT	exon 4	160	96.0
Egr1	Rn00561138_m1	ACGAGCACCTGACCACAGAGTCCTT	1 - 2 exon junction	64	98.0

*taken from Applied Biosystems web-site.
**determined from Liu et al. Brain Research 1067(1), 1-12 (2006)

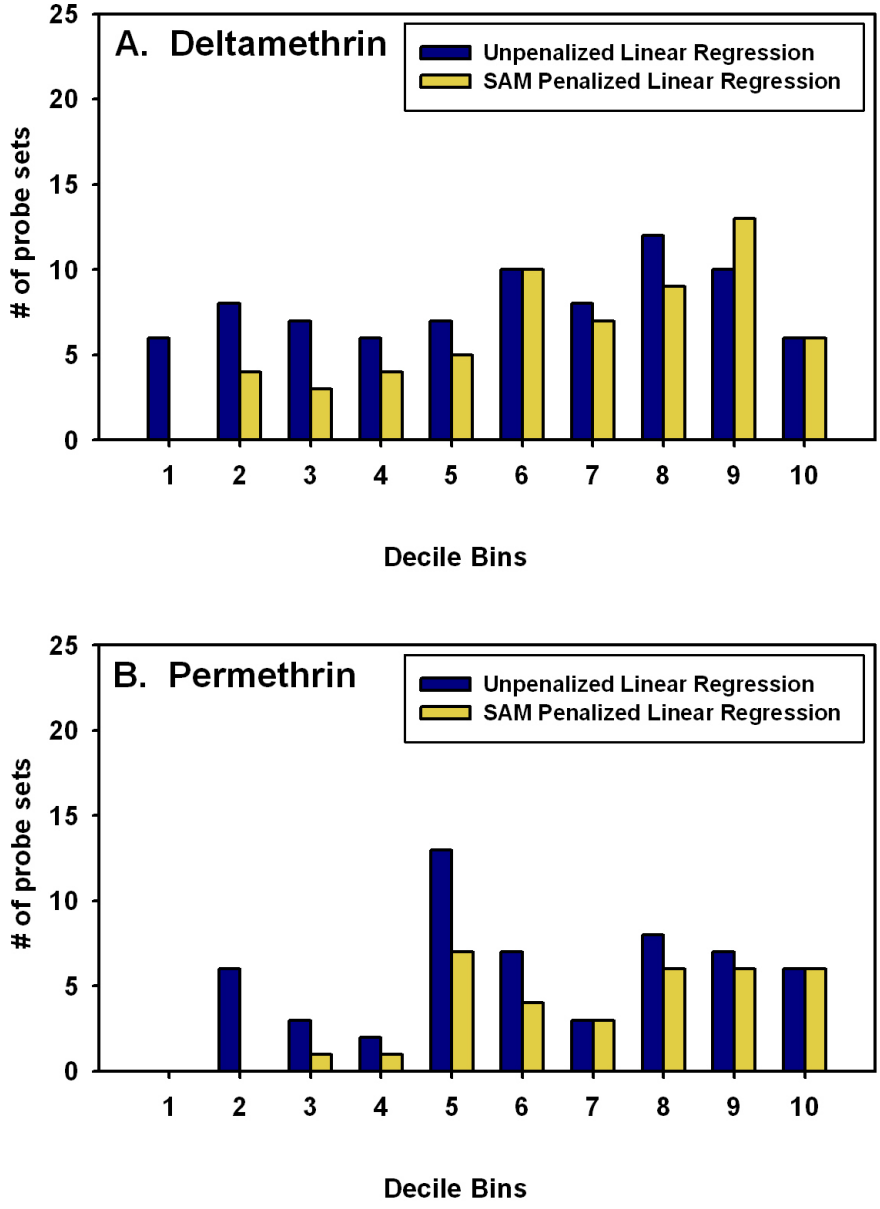

Appendix A, Figure 1. ***Identification of dose-responsive probe sets by linear regression or penalized linear (SAM) regression.*** Panels A and B are histograms of the number of probe sets identified as dose-responsive using either a linear regression (blue bars) or a penalized linear regression in SAM (yellow bars) for deltamethrin and permethrin, respectively. Decile bins were defined by ranking probe sets by the mean raw expression summary score across all treatment conditions from lowest to highest and dividing the probe sets into equal groups (n = 3104 for deciles 2-8 and 3105 for deciles 1 and 10). Probe sets within each decile that were determined to be dose-responsive with each method were counted and plotted in the panels. Note that less probe sets were detected as significantly dose-responsive in the lower decile ranges using penalized regression while the number of probe sets identified as dose-responsive in the upper deciles was similar between the two methods

Appendix B. Chapter 4 Supplementary Material

Appendix B, Table 1. ***Taqman® qRT-PCR assay information.***

Gene Symbol	Assay I.D.	Reference Sequence	Assay Position*	Amplicon Length	Amplification Efficiency (%)
β-actin	Rn00667869_m1	CTTCCTTCCTGGGTATGGAATCCTG	4 - 5 exon junction	91	95.2
Gpd1	Rn00573596_m1	GGGCCTCGTGGACAAGTTTCCCTTG	7 - 8 exon junction	79	92.4
Camk1g	Rn00788224_m1	CATTTCTGAGTCAGCCAAGGACTTT	8 - 9 exon junction	71	96.0
Egr1	Rn00561138_m1	ACGAGCACCTGACCACAGAGTCCTT	1 - 2 exon junction	64	98.0
Arc	Rn00571208_g1	GCCCCCAGCAGTGATTCATACCAGT	1 - 2 exon junction	119	98.8
Nr4a1	Rn00577766_m1	CGGGAGCCGGCCGGAGATGCCCTGT	1 - 2 exon junction	108	91.1
Nedd9	Rn01435420_m1	ATCATCAGCTGAGTCAGTTCCAGCT	6 - 7 exon junction	89	90.8

*taken from Applied Biosystems web-site.

Appendix B, Table 2. *Statistical Analysis of qRT-PCR Data*

		Two-Way ANOVA		Deltamethrin 3 h pair-wise		6 h pair-wise	
		F	p-value	F	p-value	F	p-value
Nr4a1	**TRT**	15.15	0.0005	104.81	0.0001	0	0.9476
	TIME	39.2	0.0001				
	TRT*TIME	40.53	0.0001				
Arc	**TRT**	9.11	0.0050	46.31	0.0001	0	0.9558
	TIME	25.16	0.0001				
	TRT*TIME	24.4	0.0001				
Egr1	**TRT**	0.28	0.5972	6.45	0.0219	1.36	0.2608
	TIME	6.58	0.0152				
	TRT*TIME	0.69	0.4115				
Camk1g	**TRT**	3.95	0.0553	0.16	0.6915	20.68	0.0003
	TIME	12.98	0.0011				
	TRT*TIME	9.31	0.0046				
Nedd9	**TRT**	2.71	0.1094	6.74	0.0195	0.46	0.5060
	TIME	1.52	0.2267				
	TRT*TIME	5.03	0.0319				
Gpd1	**TRT**	6.36	0.0168	154.19	0.0001	21.21	0.0003
	TIME	127.98	0.0001				
	TRT*TIME	16.71	0.0003				

Appendix B, Table 2 ***continued*****.**

		Cyfluthrin					
		Two-Way ANOVA		3 h pair-wise		6 h pair-wise	
		F	p-value	F	p-value	F	p-value
Nr4a1	**TRT**	9.51	0.0042	31.54	0.0001	0.59	0.4538
	TIME	18.26	0.0002				
	TRT*TIME	26.17	0.0001				
Arc	**TRT**	9.23	0.0047	31.77	0.0001	0.44	0.5178
	TIME	17.85	0.0002				
	TRT*TIME	24.87	0.0001				
Egr1	**TRT**	3.48	0.0712	12.13	0.0031	0.01	0.9240
	TIME	8.02	0.0079				
	TRT*TIME	7.37	0.0106				
Camk1g	**TRT**	0.14	0.7088	2.2	0.1574	3.91	0.0655
	TIME	5.15	0.0301				
	TRT*TIME	0.09	0.7627				
Nedd9	**TRT**	1.24	0.2734	1.97	0.1794	0.49	0.4934
	TIME	0.25	0.6173				
	TRT*TIME	2.22	0.1458				
Gpd3	**TRT**	3.06	0.0897	36.26	0.0001	2.3	0.1488
	TIME	27.14	0.0001				
	TRT*TIME	8.92	0.0054				

Appendix B, Table 2 ***continued*****.**

		Cypermethrin					
		Two-Way ANOVA		3 h pair-wise		6 h pair-wise	
		F	p-value	F	p-value	F	p-value
Nr4a1	**TRT**	28.15	0.0001	76.3	0.0001	2.27	0.1511
	TIME	44.66	0.0001				
	TRT*TIME	68.03	0.0001				
Arc	**TRT**	13.77	0.0008	30.48	0.0001	2.8	0.1135
	TIME	19.03	0.0001				
	TRT*TIME	32.77	0.0001				
Egr1	**TRT**	10.11	0.0033	29.5	0.0001	0.23	0.6368
	TIME	15.88	0.0004				
	TRT*TIME	20.95	0.0001				
Camk1g	**TRT**	0.37	0.5458	3.81	0.0688	2.76	0.1162
	TIME	6.52	0.0156				
	TRT*TIME	0.38	0.5424				
Nedd9	**TRT**	3.79	0.0604	10	0.0060	0.31	0.5853
	TIME	3.52	0.0697				
	TRT*TIME	7.04	0.0123				
Gpd3	**TRT**	0.65	0.4267	17.2	0.0008	1.08	0.3142
	TIME	11.09	0.0022				
	TRT*TIME	2.8	0.1041				

Appendix B, Table 2 ***continued*****.**

		Permethrin					
		Two-Way ANOVA		3 h pair-wise		6 h pair-wise	
		F	p-value	F	p-value	F	p-value
Nr4a1	**TRT**	0.39	0.5384	16.18	0.0010	3.5	0.0799
	TIME	17.52	0.0002				
	TRT*TIME	2.48	0.1254				
Arc	**TRT**	0.04	0.8506	3.76	0.0702	1.36	0.2615
	TIME	4.95	0.0333				
	TRT*TIME	0.46	0.5018				
Egr1	**TRT**	0.13	0.7229	0.54	0.4738	1.83	0.1952
	TIME	2.26	0.1425				
	TRT*TIME	0.3	0.5875				
Camk1g	**TRT**	0.18	0.6772	0.07	0.7892	0.33	0.5719
	TIME	0.02	0.8843				
	TRT*TIME	0.33	0.5712				
Nedd9	**TRT**	0.19	0.6693	0.01	0.9251	0.34	0.5660
	TIME	0.26	0.6121				
	TRT*TIME	0.15	0.6990				
Gpd3	**TRT**	0.42	0.5199	4.53	0.0493	0.41	0.5294
	TIME	0.19	0.6696				
	TRT*TIME	2.45	0.1271				

Appendix B, Table 2 ***continued*****.**

		Tefluthrin					
		Two-Way ANOVA		3 h pair-wise		6 h pair-wise	
		F	p-value	F	p-value	F	p-value
Nr4a1	**TRT**	3.29	0.0792	8.42	0.0104	2.91	0.1075
	TIME	2.36	0.1346				
	TRT*TIME	11.31	0.0020				
Arc	**TRT**	3.15	0.0855	5.25	0.0358	4.27	0.0555
	TIME	1.03	0.3183				
	TRT*TIME	9.02	0.0052				
Egr1	**TRT**	3.91	0.0567	4.98	0.0402	2.71	0.1195
	TIME	1.19	0.2841				
	TRT*TIME	7.61	0.0095				
Camk1g	**TRT**	0.89	0.3519	2.72	0.1184	0.01	0.9127
	TIME	1.36	0.2517				
	TRT*TIME	1.73	0.1982				
Nedd9	**TRT**	1.68	0.2036	3.08	0.0986	0.13	0.7237
	TIME	1.33	0.2571				
	TRT*TIME	2.56	0.1195				
Gpd3	**TRT**	0.01	0.9324	3.02	0.1014	0.26	0.6196
	TIME	1.72	0.1985				
	TRT*TIME	0.17	0.6840				

Appendix B, Table 2 ***continued*****.**

		Bifenthrin					
		Two-Way ANOVA		3 h pair-wise		6 h pair-wise	
		F	p-value	F	p-value	F	p-value
Nr4a1	**TRT**	4.15	0.0501	10	0.0060	2.37	0.1428
	TIME	4.85	0.0349				
	TRT*TIME	12.37	0.0013				
Arc	**TRT**	2.64	0.1137	3.63	0.0750	5.52	0.0320
	TIME	0.02	0.8755				
	TRT*TIME	8.92	0.0054				
Egr1	**TRT**	1.89	0.1788	0.29	0.6005	5.76	0.0289
	TIME	1.12	0.2983				
	TRT*TIME	3.61	0.0666				
Camk1g	**TRT**	0.06	0.8051	0.01	0.9104	0.28	0.6066
	TIME	0.23	0.6370				
	TRT*TIME	0.11	0.7437				
Nedd9	**TRT**	0	0.9710	0.53	0.4780	1.64	0.2180
	TIME	1.82	0.1871				
	TRT*TIME	0.03	0.8572				
Gpd3	**TRT**	0.05	0.8202	0.91	0.3552	0.1	0.7555
	TIME	0.53	0.4701				
	TRT*TIME	0.03	0.8635				

Appendix B, Figure 1. ***Dimensional reduction of microarray data: effect of mean centering on measures of significance.*** Panels in the first column of the figure plot raw expression summary values for a probe set that has a significant interaction of time and treatment in a two-way ANOVA model (*Nfkbia*, top row), a probe set that has a significant main effect of treatment and no interaction of time and treatment (*2610029k21*, middle row) and a probe set with a significant main effect of time and no interaction of time and treatment (*Ly86*, bottom row). Significant effects observed with *Nfkbia* and *2610029k21* are exemplary of effects considering 'interesting' in the present study. Effects of time with no treatment are not of interest. Panels in the middle column are box plots of the expression summaries for each condition in the study before mean normalization for *Nfkbia, 2610026K21* and *Ly68*. Significance values for analysis of the four groups with a One-Way ANOVA are listed above the panels. Note that all three of the genes are significant in the one-way ANOVA. Panels in the far right column are box plots of the expression summaries for each condition in the study after mean normalization. Note that the significant effect for *Ly68* (bottom right corner panel) in the one-way ANOVA model is eliminated. Also, the two genes with treatment effects in the two-way ANOVA still have a significant model *p*-value in one-way ANOVA. Numbers in italicized type over each box plox are coefficients of variation of the data in each group. The C.V.s do not change following mean normalization. Mean normalized data was used in the SAFE enrichment analyses throughout the present study.

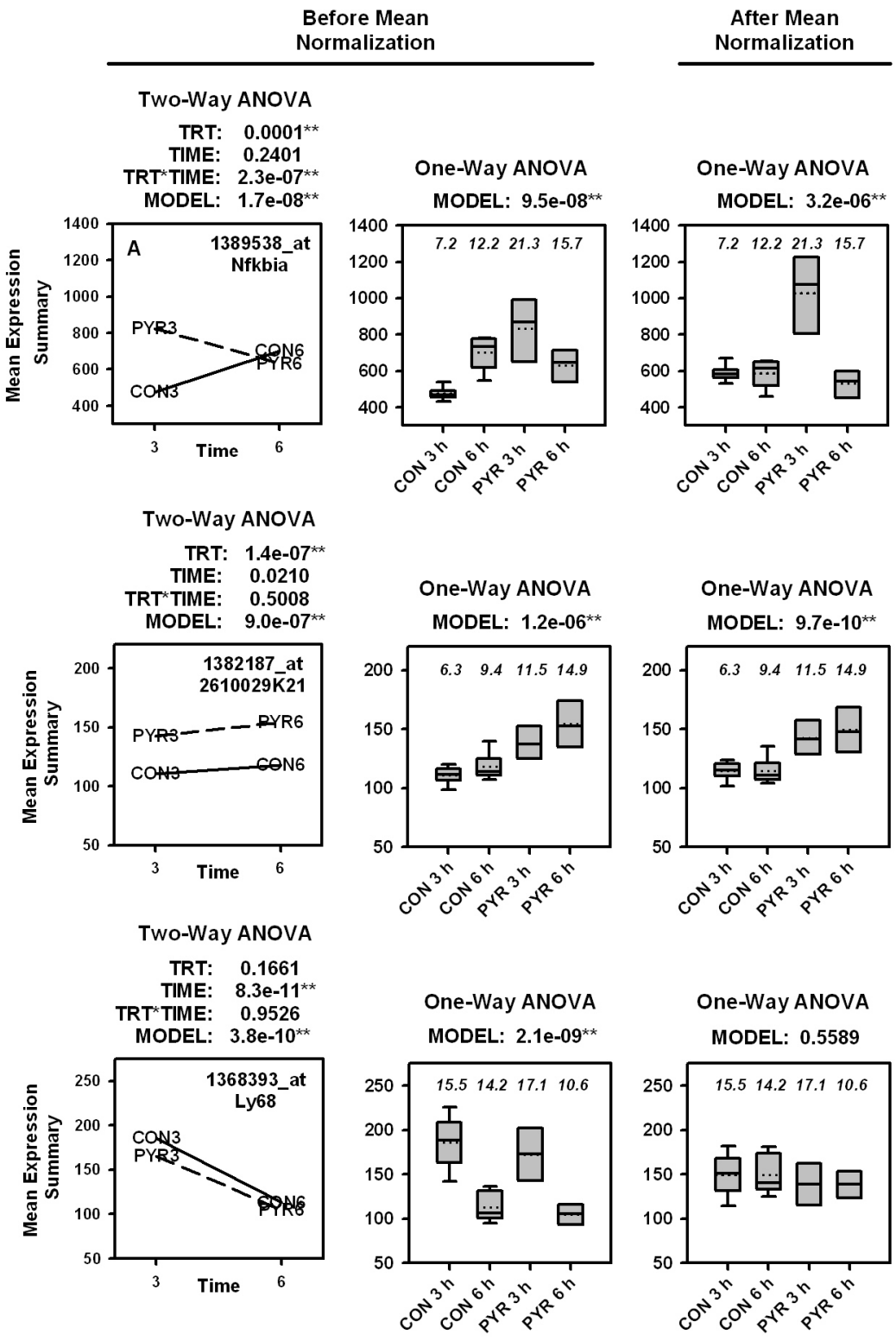
Before Mean Normalization
After Mean Normalization
Two-Way ANOVA
TRT: 0.0001**
TIME: 0.2401
TRT*TIME: 2.3e-07**
MODEL: 1.7e-08**
A
1389538_at
Nfkbia
PYR3
CON6
PYR6
CON3
Mean Expression Summary
Time
One-Way ANOVA
MODEL: 9.5e-08**
7.2 12.2 21.3 15.7
One-Way ANOVA
MODEL: 3.2e-06**
7.2 12.2 21.3 15.7
CON 3 h
CON 6 h
PYR 3 h
PYR 6 h
Two-Way ANOVA
TRT: 1.4e-07**
TIME: 0.0210
TRT*TIME: 0.5008
MODEL: 9.0e-07**
1382187_at
2610029K21
PYR3
PYR6
CON3
CON6
One-Way ANOVA
MODEL: 1.2e-06**
6.3 9.4 11.5 14.9
One-Way ANOVA
MODEL: 9.7e-10**
6.3 9.4 11.5 14.9
Two-Way ANOVA
TRT: 0.1661
TIME: 8.3e-11**
TRT*TIME: 0.9526
MODEL: 3.8e-10**
1368393_at
Ly68
CON3
PYR3
CON6
PYR6
One-Way ANOVA
MODEL: 2.1e-09**
15.5 14.2 17.1 10.6
One-Way ANOVA
MODEL: 0.5589
15.5 14.2 17.1 10.6